8-2009

Development of a canine stifle computer model to investigate cranial cruciate ligament deficiency.

Nathan Brown 1984-
University of Louisville

DEVELOPMENT OF A CANINE STIFLE COMPUTER MODEL TO INVESTIGATE CRANIAL CRUCIATE LIGAMENT DEFICIENCY

By

Nathan Brown
B.S., University of Louisville, 2007

A Thesis
Submitted to the Faculty of the
University of Louisville
J. B. Speed School of Engineering
as Partial Fulfillment of the Requirements
for the Professional Degree

MASTER OF ENGINEERING

Department of Mechanical Engineering

August 2009

DEVELOPMENT OF A CANINE STIFLE COMPUTER MODEL TO INVESTIGATE CRANIAL CRUCIATE LIGAMENT DEFICIENCY

Submitted by:_____
Nathan Brown

A Thesis Approved On

_____
(Date)

by the Following Reading and Examination Committee:

_____
Dr. Gina Bertocci, Thesis Director

_____
Dr. Denis Marcellin-Little

_____
Dr. Peter Quesada

_____
Dr. Michael Voor

ACKNOWLEDGEMENTS

This study is funded by the University of Louisville PhD Fellowship Program and Grosscurth Biomechanics Endowment

ABSTRACT

Background - Cranial cruciate ligament (CrCL) rupture in the canine stifle is a leading cause of orthopedic lameness in the dog. Several corrective surgical procedures have been developed to return dogs to pre-injury function following CrCL rupture, but no one technique has fully shown superiority in terms of functional outcomes. A complete understanding of canine stifle biomechanics prior to and following CrCL rupture is needed to evaluate the biomechanical rationale of surgical corrective procedures being employed.

Research Question - The goals of this study were to 1) develop a three dimensional rigid body canine hind limb computer model to simulate both a CrCL intact and CrCL deficient stifle during the stance phase of gait, 2) describe the stifle biomechanics in the CrCL intact and CrCL deficient stifle, and 3) to systematically assess model parameters which may influence CrCL deficiency.

Methods - A three dimensional rigid body computer model representing the skeletal structure of a 32 kg Labrador Retriever was developed using SolidWorks based on boney landmarks. Canine hind limb kinetic and kinematic parameters associated with the stance phase of gait were incorporated into the model from the scientific literature. Model simulation of the stance phase was implemented in COSMOSMotion for the CrCL intact and CrCL deficient stifle. Outcome measures assessed include stifle ligament forces and

tibial translation. Parameters thought to be associated with CrCL deficiency were systematically altered to determine the model outcome measure sensitivity. Verification of the model was attempted by comparison to a previously reported hind limb mathematical model and an in vitro study.

Results - The CrCL was found to be the primary load-bearing ligament during the stance phase in the CrCL intact stifle. The peak CrCL load of 26% body weight occurred at 40% stance in the intact stifle. The caudal cruciate ligament (CaCL) was found to be the primary load-bearing ligament in the CrCL deficient stifle. The peak CaCL load of 219% body weight occurred at 40% stance in the deficient stifle. Suppression of the CrCL consistently increased CaCL load profiles during stance. The medial collateral ligament and lateral collateral ligament were generally not loaded in the CrCL intact or CrCL deficient stifle. The peak relative cranial tibial translation following suppression of the CrCL in the baseline model was 17.8 mm. These outcome measures were verified through reasonable agreement with a hind limb mathematical model and an in vitro study.

Tibial plateau angle (TPA), patellar ligament line of action angle (PLLAA) and femoral condyle radius (FCR) were parameters for which model outcomes were most sensitive. In the CrCL intact stifle the CrCL peak load during stance increased with increasing TPA and increasing PLLAA. In the CrCL deficient stifle the CaCL peak load during stance increased with increasing TPA, increasing PLLAA, increasing FCR, increasing ground reaction force magnitude, increasing muscle force magnitude and increasing body mass. Additionally, the peak relative tibial translation during stance increased with increasing TPA, increasing PLLAA and increasing FCR. Parameters for which model outcome measures were less sensitive include ligament stiffness (all

ligaments), CrCL stiffness, ligament prestrain (all ligaments), CrCL prestrain and femoromeniscal friction coefficients.

Conclusions - A three dimensional rigid body canine hind limb computer model was developed to simulate both a CrCL intact and a CrCL deficient stifle during the stance phase of gait. This is the first 3D computer model to our knowledge capable of determining ligament forces in the CrCL intact and CrCL deficient stifle and visually describing tibial translation. This study attempts to assess several clinically relevant biomechanical parameters thought to be related to CrCL deficiency.

TABLE OF CONTENTS

Page

NOMENCLATURE

ATT	=	Anatomical Tibial Translation
BM	=	Body Mass
BW	=	Body Weight
CaCL	=	Caudal Cruciate Ligament
CrCL	=	Cranial Cruciate Ligament
CTWO	=	Cranial Tibial Wedge Osteotomy
FCR	=	Femoral Condyle Radius
FFC	=	Femoromeniscal Friction Coefficient
$(FT_{Deficient})_{Loaded}$	=	Craniocaudal distance from a fixed point on the femur to a fixed point on the tibia with a deficient CrCL loaded via weight bearing
$(FT_{Intact})_{Unloaded}$	=	Craniocaudal distance from a fixed point on the femur to a fixed point on the tibia with an intact CrCL unloaded via weight bearing
GRF	=	Ground Reaction Force
LCL	=	Lateral Collateral Ligament
LP	=	Ligament Prestrain
LS	=	Ligament Stiffness
MCL	=	Medial Collateral Ligament
MFM	=	Muscle Force Magnitude
PLLAA	=	Patellar Ligament Line of Action Angle
RTT	=	Relative Tibial Translation
TPA	=	Tibial Plateau Angle
TPLO	=	Tibial Plateau Leveling Osteotomy
TTA	=	Tibial Tuberosity Advancement
TTO	=	Triple Tibial Osteotomy

LIST OF TABLES

LIST OF FIGURES

I. INTRODUCTION

Canine stifle stability becomes compromised with degeneration of the stabilizing ligaments. Cranial cruciate ligament (CrCL) rupture is the most common orthopedic condition diagnosed in the canine stifle joint (Morris and Lipowitz 2001; Warzee, Dejardin et al. 2001; Pacchiana, Morris et al. 2003; Aragon and Budsberg 2005) and often requires surgical intervention in larger breed dogs (Lazar, Berry et al. 2005). This research will assess stability within the stifle joint through biomechanical computer modeling of the canine hind limb and compare loadings within the stifle joint associated with a CrCL intact stifle and a CrCL deficient stifle. The long-term goal of this research is to develop a tool that will allow for biomechanical characterization of common surgical procedures designed to stabilize CrCL deficient stifle joints. This would provide an evidence-based approach to surgical procedure selection. Findings from this study will generate hypotheses for future studies.

Specific aims of this study include the following:

1. Describe biomechanics of a normal canine stifle joint during the stance phase of walking gait using a 3D computer model.
2. Describe biomechanics of a CrCL deficient canine stifle joint during the stance phase of walking gait using a 3D computer model.

3. Investigate the influence of model input parameters such as tibial plateau angle, ligament stiffness, femoral condyle geometric shape, and femoromeniscal penetration on stifle ligament forces during the stance phase of gait.

The researchers hypothesize the following:

1. Stifle ligament forces will be altered in a CrCL deficient stifle during the walking stance phase of gait.
2. The caudal cruciate ligament (CaCL) will be required to carry additional loading in the CrCL deficient stifle.
3. Model input parameters such as tibial plateau slope, femoral condyle geometric shape and ligament stiffness will influence stifle ligament forces during the stance phase of gait.

II. BACKGROUND AND SIGNIFICANCE

2.1 Introduction

Cranial cruciate ligament (CrCL) rupture is a leading cause of lameness and immobility in dogs (Morris and Lipowitz 2001; Warzee, Dejardin et al. 2001; Pacchiana, Morris et al. 2003; Aragon and Budsberg 2005). The CrCL provides stability within the stifle joint, the equivalent to the knee joint of humans, along with three other stabilizing ligaments: the caudal cruciate ligament (CaCL), the medial collateral ligament (MCL) and the lateral collateral ligament (LCL). The stifle joint anatomy is illustrated in FIGURE 1.

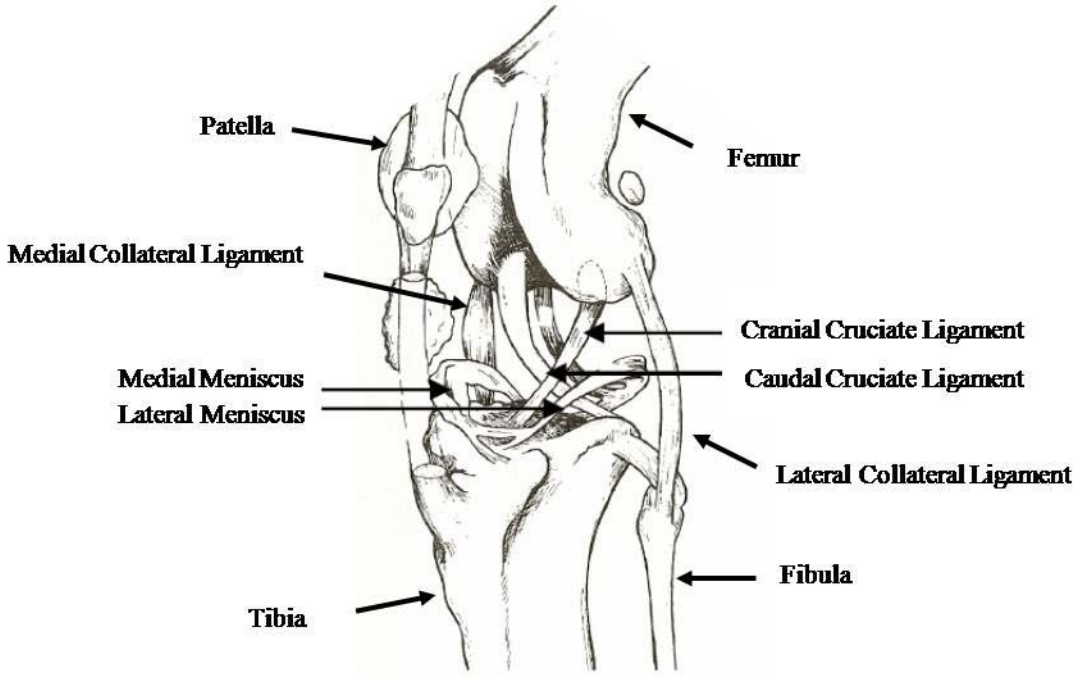

FIGURE 1 - Stifle anatomy (Adams 1986).

The CrCL in the canine is synonymous with the anterior cruciate ligament (ACL) of humans where cranial corresponds with anterior and caudal corresponds with posterior for anatomical directions. In humans rupture of the ACL is typically caused by a traumatic event, often a sports injury, but trauma often is not the cause for CrCL rupture in canines. Rupture of the CrCL has been associated with trauma, but more commonly it results from degeneration of the ligament over time until partial or complete rupture (Morris and Lipowitz 2001; Osmond, Marcellin-Little et al. 2006).

Several breeds, typically the larger breeds, are prone to CrCL degeneration as a result of anatomical characteristics coupled with stifle biomechanics (Morris and Lipowitz 2001; Lazar, Berry et al. 2005; Osmond, Marcellin-Little et al. 2006; Witsberger, Villamil et al. 2008). This inevitably leads to CrCL degeneration, stifle instability and lameness (Slocum and Devine 1984; Morris and Lipowitz 2001; Osmond, Marcellin-Little et al. 2006). Due to its high prevalence, CrCL rupture and associated lameness have sparked a multitude of orthopedic procedures designed to stabilize the stifle joint following CrCL rupture. The growing concern with these procedures, however, is that no one procedure has shown to consistently return these dogs to normal function in all cases. Also, the long-term effects of these radical procedures have not been conclusively studied. It is suspected that alteration of the stifle joint in turn alters the loading characteristics within the stifle and thus may predispose the stifle to injury within the remaining healthy components.

With new orthopedic corrective procedures still being developed, it is imperative that these procedures be biomechanically evaluated to assess their role in generating unwanted stresses within the stifle that could lead to eventual failure of surrounding

tissues. Development of a computer model of the canine hind limb representative of the normal walking gait during weight bearing would aid in understanding the biomechanics associated with the onset of CrCL rupture.

2.2 Prevalence of Cranial Cruciate Ligament Rupture and Lameness

Cranial cruciate ligament rupture is the most common orthopedic condition diagnosed in the canine stifle joint (Morris and Lipowitz 2001; Warzee, Dejardin et al. 2001; Pacchiana, Morris et al. 2003; Aragon and Budsberg 2005). Rupture of the CrCL has been associated with trauma, poor physical condition and obesity, chronic ligament degeneration, intra-articular immune complex deposition and intracondylar notch width (Vasseur, Pool et al. 1985; Morris and Lipowitz 2001; Osmond, Marcellin-Little et al. 2006). Morris (2001) and Osmond et al (2006) suggested that the intercondylar notch width was smaller in dogs with CrCL injuries causing possible impingement on the CrCL leading to degeneration. Such a correlation has also been established in humans and ACL injury predisposition (Morris and Lipowitz 2001). Vasseur et al (1985) concluded that dogs at 5 years of age weighing more than 15 kg were more likely to show degeneration within the CrCL than dogs weighing less than 15 kg. Similarly, breed variation has been concluded to correlate with CrCL deficiency. Breeds such as the Newfoundland, Rottweiler and Labrador Retriever were more likely to suffer CrCL deficiency while the Dachshund and Greyhound were less likely to suffer CrCL deficiency (Witsberger, Villamil et al. 2008).

Its estimated cost in 2003 at over 1 billion dollars annually in the United States (Wilke, Robinson et al. 2005) indicates a need for an improved understanding of the

surgical procedures employed (Aragon and Budsberg 2005; Thieman, Tomlinson et al. 2006). It has been reported that dogs suffering CrCL rupture have varying results of recovery based on the size of the dog. Dogs weighing less than 15 kg had improvement without surgery in 85% of cases while dogs weighing more than 15 kg had improvement without surgery in only 30% of cases (Lazar, Berry et al. 2005). Following CrCL disease meniscal injury occurred in 70% of cases, and nearly all meniscal tears diagnosed involved the caudal horn of the medial meniscus. Meniscal injury has still been found to occur following treatment of CrCL disease and increases pain, lameness and the progression of osteoarthritis (Thieman, Tomlinson et al. 2006).

2.3 Role of the Cruciate Ligaments

The cranial cruciate ligament (CrCL) serves to prevent hyperextension and stabilize the stifle joint by limiting internal rotation and cranial displacement of the tibia relative to the femur (Morris and Lipowitz 2001). Instability within the stifle has experimentally been demonstrated to be the primary cause of post-traumatic arthritis (Slocum and Devine 1984). Arnoczky and Marshall investigated the anatomy and function of the canine stifle (Arnoczky and Marshall 1977). Fifty cadaver stifle joints from dogs ranging in size from 15 to 20 kg were included in the study. The structure of the CrCL was evaluated through a range of extension and flexion (40° to 135° flexion) as illustrated in FIGURE 2.

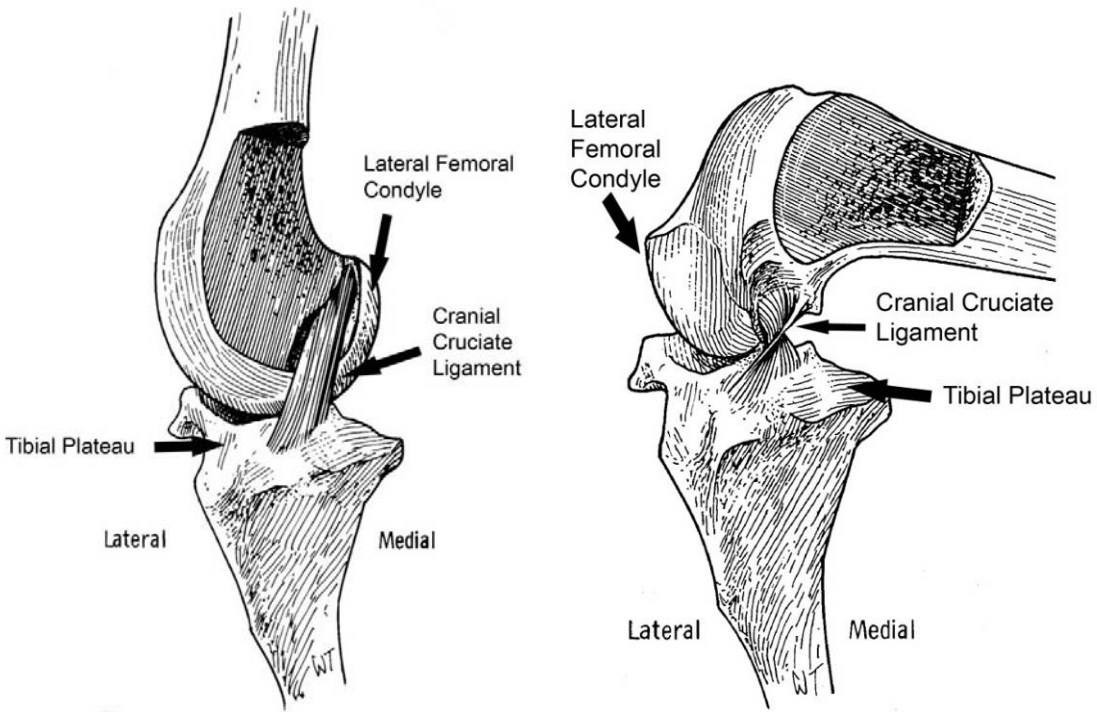

FIGURE 2 - View of the CrCL within the stifle joint in extension (left) and flexion (right) (Arnoczky and Marshall 1977).

Removal of the medial femoral condyle in FIGURE 2 clearly shows the insertion points of the CrCL on the femur and tibia. The CrCL attaches to the caudal portion of the lateral femoral condyle on the medial side. It then extends cranially, medially and distally and attaches to the cranial intercondyloid area of the tibia but does not attach to the menisci. Throughout extension and flexion, the length and tension within the CrCL changed for different portions of the ligament. With increasing flexion the CrCL twists such that the craniomedial band is taut (Arnoczky and Marshall 1977).

The caudal cruciate liagament (CaCL) is the second of the two cruciate ligaments and is illustrated in FIGURE 3.

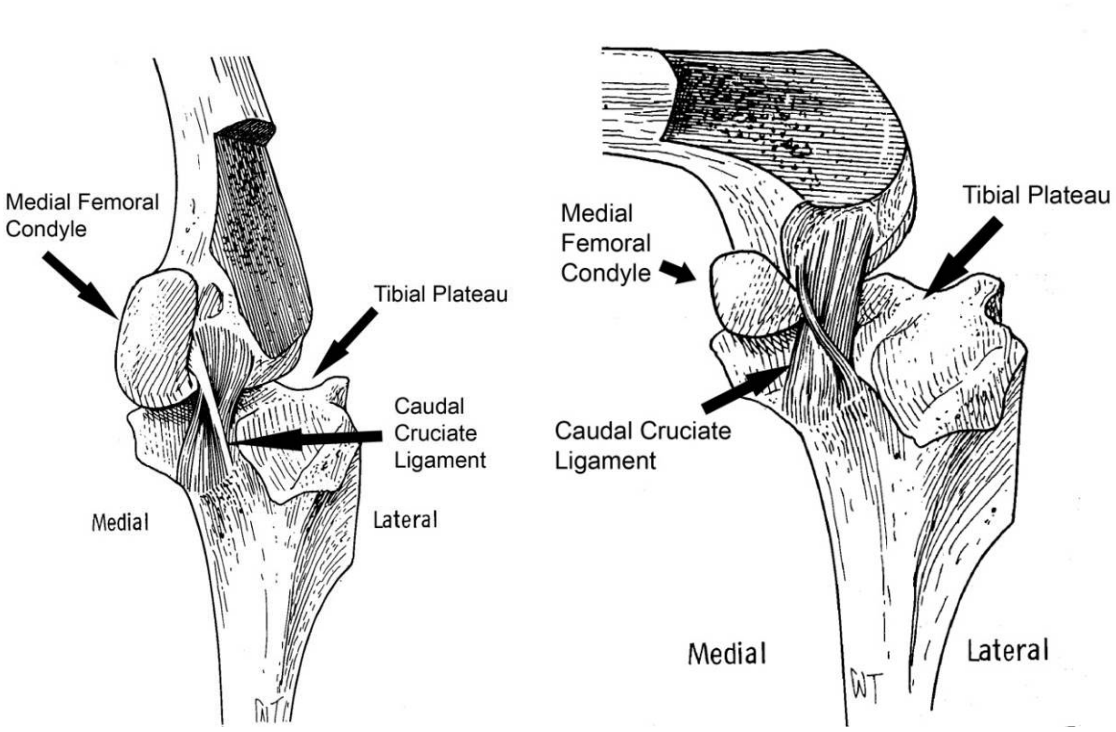

FIGURE 3 - View of the CaCL within the stifle joint in extension (left) and flexion (right) (Arnoczky and Marshall 1977).

As with the CrCL, the CaCL length and tension within the fibrous tissue vary throughout flexion and extension. The CaCL attaches to the lateral aspect of the medial femoral condyle. It then extends caudodistally to the medial aspect to the popliteal notch of the tibia. The CaCL does not attach to the menisci. Arnoczky notes that in general, the CaCL is broader than the CrCL and the CaCL remains medial to and crosses the CrCL (Arnoczky and Marshall 1977).

Following anatomical investigation Arnoczky and Marshall attempted to describe the function of the CrCL and CaCL and their roles in stabilizing the stifle joint by transecting a portion or all of each ligament (Arnoczky and Marshall 1977). Also, by measuring the displacements of the ligament insertion points throughout the range of

flexion and extension, the relative amount of tension within the ligaments was obtained. It was observed that the CrCL was generally taut in extension and loose in flexion while the CaCL was generally taut in flexion and loose in extension. Each ligament was comprised of component parts that behaved differently in flexion and extension. The CrCL contained a caudolateral band and a craniomedial band while the CaCL contained a cranial band and a caudal band (Arnoczky and Marshall 1977). Others have claimed that the CrCL is composed of three bands; the craniomedial band, the intermediate band and the caudolateral band (Slocum and Devine 1983).

Stability of the stifle was assessed by transection of the ligament bands in twenty stifle joints obtained from cadavers (Arnoczky and Marshall 1977). No cranial drawer motion was observed while the CrCL was intact. Entire transection of the CrCL resulted in an average cranial drawer motion of 2 mm in extension and 9.5 mm at 90° flexion. Internal rotation increased by 9° in extension and 26° at 90° flexion. With the CaCL intact no caudal drawer motion was observed in extension or at 90° flexion. Entire transection of the CaCL resulted in an average caudal drawer motion of 2 mm in extension and 8 mm at 90° flexion. Hyperextension increased by 12° if the CrCL was transected, was unaffected by transection of the CaCL and increased by 18° if both the CrCL and CaCL were transected. Hyperextension leads to the onset of damage to the CrCL. In flexion it was concluded that both cruciate ligaments contribute to limiting flexion, but the independent role of each cruciate ligament was not clearly established (Arnoczky and Marshall 1977).

2.4 Role of the Collateral Ligaments

A similar study to that of Arnoczky and Marshall (Arnoczky and Marshall 1977) for the cruciate ligaments was performed by Vasseur and Arnozcky (Vasseur and Arnoczky 1981) for the collateral ligaments of the stifle joint. Twenty-five cadaver stifles from medium to large breed dogs were examined. Eight of those 25 stifle joints were studied for anatomical characteristics of the collateral ligaments. The insertion regions for both the medial collateral ligament (MCL) and lateral collateral ligament (LCL) are depicted in FIGURE 4.

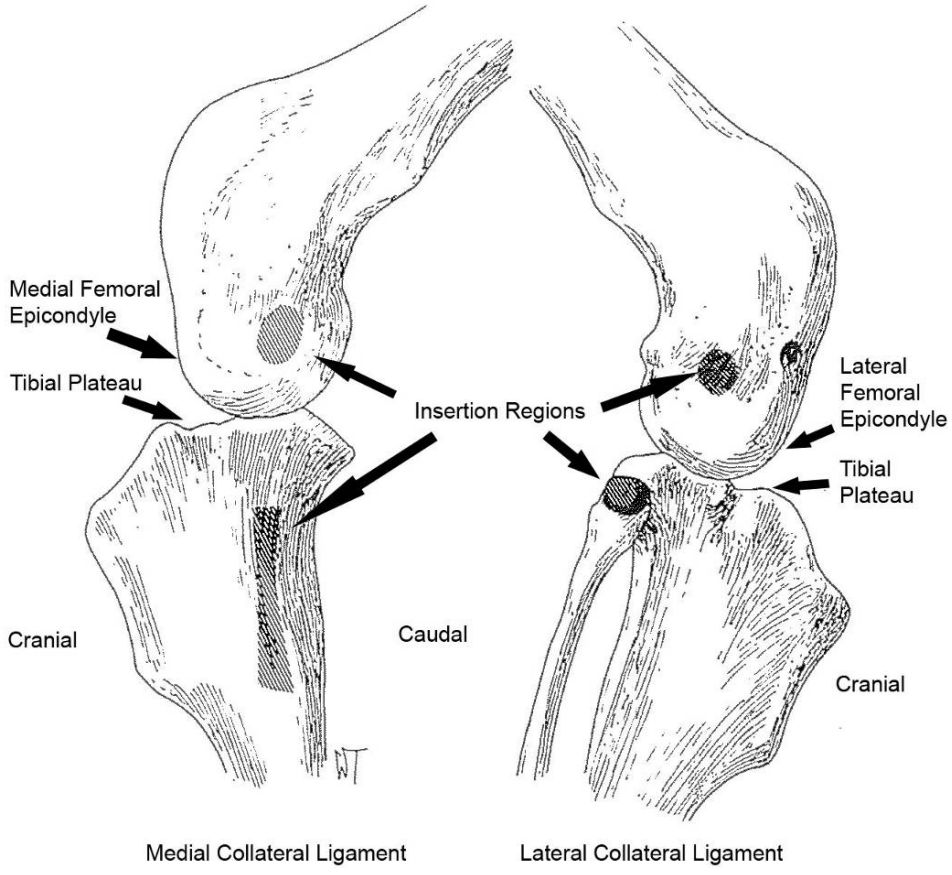

FIGURE 4 - Medial collateral ligament and lateral collateral ligament insertion regions as depicted by the shaded regions (Vasseur and Arnoczky 1981).

The MCL arises from the medial femoral epicondyle, extends distally across the medial tibial condyle, and inserts over a rectangular region of the proximal medial tibia (Vasseur and Arnoczky 1981). The MCL forms a strong attachment with the joint capsule and medial meniscus while the ligament fibers remain oriented longitudinally and of uniform width (Vasseur and Arnoczky 1981). The fibrous tissue of the MCL in both extension and flexion are displayed in FIGURE 5.

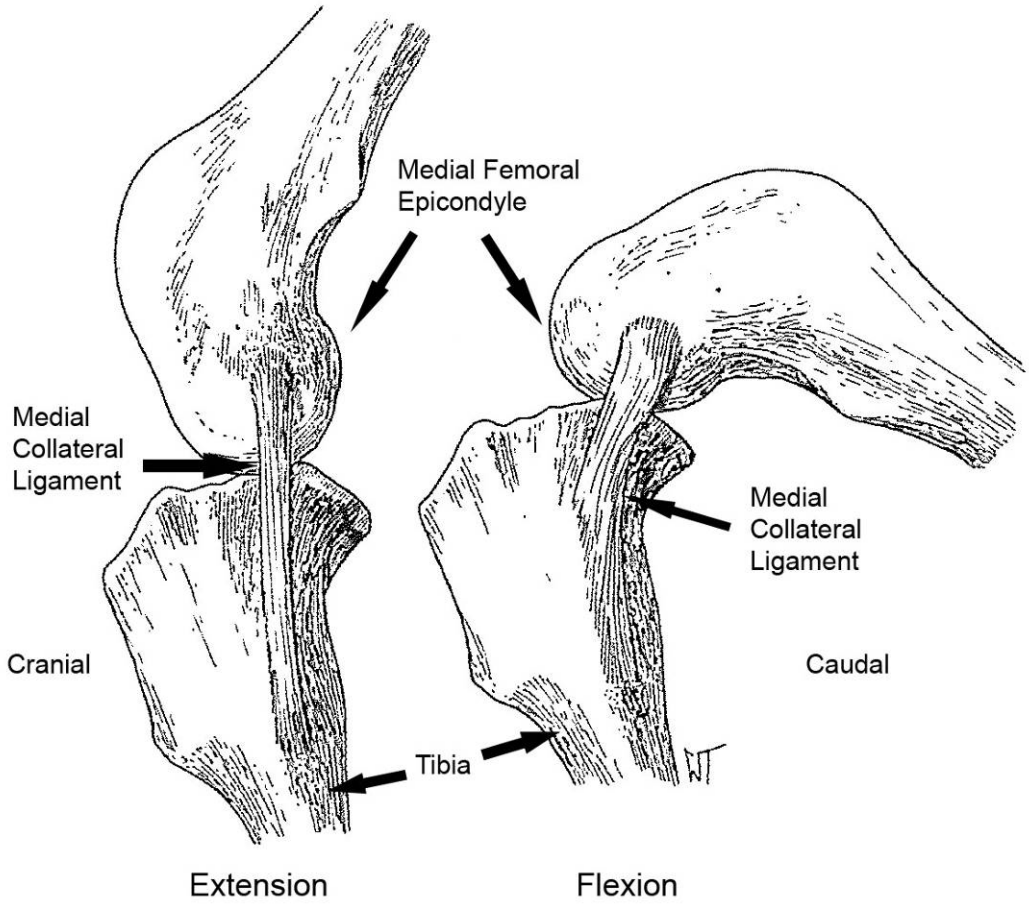

FIGURE 5 - Medial collateral ligament in extension and flexion (Vasseur and Arnoczky 1981).

The LCL originates on the lateral femoral epicondyle and extends caudodistally to insert on the fibular head (Vasseur and Arnoczky 1981). As with the MCL, the fibers of the LCL are longitudinally oriented and maintain a constant width. The fibers of the LCL, however, are not attached to the lateral meniscus and are loosely connected to the joint capsule (Vasseur and Arnoczky 1981). The fibrous tissue of the LCL in both extension and flexion are displayed in FIGURE 6.

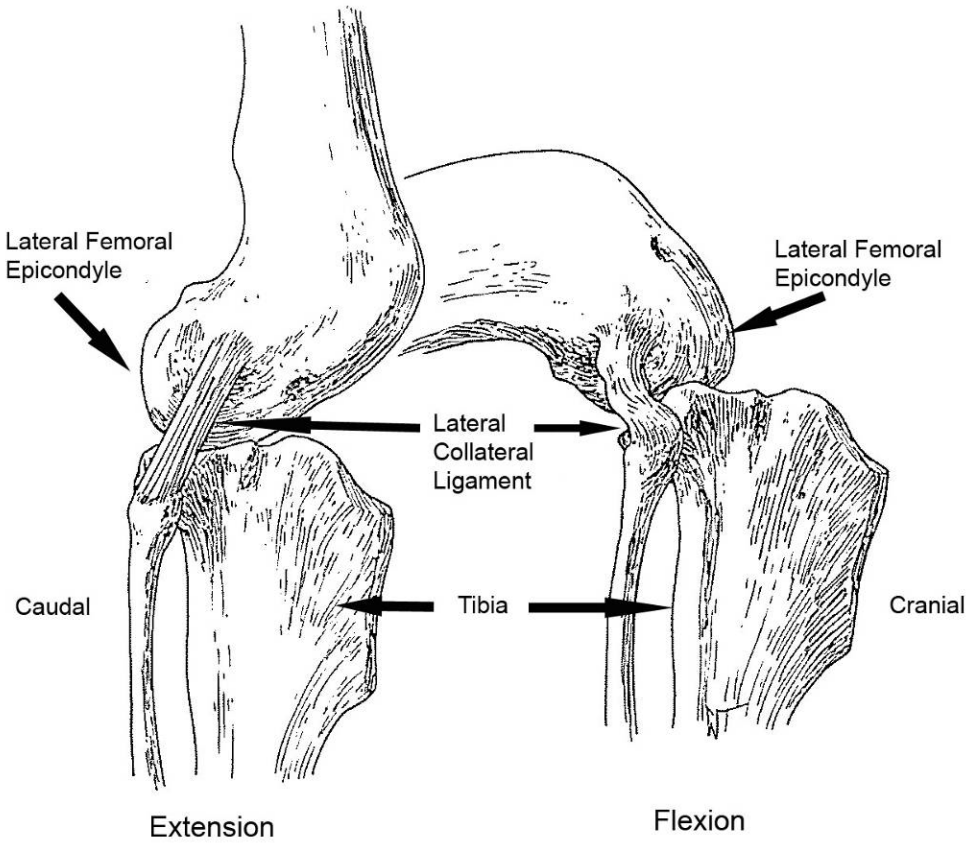

FIGURE 6 - Lateral collateral ligament in extension and flexion (Vasseur and Arnoczky 1981).

The cruciate and collateral ligaments help prevent excessive joint motion that may cause damage to joint structures (Vasseur and Arnoczky 1981). In extension the collateral

ligaments primarily restrain excessive varus and valgus angulation of the tibia while the cruciate ligaments serve as a secondary restraint. Both collateral ligaments are taut in extension. In flexion the collateral ligaments become less taut and allow more varus and valgus angulation. The LCL folds upon itself while the MCL remains partially taut with the caudal portion becoming less taut in flexion. External rotation is limited only by the collateral ligaments (Vasseur and Arnoczky 1981).

Using lead markers to define the ligament insertion points (both cranial and caudal portions), radiographs of the stifle through the range of motion were taken (Vasseur and Arnoczky 1981). The distance between the lead markers was measured from these radiographs to approximate the amount of tension within the collateral ligaments throughout the range of motion. Vasseur and Arnoczky's results indicate that the cranial and caudal portions of the LCL shortened during flexion while the caudal portion of the MCL shortened during flexion and the cranial portion remained the same length (Vasseur and Arnoczky 1981). This reiterates the anatomical investigation as depicted in FIGURE 5 and FIGURE 6 in the increased laxity of the collateral ligaments in flexion.

The role of the collateral ligaments in joint stability was examined in 10 of the cadaver stifles (Vasseur and Arnoczky 1981). Tibial rotation, varus and valgus angulation, and joint stability with combined cruciate ligament transection were assessed following transection of the collateral ligaments. Transection of either the LCL or MCL alone resulted in increased internal rotation when the joint was extended but had little effect when the joint was flexed. External rotation was affected by transection of either collateral ligament in both flexion and extension. A moderate increase in external rotation

occurred in extension with transection of the LCL while a slight increase occurred in flexion. Transection of the MCL resulted in a slight increase in external rotation in extension with a moderate increase in flexion. Varus angulation slightly increased with transection of the LCL in flexion while valgus angulation increased slightly with transection of the MCL in flexion and extension (Vasseur and Arnoczky 1981).

Joint stability following transection of the collateral ligaments coupled with transection of the cruciate ligaments was also examined (Vasseur and Arnoczky 1981). Transection of the LCL coupled with CrCL transection resulted in a moderate increase in varus angulation but no change in valgus angulation in both flexion and extension. Internal rotation slightly increased in extension but was more prominent in flexion. No increase in external rotation occurred (Vasseur and Arnoczky 1981).

Similar effects occurred with transection of the CaCL and also with transection of the MCL (Vasseur and Arnoczky 1981). Results for transection of either cruciate ligament were the same. Valgus angulation moderately increased in flexion and extension while varus angulation was not affected. Internal rotation increased slightly in extension but was more prominent in flexion. Finally, no effect on external rotation occurred (Vasseur and Arnoczky 1981).

2.5 Biomechanics of the Stifle Joint

2.5.1 Cranial Drawer Sign

Rupture of the CrCL can be observed noninvasively by the cranial drawer sign (Slocum and Devine 1983). The cranial drawer sign is determined by placing the thumb and index finger of one hand on the patella and lateral fabella. The thumb and index finger of the other hand are placed on the head of the fibula and tibial tubercle. The tibia

is then moved cranially. Rupture of the CrCL is present with excessive cranial tibial movement (Slocum and Devine 1983). This procedure is illustrated in FIGURE 7.

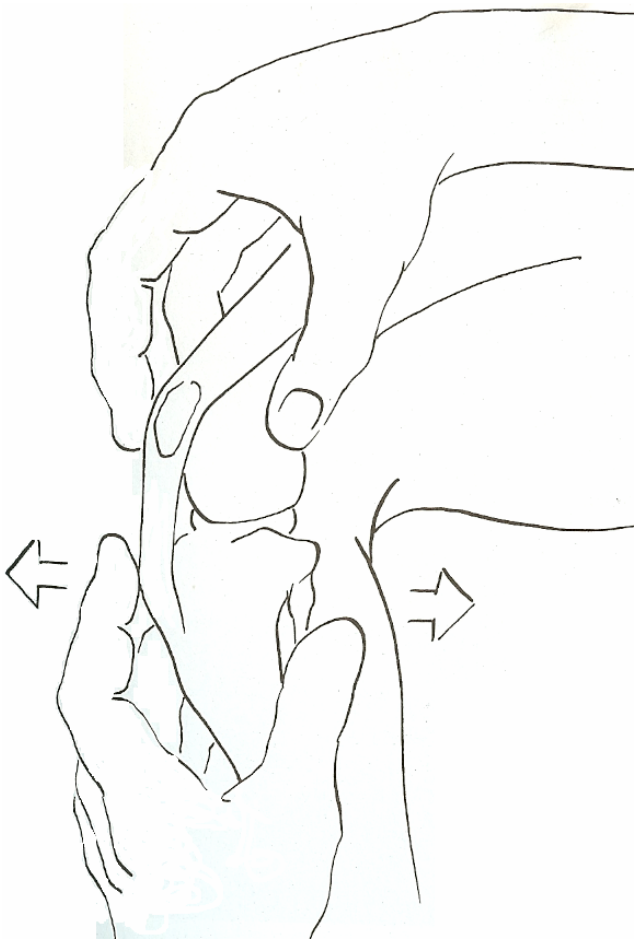

FIGURE 7 - Cranial drawer sign test (Slatter 2003).

2.5.2 Tibial Compression Test

The cranial drawer sign may detect deficiency of the CrCL, but it does not simulate weight-bearing which is typically when a dog experiences lameness due to a deficient CrCL. The displacement of the tibia is instead induced by the examiner by applying a craniocaudal force to the proximal tibia. The tibial compression test can also

detect CrCL rupture by simulating weight-bearing (Slocum and Devine 1983). The tibial compression mechanism was introduced in 1978 to detect cranial drawer motion (Morris and Lipowitz 2001). This test is performed similarly to the determination of the cranial drawer sign, but the motion of the tibia is induced by gripping the metatarsal bones and flexing the tarsal joint to simulate weight bearing. Movement of the tibia relative to the femur during this test is indicative of CrCL rupture (Slocum and Devine 1983). FIGURE 8 shows the tibial compression test.

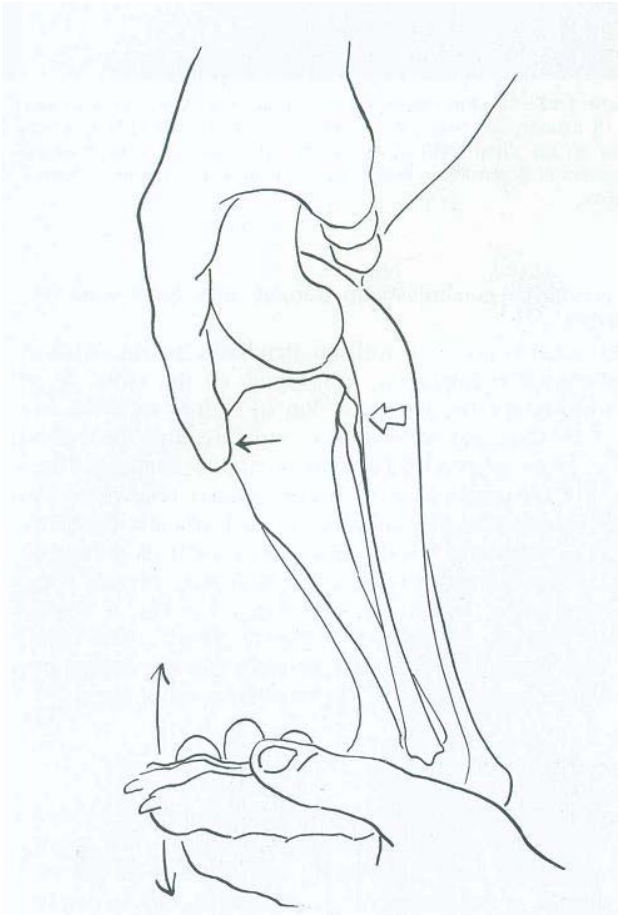

FIGURE 8 - Tibial compression test (Slatter 2003).

2.5.3 Cranial Tibial Thrust

Slocum and Devine (1983) further expanded on the tibial compression test by suggesting a steeper tibial plateau angle (TPA), the proximal surface of the tibia on which the menisci and femoral condyles rest, could induce CrCL rupture (Slocum and Devine 1983; Slocum and Devine 1984; Slocum and Slocum 1993; Morris and Lipowitz 2001). Slocum recognized that a force within the stifle acts to thrust the tibia cranially during weight bearing (Slocum and Devine 1983). They postulated this cranial tibial thrust (CTT) is dependent on tibial compression and the angle of the tibial plateau. Cranial drawer motion during the tibial compression test results from a deficient CrCL while CTT may lead to CrCL degeneration (Slocum and Devine 1983).

Slocum performed the tibial compression test on 1673 dogs during regular physical examinations (Slocum and Devine 1983). These dogs had no signs of stifle problems. Additionally, Slocum performed the tibial compression test on 65 stifles from dogs with confirmed CrCL rupture before and after anesthesia. The results of the tibial compression tests on these 1673 healthy dogs (3346 stifles) and the 65 CrCL deficient stifles from dogs with confirmed CrCL rupture were negative and positive, respectively. This outcome reiterates the validity of the tibial compression test in determining CrCL deficiency. The tibial compression tests before and after anesthesia indicated a static component contributing to cranial drawer motion while the dog is subdued as well as the dynamic factors such as the muscles while the dog is alert (Slocum and Devine 1983).

In addition to the tibial compression tests, Slocum placed cadaveric hind limbs in a normal standing position with the stifle at 140° and then dissected them to determine the necessary structures for joint stability (Slocum and Devine 1983). The paw was

pushed towards the femur while muscle groups and ligaments were excised until this weight-bearing angle could no longer be maintained. The tarsal tendon and biceps femoris muscle were deemed necessary to maintain the stance position (Slocum and Devine 1983).

An average TPA of 22.6° with a standard deviation of 4.5° was determined from radiographs of 16 stifles (Slocum and Devine 1983). Since there is an inclination of the tibial plateau, the weight-bearing compressive force transferred from the femur to the tibia will have a component along the axis of the tibia and a component directed cranially perpendicular to the axis of the tibia as in FIGURE 9. The functional axis of the tibia is F, the tibial plateau is P and the tibial plateau angle is Θ, which is relative to the perpendicular of the functional axis. If the axis of the tibia and the plateau slope are not perpendicular, the weight-bearing load W is broken into a compressive force, C, and a cranial thrust force, T

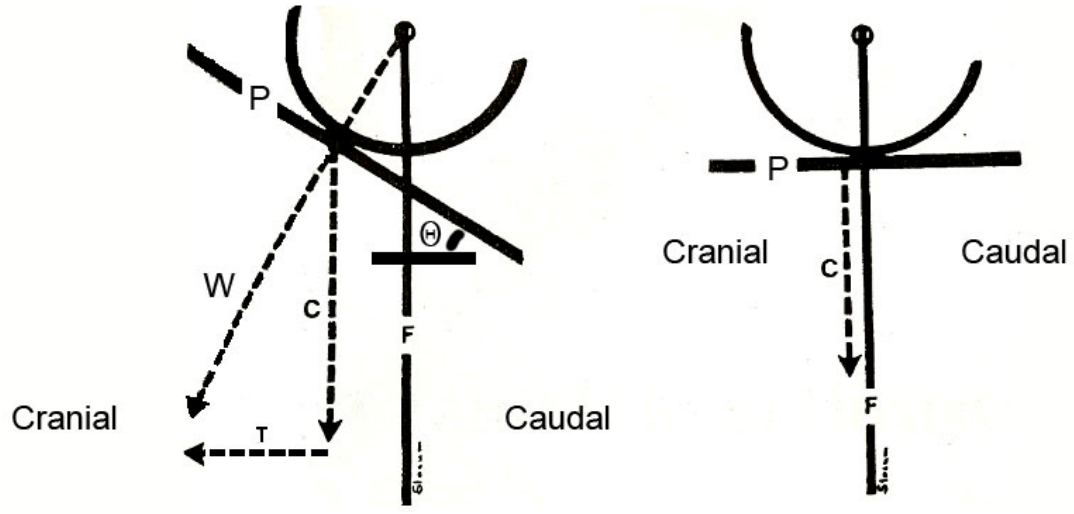

FIGURE 9 - Cranial tibial thrust in relation to tibial plateau angle (Slocum and Devine 1983).

Cranial tibial thrust is countered by the CrCL, but a deficient CrCL attempting to counteract CTT may become further predisposed to degeneration and eventual rupture (Slocum and Devine 1983). A ruptured or partially torn CrCL can no longer oppose the cranial thrust force and cranial drawer motion is observed. Cranial drawer motion of the tibia may then result in impingement of the horn of the medial meniscus as it interacts with the femoral condyle (Slocum and Devine 1983).

2.6 Anatomical Characteristics Associated with the Onset of CrCL Rupture

2.6.1 Tibial Plateau Angle

The tibial plateau angle (TPA) is the angle created by the slope of the medial tibial condyle and the perpendicular to the functional axis of the tibia as depicted in FIGURE 10 (Warzee, Dejardin et al. 2001). The functional axis of the tibia connects the center of the tarsus joint and the midpoint of the line joining the intercondylar tubercles.

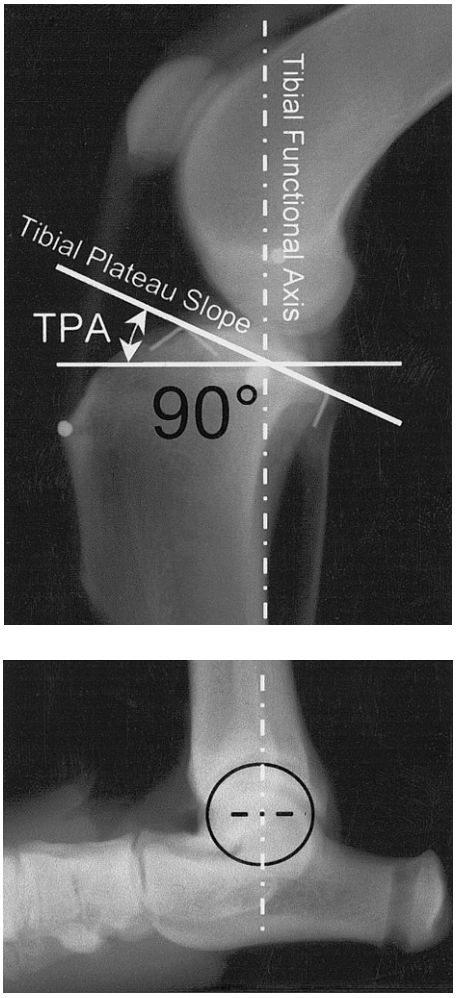

FIGURE 10 - Radiograph of the canine stifle and tarsus joints depicting the determination of the tibial plateau slope (Warzee, Dejardin et al. 2001).

Morris et al (2001) used lateral radiographs to compare the tibial plateau angle of larger breed dogs such as Golden Retrievers and Rottweilers experiencing CrCL rupture with those having healthy stifle joints. Fifty-six dogs (group 1) had CrCL injuries with 14 (group 1a) of those 56 having one healthy stifle. Thirty-one dogs (group 2) had no stifle injuries and served as controls. Sixty-six TPAs, 14 TPAs, and 30 TPAs were measured for groups 1, 1a and 2, respectively. The mean TPA from the radiographs for groups 1, 1a and 2 were 23.8°, 24.7° and 18.1°, respectively. CrCL injury corresponded with higher

TPAs, but the authors suggested that more dogs are needed to establish norms. A 95% upper prediction limit using the central limit theorem for a normal TPA of 21.2° was presented, but a normal TPA may differ among breeds (Morris and Lipowitz 2001).

Since tibial plateau slope is commonly regarded as a factor contributing to the onset of CrCL rupture, Baroni et al (2003) investigated the repeatability of obtaining TPA measurements from radiographs as compared to anatomic measurements. Sixteen hind limbs from cadavers weighing more than 20 kg were reviewed using two radiographic methods, and the effects of film digitization and radiographic beam placement were monitored. The subjective impression was that the conventional TPA measurement method underestimates the actual angle. The conventional method for measuring TPA was that explained by Warzee (2001) in which the TPA is the angle between the slope of the medial tibial condyle and the perpendicular to the functional axis of the tibia. The slope of the medial tibial condyle is determined by establishing a line between the small cranial margin of the tibial plateau and the insertion point of the CaCL (Baroni, Matthias et al. 2003). Baroni et al (2003) hypothesized that the conventional method underestimates the TPA because the choice of rationale for the landmarks used in establishing the tibial plateau slope has not been established (Baroni, Matthias et al. 2003).

The slope of the medial tibial condyle, however, consistently appeared steeper at the femorotibial contact point. Baroni et al (2003) proposed an alternative method for measuring the TPA. The alternative method instead defines the tibial plateau slope by tracing a line tangential to the cranial linear portion of the medial tibial condyle at the point of femorotibial contact. Both the conventional method and the alternative method

were compared to anatomical measurements. Anatomical measurements were obtained by disarticulating the limbs and digitally photographing the proximal portion of the tibia. The angle formed between the medial tibial condyle and the functional axis of the tibia was measured (Baroni, Matthias et al. 2003). All three methods are displayed in FIGURE 11.

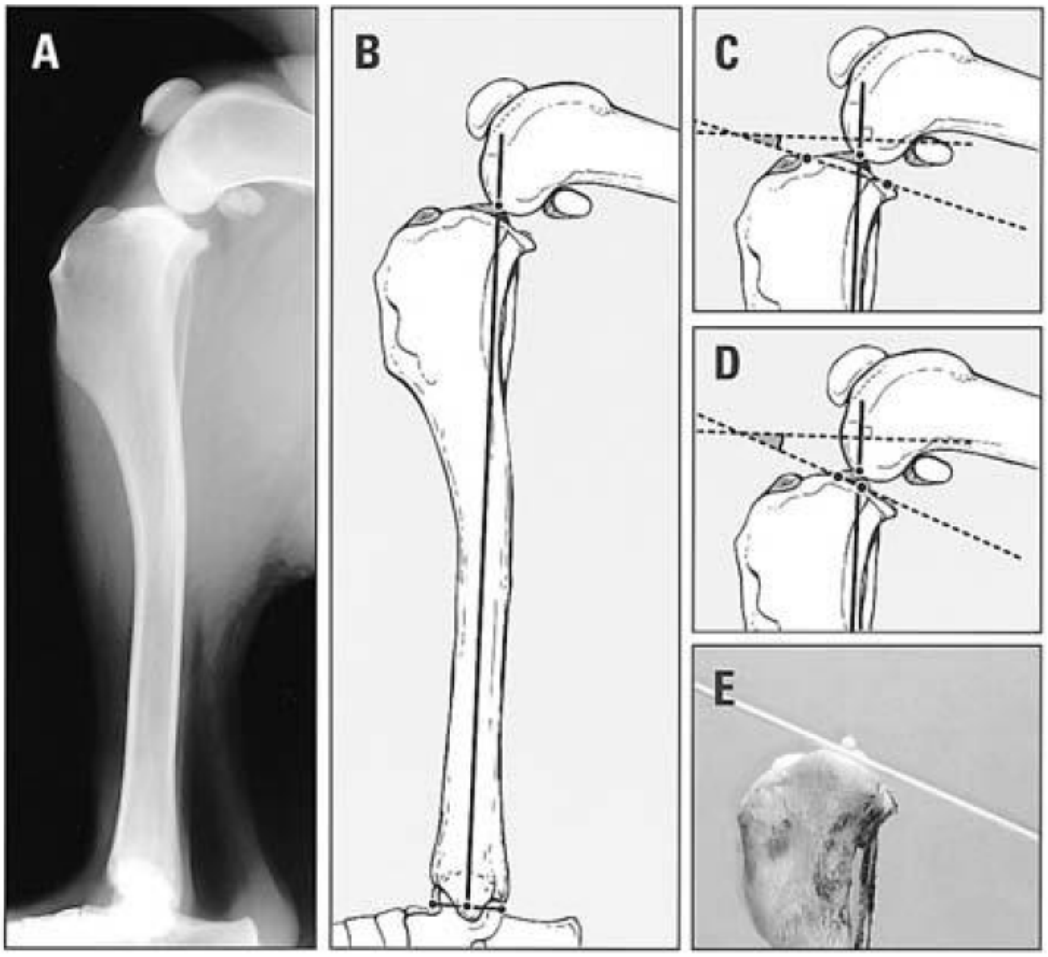

FIGURE 11 - Lateral radiograph, A, of the canine hind limb with the depiction of the functional axis of the tibia, B. The plateau slope is depicted in C using the conventional method, D using the alternative method, and E using the anatomical method (Baroni, Matthias et al. 2003).

Examiners of varying experience were included in the study (Baroni, Matthias et al. 2003). Three examiners used the conventional method and three used the alternative method. Their results showed that measurements taken using the alternative method did not differ significantly from anatomical measurements while those taken using the conventional method did. Mean difference in the two methods was 7° with the conventional method underestimating the plateau slope. Experience also influenced the measurements taken in that the four most experienced examiners detected differences between film digitization and radiographs taken with beam placement while the two least experienced examiners did not (Baroni, Matthias et al. 2003). Therefore, care should be taken in determining the TPA since many surgical procedures attempt to neutralize cranial tibial thrust by altering the plateau angle.

Reif and Probst (2003) conducted a study to compare the TPA of Labrador Retrievers deemed to be normal without signs of CrCL rupture with those having complete or partial rupture of the CrCL. Such a comparison is often difficult because the factors that predispose dogs to CrCL rupture have not been conclusively established so determination of a normal population is somewhat subjective. In order to avoid this dilemma, Reif and Probst (2003) attempted to establish a control group of normal Labrador Retrievers by examining the medical records of 166 Labrador Retrievers that underwent treatment for CrCL rupture. It was determined that only 14% of dogs had an onset of CrCL rupture at or after the age of 8 years, and no dogs older than 10 years of age were treated. Most dogs had been admitted for treatment between 3 and 5 years of age (Reif and Probst 2003).

After establishing an age range, Reif and Probst (2003) attempted to compare the TPA of dogs with and without CrCL rupture within these ranges. Group 1 consisted of 42 Labrador Retrievers with CrCL rupture and a mean age of 5.4 years. Group 2 consisted of 39 Labrador Retrievers without CrCL rupture and a mean age of 10 years. The mean (+/- SD) TPA for groups 1 and 2 were 23.5 +/- 3.1 degrees and 23.6 +/- 3.5 degrees, respectively. There was no statistical difference between the two groups. One breed was used to eliminate variation in breed characteristics. It was concluded that TPA should not be the sole factor in estimating the likelihood of CrCL disease in the Labrador Retriever (Reif and Probst 2003).

2.6.2 Tibia Deformities

Deformities of the proximal tibia may also lead to CrCL degeneration (Morris and Lipowitz 2001). Osmond et al (2006) investigated the morphologic changes present in the canine tibia with a steep TPA. CT scans were reconstructed as three-dimensional models using the software Mimics (Materialise, Ann Arbor, MI) for later use in CAD software. These models were then manipulated to introduce caudal and proximal deformities in the tibia. The deformities introduced to the models were first, the deformity that would result from premature closure of the caudal aspect of the medial tibial condyle (tibial plateau deformity) and second, the deformity that would result from premature closure of the caudal aspect of the proximal tibia physis as a whole (proximal shaft deformity). These two deformities were simulated by altering the reconstructed 3D model with wedge angles of 10° and 15° for each deformity as depicted in FIGURE 12 (Osmond, Marcellin-Little et al. 2006).

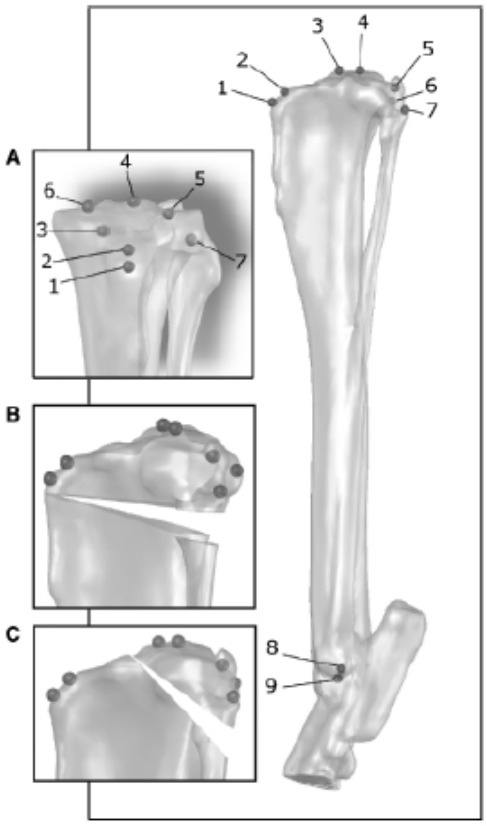

FIGURE 12 - The proximal tibia, A, was modified to represent a proximal shaft deformity, B, and a tibial plateau deformity, C (Osmond, Marcellin-Little et al. 2006).

These modeled deformities established a basis for measurements that could be compared to measurements obtained from radiographs (Osmond, Marcellin-Little et al. 2006). The model measurements were then compared to radiographs of sixty-seven dogs with CrCL rupture along with fourteen control group dogs that had no signs of CrCL rupture. It was determined that dogs with proximal shaft deformities could not be identified by TPA alone, and their findings indicated that TPA and proximal tibial shaft deformities do not statistically coincide. This study indicates possibly tibial deformities in addition to TPA contribute to CrCL injuries, but most studies focus on the TPA.

Therefore, tibial deformities, which may not coincide with TPA, may predispose dogs to CrCL rupture (Osmond, Marcellin-Little et al. 2006).

2.6.3 Bone Characteristics

Brianza et al (2007) studied the characteristics of the radius and ulna of thirty-two canines. The investigation centered on discerning geometrical, densitometric and mechanical properties of bone. Differences in animal size and species were thought to influence these characteristics. Axial compression tests were performed, and bone properties such as geometry and volume were calculated based on CT scans. Bones were loaded until failure to determine ultimate stress. The mechanical properties for bone based on sex were also provided. The properties of ultimate load, maximum stress, work to failure, bone mineral density and bone mineral content were on average higher in males, while cortical volume percentage was on average higher in females. Bone mineral content and bone mass varied linearly with body mass (Brianza, D'Amelio et al. 2007). This research utilized the forelimb rather than the hind limb, but bone characteristics could possibly be extrapolated from this study if stresses present during ligament tensile testing approach those experienced by bone failure testing in the hind limb. Since the maximum stresses reported for female canines were 455 +/- 103 MPa (mean +/- SD) (Brianza, D'Amelio et al. 2007) and the maximum stress reported by Vasseur (1985) in the CrCL at failure was less than 140 MPa, the bones could likely be approximated as non-deformable rigid bodies in a theoretical model.

2.6.4 Ligament Characteristics

The ligaments of the canine stifle serve as passive restraints to excess movement. As described previously, the canine stifle contains the cranial cruciate ligament (CrCL), caudal cruciate ligament (CaCL), medial collateral ligament (MCL) and lateral collateral ligament (LCL). Of the four stabilizing ligaments, the CrCL is most commonly associated with orthopedic lameness (Morris and Lipowitz 2001; Warzee, Dejardin et al. 2001; Pacchiana, Morris et al. 2003; Aragon and Budsberg 2005).

Vasseur et al (1985) investigated the canine stifle to establish correlations between age, weight, and condition of the CrCL. Microscopic degeneration of the CrCL was examined in dogs of varying age and breed. The biomechanical properties of the CrCL were also assessed, and the degeneration within the CrCL was compared to the remaining stabilizing ligaments (Vasseur, Pool et al. 1985).

Results from examining the CrCL microscopically indicated that the central region of the CrCL was most frequently the region with the most degeneration (Vasseur, Pool et al. 1985). The CaCL also showed signs of degeneration, but the extent of degeneration was typically less than that observed in the CrCL. Less degeneration was noted in the MCL, and rarely was degeneration present in the LCL. Vasseur et al (1985) attributed the increased microscopic degeneration in the inner portion of the CrCL to older age (5 years), increased weight (greater than 15 kg), and reduced blood supply. Vasseur noted that the inner region of the CrCL had previously been shown to fail first in CrCL rupture which correlates with these results (Vasseur, Pool et al. 1985).

CrCL mechanical properties were determined in 59 stifles that had been cleared of all tissues other than the CrCL by testing in tension to failure (Vasseur, Pool et al. 1985).

All but one CrCL failed by tearing within the mid-portion of the ligament. The other specimen failed by avulsion of the tibia boney component. The mean length of the CrCL was 18.6 +/- 3.8 mm. Statistically significant decreases with age were present in the values of modulus, maximum stress and strain energy to failure. Comparing these measures by weight indicated that maximum stress and strain energy to failure had a significantly smaller decrease in smaller dogs with aging while there was no significant difference in modulus. These results would indicate, older, larger dogs are more prone to CrCL rupture, and the rupture would likely occur in the mid-portion of the CrCL (Vasseur, Pool et al. 1985). The correlation with age is in direct contrast to the conclusion of the study by Reif (2003) that most dogs experiencing CrCL deficiency that were treated were under 5 years old.

2.6.5 Effects of the Menisci

Kowaleski includes the menisci as another source opposing cranial drawer motion (Kowaleski, Apelt et al. 2005). Pozzi et al performed an in vitro study to monitor the effects of the meniscus on stifle stability (Pozzi, Kowaleski et al. 2006). Since some corrective procedures involve performing a meniscal release to prevent meniscal injury following CrCL rupture, the role of the meniscus as a stabilizer must be addressed. At the time of CrCL rupture, the medial meniscus may be torn, but it is believed that injury to the meniscus occurs over time when the stifle becomes instable (Pozzi, Kowaleski et al. 2006). When the CrCL has ruptured and no longer stabilizes the stifle joint, it is believed the medial meniscus serves as a wedge between the tibia and femur to prevent tibial translation relative to the femur as has been concluded in human knee studies following anterior cruciate ligament transection (Pozzi, Kowaleski et al. 2006). Acting as a

secondary stabilizer exposes the medial meniscus to shearing forces that may predispose it to injury during weight bearing (Pozzi, Kowaleski et al. 2006). A meniscal release is often performed to prevent subsequent injury following CrCL corrective procedures (Thieman, Tomlinson et al. 2006). Therefore, both the stabilizing ligaments and the menisci should be considered when assessing the effects of stifle corrective procedures.

2.7 Canine Gait

2.7.1 Normal Gait

Canine gait can be monitored noninvasively using kinematic motion tracking and kinetic ground force reaction data. Current biomechanics laboratories use three elements to evaluate canine gait: human perception, quantitative measurement, and biomechanical analysis (DeCamp 1997). Human perception introduces subjectivity and is not as efficient or accurate as modern equipment. DeCamp (1997) described the current state of modern gait analysis and measured ground reaction forces normalized by body weight for the forelimb and hind limb during the stance phase of gait in all three directions. Craniocaudal ground reaction force amplitudes may be reduced for dogs experiencing moderate to severe lameness. Both the walk and trot were evaluated in DeCamp's (1997) study, but this research focuses on the walking gait. It was found that the duration of the stance phase and braking and propulsion impulses increased with increasing physical size. Due to this variation, large breed dogs should not be directly compared with small breed dogs in gait analysis (DeCamp 1997).

Ground reaction forces were obtained by leading the dog to walk at 0.3 m/s across a force plate. Using a constant walking gait velocity prevented altered ground reaction forces due to varied limb speeds associated with faster gaits (DeCamp 1997). Peak

vertical hind limb forces increased while vertical impulses decreased with an increased dog walking velocity (DeCamp 1997). Coefficients of variation in vertical ground reaction forces were shown to fall within 5.8 to 8.5%. Multiple handlers in the experiment were of less concern than trial repetitions and individual dog variation. DeCamp (1997) reported that variance in ground reaction forces attributed to handlers was between 0 and 7% while trial repetition and individual dog variation was between 29 and 85% and 14 and 69%, respectively (DeCamp 1997). Redistribution of weight-bearing forces during lameness also occurred (DeCamp 1997). Lameness in one rear limb often caused redistribution of weight-bearing forces to the other rear limb and may increase pre-injury values by as much as 130%. This lameness in the hind limb does not appear to affect the forelimbs (DeCamp 1997). Therefore, the apparent healthy hind limb should not be used as a control for a hind limb experiencing lameness (DeCamp 1997).

For CrCL deficient stifles, peak vertical forces and peak vertical impulses were reduced (DeCamp 1997). Improvements in ground reaction forces have been documented following corrective surgeries when compared to those not treated. Measured ground reaction forces returned to normal within 5 to 6 months following surgery. Improvement was seen with extracapsular and intracapsular techniques, with the intracapsular techniques better approaching normal limb function. Joint angles at a walk and trot were measured for large breed dogs. At a walk, the average coxofemoral joint angles ranged from 108° to 140°, the average stifle joint angles ranged from 120° to 145°, and the average tarsus joint angles ranged from 132° to 160° (DeCamp 1997).

DeCamp (1997) focused on kinematic gait analysis in CrCL deficient stifles. A lack of treatment shows gait lameness measures to be severe and persistent. Ground

reaction forces have been shown to return to normal following corrective surgery, but osteoarthritis can progress regardless of treatment. Kinetic analysis has shown improvement in lameness after six months following surgery but not a return to normal function, which suggests kinematic analysis may be more sensitive than force plate analysis (DeCamp 1997).

2.7.2 Gait Symmetry

Gait symmetry was assessed using both force plate data and kinematic data (Schaefer, DeCamp et al. 1998). Due to the cumbersome qualities of using force plates and the high inter-trial variance, Schaefer studied the hind limb symmetry of the canine trot using the kinematic motion tracking system. Eight large breed dogs between 22 and 40 kg that were believed to be healthy were included in the testing. Using reflective markers the motion capture data was processed to give joint angles for both hind legs of all subjects at a trot. The mean values for each limb were then compared. Intratrial differences in temporal and distance variables between the right and left hind limbs were negligible and hind limb symmetry was apparent in healthy dogs. Measured variances were attributed to the dog and trial variations (Schaefer, DeCamp et al. 1998). Variation from symmetry would thus be suggestive of lameness and possible adverse limb function.

2.7.3 Cranial Cruciate Deficient Gait

DeCamp et al (1996) performed a study that kinematically assessed the canine gait following transection of the CrCL. Six healthy, large-breed dogs with a mean weight of 26.4 kg were included in the study. Each dog was walked at a rate between 1.80 and 2.10 m/s and was fitted with reflective markers to track the kinematic motion of the hind

limb. This procedure was performed prior to CrCL transection, and 1, 3 and 6 months following transection of the right CrCL. The factors measured for each dog at each session included lameness scores, drawer movement, dog velocity, maximal foot velocity, stride length, stride frequency, and joint angles and velocities for the coxofemoral, stifle and tarsus joints (DeCamp, Riggs et al. 1996).

Lameness, drawer movement and stride frequency increased following transection while stride length decreased (DeCamp, Riggs et al. 1996). No differences were observed for the mean maximal foot velocity and mean dog velocity prior to and after CrCL transection. During the stance phase, the stifle joint was more flexed following CrCL transection, while the tarsus and coxofemoral joints were more extended following CrCL transection. This change in hind limb movement is likely an adaptive response to the unstable joint, painful stimuli or a ruptured meniscus. These changes in gait may help in the recognition of primary and compensatory kinematic patterns due to musculoskeletal abnormalities. All dogs were assessed after the last follow-up, and each had a ruptured meniscus (DeCamp, Riggs et al. 1996).

2.8 Corrective Surgical Procedures for Stifle Joint Stabilization

Several corrective surgical procedures have been proposed to restore stability to the stifle following CrCL deficiency. These procedures can be grouped into three categories: intra-articular reconstruction (within the joint capsule), extra-articular reconstruction (outside the joint capsule) and osteotomies (bone reconstruction).

2.8.1 Intra-articular Technique

Intra-articular reconstruction uses a biological or synthetic tissue to replace the defective CrCL (Slatter 2003). This graft often loses strength after being implanted so it is suggested to use a graft that is as strong as or stronger than the tissue to be replaced. Such grafts could include the patellar tendon. Synthetic materials are attractive because they prevent the need of obtaining a biological graft, but the biological reaction to foreign materials may result in chronic inflammatory response. Braided polyester tapes were concluded to be effective as a replacement for the CrCL (Slatter 2003). FIGURE 13 shows the intra-articular technique.

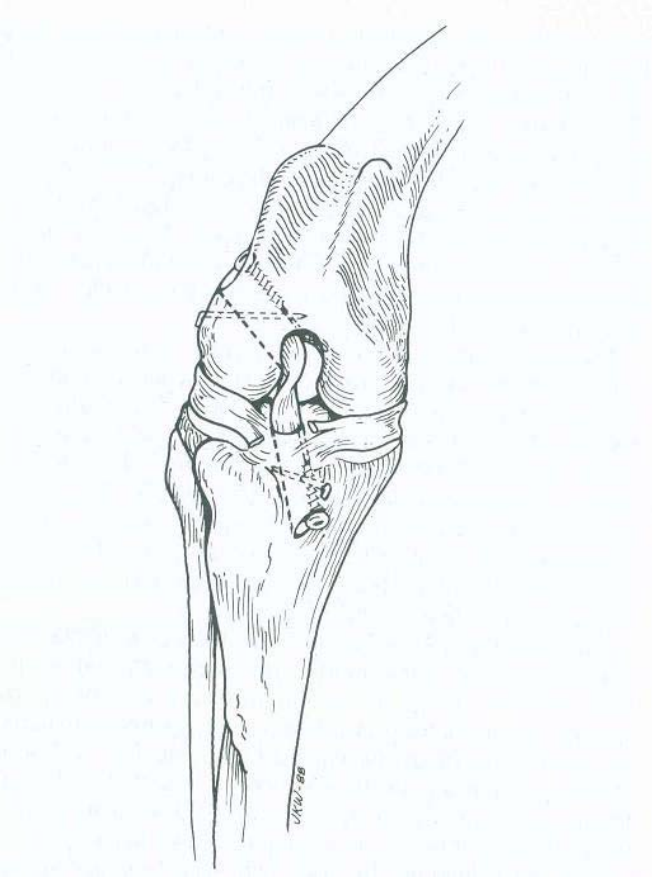

FIGURE 13 - Intra-articular technique showing the graft and fixation of the graft (Slatter 2003).

Placement of the graft involves drilling holes in the femur and tibia to correspond with the origin and insertion of the CrCL (Slatter 2003). The graft is then fastened in these holes at a tension higher than needed because the tension within the graft will immediately decrease due to stress relaxation (Slatter 2003). Intra-articular results where materials were used to replace and mimic the role of the CrCL varied so extra-articular techniques were developed (Slocum and Slocum 1993).

2.8.2 Extra-articular Technique

Extra-articular techniques sought to eliminate cranial drawer motion without affecting joint range of motion (Slocum and Slocum 1993). They are quicker to perform and generally easier since they are outside the joint capsule (Slatter 2003). The extra-articular repair technique to compensate for CrCL deficiency involves a stifle arthrotomy and removal of what remains of the CrCL. Through two holes in the tibial tuberosity, nylon leader sutures connect to the lateral fabella located on the caudal aspect of the femur (Lazar, Berry et al. 2005). This technique provides stifle stability without altering the stifle anatomy (Havig, Dyce et al. 2007). In 1993, Slocum claimed results from extra-articular procedures had been inconsistent in returning normal pre-injury function regardless of the type of dog which led to the development of osteotomy procedures (Slocum and Slocum 1993). FIGURE 14 shows an extra-articular procedure that uses three sutures.

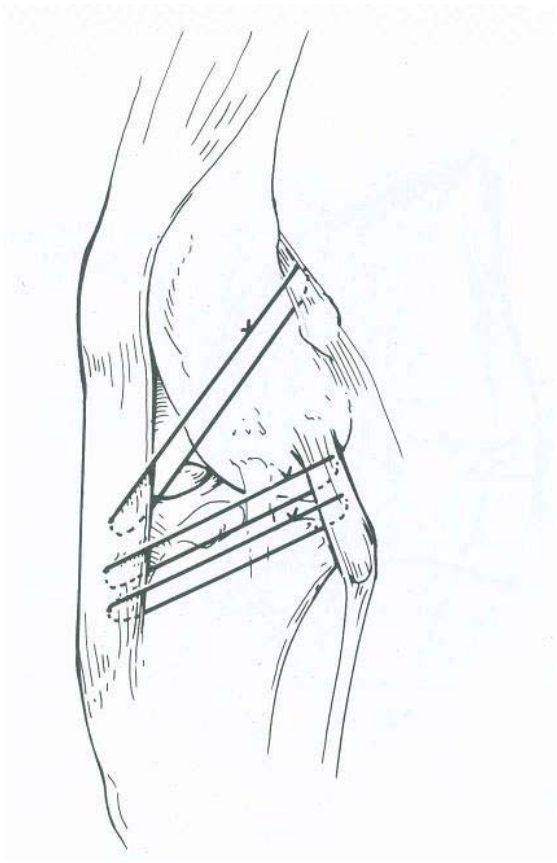

FIGURE 14 - Extra-articular technique using three sutures (Slatter 2003).

2.8.3 Cranial Tibial Wedge Osteotomy

Slocum and Devine (1984) developed several corrective procedures intended to eliminate cranial tibial drawer as a result of cranial tibial thrust. The cranial tibial wedge osteotomy (CTWO) performed in 1984 was the first attempt to eliminate cranial drawer motion of the tibia associated with CrCL deficiency. This procedure followed from the insufficient results present with many other procedures. Since cranial tibial translation is antagonistic to the role of the CrCL, inadequately stabilizing tibial thrust would induce stress on the CrCL and lead to inevitable failure of the procedure (Slocum and Devine 1984). The CTWO was developed to be performed in adjunct with CrCL repair so as to eliminate the cranial tibial thrust, allowing the CrCL repair to fully heal without added

stress (Slocum and Devine 1984). The wedge was cut into the axis of the tibia, and the proximal portion of the tibia was rotated flush so that the tibial plateau angle was altered to be perpendicular to the long axis of the tibia as depicted in FIGURE 15.

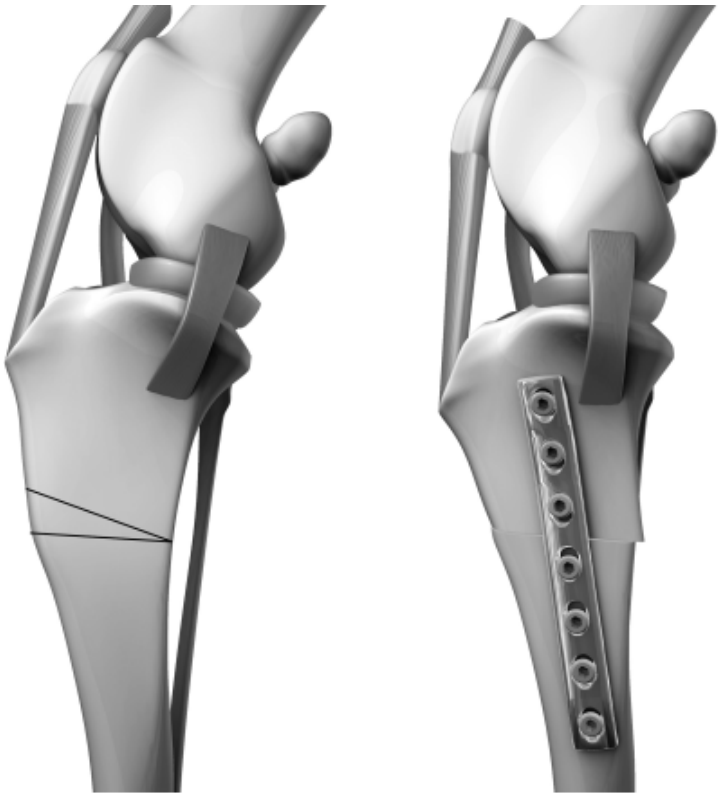

FIGURE 15 - The cranial tibial wedge osteotomy involves removing a wedge from the tibia (left) and fusing the remaining proximal and distal portions of the tibia (right) (Kim, Pozzi et al. 2008).

The procedure was performed on 19 stifles with wedge angles varying from 18 to 30 degrees (Slocum and Devine 1984). It was most commonly performed in adjunct with semitendinosus and gracilis muscle advancement medially and biceps femoris advancement laterally. No variations were found for different wedge angles, but 22.5° was considered the angle to eliminate cranial thrust. Improvement was seen in the

majority of dogs treated, but the long-term effects were still unknown at the time. Concern was particularly expressed for increased loading of the CaCL following surgery since increased stress may result in the CaCL following tibial plateau rotation (Slocum and Devine 1984).

2.8.4 Tibial Plateau Leveling Osteotomy

Following the CTWO Slocum and Devine introduced a new procedure in 1993 called the tibial plateau leveling oseotomy (TPLO) (Slocum and Slocum 1993). This method also sought to eliminate cranial tibial thrust in CrCL deficient stifle joints. Slocum (1993) observed the biomechanics, and thus need for this procedure, by comparing the traditional approach to stifle biomechanics with a more active approach (Slocum and Slocum 1993).

Prior to Slocum's (1993) introduction of the TPLO, the CrCL and CaCL were treated as two members of a four-bar linkage with the other two members being the bone connections between the proximal portions and distal portions of the ligaments. This traditional approach, however, failed to explain the existence of partial or complete ruptures except by trauma and neglected structures outside of the stifle joint. Also, it did not explain impingement and rupture of the caudal horn of the medial meniscus and failed to explain the successes and failures of previous corrective procedures (Slocum and Slocum 1993).

Slocum (1993) included forces due to muscles and weight bearing in his more active assessment. The muscle forces served as active stabilizers of the stifle joint while the ligaments served as passive stabilizers. When the muscles do not entirely eliminate cranial drawer motion, the passive stabilizers become necessary. With a ruptured CrCL

and degenerated meniscus, the passive elements can no longer prevent cranial drawer motion. Slocum, however, suggested that modification of the tibial plateau slope to be perpendicular to the long axis of the tibia will cause weight-bearing forces to act along the axis of the tibia entirely. TPLO surgery thus eliminates cranial tibial thrust, but does not replace the passive restraint of the ruptured CrCL (Slocum and Slocum 1993).

Slocum (1993) explained the procedure which averages 75 minutes and requires licensing from Slocum Enterprises. Upon signs of CrCL rupture, the lameness is corrected by making a radial cut in the proximal portion of the tibia. The distal extent of the smaller, more proximal portion of the tibia is then rotated caudally to achieve the desired plateau angle and then set with a brace plate and screws and allowed to heal as depicted in FIGURE 16 (Slocum and Slocum 1993).

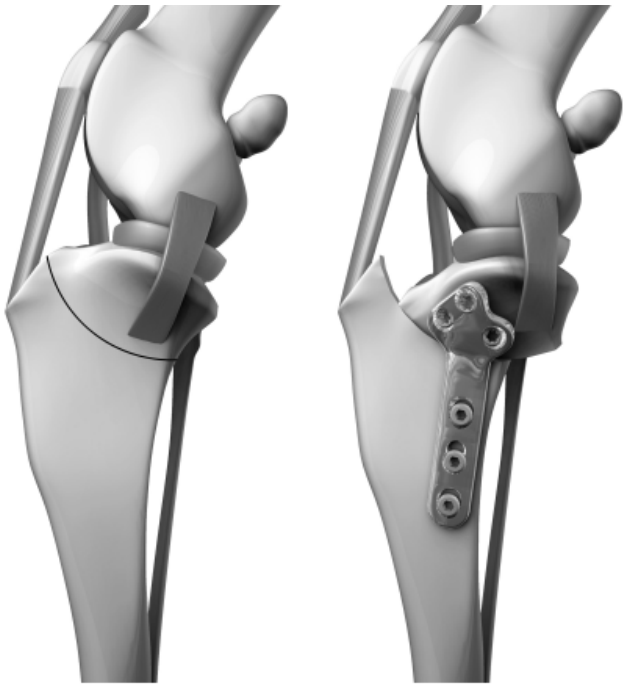

FIGURE 16 - The tibial plateau leveling osteotomy rotates the proximal portion of the tibia so that the slope is perpendicular to the functional axis of the tibia. A plate secures the rotated tibia for fusion of the two tibia pieces (Kim, Pozzi et al. 2008).

Success of the procedure observed by the fourth post-operative month showed good results in five areas: full flexibility of the stifle, full muscular development, joint calmness and freedom from inflammation, no progression in osteoarthrirtis, and return of full function (Slocum and Slocum 1993). The TPLO procedure showed improved results for dogs suffering from CrCL degeneration, but Slocum had not fully investigated the long-term effects this radical procedure has on the biomechanics of the stifle joint. Over rotation of the plateau slope was found to induce CaCL stress and was considered the source of lameness for some dogs that did not fully recover (Slocum and Slocum 1993). Warzee (2001) performed a study proposing that leveling of the tibial plateau slope converts the cranial tibial thrust to caudal tibial thrust and predisposes the CaCL to fatigue failure from added stress. Meniscal injuries can follow TPLO procedures if a meniscal release is not performed. The causes of meniscal injury due to TPLO are still unknown (Warzee, Dejardin et al. 2001).

2.8.5 Combination of TPLO and Cranial Tibial Wedge Osteotomy

For dogs with excessively steep tibial plateau angles (TPA >34º) a combination of the TPLO and the CTWO was advised for CrCL deficient stifles (Talaat, Kowaleski et al. 2006). Since rotation of the tibial plateau leaves the un-rotated, cranial, proximal portion of the tibia with less support, the patellar ligament may induce stresses that the tibial tuberosity cannot adequately withstand due to the reduced caudal boney support which could lead to fracture. For dogs with a higher TPA the increased rotation needed to obtain a postoperative TPA of approximately 5º leaves the tibial tuberosity even further compromised. It is recommended that the tibial plateau be rotated no further than the insertion point of the patellar ligament and the remainder of the rotation of the tibial

plateau be obtained by performing a CTWO. Inclusion of the CTWO relocates the insertion of the patellar ligament more distally which does not occur with the TPLO (Talaat, Kowaleski et al. 2006). The combination TPLO and CTWO is depicted in FIGURE 17. The extent of rotation of the tibial plateau should be restricted to the insertion point of the patellar ligament as shown to prevent fracture of the tibial tuberosity (Talaat, Kowaleski et al. 2006).

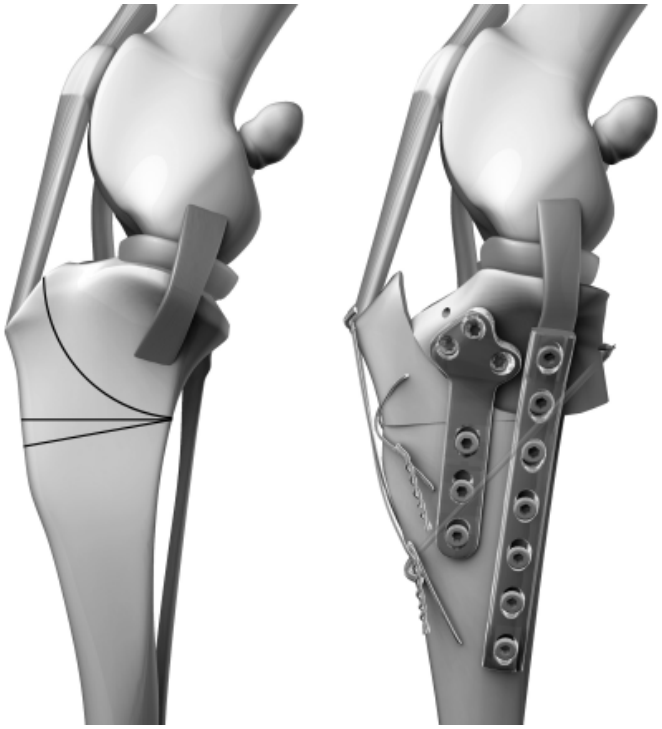

FIGURE 17 - The combination TPLO and CTWO preoperative tibia with the osteotomy cut lines displayed on the left, and the postoperative result on the right (Kim, Pozzi et al. 2008).

Talaat et al (2006) also reported the outcome of 15 dogs (18 stifle joints) undergoing the combination of TPLO and CTWO. The mean weight was 45 kg and the

mean age was 2.8 years. Mean preoperative TPA was 42 º while the mean postoperative TPA was 8º. Following the procedure at a mean of 23 weeks, a postoperative examination was conducted, and no lameness and mild lameness was recorded in 11 and 4 stifles, respectively. The complication rate, however was 77.8% (14 stifles), and a second corrective procedure was performed in 6 stifles, which was a higher rate than those reported for TPLO alone. Long-term telephone follow-up evaluations at a mean of 30.8 weeks following initial surgery indicated satisfaction from all owners participating. The mean time of 18 weeks was needed for complete healing described by radiographs, and no fractures of the tibial tuberosity were present in this study which may be due to the prevention of rotation beyond the tibial tuberosity (Talaat, Kowaleski et al. 2006).

2.8.6 Tibial Tuberosity Advancement

Another proposed osteotomy to stabilize the stifle joint is the tibial tuberosity advancement (TTA). The TTA cuts the tibial tuberosity from the tibia and moves it cranially along with the patellar ligament (Hoffmann, Miller et al. 2006). The cut portion is then set with a titanium plate at the tibial crest and a titanium cage implanted in the proximal gap that determines the amount of cranial advancement. Moving the tibial tuberosity cranially alters the direction of force applied by the quadriceps through the patellar ligament. Rather than altering the plateau slope to alter the normal force of weight bearing to eliminate cranial tibial thrust, the TTA serves to eliminate CTT by countering the normal force of weight bearing with the patellar force. This was achieved by advancing the tibial tuberosity so that the patellar ligament is perpendicular to the tibial plateau (Hoffmann, Miller et al. 2006). FIGURE 18 shows the alteration to the tibial tuberosity in TTA.

FIGURE 18 - Tibial tuberosity advancement involves cutting the cranial aspect of the tibia along the cut line, left, and fixing the cut portion more cranially to alter the insertion direction of the patellar ligament, right (Kim, Pozzi et al. 2008).

2.8.7 Triple Tibial Osteotomy

Bruce et al (2007) developed an osteotomy procedure that combined the TTA and CTWO. This combination attempted to gain the benefits of both procedures while using less radical modifications to the tibia. As with the TTA, this procedure reduces the TPA such that the plateau becomes perpendicular to the patellar ligament. As depicted in FIGURE 19 the three osteotomies are made in the proximal portion of the tibia. The wedge is removed, and rotation of the proximal fragment simultaneously closes the wedge gap and advances the tibial tuberosity (Bruce, Rose et al. 2007).

FIGURE 19 - The triple osteotomy combines the CTWO with the TTA by performing three osteotomies in the tibia (Kim, Pozzi et al. 2008).

The triple tibial osteotomy (TTO) was performed on 64 stifles following CrCL injury in 52 dogs (Bruce, Rose et al. 2007). Each procedure was performed by Warrick J. Bruce, one of the authors, following a preoperative radiograph to determine the TPA and the necessary wedge angle to be removed. The TTO also involved removal of the remnants of the CrCL if completely ruptured. Depending on the degree of meniscal damage, a partial or total meniscectomy was performed if needed. When the osteotomies were completed and the fragments were secured, radiographs were taken to determine the postoperative TPA. Postoperative tibial plateau angles (mean 16.1°) were greater than in other procedures. A follow-up assessment was conducted at 6 weeks following the

surgery, and a long-term assessment was conducted 11 months following surgery (Bruce, Rose et al. 2007).

Complication rate for this study was 36.0%, and the most common complication (23.4% of cases) was fracture of the distal end of the tibial crest (Bruce, Rose et al. 2007). At the first follow-up, mild lameness and cranial drawer motion were present in all cases, and 89.1% of cases had a positive tibial compression test. An increase in thigh circumference and stifle range of motion was significant from the preoperative assessments and the short-term follow-up assessments. All joints had evidence of radiographic bone healing. Similar results were obtained for the long-term follow-up. All owners that responded expressed satisfaction with the procedure (Bruce, Rose et al. 2007).

2.8.8 Stifle Replacement

Liska et al (2007) performed a custom total knee replacement for a 20 kg dog experiencing femoral condylar bone loss after a hunting accident. Though this article does not directly relate to stifle instability due to CrCL rupture, it does address utilizing DICOM CT scans to develop a 3D model that could then be used for stereo lithography (STL). The computed tomography (CT) scan was imported and processed in Mimics, version 7.10 (Materialise, Ann Arbor, MI). With a 3D reconstructed model of the canine's injured hind limb, a prosthetic component was designed and fitted to the computer model before surgery. This allowed for assessment of the accuracy of the prosthetic component and aided surgical rehearsal. The surgical procedure was described, and this technique did not require replacement of the CaCL and CrCL since it eliminated

cranial-caudal translation through the implant (Liska, Marcellin-Little et al. 2007). The implant is displayed in FIGURE 20.

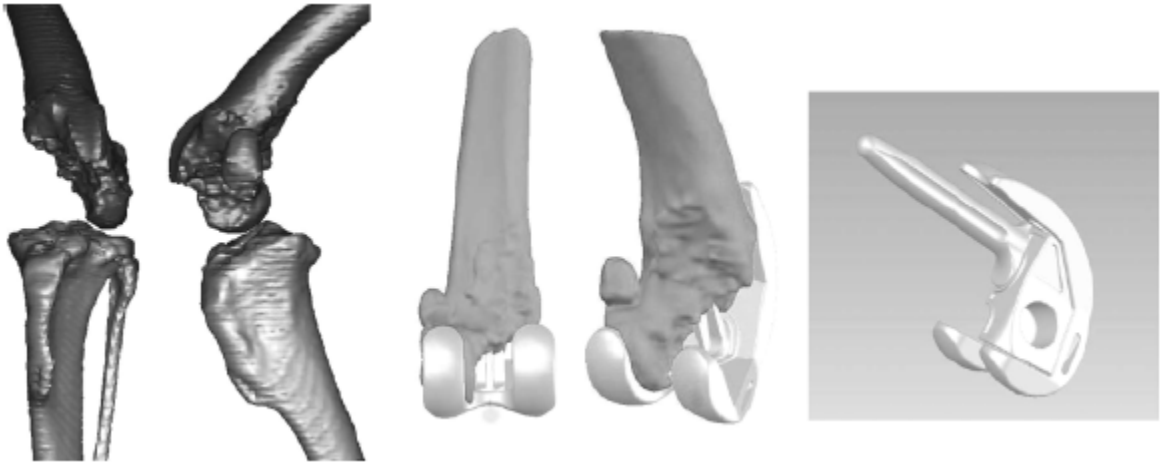

FIGURE 20 - The solid model of the damaged stifle, left, is fitted with the stifle implant, center, that was designed in a CAD software package, right (Liska, Marcellin-Little et al. 2007).

2.9 Assessments of Corrective Surgical Procedures for Stifle Joint Stabilization

The multitude of corrective surgical procedures to correct or compensate for CrCL deficiency suggests that no one procedure is universally accepted (Aragon and Budsberg 2005; Lazar, Berry et al. 2005). Aragon and Budsberg attempted to use evidence-based medicine, or "the systematic evaluation of research evidence, clinical expertise, and patient values in an effort to improve medical and surgical techniques" (Aragon and Budsberg 2005). Upon reviewing the available literature, it was concluded that there is no one procedure that has enough data to claim superiority over other

procedures, to present long-term success of normal limb function, or to prevent osteoarthritis (Aragon and Budsberg 2005). According to Lazar et al, 36% of small animal surgeons preferred lateral suture stabilization, 25% preferred tibial plateau leveling osteotomy, 22% preferred a fasical strip technique and 13% preferred fibular head transposition for treating CrCL injury in larger breed dogs (Lazar, Berry et al. 2005).

Extra-articular techniques have shown to restore joint stability while sacrificing joint kinematics (Warzee, Dejardin et al. 2001). Additionally, this added constraint increases compression of joint surfaces which may lead to articular cartilage and meniscal damage (Warzee, Dejardin et al. 2001). Intra-articular procedures have been prone to early failure and replacing the CrCL often does not exceed 30% of the strength of the normal CrCL (Warzee, Dejardin et al. 2001). Most studies done in retrospect report good results for all techniques in returning the dog to normal function, but they have not proven to prevent meniscal damage, prevent arthritis or ensure long-term stifle stability (Warzee, Dejardin et al. 2001). Restoration of femorotibial contact mechanics may not be achieved following surgical intervention to restore stifle stability (Kim, Pozzi et al. 2009).

2.9.1 Retrospective Studies

Pacchiana et al (2003) performed a retrospective study of cases using the TPLO procedure and compared the results with other procedures. This study was based on medical records for dogs undergoing TPLO at the University of Minnesota Veterinary Teaching Hospital from July 1998 to June 2001 that also underwent follow ups. Pertinent information such as age, weight, breed, additional operative procedures, etc.

were obtained from the medical records. Complications associated with the TPLO procedure were then tabulated. Complications included intra-operative complications, acute postoperative complications and chronic postoperative complications (Pacchiana, Morris et al. 2003).

Three hundred ninety-seven cases were included in the study and included both hind limbs in unilateral and bilateral cases. Labrador Retrievers, Rottweilers, Golden Retrievers, Newfoundlands and German Shepherds were the most prevalent breeds. Intra-operative complications were seen in 5% of cases; acute postoperative complications occurred in 46% of cases; and chronic postoperative complications occurred in 49% of cases. Complications varied in extent and type, but Rottweilers were noted to have more complications than expected. Complications included loosening of screws, tibial tuberosity fractures, desmitis of the distal patellar tendon, osteomyelitis, edema of the distal portion of the limb, soft tissue infection, intra-articular screw impingement, subsequent meniscal tears, fixation plate breakage, patellar luxations, and delayed healing (Pacchiana, Morris et al. 2003). It was reported that the combined complication rate of the TPLO procedure based on previous literature was 19.5% while this study showed a complication rate of 28% for both major and minor complications. Major complications included loose or broken implants, presence of infection, patella tendon desmitis fractures of the tibia, fibula or patella, and complications requiring further treatment or surgery. Removal of minor complications reduces the complication rate to 13%. Complications specific to TPLO included intra-articular screw impingement, tibial tuberosity fracture, and broken implants (Pacchiana, Morris et al. 2003).

Priddy et al (2003) conducted a study assessing TPLO based on complications and owner comments for 193 cases that spanned from 1997 through 2001 (Priddy, Tomlinson et al. 2003). Following TPLO surgery Slocum and Slocum (1993) commented that the most common complications are plate breakage, screw loosening, pin migration and wire breakage, but neither the outcome from those complications nor the prevalence of those complications was known (Priddy, Tomlinson et al. 2003). Therefore, Priddy et al attempted to report the rate of complications for unilateral TPLO procedures as well as bilateral (performed during one or separate anesthetic episodes) procedures. Dogs having previous stifle surgery, autoimmune joint disease or concurrent systemic disease were excluded from the study (Priddy, Tomlinson et al. 2003).

Medical records were retrieved and assessed, and a questionnaire regarding activity levels and lameness was sent to owners. Complications were seen in 47 (24.4%) dogs. Thirty-five, 8 and 2 dogs had 1, 2 and 3 complications, respectively, while 1 dog had 4 complications and 1 dog had 5 complications. Most commonly the complications included osteomyelitis, fracture of the fibular head, a broken drill bit, avulsion of the tibial tuberosity and incisional infection (Priddy, Tomlinson et al. 2003). Dogs undergoing bilateral TPLOs during one anesthetic episode had a significantly higher complication rate than dogs undergoing a single TPLO at a time. It was determined that the choice of saw blade size used during the osteotomy could not be statistically assessed in relation to complication rate due to the lack of 18 mm and 30 mm saw blades used compared to 24 mm blades. Owner satisfaction from the survey was high as 93% indicated satisfaction with the procedure. Therefore, owner assessment may not entirely

indicate a low complication rate or guarantee the integrity of the procedure (Priddy, Tomlinson et al. 2003).

A common issue with CrCL rupture and corrective procedures is the progression of osteoarthritis (OA) which often occurs following the loss of CrCL function. The progression of OA can occur following CrCL rupture in both treated and untreated stifles (Lazar, Berry et al. 2005). Rayward et al (2004) investigated 40 dogs treated for CrCL degeneration with the TPLO procedure. Radiographic assessments were conducted by a single, experienced radiology specialist. Radiographs were taken prior to surgery, 6 weeks following surgery and 6 months following surgery, and scored on a scale of 0 to 4 based on the extent of osteophytosis with 0 representing no osteophytosis and 4 representing severe osteophytosis. The most common breeds were Golden Retriever and Labrador Retriever, with complete CrCL rupture present in 33 dogs and partial rupture in 7 dogs (Rayward, Thomson et al. 2004).

Osteoarthritis results in changes of the articular cartilage, synovium, subchondral and trabecular bone (Rayward, Thomson et al. 2004). Radiography has been the standard for many years in detecting osteoarthritis. When using radiography osteophyte assessment is typically used because osteophytes occur early in the disease process. In as little as three days to two weeks, osteophytes become visible radiographically. This method has shown good agreement for both intra-rater and inter-rater assessments. This study found that from the initial radiographic assessment to the 6-month radiographic assessment 40% of the dogs who had undergone TPLO had an increase in osteoarthritis while 57.5% showed no change and 2.5% had a decreased osteoarthritis score. It was noted that no significant correlation between body weight and osteoarthritis progression

was seen, though 20 kg was used as a minimum weight for the study. Also, the meniscal characteristics were not found to correlate with osteoarthritis progression in this study. These results were therefore comparable or better than those reported for other surgical techniques (Rayward, Thomson et al. 2004).

Conzemius (2005) reports that 1 of 3 surgical techniques are typically performed in large breed dogs suffering CrCL rupture. Those techniques are the lateral suture stabilization (LSS), intracapsular over-the-top stabilization (ICS) and tibial plateau leveling osteotomy (TPLO). The variability of these procedures has led to much debate as to which provides the best outcome. Several previous studies had compared the LSS and ICS, but they lacked patient evaluation and breed variation. Additionally, these studies varied in timing of post-operative exam and did not include TPLO procedures (Conzemius, Evans et al. 2005).

Conzemius (2005) included 131 Labrador retrievers experiencing CrCL rupture from June 1998 to September 2002 that underwent one of these three procedures, the LSS, ICS or TPLO. All dogs also had either complete or partial medial meniscectomies. Force plate data for a walk was obtained prior to surgery as well as at follow-up. Forty-seven LSS procedures, 20 ICS procedures and 64 TPLO procedures were performed. The TPLO procedure was found to most closely return peak vertical ground reaction forces to normal at 6 months. The LSS, however, was found to most closely return vertical impulses to normal values at 6 months. The ICS procedure had significantly less peak vertical ground reaction forces and vertical impulses. Comparison to dogs with CrCL rupture without corrective treatment was not included due to the widely accepted trend that these dogs do not have a favorable outcome. It was concluded that TPLO and LSS

performed better than ICS, and if choosing between the LSS and TPLO, postoperative limb function should be considered (Conzemius, Evans et al. 2005).

A retrospective comparison of the TPLO and the extracapsular repair (ECR) technique was performed by Lazar et al (2005). In order for inclusion in the study, the dog had to meet the following criteria: weighed at least 22.7 kg, have had more than 12 months elapse between surgery and final examination, have had radiographs taken preoperatively and upon final examination, had no previous or additional stifle injury, and had no injury at surgery other than CrCL rupture and possible medial meniscus injury. For this study 27 stifles from 22 dogs underwent ECR performed by three surgeons while 52 stifles from 44 dogs underwent TPLO performed by one surgeon. Mediolateral radiographic projections along with either a craniocaudal or caudocranial radiographic projection were evaluated at preoperative and final examinations (at least 12 months following surgery). These radiographs were then scored on a scale of 0 to 3 (3 being most severe) for the extent of osteoarthritis based on 32 criteria by 2 of the authors. Osteoarthritis (OA) scores could range from 0 to 96 with 96 representing the worst case (Lazar, Berry et al. 2005).

Preoperative weight for those dogs that underwent ECR was significantly less than those undergoing TPLO with a mean +/- SD weight of 33.4 +/- 9.3 kg and 38.9 +/- 9.1 kg, respectively. More dogs (74%) that underwent ECR had torn menisci while 42% who underwent TPLO had torn menisci. Preoperative and final examination OA scores for ECR were 13.0 +/- 8.4 and 27.6 +/- 11.0, respectively. TPLO pre-operative and post-operative scores were 15.9 +/- 8.4 and 22.9 +/- 9.7, respectively. No significant difference was observed between the ECR and TPLO OA scores. However, using a log

logistic regression model when comparing the difference between the final examination and preoperative OA scores for each dog for both techniques, those with a difference greater than 6 were 5.78 times more likely to have undergone ECR. This indicates that a more severe change in OA is more likely to occur following ECR than TPLO. Medial meniscus status did not have a significant effect on OA score based on surgical visual inspection (Lazar, Berry et al. 2005).

Several sources of error in the study (Lazar, Berry et al. 2005) are acknowledged by the authors including the score weighting and the inability to conceal TPLO procedures from ECR procedures from the radiograph reviewers due to obvious differences apparent on the radiographs. The radiographic method for determining OA, however, allows for specific isolation of the stifle joint but does not necessarily correspond with limb function as would be evident with force plate and kinematic analysis (Lazar, Berry et al. 2005).

Robinson et al (2006) proposed that TPA following TPLO would significantly affect limb function as detected by force plate analysis in Labrador Retrievers. Case reports were obtained for 32 dogs that had postoperative walking trials at least 4 months following surgery from 1999 to 2003. TPAs were obtained via radiographs. The mean preoperative TPA was 25.3 +/- 2.6° and the mean postoperative TPA was 7.8 +/- 3.7°. There was no significant relationship between pre- and postoperative ground reaction forces, vertical impulses or TPAs. Therefore, the hypothesis was rejected (Robinson, Mason et al. 2006).

As suggested by Slocum and Slocum, a medial meniscal release is often performed accompanying the TPLO procedure (Slocum and Slocum 1993). Thieman et al

(2006) attempted to assess the outcome of TPLO procedures and the onset of meniscal tears following TPLO when a meniscal release was or was not performed. The literature was lacking this information and thus limited a surgeon's justification for meniscal release (Thieman, Tomlinson et al. 2006). Their study compared the rates of subsequent meniscal tears following TPLO in 3 groups of dogs based on method of stifle joint exploration. The 3 methods were arthrotomy with meniscal release, arthrotomy without meniscal release and arthroscopy without meniscal release. Subsequent meniscal tears were not reduced by performing meniscal release. Owner assessment was also investigated and it was concluded that meniscal release had no effect on owner assessment (Thieman, Tomlinson et al. 2006).

To assess the amount of motion loss associated with TPLO, Jandi and Schulman (2007) conducted a study examining the amount of stifle flexion and extension before and after surgery and its relation to clinical lameness. This study investigated 412 stifles in 280 dogs. The dogs were reevaluated for lameness and stifle extension and flexion at 12 and 24 months following surgery. Flexion and extension angles were measured using goniometers to within 1°. Each dog was then placed in one of three groups; group 1 showed no loss of motion or improved range of motion, while group 2 had motion loss of less than 10° and group 3 had motion loss greater than 10°. Both authors independently examined the dogs for lameness evaluation (Jandi and Schulman 2007).

The mean age and weight of the dogs included in the study by Jandi and Schulman (2007) was 6.1 years and 36.6 kg, respectively. Of the 412 stifles, 322 were in group 1, 78 were in group 2 and 12 were in group 3. It was concluded the TPLO procedure did not significantly affect improvement or loss of stifle flexion or extension,

but the correlation between the loss of stifle extension or flexion and clinical lameness scores was significant. This indicates TPLO was not the sole factor responsible for motion loss (Jandi and Schulman 2007).

The tibial tuberosity advancement has been adopted more recently than the TPLO, but several studies regarding the viability of the TTA procedure have already been conducted. Hoffmann et al (2006) assessed the TTA procedure in 65 stifles. All dogs weighed greater than 10 kg with a mean weight of 39.7 kg. Fifty-eight percent received a TTA of 9 mm, 37% received a TTA of 6 mm, and 5% received a TTA of 12 mm. Twenty-seven complications were recorded with this procedure while most were minor. The major complications included joint pain and effusion, medial meniscal injury and joint crepitus. Implant failure occurred in one dog, but this dog had received a bilateral TTA, and the owner acknowledged that the dog was not properly restrained in activity following the surgery. Owner assessment of the overall outcome of the procedure was good to excellent (Hoffmann, Miller et al. 2006).

2.9.2 In Vitro Studies

Fifteen cadaveric hind limbs were included in a study by Warzee et al (2001) to investigate experimentally the effects of tibial plateau leveling on tibial subluxation, tibial axial rotation, optimal tibial plateau rotation angle and CaCL strain. This study used hind limbs with muscular tissue removed and passive restraints, such as the ligaments, initially intact. The CrCL was then transected and tibial subluxation and rotation were assessed. The TPA was then altered by employing the TPLO procedure (Slocum and Slocum 1993) to within +/- 0.5° of 0° based on preliminary radiographs. By then transecting the CrCL, its role in stability would become apparent. Induced strain following the rotation of the

plateau slope was also measured in five test hind limbs that were fitted with a strain-gage force transducer in the CaCL (Warzee, Dejardin et al. 2001).

The test specimens were placed in an apparatus to simulate the midpoint of stance with the joint angles matching those of previously reported data (Warzee, Dejardin et al. 2001). A spring-loaded link served as the quadriceps muscle, and an axial load of 33% body weight was applied to the femur. The minimum plateau angle necessary was determined following transection of the CrCL by rotation of the tibial plateau until cranial tibal subluxation was stable and prevented under the applied load (Warzee, Dejardin et al. 2001).

Following tibial plateau leveling, caudal subluxation was experienced (6.3 mm +/- 1.8 mm). Further caudal subluxation (8.9 mm +/- 1.1 mm, total) resulted from transection of the CaCL. Strain gage output monitoring CaCL strain increased with increasing tibial plateau rotation indicating an increase in the strain within the CaCL with rotation of the tibial plateau. These results indicated that cranial tibial thrust was converted to caudal tibial thrust following tibial plateau rotation, which possibly predisposes the CaCL to injury (Warzee, Dejardin et al. 2001). Internal tibial rotation was reduced but not eliminated following tibial plateau leveling and may be a result of the collateral ligaments remaining taught through the range of motion. This study did not replicate all muscle forces and the extents of the forces generated by those muscle forces replicated were estimates (Warzee, Dejardin et al. 2001).

Reif et al (2002) performed similar testing to Warzee by using six canine cadaveric hind limbs subjected to weight bearing before and after TPLO. The hind limbs were cleared of muscle tissue while the stifle ligaments remained intact. It was

hypothesized that cranial tibial thrust would be caused by axial loading in a CrCL-deficient stifle, caudal tibial thrust would result from axial loading following TPLO and increasing axial tibial loads would result in increasing caudal tibial thrust (Reif, Hulse et al. 2002).

A circular osteotomy of the proximal portion of the tibia was performed on each specimen. The distal portion of the tibia was removed, and cranio-caudal translation of the proximal portion of the tibia was monitored by a potentiometer following application of a 22 N axial load to the distal portion of the tibia in the direction of the tibial functional axis. Cranial tibial translation was experienced in the CrCL-deficient stifles. After the TPLO the specimens were placed under a series of increasing weight-bearing loads varying linearly from 13 to 45 N. Cranial translation of the tibia was elicited by applying a 5 mm/s pull on the tibial crest in the cranial direction. The resistance of the specimen to cranially subluxate (caudal tibial thrust) increased with the increased weight-bearing input forces. Therefore, caudal tibial thrust was produced from the axial weight-bearing loads following rotation of the tibial plateau and increased with increasing axial weight-bearing loads. The three hypotheses were confirmed and it was concluded that the TPLO procedure converts cranial tibial thrust to caudal tibial thrust that increases with the amount of weight bearing. Limitations included neglecting muscle forces, removal of the distal portion of the tibia and testing at only a stifle flexion angle of 60° (Reif, Hulse et al. 2002).

An in vitro study conducted by Kowaleski et al (2005) attempted to compare TPLO outcomes using a centered and distal osteotomy position. Previous work by Kowaleski had shown that the TPLO position with respect to the tibial intercondylar

tubercles affected TPA postoperatively. With this conclusion a study examining the variation in TPA and tibial long axis shift (TLAS) using the centered and distal TPLO procedures was conducted as depicted in FIGURE 21.

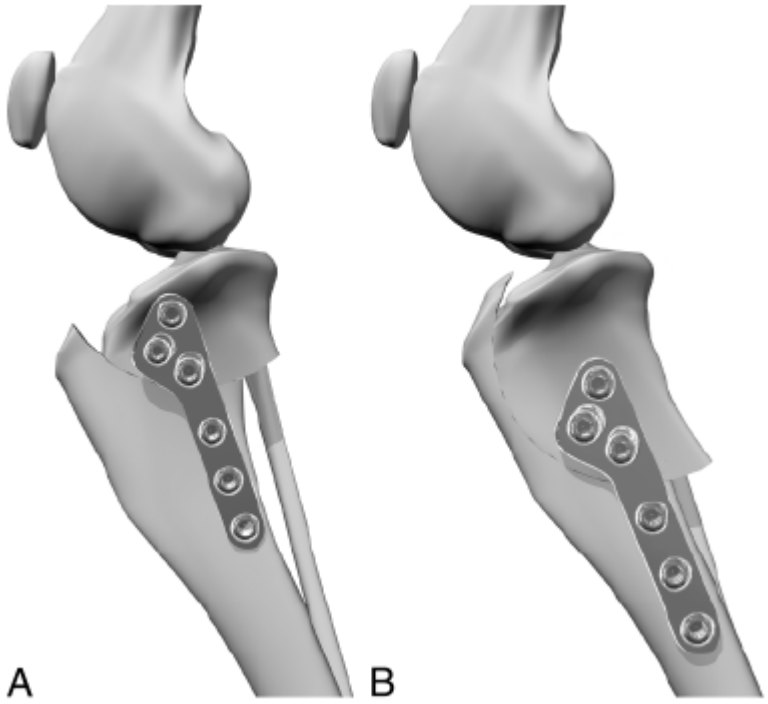

FIGURE 21 - The centered TPLO, A, and distal TPLO, B (Kowaleski, Apelt et al. 2005).

Six dog cadavers weighing between 20 and 25 kg determined to be free of joint disease in the stifles were used in the study. One hind limb received the centered TPLO and the other received the distal TPLO. A 30% body weight load was applied to each limb that had been cleared of muscle tissue leaving the stifle capsule, patellar tendon and collateral ligaments intact. A quadriceps force and Achilles mechanism were simulated using cables, turnbuckles and springs (Kowaleski, Apelt et al. 2005).

Fiduciary markers were used to allow for accurate measurements from radiographs (Kowaleski, Apelt et al. 2005). The intact stifle was loaded at set joint angles

and then radiographically assessed. Transection of the CrCL was then performed along with a lateral parapatellar arthrotomy and another radiograph was obtained. The right and left hind limbs were then divided into two groups so that half would receive the centered TPLO and half would receive the distal TPLO with the degree of rotation based on the previously measured TPAs. Cranial tibial subluxation (CTS) was significantly lower in the centered TPLO procedure than in the distal TPLO procedure, but both methods reduced the amount of CTS as compared with CrCL transection without TPLO. There was still some degree of CTS with the centered TPLO procedure, however, which may explain why some TPLO procedures do not entirely eliminate cranial tibial thrust. Several muscle forces were neglected, but the goal was to compare the two procedures so all forces were not deemed necessary. Their results indicated that the centered TPLO is more biomechanically sound than the distal TPLO procedure (Kowaleski, Apelt et al. 2005).

In order to monitor the effects of TPLO on meniscal injury, Pozzi et al (2006) compared tibial translation following CrCL transection with and without meniscal release before and after TPLO. This experiment included using a tension cable to serve as the quadriceps and a weight bearing load of 20% body weight. Specimens included both hind limbs from cadavers weighing between 25 and 35 kg with TPAs of 24-30°. Fiduciary markers and radiographs were used to measure TPAs and tibial translation. The femoral long axis was 20° from vertical while the stifle angle was 105 +/- 5°. Radiographs were analyzed and surgical procedures were performed by one investigator (Pozzi, Kowaleski et al. 2006).

Two experiments were performed (Pozzi, Kowaleski et al. 2006). The first experiment involved sixteen pairs of hind limbs which were randomly assigned to two groups. One group would contain an intact CrCL and the other group would contain a transected CrCL. For the first experiment, radiographs were obtained when the limb was initially loaded as previously described for all specimens. For the group designated to have CrCL transection, the CrCL was then transected and another radiograph was obtained. Medial meniscal release (MMR) and medial caudal pole hemimeniscectomy (MCH) were performed on all stifles while obtaining a radiograph following each procedure. The same set of procedures was used in the group without CrCL transection, except the step to transect the CrCL was omitted (Pozzi, Kowaleski et al. 2006). From the radiographs, cranial tibial subluxation and caudal pole travel distance were determined following the operative procedures. Transection of the CrCL resulted in significant tibial translation, but no significant differences were determined between the meniscectomy procedures. Stifle stability was minimally impacted by meniscal release when the CrCL was intact; however, the meniscus was not the primary stabilizer of cranial drawer motion (Pozzi, Kowaleski et al. 2006).

Similarly, the second experiment included 15 pairs of hind limbs separate from the first experiment (Pozzi, Kowaleski et al. 2006). Theses stifles underwent CrCL transection and TPLO to attain a TPA of 5-7°. Radiographs were obtained as described for the first experiment and also included radiographs following the TPLO procedure. After loading the limbs as previously described, the displacement of the caudal pole of the medial meniscus was reduced from that of the first experiment. This suggests that rotation of the tibial plateau may reduce the extent that the meniscus serves as a wedge to

prevent cranial tibial subluxation. In turn, the TPLO procedure may help prevent medial meniscal damage due to increased meniscal stretch imposed by CrCL rupture. The testing of only one phase of stance introduces a limitation to this claim as it may not apply to all phases of stance (Pozzi, Kowaleski et al. 2006).

To study the effects of tibial tuberosity advancement (TTA) on tibiofemoral shear forces, Apelt et al (2007) performed an in vitro experiment to measure the changes in cranial tibial subluxation (CTS) and patellar tendon angle (PTA) following CrCL transection. The authors hypothesized that advancement of the tibial tuberosity would be neutralized by the patellar ligament at an angle of 90° relative to the tibial plateau in the CrCL deficient stifle. In addition, a PTA less than 90° would result in femorotibial shear forces in the caudal direction (Apelt, Kowaleski et al. 2007).

Apelt et al (2007) attempted to replicate the biomechanics during stance using 10 cadaveric hind limbs with no signs of orthopedic disease. Each hind limb was set up so that the femur was at 70° from the horizontal top platform, the stifle joint angle was 135° and the tarsus joint angle was 145°. A load equal to 30% body weight was applied. To simulate the quadriceps and Achilles tendon, cables were placed under tension and connected to the patella and femorofabeller articulations. With the limb loaded a lateral radiograph was taken. The CrCL was then transected, the limb was set up as before, and another lateral radiograph was taken. The TTA procedure was then performed with maximum advancement allowed by the hardware of the TTA, the limb was reloaded, and another lateral radiograph was obtained. Finally, the extent of the advancement was incrementally decreased until the tibia subluxated indicating cranial drawer motion.

Radiographs were obtained at each increment, and the increment just prior to subluxation was considered the critical point (Apelt, Kowaleski et al. 2007).

The results of study by Apelt et al (2007) indicated that cranial tibial subluxation (CTS) occurred following transection of the CrCL and was converted to caudal tibial subluxation at maximal tibial tuberosity advancement. At the critical point, the CTS was reduced. The mean patellar angle prior to transection, following transection, at maximal TTA and at the critical point was 105.8°, 80.4°, 80.8° and 90.3°, respectively. In summary, CTS was converted to caudal tibial subluxation when the patellar tendon became perpendicular to the tibial plateau so a PTA of 90° should be attained clinically when performing the TTA to eliminate CTS (Apelt, Kowaleski et al. 2007).

Stifle contact mechanics and kinematics prior to and following both the TPLO and TTA have been assessed (Kim, Pozzi et al. 2009; Kim, Pozzi et al. 2009). While the TPLO procedure eliminated tibial translation that resulted from transection of the CrCL, it did not restore normal contact mechanics between the femur and tibia. Contact pressures were redistributed on the tibial plateau more caudally and may increase the risk for osteoarthritis (Kim, Pozzi et al. 2009). The TTA resulted in both elimination of tibial translation following CrCL transection as well as a return of contact mechanics experienced prior to CrCL transection (Kim, Pozzi et al. 2009).

2.10 Canine Models

2.10.1 Mathematical Models

In order to develop a theoretical model of the canine hind limb, Shahar and Milgram (2001) dissected a hind limb of a canine cadaver to obtain morphometric and anatomic data. The dog used in the study weighed 23 kg and was of mixed breed. Data

obtained from this study included muscle mass, total muscle length, muscle fiber length, physiologic cross-sectional area (PCSA), architectural index (AI) and origin and insertion locations for all muscles of the hind limb. Only muscles that had both origin and insertion on the tibia-tarsal-metatarsal unit were discarded. The values obtained for the AI of each muscle were compared to published values for the human and cat, and the AI for the dog in this study was similar to the AI for the human and cat in most muscles. Differences were attributed to interspecies differences (Shahar and Milgram 2001).

In addition to the musculature data, Shahar and Milgram (2001) obtained origin and insertion coordinates for each muscle along with the coordinates of important boney landmarks through the use of an electronic coordinate measuring device. These coordinates were based on three coordinate systems with origins in the pelvis, femur and tibia. Transferring one set of coordinates in one system, the tibial system, to another system, the femoral system, would require the use of coordinate transformations (Shahar and Milgram 2001). This would also allow for determining the locations of muscle origins and insertions throughout gait to determine the forces within each muscle as was done in subsequent studies (Shahar and Banks-Sills 2002; Shahar and Banks-Sills 2004; Shahar and Milgram 2006).

Shahar and Banks-Sills developed a three dimensional mathematical model of the canine hind limb during three-legged stance (Shahar and Banks-Sills 2002). Such a model requires the knowledge of external ground reaction forces and pelvo-sacral joint reaction forces and moments, and the internal forces transmitted by ligaments and muscles. Since there are far more musculoskeletal forces than equations of equilibrium, the body has no unique solution. This model, like several other models, utilizes

optimization techniques to solve the indeterminate problem. At the time only one other paper (Arnoczky, Torzilli et al. 1977) described the biomechanics around the canine hip, but it was a two-dimensional assessment. Two optimization techniques were used to simulate muscle forces for this model (Shahar and Banks-Sills 2002).

Shahar's model of the right hind limb was created using rigid bodies for the pelvis, femur and tibia with the bones below the tarsal joint considered as part of the tibia (Shahar and Banks-Sills 2002). Only the mid-stride phase of stance was considered. It was assumed the internal forces balance the external forces. Geometric data was obtained by cadaver dissection (Shahar and Milgram 2001), and joint angles were 40° for the axis of the pelvis relative to horizontal, 105° for the femur in flexion and 10° for the femur in abduction, and 50° for the tibia in flexion. Forces acting on the pelvis were taken as the forces within the 23 muscles that insert on the pelvis, hip reaction forces, and the pelvo-sacral force and moment. The weight of the pelvis was considered negligible, and hip joint reaction moments were assumed zero due to the use of a ball-and-socket joint. Each muscle force was applied at its location of insertion while the hip reaction force was assumed to act at the center of the acetabulum, and the pelvo-sacral force and moment were assumed to act at the midline of the pelvis. A similar setup was utilized for the forces acting on the femur and tibia, and input ground reaction forces of 34% body weight (BW) vertically, 6% BW caudo-cranially, and 1% BW latero-medially were used. It was assumed that the stifle ligaments provided no resistance to flexion or extension and the joint was assumed a hinge joint (Shahar and Banks-Sills 2002).

To solve the equilibrium equations, two muscle optimization techniques were used. The two techniques were the minimization of the sum of muscle forces (MSMF)

and the minimization of the maximal muscle stress (MMMS). The MSMF method resulted in the activation of 5 muscles while the MMMS method resulted in the activation of 20 muscles. Electromyography (EMG) studies have shown more muscles to be active than can be approximated by linear optimization which indicates that the MMMS optimization technique may be a better approximation than the MSMF optimization technique (Shahar and Banks-Sills 2002). Hip joint reaction forces were comparable to in vivo studies, but stifle reaction forces and ligament forces were not reported. This paper gives a first approximation of the canine hind limb forces and served as the basis for several subsequent hind limb modeling papers (Shahar and Banks-Sills 2002).

To further elaborate on the canine hind limb model proposed in 2002, Shahar and Banks-Sills established a quasi-static three dimensional model of the canine stifle which evaluated 10% increments of stance in the gait cycle of a slow walk (Shahar and Banks-Sills 2004). Goals of this study included calculation of forces within the stifle ligaments and stifle joint reaction forces during each increment of stance. This 2004 study also compared the biomechanics of a healthy stifle with a CrCL deficient stifle by simulating the absence of the CrCL. Boundary conditions at each increment of stance were established from the MMMS optimization technique as described in the study by Shahar (2002) for input hip joint reaction forces and hind limb muscle forces (Shahar and Banks-Sills 2004). Ground reaction forces and kinematic data were obtained from previous studies for each increment of stance (Budsberg, Verstraete et al. 1987; Hottinger, DeCamp et al. 1996).

The Shahar (2004) model included assumptions such as negligible hind limb weight, the bones were considered rigid bodies, the menisci effects were ignored,

coefficients of friction between cartilaginous structures were ignored, the patellar ligament was considered inextensible, and the patella only rotated in the sagittal plane. The stifle ligaments were considered as single entities and not multiple bundles (Shahar and Banks-Sills 2004).

Four stifle ligaments were included in the model; the CrCL, CaCL, LCL and MCL were treated as nonlinear springs with a second order force-length relationship as done in the human knee study by Blankevoort et al (1991). The forces within the ligaments were based on the amount of strain due to stretching, and the force for each ligament was then calculated using strain based spring constants (Shahar and Banks-Sills 2004). The CrCL loading results of this study are similar to those for other quadrupeds measured in vivo (Holden, Grood et al. 1994). The CrCL is loaded throughout the stance phase and reaches a peak of 12% body weight (BW) at 40% of stance. The peak load of the LCL was 2.5% and occurred at 80% of stance. The CaCL and MCL were not loaded in the CrCL intact stifle. In contrast the CrCL deficient stifle showed loading within the LCL for the entire stance phase and loading within the caudal cruciate ligament became present with a peak of 11% BW at 50% stance (Shahar and Banks-Sills 2004). The stifle ligament loadings calculated by this model are displayed in FIGURE 22.

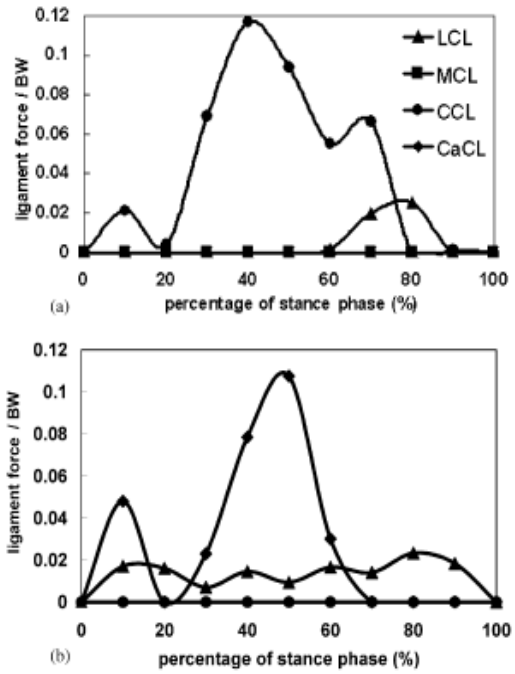

FIGURE 22 - Stifle ligament loadings prior to and following CrCL rupture (Shahar and Banks-Sills 2004).

Using the stifle models developed by Shahar and Banks-Sills (Shahar and Banks-Sills 2002; Shahar and Banks-Sills 2004), Shahar and Milgram developed another three dimensional model capable of simulating rotation of the tibial plateau (Shahar and Milgram 2006). In this model the same assumptions as previously described in the quasi-static model (Shahar and Banks-Sills 2004) were employed along with the same input boundary conditions for ground reaction forces, kinematic data, and MMMS optimization values for hind limb muscle forces and hip joint reaction forces. Simulation of tibial plateau rotation in the theoretical model (Shahar and Milgram 2006) mimicked the popular TPLO corrective surgery. Plateau rotation in the sagittal plane was achieved in the model through utilization of a rotation matrix that altered the coordinates of points describing the surface geometry of the tibial plateau (Shahar and Milgram 2006).

TPLO had not been conclusively shown to perform better than other corrective procedures and possible adverse biomechanical effects have been suggested (Warzee, Dejardin et al. 2001; Aragon and Budsberg 2005; Lazar, Berry et al. 2005). This three dimensional model had advantages over the two dimensional model of Slocum by considering muscle forces. The TPA of the dog used for the model was 22°. The rotation matrices altered the TPA to 0° and 5°. It was shown that the CaCL became loaded when the TPA was rotated caudally (distal portion of the proximal tibial fragment) by 22° so that the TPA was 0°, and the CrCL, if intact prior to rotation, became less loaded, but the loading was not entirely eliminated. For a CrCL deficient stifle, CaCL loadings were significant in all cases (Shahar and Milgram 2006). It was concluded that cranial tibial thrust was converted to caudal tibial thrust after rotation so that the TPA was 0°, but rotation to a TPA of 5° did not eliminate cranial tibial thrust. Due to its correlation with measured forces in goats (Holden, Grood et al. 1994), this model was considered partially validated, but several assumptions and limitations remain as were described for each of Shahar's mathematical models (Shahar and Banks-Sills 2002; Shahar and Banks-Sills 2004; Shahar and Milgram 2006).

2.11 Human Studies

The models of Shahar (Shahar and Banks-Sills 2002; Shahar and Banks-Sills 2004; Shahar and Milgram 2006) were based on the work of Blankevoort et al (1991) to further the development of a mathematical model of human knee biomechanics. Blankevoort et al (1991) attempted to determine the effects of the articular surfaces and articular contact of the tibia and femur on model outputs. The kinematic characteristics of the model were compared to experimental passive motion of the knee. Varied parameters

of the model included the rigidity of the contact surfaces and the surface geometry as described by polynomial approximations (Blankevoort, Kuiper et al. 1991).

The geometries of the knee were based on previous studies from which experimental kinematic data were also available (Blankevoort, Kuiper et al. 1991). Effects of the meniscus and friction were neglected. The model was assessed over a range of joint positions to approximate joint motion. The ligaments were described by two or more line elements that represented different fiber bundles, and the ligaments were assumed elastic. Therefore, the force within the ligament elements were a function of the length of the ligaments described by the distance between origin and insertion points. Ligament forces were described by first and second order relationships. Determination of which force-length relationship was used was based on the amount of strain imposed within each ligament as compared to previously reported reference strains (Blankevoort, Kuiper et al. 1991). Ligament stiffness values for each element ranged from 2000 to 9000 N per unit strain. Internal and external rotation was described over a range of flexion angles by inputting an axial torque about the long axis of the tibia. Equilibrium equations for the knee were then solved using the Newton-Raphson iteration procedure. The results indicated good agreement with experimental studies (Blankevoort, Kuiper et al. 1991).

A computer model of the human lower extremity was developed by Liacouras and Wayne (2007) using CT scans to develop an Initial Graphics Exchange Specification (IGES) file. The goals of this study were to develop a solid body computer model from commercial software that could be subjected to varying scenarios to approximate the response of a biomechanical system. The scenarios tested for the lower extremity were syndesmotic injury and repair and ankle inversion following ligament transection. In

order to validate this computer model, the results were compared with physical cadaver representations (Liacouras and Wayne 2007).

From the IGES files solid models were generated and assembled in SolidWorks (SolidWorks Corp, Concord, MA). To kinetically simulate the injuries, COSMOSMotion (Structural Research and Analysis Corp, Santa Monica, CA) was employed to allow for a dynamic response to input loads (Liacouras and Wayne 2007). After assembling the lower extremity bones, boundary control structures were developed to ensure alignment or restriction of particular movements. Three boundary structures were used for the syndesmotic scenario. Two of these structures were cylinders that established a cylindrical joint for the long axis of the tibia. This joint allowed for axial loading of 15 lbf (66.7 N) compression and a torsional loading of 24 in.-lbf (2.7 N-m) about the long axis of the tibia. To prevent the foot from penetrating the horizontal plane on which it rested, as in to simulate the ground, the third structure used was a flat plate in contact with the bottom of the foot. The tibia, fibula and talus were allowed to move while all other bones were fixed. The ankle inversion scenario required only one boundary structure in order to orient the medial-lateral input force of 10 lbf (44.5 N). For this scenario only the tibia was fixed while all other bones were free to move (Liacouras and Wayne 2007).

Three-dimensional contacts were implemented to prevent intersection of articulating bone surfaces (Liacouras and Wayne 2007). Ligaments were represented as linear springs based on stiffness values from the scientific literature or assumed values where no literature values were obtained. A pre-strain of 0.5 to 2% was applied to each ligament, and the input loads previously described were introduced over time intervals to

allow the system to reach equilibrium with each input. To simulate ligament rupture during the syndesmotic injury, the springs representing the anterior and posterior tibiofibular ligaments along with springs representing 8 cm of the interosseous membrane near the ankle were suppressed. Likewise, in the ankle inversion study, the spring representing the calcaneofibular ligament was suppressed (Liacouras and Wayne 2007).

Sensitivity of the model to applied loads and ligament stiffness was also assessed (Liacouras and Wayne 2007). The torsional loading was determined to have a more significant impact on the model than the compressive loading. Limitations in the study noted by the authors included the use of only one foot in the computer model while using several in the cadaver studies. Also, representing the ligaments as single-element linear springs was assumed to approximate the linear portion of ligament response. The effects of muscle forces were neglected in the model (Liacouras and Wayne 2007).

2.12 Scientific Literature Conclusions

Repair of the CrCL deficient stifle remains common in orthopedic surgery for large breed dogs. Several corrective procedures with varying degrees of invasiveness have been developed, but no one procedure has proven to be consistently superior or overwhelmingly preferred. Previously, these radical procedures were developed by considering only a few structures of the hind limb, and the success of the procedure was determined from retrospective studies. Computer models attempting to further the understanding of the biomechanics within the stifle joint as a whole have begun to become available due to previous models proposed in human biomechanics research. Further biomechanical research is needed to understand the canine stifle joint, the role of the CrCL, and the effects of radical repair techniques to stabilize the CrCL deficient

stifle. Orthopedic surgeons may then have the tools necessary to make the most informed decisions on a case by case basis.

III. MATERIALS & METHODS

Anatomical information from a large breed dog was be used to develop the geometrical characteristics of a three dimensional, computer generated model of the canine hind limb using the computer aided design software SolidWorks (SolidWorks Corp, Concord, MA). Both kinetic and kinematic inputs supplied from the scientific literature were applied to the model. Biological structures modeled included bones, ligaments, menisci, and muscle actuators. The hind limb joints were constructed using movement constraints. Once constructed the canine hind limb model was used to simulate 10% discrete phases of stance in COSMOSMotion (Structural Research and Analysis Corp, Santa Monica, CA) to describe the biomechanics of both a CrCL intact and CrCL deficient stifle joint. Loadings within the stifle ligaments were assessed for each case and compared to the scientific literature. The sensitivity of the model to varied input parameters was also addressed.

3.1 Model Development

The hind limb model was constructed based on identification of boney landmarks from anatomic and radiographic images. Rigid body model components included the pelvis, femur, tibia, tarsus, metatarsals and phalanges. Ligament and key muscle insertion points were identified on these components based on the anatomical geometry.

3.1.1 Canine Subject

A 32 kg English Labrador Retriever was used for hind limb measurements. The hind limb lengths were 14 cm from the iliac crest to the greater trochanter, 22 cm from the greater trochanter to the stifle, 20 cm from the stifle to the tarsus, and 10 cm from the tarsus to the fifth metatarsal. These measurements were obtained using a tape measure and boney locations were determined by palpation. FIGURE 23 displays the dog from which measurements were obtained.

FIGURE 23 - Canine subject.

3.2 Three Dimensional Rigid Body Canine Hind Limb Computer Model Components

Pertinent components of the hind limb were incorporated into the 3D rigid body model. Each component was defined based on the role it plays in the hind limb. Bones were modeled as rigid bodies while ligaments were modeled as extensible nonlinear

springs. The menisci were treated as incompressible frictionless surfaces, and the muscles were treated as force actuators.

3.2.1 Bone Modeling

Bones were modeled as non-deformable rigid bodies. Bone geometry was replicated based on anatomical images and assessment of boney landmarks from the literature. Boney prominences were included where applicable to establish ligament and muscle insertion points and locate and orient kinetic and kinematic inputs reported in the literature. A tibial plateau angle of 22° was used (Morris and Lipowitz 2001; Reif and Probst 2003). The bones were neither analyzed for their structural integrity nor their response to varied kinetic and kinematic inputs during discrete phases of stance. The fibula and patella were neglected as modeled components in this first approximation. Rather, the LCL attachment at the fibula and the direction of the patellar ligament force vector at the tibial tuberosity approximated the role of these structures in stifle stability.

3.2.2 Ligament Modeling

The stifle ligament forces were the primary outcome measures investigated using the model. Ligament forces were expected to vary during each phase of stance due to varied ground reaction forces, muscle forces, joint angles and locations of ligament origins and insertions. In theoretical models ligaments have commonly been modeled as springs. Both linear and nonlinear spring approximations have been used (Blankevoort, Kuiper et al. 1991; Shahar and Banks-Sills 2004; Shahar and Milgram 2006; Liacouras and Wayne 2007). Blankevoort et al (1991) used a nonlinear spring method to develop a mathematical model of the human knee. Shahar (2004, 2006) adapted the method used by

Blankevoort (1991) for use in a mathematical model of the canine stifle. Liacouras (2007) used linear springs to develop a human lower leg computer model. Nonlinear springs will be used in this study as a first approximation of ligaments, and it was assumed that no ligament failed during simulation.

Each ligament was treated as a single line element that is directed along the vector from the ligament origin to the ligament insertion. Since ligaments only act as a restraint in tension, the force response for each of the four stifle ligaments was approximated using

$$F = k_j\left(\varepsilon_j - \varepsilon_m\right); \qquad 2\varepsilon_m < \varepsilon_j \tag{1}$$

$$F = \frac{1}{4} k_j \frac{\varepsilon_j^{\,2}}{\varepsilon_m}; \qquad 0 < \varepsilon_j \le 2\varepsilon_m \tag{2}$$

$$F = 0; \qquad \varepsilon_j \le 0 \tag{3}$$

where k_j is the stiffness value for ligament j, ε_j is the strain in ligament j and ε_m is the parameter that determines the ligament response transition from the toe region to the linear region (Blankevoort and Huiskes 1991; Shahar and Banks-Sills 2004). The parameter ε_m was set at 0.03 (Blankevoort and Huiskes 1991; Shahar and Banks-Sills 2004).

As described by (Shahar and Banks-Sills 2004), the unstressed ligament lengths were based on a reference position and the associated reference strains for each respective ligament. A stifle at full extension (Shahar and Banks-Sills 2004) corresponding to a stifle angle of 162° (Jaegger, Marcellin-Little et al. 2002), was used as the reference position. The unstressed ligament length for each ligament j is therefore determined using

$$L_{0j} = \frac{L_{REF}}{1 + \varepsilon_{REF}} \tag{4}$$

where L_{REF} is the linear distance from the origin to the insertion of each ligament at the reference position and ε_{REF} is the inherent strain in each ligament at the reference position. The values that were used for the inherent strain at the reference position are listed in TABLE I (Shahar and Banks-Sills 2004).

TABLE I

INHERENT STRAINS FOR EACH LIGAMENT AT THE REFERENCE POSITION

(SHAHAR AND BANKS-SILLS 2004)

Ligament	ε_{REF}
CrCL	0.04
CaCL	0.04
MCL	-0.25
LCL	0.08

The strain within each ligament was then determined using

$$\varepsilon_j = \frac{\left(L_j - L_{0j}\right)}{L_{0j}} \tag{5}$$

where Lj is the length of ligament j during simulation. Failure in the CrCL along its axis was measured at or above four times body weight at two stifle angles in Greyhounds and Rottweilers (Wingfield, Amis et al. 2000). Stifle ligament force values above this threshold in the model were deemed unrealistic.

The modeled linear distances between insertion and origin for each ligament at full extension are listed in TABLE II.

TABLE II

LIGAMENT LENGTHS AT THE REFERENCE POSITION

Ligament	L_{REF} (mm)
CrCL	18.9
CaCL	11.5
MCL	58.9
LCL	25.9

Approximate ligament lengths for similarly sized dogs have been reported in the literature. Vasseur et al (1985) and Wingfield et al (2000) reported an average CrCL length of 18.6 mm and 18.7 mm, respectively, for dogs ranging from 32 to 46 kg. Vasseur and Arnoczky (1981) reported MCL and LCL lengths of approximately 70 mm and 30 mm, respectively, at full extension for dogs weighing between 20 and 50 kg. Likewise, Arnoczky and Marshall (1977) reported average CaCL lengths of 11 mm for dogs weighing between 15 and 20 kg.

Ligament stiffness values were based on ligament cross sectional area (CSA) perpendicular to the ligament long axis at the ligament midsection. Two studies have reported measured CSA values of the CrCL. A previous study which measured the CSA as well as the tensile strength along the ligament long axis reported average midsection CSA values of 20.41 mm^2 and 26.40 mm^2 for the Racing Greyhound (31 kg average weight) and Rottweiler (42 kg average weight), respectively (Wingfield, Amis et al. 2000). Tensile data for these breeds was reported as tangent moduli of 221 MPA and 198 MPA for the Racing Greyhound and Rottweiler, respectively (Wingfield, Amis et al. 2000). Additionally, a previous study reported a fit equation which correlates the CrCL

CSA with weight (Vasseur, Pool et al. 1985). However, this study did not report CrCL tensile strength as a function of either weight or CSA.

Little experimental information is available for the CaCL, LCL and MCL in canines, so the stiffness values used in previous canine studies were often adapted from human studies (Shahar and Banks-Sills 2004). In this study the remaining ligaments were assumed to have the same tensile material properties as the CrCL, but it was assumed the CSA for each ligament would vary. Cross sectional areas for these remaining ligaments were obtained through the use of medical imaging data.

A computed tomography (CT) scan of the hind limb was obtained for a 9 month old, 58 kg male dog using a Sensation 16 scanner (Siemens AG, Berlin and Munich, Germany), 0.669 mm slices and a 0.742 pixel size*. This scan was imported into Mimics 12.11 (Materialise, Ann Arbor, MI). A three dimensional model of the stifle containing the bone and ligament structures was developed using segmentation. The measurement tools in Mimics were used to approximate the elliptical major and minor axes of the ligament midsection CSA. The stifle model is shown in FIGURE 24 while the respective CSAs are listed in TABLE III.

*CT scan provided by Dr. Marcellin-Little, DEDV from the College of Veterinary Medicine, NC State University

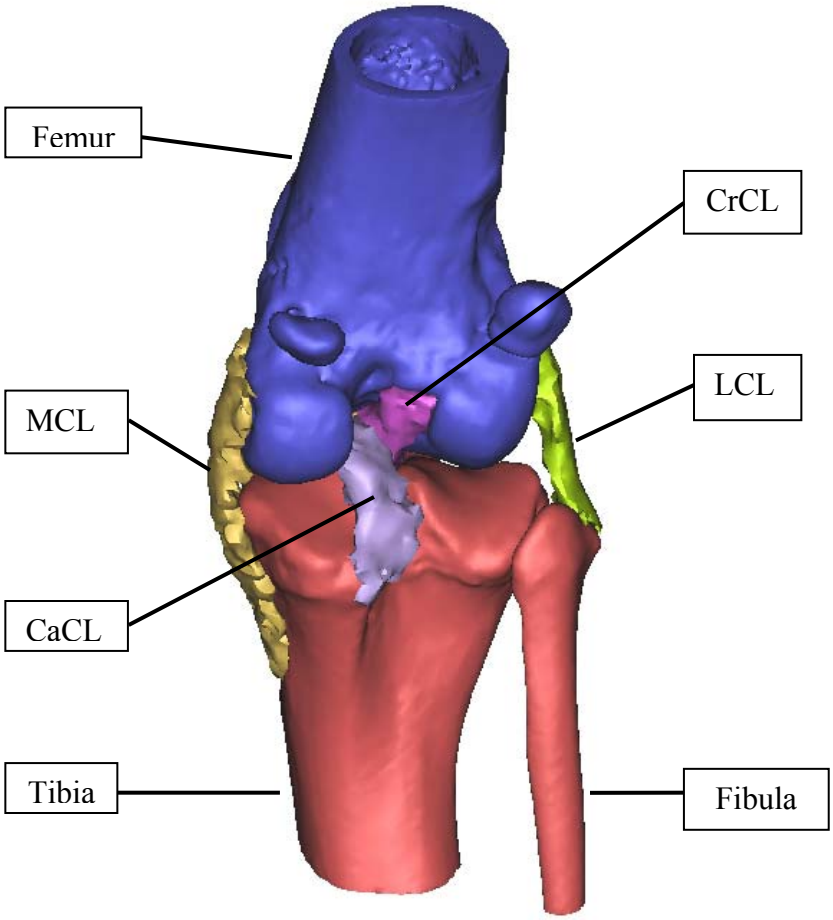

FIGURE 24 - Caudal aspect of the stifle reconstructed from medical imaging data.

TABLE III

ELLIPTICAL LIGAMENT CSAS OBTAINED FROM MEDICAL IMAGING DATA

Ligament	CSA (mm^2)
CrCL	31.8
CaCL	53.8
MCL	47.8
LCL	27.5

Since the dog from which the CT scan was obtained had a body mass of 58 kg and the dog from which the model was developed had a body mass of 32 kg, a scaled value for each CSA obtained from the CT scan was used in the model. The CrCL CSA

for a dog body mass of 32 kg was determined by fitting a linear trend line to three points. Two points were the average CrCL CSA reported for the average dog body mass for the Racing Greyhound and the Rottweiler (Wingfield, Amis et al. 2000). The third point was the CrCL CSA obtained from the reconstructed medical imaging data. FIGURE 25 shows these three points with the linear trend line.

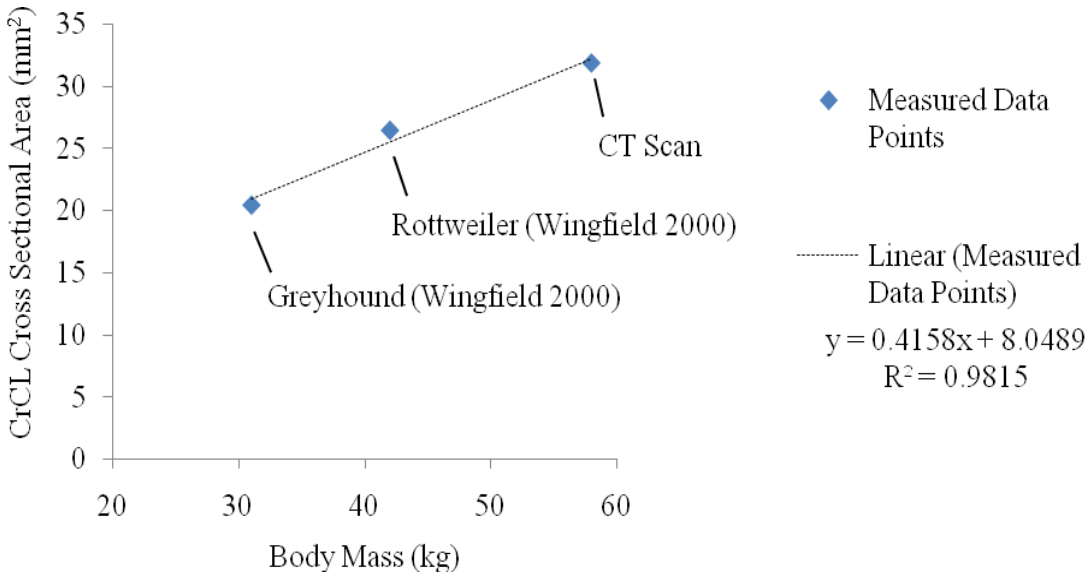

FIGURE 25 – Cross sectional area as a function of body mass.

From the linear trend line, a CSA for a dog body mass of 32 kg was obtained as 21.2 mm^2. A proportional relationship between the CSA and weight was then applied to the remaining ligament CSAs in TABLE III. The adjusted values are listed in TABLE IV.

TABLE IV

PROPORTIONALLY ADJUSTED ELLIPTICAL LIGAMENT CSAS

Ligament	CSA (mm^2)
CrCL	21.2
CaCL	35.9
MCL	31.9
LCL	18.4

Stiffness values for each respective ligament were then approximated using the minimum tangent modulus reported (Wingfield, Amis et al. 2000) of 199 MPa. The stiffness values for each ligament are listed in TABLE V.

TABLE V

LIGAMENT STIFFNESS VALUES

Ligament	Stiffness (N/ε)
CrCL	4230
CaCL	7150
MCL	6350
LCL	3650

Stiffness values for each of the four ligaments in the human knee were previously compared (Blankevoort, Kuiper et al. 1991). These values varied from 3000 to 12,000 N/ε for the ACL, 4500 to 20,000 N/ε for the PCL, 3000 to 7300 N/ε for the LCL and 5200 to 8300 N/ε for the MCL.

3.2.3 Meniscus Modeling and 3D Contact

The menisci were modeled as non-deformable rigid bodies. COSMOSMotion (Structural Research and Analysis Corp, Santa Monica, CA) allows the incorporation of simulating three dimensional contacts between modeled components. The menisci were

treated as components fixed to the tibia which interacted with the femoral condyles. Friction was treated as negligible with static and dynamic frictional coefficients of 0.05 since articular cartilage has low coefficients of friction (Fung 1993; Robertson, Caldwell et al. 2004; Shahar and Banks-Sills 2004; McCann, Ingham et al. 2009).

3.2.4 Muscle Modeling

Muscle forces were approximated and simplified due to an inability to replicate the role of all muscles of the hind limb during the stance portion of walking. Since the length of a muscle is not an exact indicator of the amount of contraction (Robertson, Caldwell et al. 2004), force-length relationship approximations that were used to represent ligaments were deemed inadequate. Several techniques have been devised to quantify the amount of force imparted to the hind limb from each muscle, but an entirely conclusive method is not currently available (Robertson, Caldwell et al. 2004). Muscle optimization techniques and electromyography measurements approximate the extent of muscle action but do not directly measure the force generated within a muscle (Robertson, Caldwell et al. 2004). Therefore, major muscles imperative for hind limb stability and to maintain joint angles were approximated as input forces.

Shahar performed an initial mathematical study of the canine hind limb in three-legged stance using two optimization techniques (Shahar and Banks-Sills 2002). One of these techniques, the minimization of the sum of muscle forces (MSMF), resulted in primary muscle forces from the deep gluteal, rectus femoris, biceps femoris, adductor magnus et brevis and lateral and intermediate vastus. All other muscle forces were zero (Shahar and Banks-Sills 2002). The second optimization technique, the minimization of maximal muscle stress (MMMS), resulted in activation of several more muscles (Shahar

and Banks-Sills 2002). This MMMS technique was applied in a subsequent quasi-static model at 10% discrete intervals of stance (Shahar and Banks-Sills 2004). Slocum (1983) noted during an in vitro study that the tarsus tendon and biceps femoris muscle were necessary to maintain stability during weight bearing at a stifle angle of 140°. Also, an electromyography study noted primary activity during the stance phase of gait in the following muscles: interosseus, gastrocnemius (medial and lateral portions), flexor digitorum superficialis, hallucis longus, popliteus, gracilis, adductor, semimembranosus (cranial and caudal portions), semitendinosus, biceps femoris (cranial and caudal portions), vastus lateralis, rectus femoris and gluteus medius (Wentink 1976). Accordingly, these muscle inputs from these studies were considered as necessary for hind limb stability in the proposed model.

3.3 Model Stability

In order to maintain stability without over constraint, the proposed model was subjected to imposed joint constraints. Imposed joint constraints included mates defined within the assembly that prevented unrealistic free motion. Such constraints limited the movement of the constitutive components of the hind limb by removing degrees of freedom. Secondly, ground reaction forces and muscle input forces actuated the model.

3.3.1 Joint Assumptions

The model was constructed using some constraining simplifications. Movement of the hind limb was constrained to the sagittal plane. The pelvis was considered fixed and immovable. The head of the femur was connected with the pelvis via a ball and socket joint with ligament and capsular constraints neglected. During each simulation the

hip angle was fixed, which prevented movement of the femur. The femoral condyles and menisci connected to the tibial plateau were able to interact as described using 3D contacts. The tarsus was treated as a frictionless hinge joint. The plantar surface of the phalanges was constrained to remain parallel to the ground surface and was constrained to vertical movement only. This setup allowed cranial-caudal and superior-inferior translation of the tibia as well as flexion-extension of the stifle joint. The extent of these movements was thus determined by the input ground reaction forces and muscle actuation forces and limited by the stifle ligaments.

3.4 Model Inputs

For each 10% discrete phase of stance, the hind limb computer model was subjected to both kinematic and kinetic inputs. The kinematic inputs included the joint angles of the hip, stifle and tarsus. The kinetic inputs included the ground reaction forces and muscle forces. All sets of inputs were obtained from the scientific literature.

3.4.1 Kinematic Data

Joint angles for the hip, stifle, and tarsus were prescribed based on the scientific literature. These angles are determined by the functional axes of the pelvis, femur, tibia and tarsal bones as defined in FIGURE 26 by connecting the distal lateral aspect of the fifth metatarsal bone (1), the lateral malleolus of the distal portion of the tibia (2), the lateral epicondyle of the femur and the fibular head (3), the greater trochanter of the femur (4), and the medial portion of the iliac crest (5).

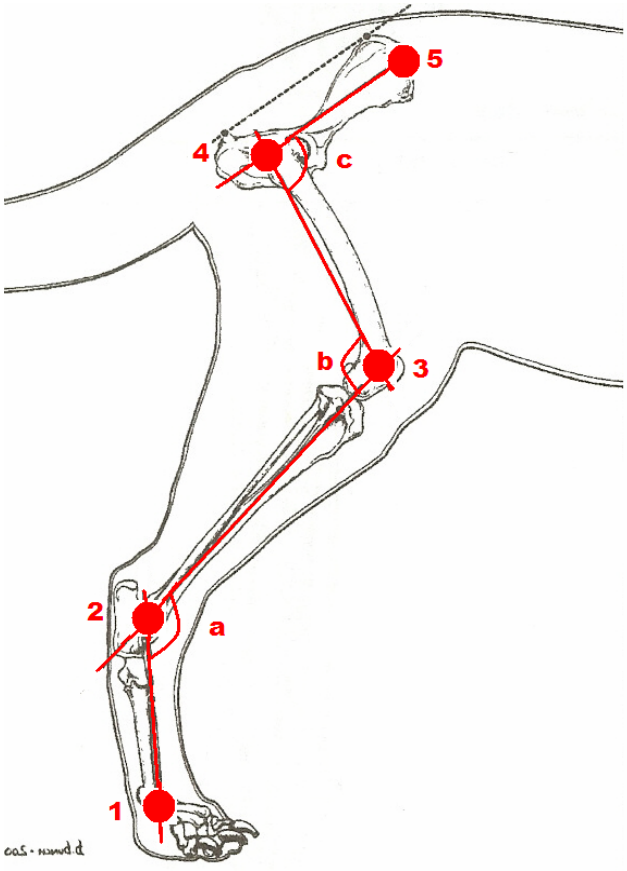

FIGURE 26 - Joint angles of the tarsus (a), stifle (b) and hip (c) of the canine hind limb (Jaegger, Marcellin-Little et al. 2002).

DeCamp et al (1997) reported the mean joint angles for the hip, stifle and tarsus for 15 healthy large breed dogs of unspecified weight in both the stance and swing phases of a walk. These results are displayed in FIGURE 27, and TABLE VI lists the discrete values used in the canine hind limb computer model.

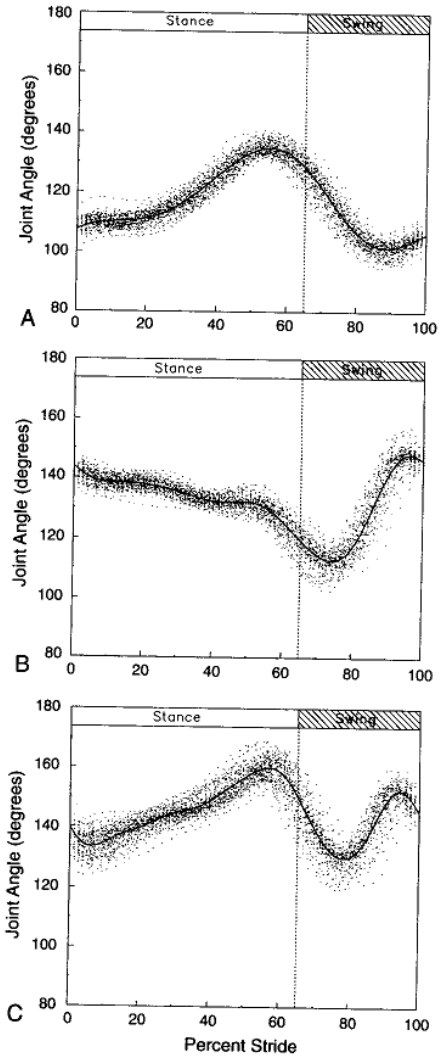

FIGURE 27 - Joint angles of the hip (A), stifle (B) and tarsus (C) of the canine hind limb during the stance and swing phases at a walk. The solid line is the mean for 5 repetitions of 15 large mixed-breed dogs (DeCamp 1997).

TABLE VI

DISCRETE JOINT ANGLES OF THE CANINE HIND LIMB FOR THE HIP, STIFLE AND TARSUS DURING THE STANCE PHASE AT A WALK (DECAMP 1997)

	Joint Angle (degrees)		
Stance Phase (%)	Hip	Stifle	Tarsus
0	108	144	140
10	110	139	134
20	111	138	136
30	112	138	140
40	113	137	143
50	116	135	146
60	122	134	149
70	129	134	155
80	134	134	160
90	135	128	157
100	129	119	150

3.4.2 Ground Reaction Force Kinetic Data

The x, y and z coordinate directions for ground reaction forces in FIGURE 29 correspond with those illustrated in FIGURE 28. The hind limb model did not utilize the x, the lateromedial, or y, the craniocaudal, coordinate forces since the model was constrained to movement in the y-z plane, and the phalanges were restricted to vertical motion in the z direction.

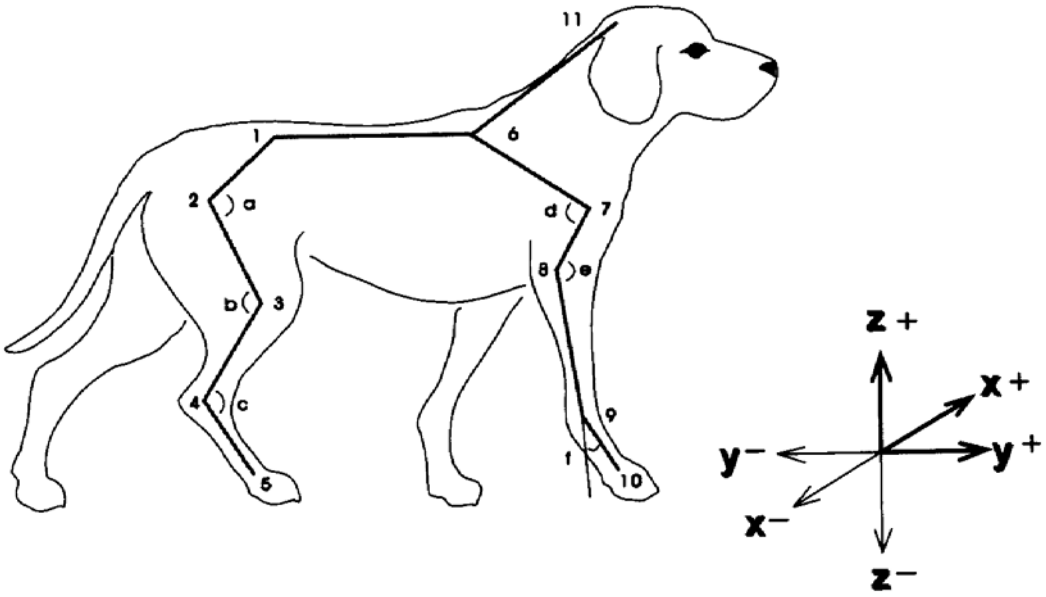

FIGURE 28 - Coordinate directions (DeCamp 1997).

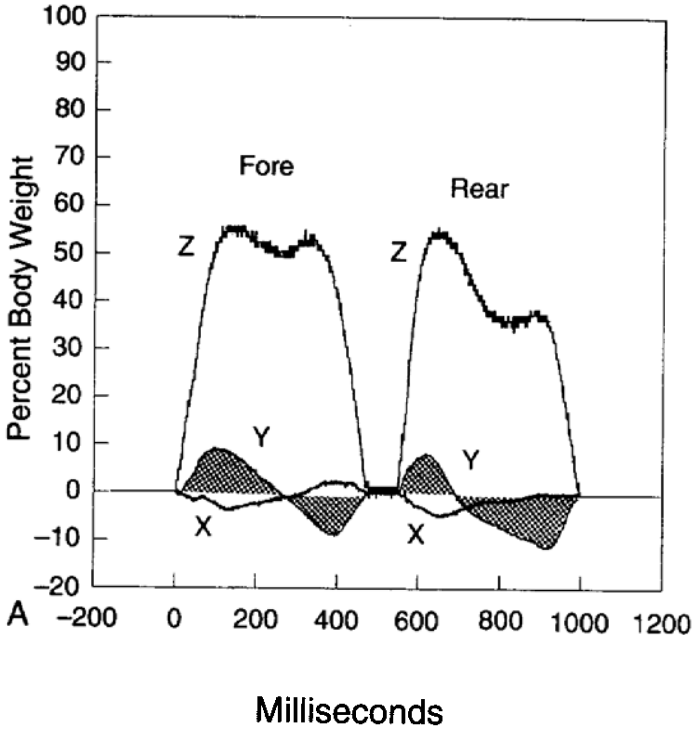

FIGURE 29 - Ground reaction force trend data in all directions during the stance phase for the fore and rear limbs of the canine normalized by body weight (DeCamp 1997).

FIGURE 29 displays the ground reaction forces for one forelimb and one hind limb during the stance phase normalized by body weight (DeCamp 1997). The maximum reaction force of the hind limb occurs between 20% and 30% of stance and its magnitude is 55% body weight. Similar ground reaction force trends were used by Shahar (2004) as listed in TABLE VII, but the peak vertical force magnitude was less at 44% body weight. The discrete values listed in TABLE VII will be used in this study.

TABLE VII

DISCRETE APPLIED GROUND REACTION FORCES FOR EACH STANCE PHASE FOR THE HIND LIMB OF THE CANINE NORMALIZED BY BODY WEIGHT (SHAHAR AND BANKS-SILLS 2004)

Phase of Stance (%)	Vertical GRF (% BW)
0	0
10	14
20	36
30	44
40	43
50	37
60	32
70	32
80	32
90	20
100	0

3.4.3 Muscle Force Kinetic Data

The input muscle forces included stifle extensors and flexors that cross the stifle joint. The inclusion of these muscles is supported by previous studies (Wentink 1976; Shahar and Banks-Sills 2004). The magnitudes of the muscle forces were based on the muscle optimization technique of Shahar (2004). TABLE VIII lists the key muscle forces

and the magnitudes of those muscle forces normalized by body weight. Based on the proximity of independent muscle origins and insertions, key muscles were combined into muscle groups. Each muscle group was simulated by an action only force that acts along the linear vector of the approximate muscle group insertion.

TABLE VIII

DISCRETE MUSCLE REACTION FORCES FOR EACH STANCE PHASE FOR THE HIND LIMB OF THE CANINE NORMALIZED BY BODY WEIGHT (SHAHAR AND BANKS-SILLS 2004)

	Hind Limb Muscle Forces During Each Stance Phase (% Body Weight)								
Muscle	10%	20%	30%	40%	50%	60%	70%	80%	90%
Tensor Fasciaelatae, caudal	3.0	8.2	0.0	0.0	0.0	11.9	15.7	16.8	12.9
Tensor Fasciaelatae, cranial	0.7	1.8	0.0	0.0	0.0	2.6	3.5	3.7	2.9
Vastus Lateralis and Intermedius	6.1	16.8	11.1	10.0	14.7	24.3	32.1	34.4	26.5
Vastus Medialis	5.3	14.8	10.9	9.8	12.9	21.4	28.2	30.3	23.3
Rectus Femoris	5.3	14.7	0.0	0.0	7.1	21.3	28.1	30.1	23.2
Biceps Femoris	4.7	12.9	12.1	14.6	11.3	18.7	9.5	8.9	0.1
Semimembranosus, tibial	0.0	0.0	3.0	3.7	2.8	0.0	3.1	0.0	0.0
Semitendinosus	0.0	0.0	5.2	6.2	4.8	0.0	0.0	0.0	0.0
Sartorius, cranial	0.8	2.3	0.0	0.0	0.0	3.3	4.3	4.7	3.6
Sartorius, caudal	0.3	1.0	0.0	0.0	0.0	1.4	1.8	2.0	1.5
Gracilis	1.5	4.3	3.0	3.5	0.9	0.0	0.0	0.0	0.0
Gastrocnemius, medial	0.0	0.0	2.6	7.3	0.0	0.0	0.0	0.0	0.0
Gastrocnemius, lateral	0.0	0.0	0.0	1.8	0.0	0.0	0.0	0.0	0.0
Flexor Digitorum Superficialis	8.5	6.9	22.1	26.7	17.3	0.0	0.0	0.0	0.0

In the model the muscles listed in TABLE VIII were grouped as follows: group 1 (femoral stifle extensors) consisted of the vastus lateralis, vastus intermedius, vastus medialis, rectus femoris and sartorius (cranial); group 2 (medial femoral stifle flexors) consisted of the semimembranosus (tibial connection), sartorius (caudal), gracilis and

semitendinosus; group 3 (lateral femoral stifle flexors) consisted of the biceps femoris, tensor fasciaelatae (cranial) and tensor fasciaelatae (caudal); group 4 (tibial stifle flexors) consisted of the gastrocnemius (medial and lateral) and flexor digitorum superficialis.

Initially, the muscle group force vectors were oriented as follows: group 1 was directed along a vector connecting the tibial tuberosity and a patellar attachment point; group 2 was directed parallel to the femur long axis; group 3 was directed parallel to the femur long axis; group 4 was directed parallel to the tibia long axis.

3.5 Simulation Software

The model was constructed in the computer aided design (CAD) three dimensional modeling software SolidWorks 2008 (SolidWorks Corp, Concord, MA). It was then analyzed in COSMOSMotion 2008 (Structural Research and Analysis Corp, Santa Monica, CA) which simulates rigid-body motion based on a physics solver and allows for input of external forces.

3.5.1 SolidWorks

SolidWorks (SolidWorks Corp, Concord, MA) is commercially available CAD software that allows for the creation of individual three dimensional rigid body component parts. Assemblies based on the incorporation of these components can be further constructed with the inclusion of assigned constraints called mates. Further analysis using motion studies can be performed on these parts and assemblies through the use of the add-in COSMOSMotion (Structural Research and Analysis Corp, Santa Monica, CA).

3.5.2 COSMOSMotion

COSMOSMotion (Structural Research and Analysis Corp, Santa Monica, CA) allowed the simulation of dynamic rigid body mechanics of the three dimensional model developed in SolidWorks. COSMOSMotion allows for the inclusion of input forces, torques, springs, dampers, contact interfaces and gravitational effects. COSMOSMotion utilizes the ADAMS/Solver software (MSC Software Corp, Santa Ana, CA) to perform the physics based motion dynamics calculations based on component material properties, mass and inertia. The iterative solver that will be used is the GSTIFF solver which solves the equations of motion until the preferred error tolerance has been satisfied.

3.6 Application of the Hind Limb Model

The hind limb stifle ligament loads were evaluated at 10% discrete intervals ranging from initial stance to final stance. Therefore, the joint angles shown in TABLE VI (DeCamp 1997) and the corresponding ground reaction forces described in TABLE VII (Shahar 2004) and muscle forces described in TABLE VIII were applied to the hind limb model to simulate a given instance of the stance phase cycle. The stifle ligament forces and tibial translation were the outcome measures.

By approximating the stifle ligaments as springs, the changes in length of these springs would parallel the stretching of ligament tissue. Therefore, by monitoring the amount of stretch within the springs, the extent of stretching within the ligament during the stance phase would indicate the extent of the stifle ligament forces. By simulating both a CrCL intact stifle and a CrCL deficient stifle, the forces within the remaining ligaments prior to CrCL rupture and following CrCL rupture could be compared. Rupture of the CrCL was simulated by suppressing that ligament in the model.

3.6.1 Parametric Sensitivity Analysis

Since the proposed model is theoretical, uncertainty due to the input parameters exists. To evaluate the sensitivity of model outputs to changes in model input parameters, a parametric sensitivity analysis was conducted. Such an analysis alters one input by predetermined percentage values while holding all other inputs constant. The resulting change to the model outputs determines how sensitive the model is to that altered input parameter. This process was repeated for all applicable input parameters. The varied input parameters that generate the greatest change in model outputs are the input parameters for which the model is most sensitive.

3.6.2 Input Parameters

The varied input parameters of the proposed model included: ligament linear stiffness, unstressed ligament lengths (as determined by the reference strains), tibial plateau angle, femoromeniscal contact friction coefficients, muscle force magnitude, patellar ligament line of action angle, ground reaction force magnitude, body mass and femoral condyle radius.

3.6.2.1 Tibial Plateau Angle

Tibial plateau angle (TPA) has been the basis for much research and many surgical procedures. A greater TPA is commonly associated with an increased risk of CrCL deficiency (Morris and Lipowitz 2001). Also, a CrCL deficient stifle with a high TPA is commonly regarded as less stable (Slocum and Devine 1983). The basis for the model was a TPA of 22° as used in a previous study (Shahar and Milgram 2006). A TPA of 18°

has been reported as less likely to result in CrCL deficiency while TPAs greater than 22° have been reported to be more likely to be associated with CrCL deficiency (Morris and Lipowitz 2001). An average TPA of 26.5° was also reported in an in vitro study assessing the TPLO procedure (Warzee, Dejardin et al. 2001). Therefore, the six cases tested were TPAs of 18°, 20°, 22° (baseline), 24°, 26° and 28°.

3.6.2.2 Ligament Stiffness

Ligament stiffness values were determined based on previously reported data for two breeds (Wingfield, Amis et al. 2000). Since the model ligament stiffnesses were developed using medical imaging data from a dog larger than the dog from which the model geometry was developed, uncertainty in appropriate ligament CSA and stiffness applied to the model exists. All ligament stiffness values determined for use in the model were altered by the same percentage changes. The 5 cases tested were ligament stiffness percentage changes of -20%, -10%, 0% (baseline), 10% and 20%.

3.6.2.3 Cranial Cruciate Ligament Stiffness

Also of interest is the simulation of stiffness changes present in the CrCL only while all other ligament stiffnesses are held constant. Such a scenario may be representative of alteration of CrCL material properties as a response to stress exposure. The 5 cases tested were CrCL stiffness percentage changes of -20%, -10%, 0% (baseline), 10% and 20%.

3.6.2.4 Ligament Prestrain

Ligament prestrain is a representation of the amount of inherent stretch present within a ligament for a given position. Since the values used in the model were

essentially adopted from previous human studies (Blankevoort, Kuiper et al. 1991; Shahar and Banks-Sills 2004), uncertainty in the amount of prestrain in canine stifle ligaments is present. Alteration to ligament prestrain would be synonymous with either a looser or tighter ligament. The 5 cases tested were ligament prestrain percentage changes of -20%, -10%, 0% (baseline), 10% and 20%.

3.6.2.5 Cranial Cruciate Ligament Prestrain

As with ligament stiffness, alteration of only the CrCL prestrain while all other ligament prestrains are held constant simulated possible changes to the CrCL due to altered stifle biomechanics or CrCL degeneration. More prestrain represented a tighter CrCL while less prestrain represented a looser CrCL. The 5 cases tested were CrCL prestrain percentage changes of -20%, -10%, 0% (baseline), 10% and 20%.

3.6.2.6 Muscle Force Magnitude

Input muscle force magnitudes were determined previously from optimization techniques (Shahar and Banks-Sills 2002; Shahar and Banks-Sills 2004). Uncertainty in these values was assessed by altering all input muscle force magnitudes by the same percentage. The 5 cases tested were muscle force magnitude percentage changes of -20%, -10%, 0% (baseline), 10% and 20%.

3.6.2.7 Patellar Ligament Line of Action Angle

The direction of the patellar ligament relative to the TPA has also been the basis for much research and many surgical procedures. The 9 cases tested were a patellar ligament line of action angle (PLLAA) of -20°, -15°, -10°, -5°, 0° (baseline), 5°, 10°, 15°, and 20°. FIGURE 30 illustrates the angle of rotation of the patellar ligament force line of

action with cranial rotation (clockwise about the tibial tuberosity) corresponding to positive.

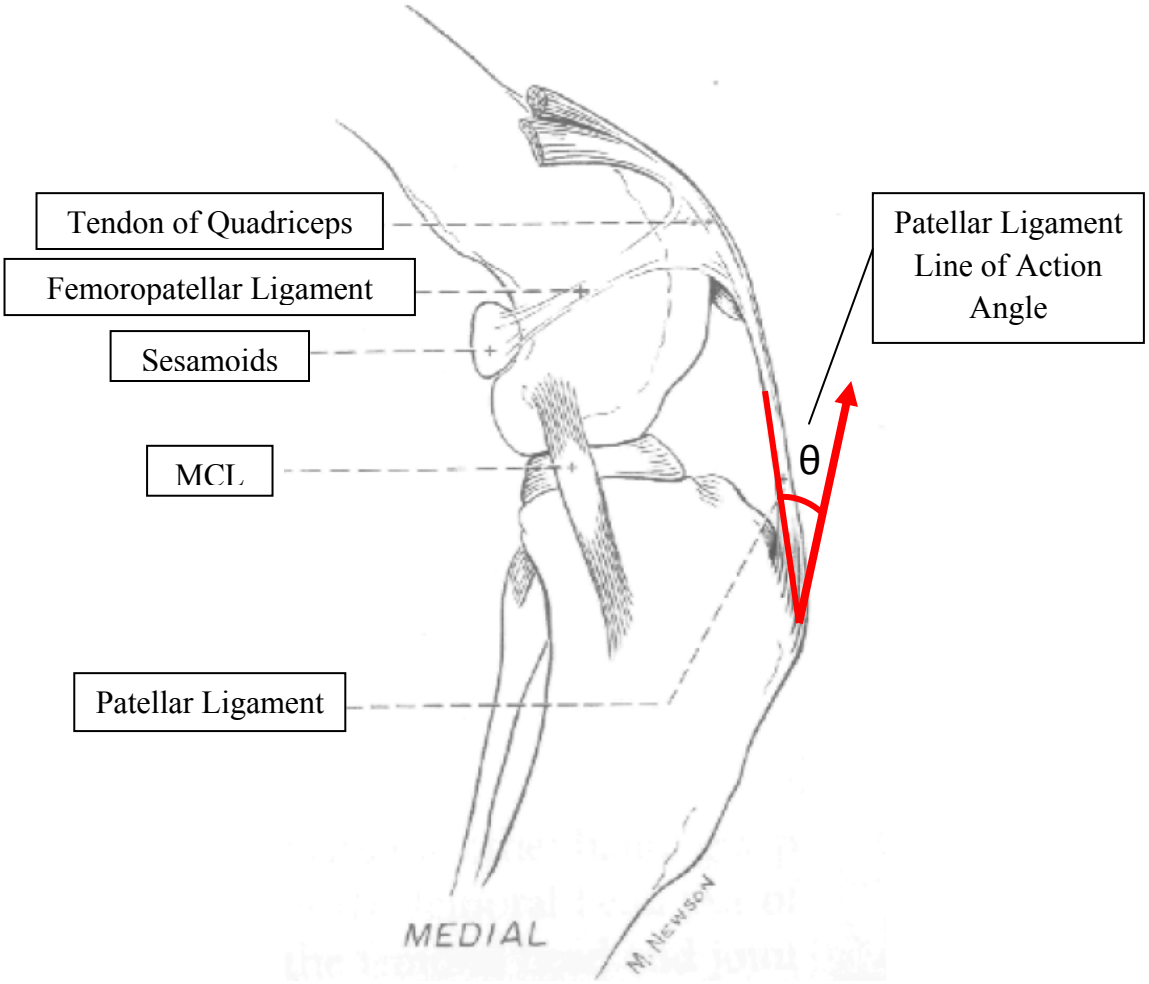

FIGURE 30 - Patellar ligament line of action angle, θ.

3.6.2.8 Ground Reaction Force Magnitude

Ground reaction forces are readily obtained using force plates and have been correlated with body weight (DeCamp 1997). Alteration of ground reaction forces in the model, however, simulated a change in weight that represents either an underweight or an overweight dog. The 5 cases tested were GRF magnitude percentage changes of -20%, -10%, 0% (baseline), 10% and 20%.

3.6.2.9 Body Mass

Since several parameters (GRF, ligament CSA and muscle force) were derived from and therfore directly related to body mass, alteration of body mass directly alters these parameters. Alteration of body mass and subsequent alteration of these parameters simulated variation in dog size while holding the model geometry, or dog height, constant. The 5 cases tested were body mass percentage changes of -20%, -10%, 0% (baseline), 10% and 20%.

3.6.2.10 Femoromeniscal Friction Coefficients

Friction between articulating surfaces in synovial joints is often considered negligible (Robertson, Caldwell et al. 2004; Shahar and Banks-Sills 2004). Frictional coefficients of 0.09 have been reported in osteoarthritic joints (Fung 1993), and in vitro frictional coefficient measurements have been reported below 0.03 in the healthy bovine knee (McCann, Ingham et al. 2009). The 4 cases tested were static and dynamic femoromeniscal friction coefficients of 0.03, 0.05 (baseline), 0.07 and 0.09.

3.6.2.11 Femoral Condyle Radius

Femoral condyle radius, FCR, has not been as extensively studied for its role in stifle stability as has the TPA or PLLAA. However, both the distal femur and the proximal tibia comprise the stifle joint and therefore both contribute to stifle biomechanics. The FCR was defined by superimposing an arc on a digital radiograph along the constant radius, articulating portion of the femoral condyle. FIGURE 31 illustrates this process.

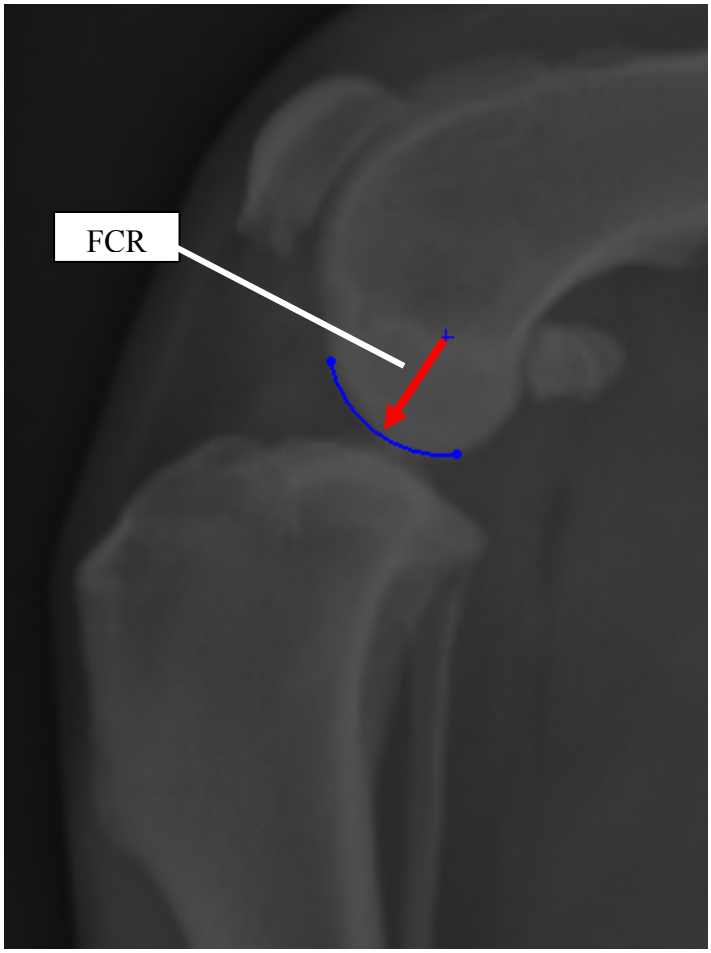

FIGURE 31 - Femoral condyle radius (FCR) as determined by radiograph.

The femoral condyle radius as depicted in FIGURE 31 was determined from radiographs for the breeds listed in

TABLE IX

FEMORAL CONDYLE RADII MEASUREMENTS FOR VARIOUS BREEDS

Breed	Patient number	Age (Y)	FCR (mm)
American Cocker Spaniel	#140231	13.1	6.9
Beagle	#128221	7.6	7.5
Bernese Mountain Dog	#117652	6.0	10.4
Dachshund	#119878	0.8	5.9
German Shepherd Dog	#132367	5.0	13.8
German Shepherd Dog	#146773	3.3	12.4
Great Dane	#150264	2.3	20.6
Greyhound	#101640	3.8	12.3
Greyhound	#128179	7.1	11.0
Labrador Retriever	#107117	7.0	12.1
Labrador Retriever	#150599	1.6	11.6
Labrador Retriever	#145809	2.5	10.4
Mastiff	#144394	2.1	17.8
Newfoundland	#127281	4.5	15.0
Newfoundland	#142808	4.6	13.0
Newfoundland	#144264	3.4	13.1
Pembroke Welsh Corgi	#149825	1.5	8.4
Rottweiler	#141512	2.1	14.6
Scottish Terrier	#115267	7.8	6.3
West Highland White Terrier	#130215	5.6	7.0

*Radiographs provided by Dr. Marcellin-Little, DEDV from the College of Veterinary Medicine, NC State University

Breeds such as the Newfoundland, Rottweiler and Labrador Retriever have been reported to be more likely to suffer CrCL deficiency while the Dachshund and Greyhound have been reported to be less likely to suffer CrCL deficiency (Witsberger, Villamil et al. 2008). The 6 cases tested were femoral condyle radii of 6 mm, 10 mm, 14 mm, 16 mm (baseline), 18 mm and 22 mm to include the range of values in TABLE IX.

3.6.3 Outcome Measures

The outcome measures used to determine model sensitivity included the stifle ligament forces and the tibial translation. Stifle ligament forces were normalized by body weight. The relative tibial translation was quantified as the difference between the distance from the tibial tuberosity and a fixed location on the femur pre- and post-stifle loading. Two normalized tibial translation measures were also used and are defined in TABLE X.

TABLE X

NORMALIZED TIBIAL TRANSLATION MEASURES

Method	Description	Equation*
1	Anatomical Tibial Translation (mm/mm)	$\frac{(FT_{deficient})_{loaded} - (FT_{intact})_{loaded}}{(FT_{intact})_{loaded}}$
2	Relative Tibial Translation per Body Mass (mm/kg)	$\frac{(FT_{deficient})_{loaded} - (FT_{intact})_{loaded}}{DogWeight}$

*FT is defined as the distance (in the cranial direction) from a fixed point on the femur to a fixed point on the tibia. Deficient or Intact denotes the status of the CrCL, and Loaded or Unloaded denotes whether or not FT is representative of weight bearing (loaded) or not (unloaded).

3.6.4 Model Verification

Output from the model was compared to results in the scientific literature to verify the model. The literature contains two types of studies from which applicable results can be compared to this model: in vitro and mathematical studies.

In vitro studies attempted to simulate weight bearing of the hind limb at mid-stride (Warzee, Dejardin et al. 2001). Warzee et al (2001) attempted to quantify the role

of the CrCL in stifle stability by measuring the amount of tibial translation following CrCL transection. The limb was stripped of muscle tissue leaving the stifle connective tissues intact, loaded with a ground reaction force and fitted with basic mechanical constraints to prevent the limb from collapsing by simulating the action of the quadriceps and gastrocnemius muscles. The outcome measures included the extent of cranial tibial translation prior to and following CrCL transection.

The second type of study is a theoretical mathematical model that attempted to simulate the loading within the stifle ligaments through the use of muscle force optimization (Shahar and Banks-Sills 2004). This study was based on the anatomical structures of a single canine hind limb and evaluated using equations of equilibrium and mathematical solvers (Shahar and Banks-Sills 2004). The outcomes of this study were stifle ligament forces at 10% increments of stance.

The results from these two studies were compared to the outcome measures of the stifle ligament forces and the cranial tibial translation described by the three dimensional canine hind limb computer model.

IV. RESULTS

The model was developed through several iterations of increasing complexity. Since future dissertation work will involve development of a model based on medical imaging data, the current proposed model was developed using geometric modeling functions available in SolidWorks (SolidWorks Corp, Concord, MA) to approximate boney geometry and key boney landmarks. The kinematic and kinetic inputs were then applied to this model, and ligament elements were implemented as described. Ligament forces, as well as the amount of tibial translation, were then determined for a CrCL intact and CrCL deficient stifle through simulation in COSMOSMotion (Structural Research and Analysis Corp, Santa Monica, CA). A parametric sensitivity analysis was conducted to assess the sensitivity of the model to varied input parameters.

4.1 Model Progression

Initially, the model was represented by a series of linkages, pins and brackets as shown in FIGURE 32.

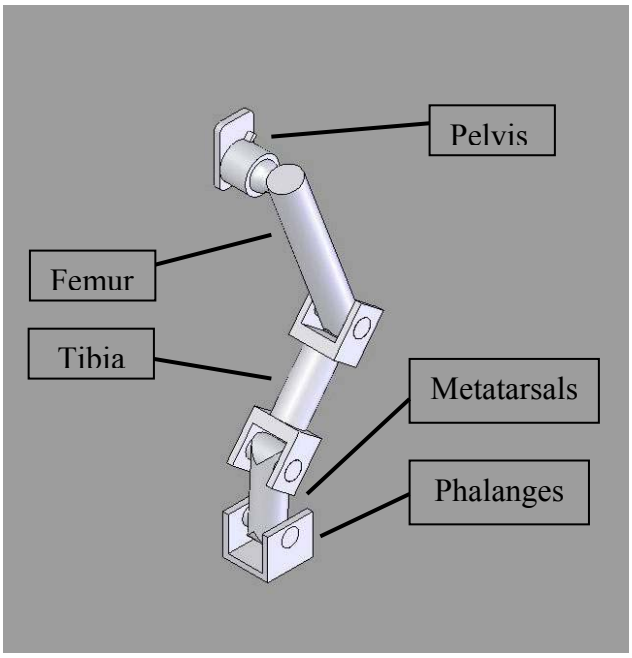

FIGURE 32 - Preliminary linkage model of hind limb.

Further modeling reduced the number of components to only those associated with the hind limb bones utilizing mates to define the joints rather than pins and brackets. This model version was still represented by primitive geometry as shown in FIGURE 33.

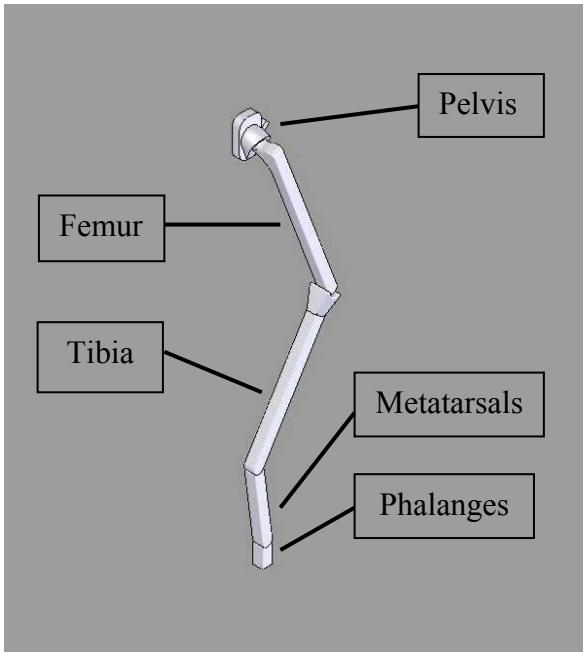

FIGURE 33 - Preliminary primitive model representing hind limb.

Bone geometry and joint representation was refined until the model shown in FIGURE 34 was developed.

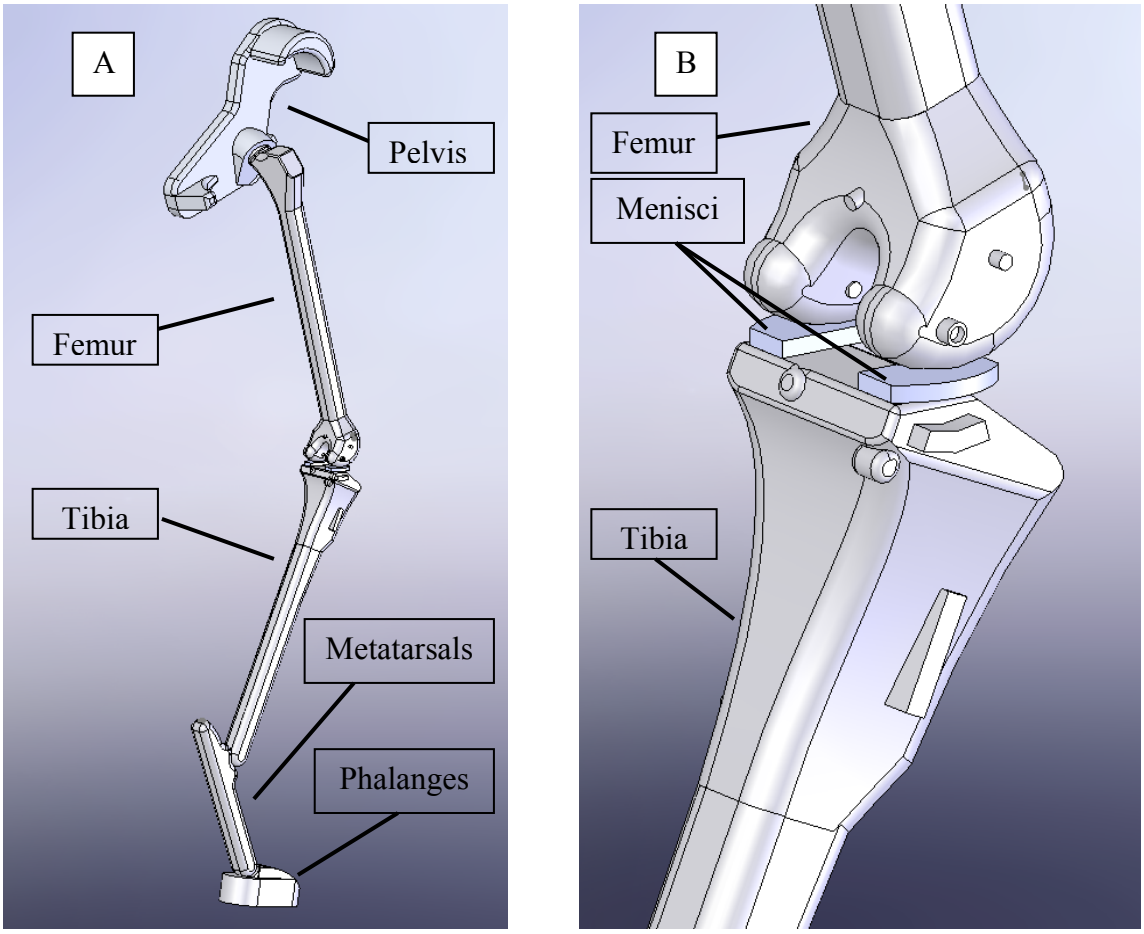

FIGURE 34 - Canine hind limb model (A) and stifle (B).

4.2 Model Description

FIGURE 35 details the stifle ligament elements while FIGURE 36 details the input muscle group and ground reaction force vectors.

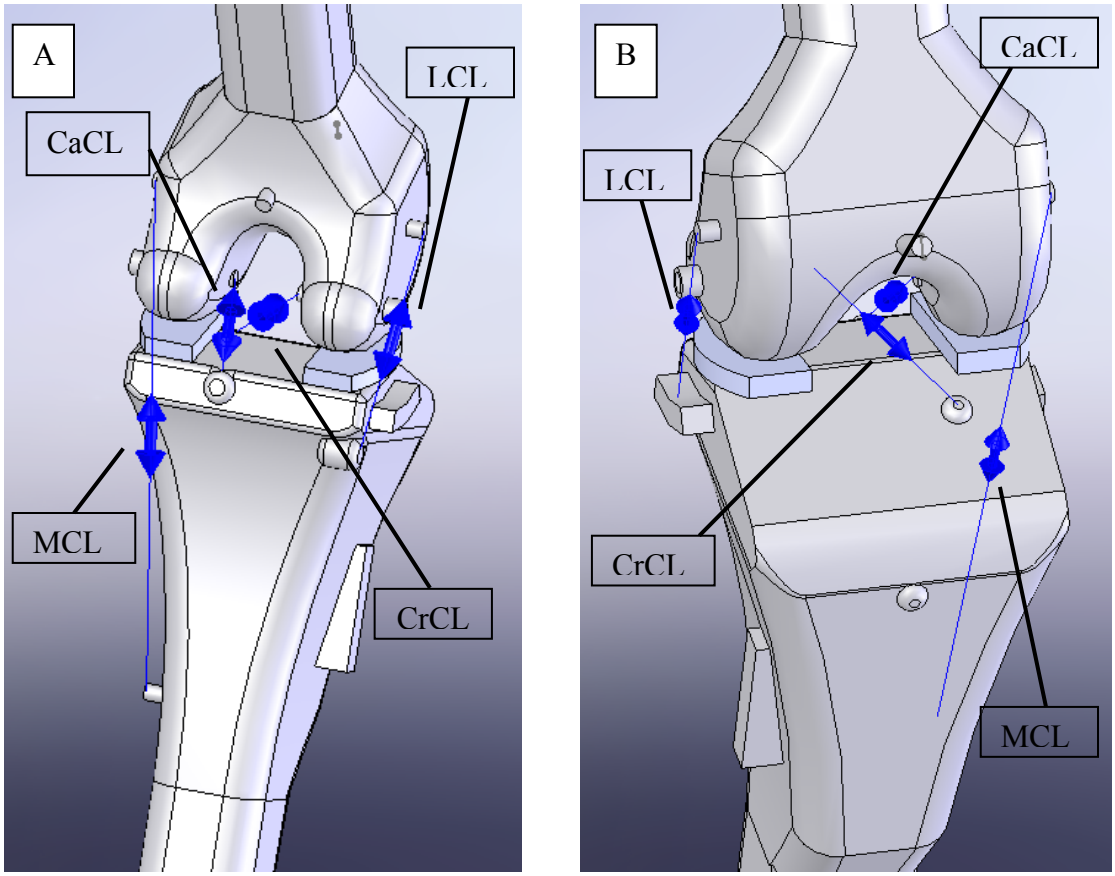

FIGURE 35 - Stifle ligament elements from caudal (A) and cranial (B) views.

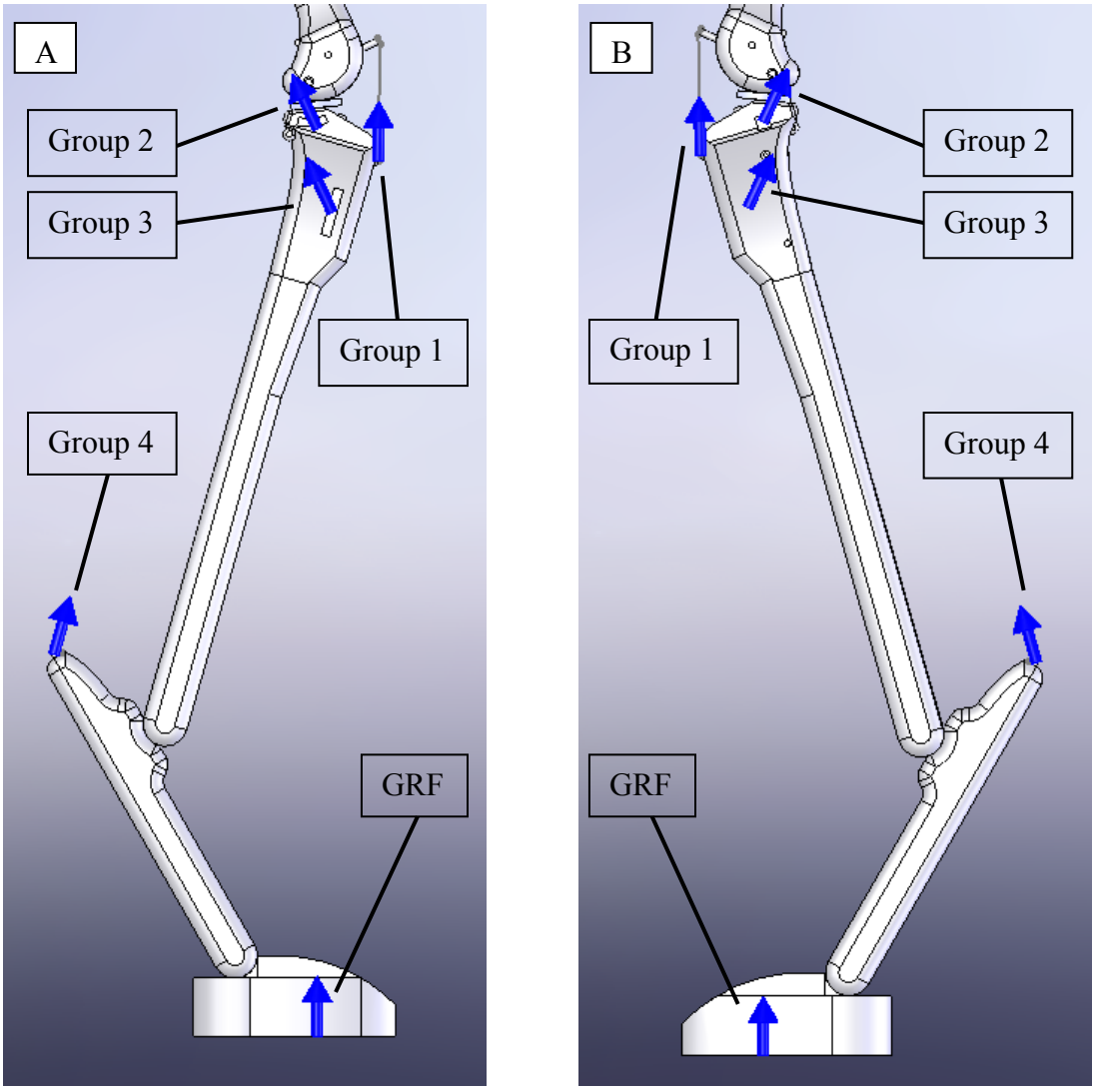

FIGURE 36 - Muscle group and ground reaction force vectors. Muscle groups 1, 2, 3 and 4 are the femoral stifle extensors, medial femoral stifle flexors, lateral femoral stifle flexors and tibial stifle flexors, respectively. Lateral (A) and medial (B) views.

4.2.1 Ligament Forces (Baseline Model)

Ligament forces were determined using the model shown in FIGURE 34 for discrete phases of stance (10% intervals). Model ligament forces normalized by body

weight for the CrCL intact and CrCL deficient stifle are displayed in FIGURE 37 and FIGURE 38, respectively.

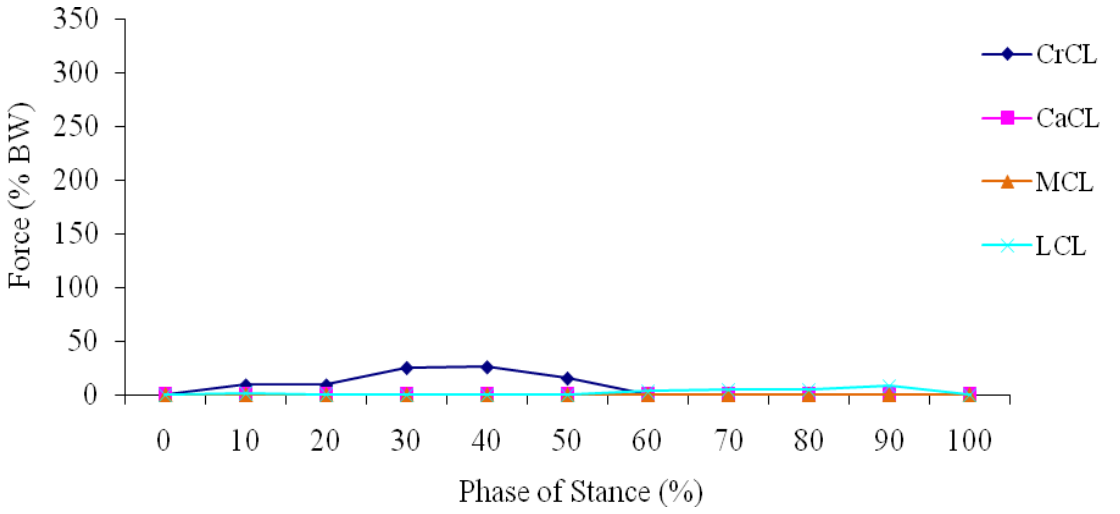

FIGURE 37 - Stifle ligament forces during stance in the CrCL intact stifle.

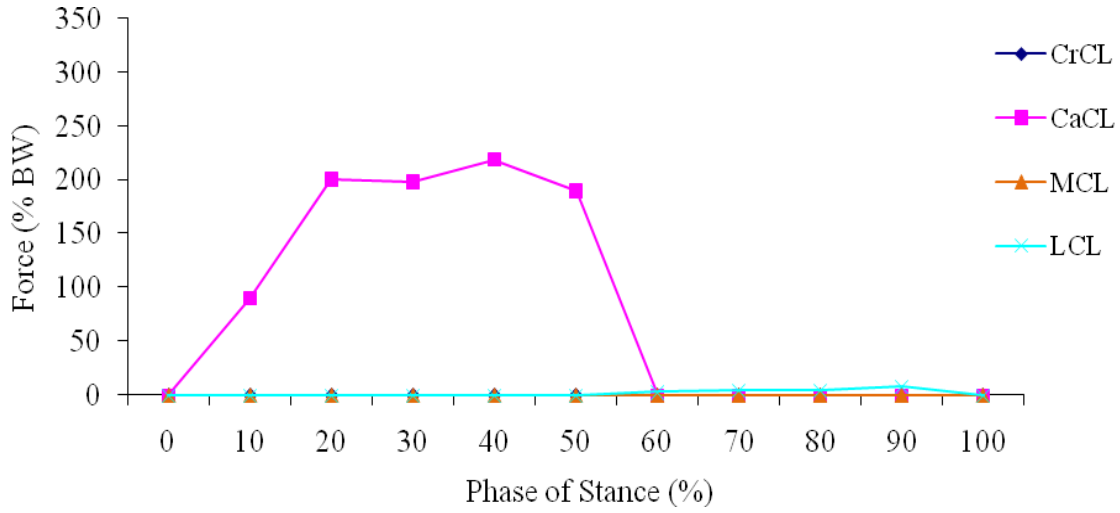

FIGURE 38 - Stifle ligament forces during stance in the CrCL deficient stifle.

In the CrCL intact stifle the peak CrCL force was 26% body weight (BW) and occurred at 40% stance. The CaCL was unloaded thoughout stance. The peak LCL force was 8% BW and occurred at 90% stance. The MCL was unloaded throughout stance. In the CrCL deficient stifle the peak CaCL force was 219% BW and occurred at 40% stance. The peak LCL force was 8% BW and occurred at 90% stance. The MCL was unloaded throughout stance.

4.2.2 Tibial Translation (Baseline Model)

Relative tibial translation between the CrCL intact and CrCL deficient stifle for each phase of stance is plotted in FIGURE 39.

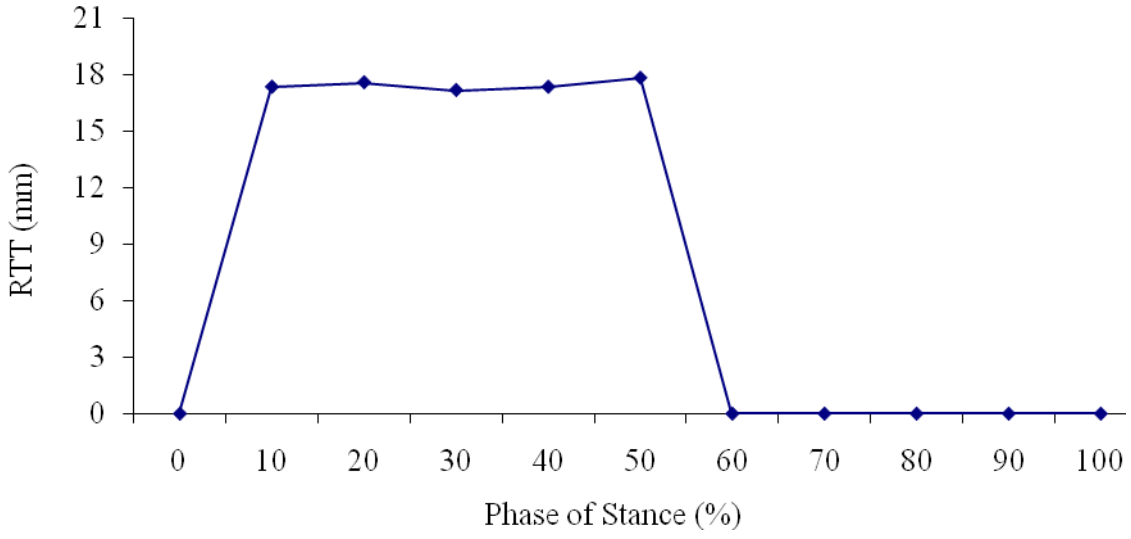

FIGURE 39 - Relative tibial translation (difference between CrCL intact and CrCL deficient tibial translations) for each phase of stance.

A peak relative tibial translation of 17.8 mm resulted at 50% stance. This corresponded with a relative tibial translation per body weight of 0.56 mm/kg and an anatomical tibial translation of 1.43.

4.3 Parametric Sensitivity Analysis

The baseline model ligament forces and tibial translation measures described in Sections 4.2.1 and 4.2.2, respectively, were the basis for comparison in the parametric sensitivity analysis. Each sensitivity analysis was conducted by varying a parameter by either a percentage change or a clinically applicable range. Each analysis was then assessed based on its deviation from the baseline results.

4.3.1 Tibial Plateau Angle

4.3.1.1 Ligament Forces for Tibial Plateau Angle Variation

Tibial plateau angle was altered in two degree intervals to simulate a common range representative of various breeds and CrCL deficieny likelihood. The six scenarios evaluated were a TPA of 18°, 20°, 22° (baseline), 24°, 26° and 28°.

The ligament forces during stance for the CrCL intact stifle and CrCL deficient stifle with a TPA of 18° are shown in FIGURE 40 and FIGURE 41, respectively.

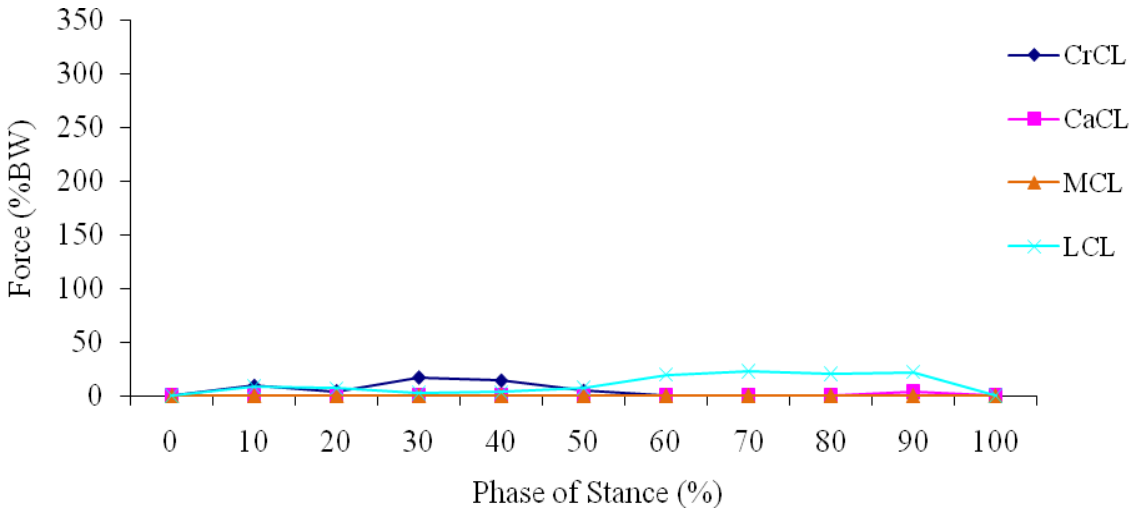

FIGURE 40 - Ligament forces for CrCL intact stifle (18° TPA).

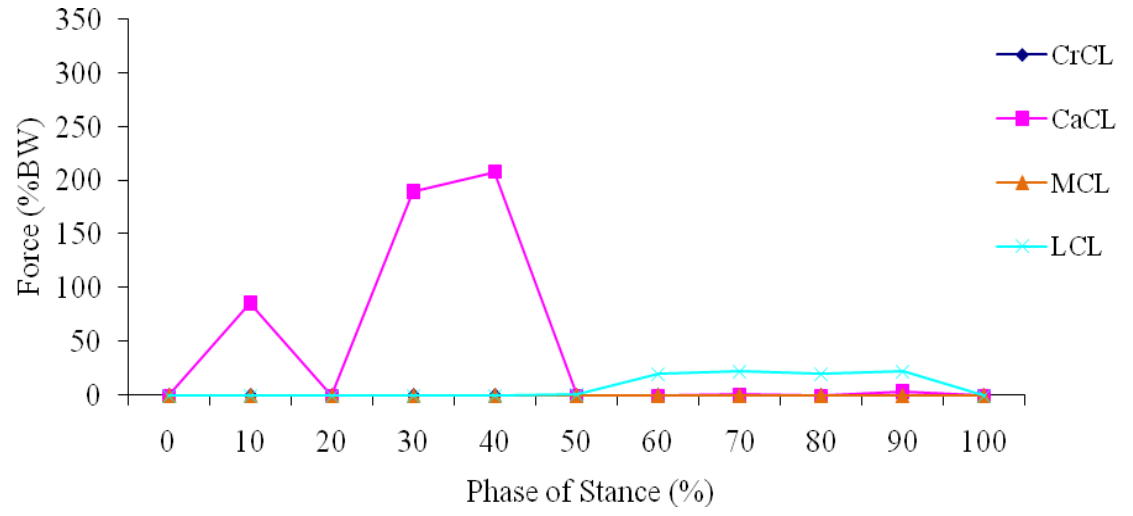

FIGURE 41 - Ligament forces for CrCL deficient stifle (18° TPA).

For the CrCL intact stifle the peak CrCL force was 17% body weight (BW) and occurred at 30% stance. The peak CaCL force was 4% BW and occurred at 90% stance. The peak LCL force was 23% BW and occurred at 70% stance. The MCL was unloaded

throughout stance. For the CrCL deficient stifle the peak CaCL force was 208% BW and occurred at 40% stance. The peak LCL force was 22% BW and occurred at both 70% and 90% stance. The MCL was unloaded throughout stance.

The ligament forces during stance for the CrCL intact and CrCL deficient stifle with a TPA of 20° are shown in FIGURE 42 and FIGURE 43, respectively.

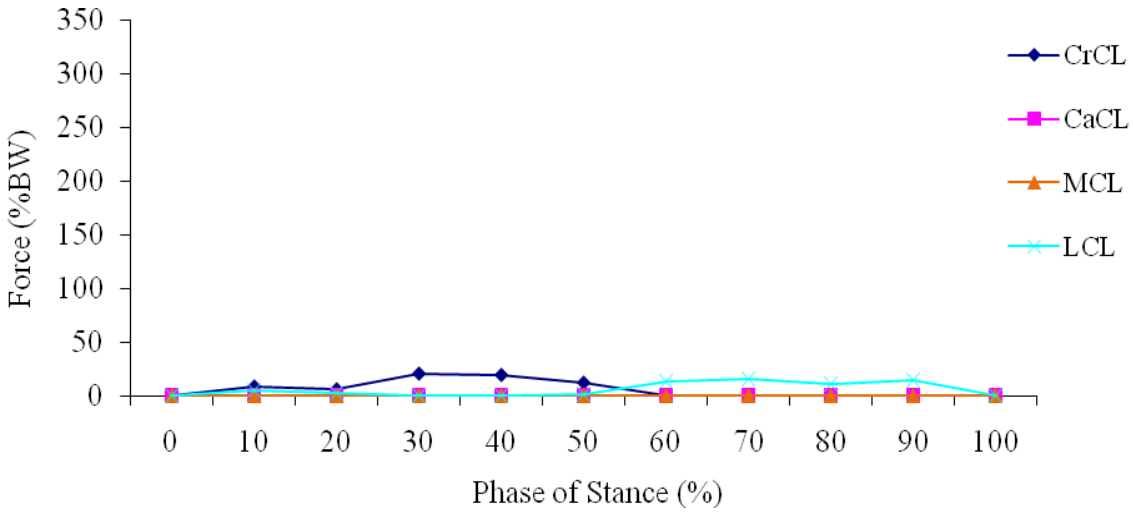

FIGURE 42 - Ligament forces for CrCL intact stifle (20° TPA).

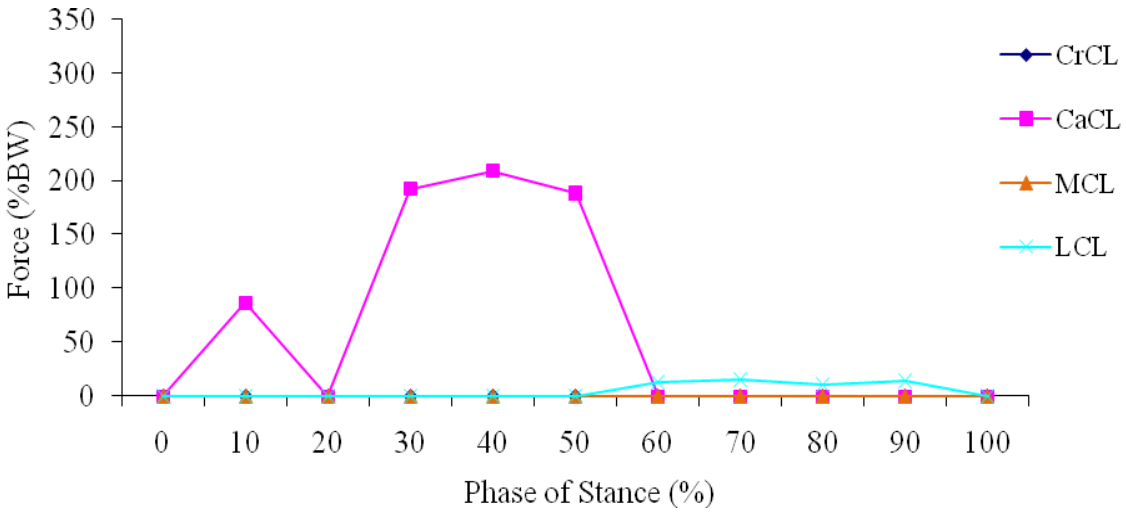

FIGURE 43 - Ligament forces for CrCL deficient stifle (20° TPA).

For the CrCL intact stifle the peak CrCL force was 21% body weight (BW) and occurred at 30% stance. The CaCL was unloaded thoughout stance. The peak LCL force was 15% BW and occurred at 70% stance. The MCL was unloaded throughout stance. In the CrCL deficient stifle the peak CaCL force was 209% BW and occurred at 40% stance. The peak LCL force was 15% BW and occurred at 70% stance. The MCL was unloaded throughout stance.

The ligament forces during stance for the CrCL intact and CrCL deficient stifle with a TPA of 22° (baseline) are shown in FIGURE 44 and FIGURE 45, respectively.

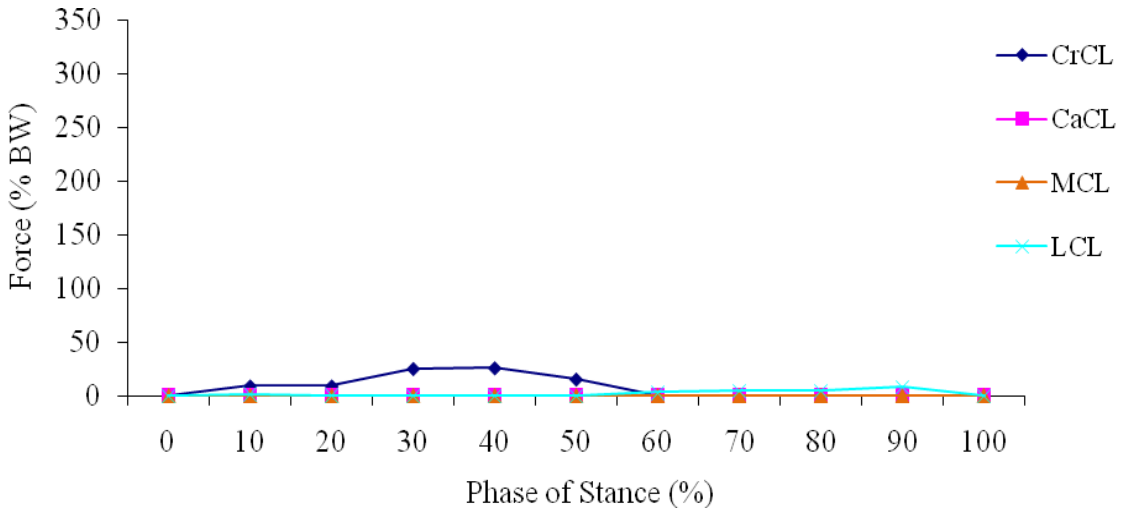

FIGURE 44 - Ligament forces for CrCL intact stifle (22° TPA).

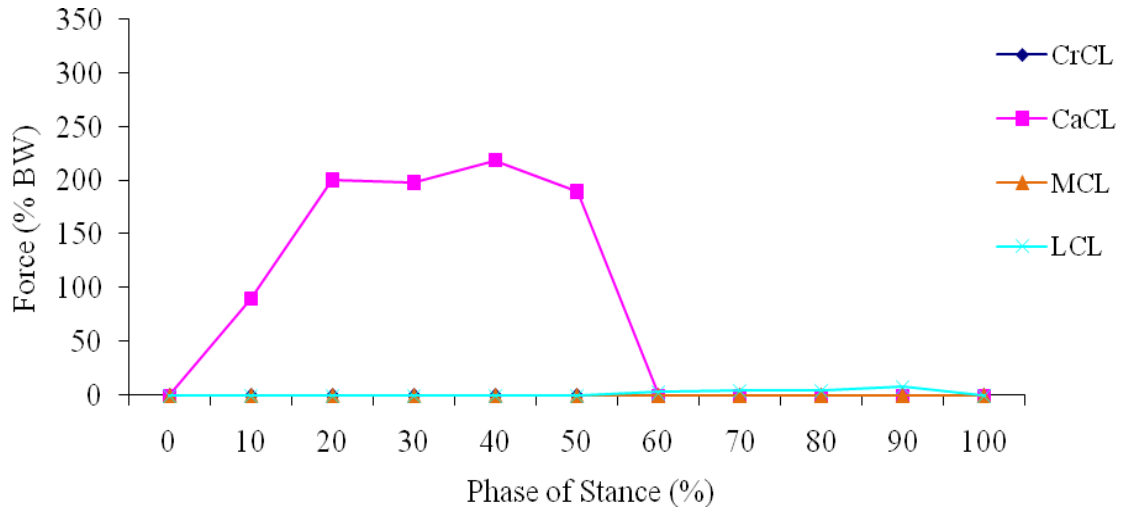

FIGURE 45 - Ligament forces for CrCL deficient stifle (22° TPA).

For the CrCL intact stifle the peak CrCL force was 26% body weight (BW) and occurred at 40% stance. The CaCL was unloaded thoughout stance. The peak LCL force was 8% BW and occurred at 90% stance. The MCL was unloaded throughout stance. For the

CrCL deficient stifle the peak CaCL force was 219% BW and occurred at 40% stance. The peak LCL force was 8% BW and occurred at 90% stance. The MCL was unloaded throughout stance.

The ligament forces during stance for the CrCL intact and CrCL deficient stifle with a TPA of 24° are shown in FIGURE 46 and FIGURE 47, respectively.

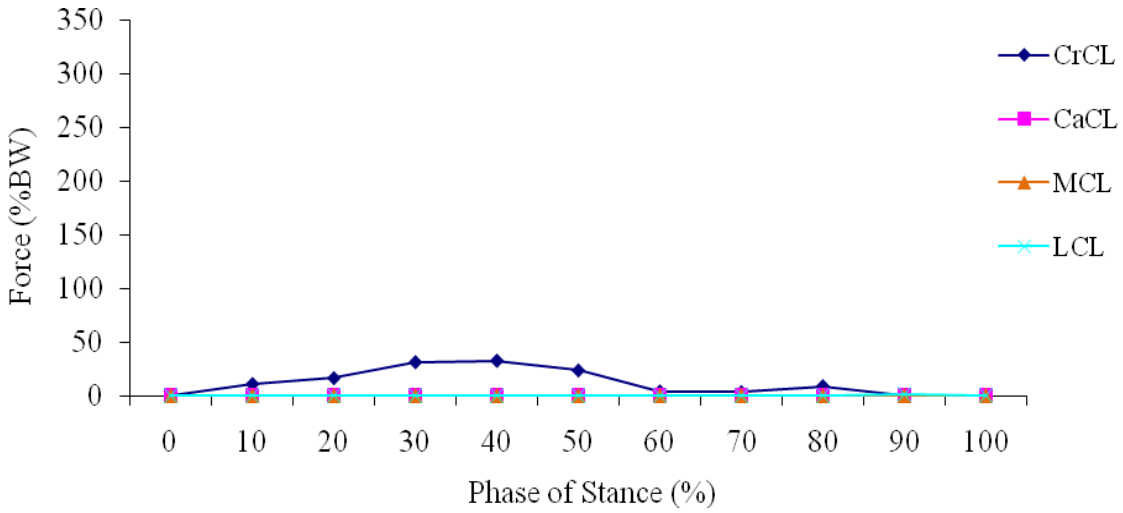

FIGURE 46 - Ligament forces for CrCL intact stifle (24° TPA).

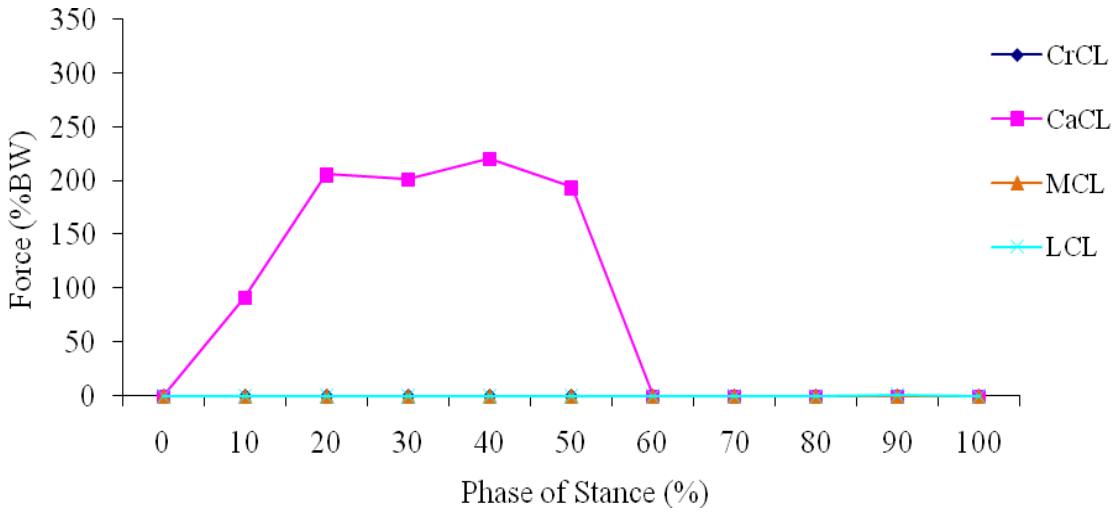

FIGURE 47 - Ligament forces for CrCL deficient stifle (24° TPA).

For the CrCL intact stifle the peak CrCL force was 32% body weight (BW) and occurred at 40% stance. The CaCL was unloaded thoughout stance. The peak LCL force was 2% BW and occurred at 90% stance. The MCL was unloaded throughout stance. For the CrCL deficient stifle the peak CaCL force was 220% BW and occurred at 40% stance. The peak LCL force was 2% BW and occurred at 90% stance. The MCL was unloaded throughout stance.

The ligament forces during stance for the CrCL intact and CrCL deficient stifle with a TPA of 26° are shown in FIGURE 48 and FIGURE 49, respectively.

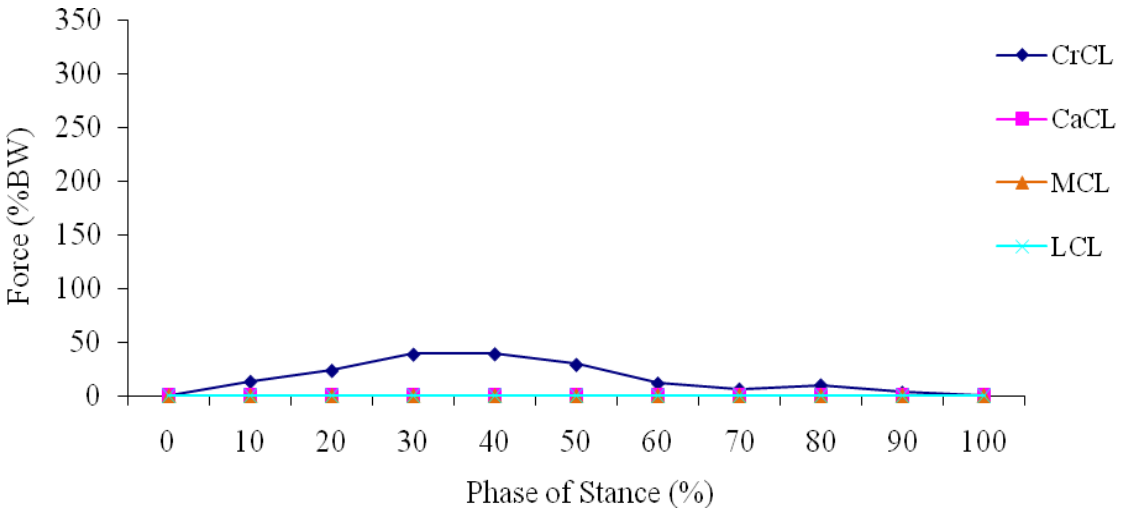

FIGURE 48 - Ligament forces for CrCL intact stifle (26° TPA).

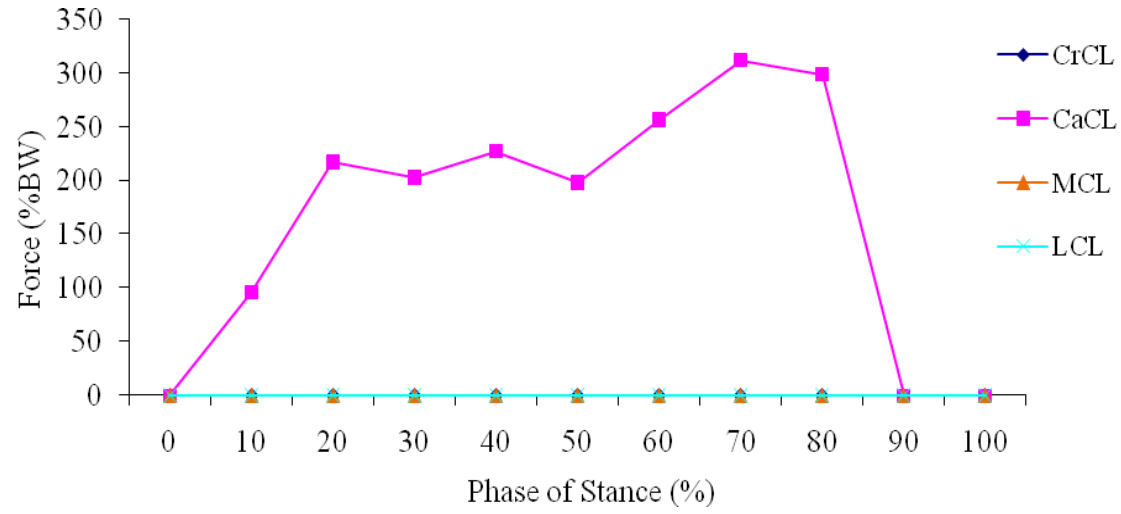

FIGURE 49 - Ligament forces for CrCL deficient stifle (26° TPA).

For the CrCL intact stifle the peak CrCL force was 39% body weight (BW) and occurred at 40% stance. The CaCL, LCL and MCL were unloaded throughout stance. For the

CrCL deficient stifle the peak CaCL force was 311% BW and occurred at 70% stance. The LCL and MCL were unloaded throughout stance.

The ligament forces during stance for the CrCL intact and CrCL deficient stifle with a TPA of 28° areshown in FIGURE 50 and FIGURE 51, respectively.

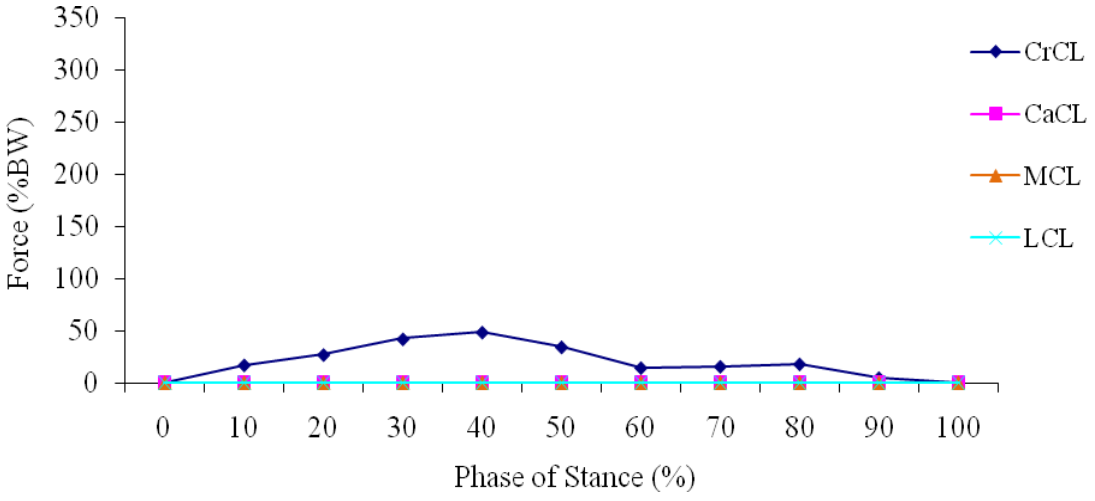

FIGURE 50 - Ligament forces for CrCL intact stifle (28° TPA).

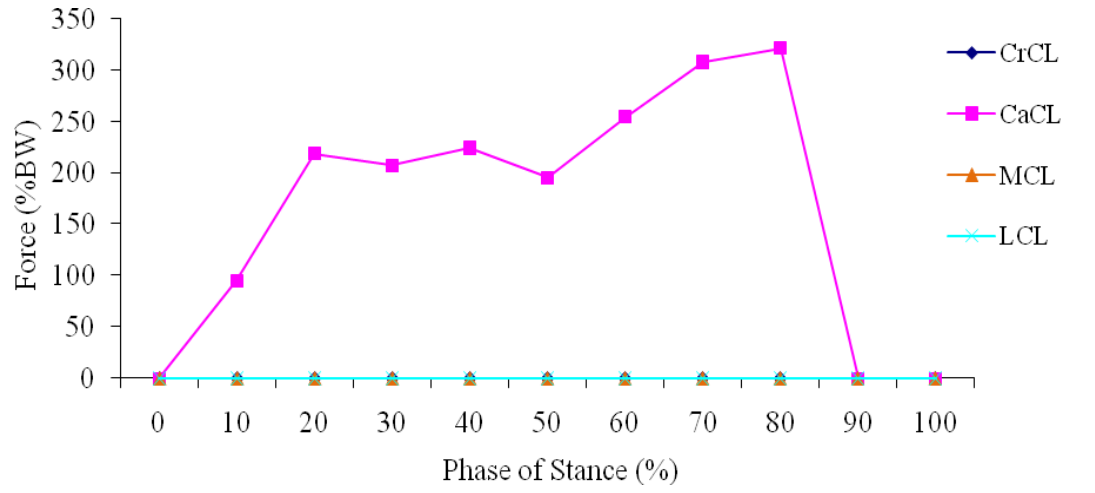

FIGURE 51 - Ligament forces for CrCL deficient stifle (28° TPA).

For the CrCL intact stifle the peak CrCL force was 49% BW and occurred at 40% stance. The CaCL, LCL and MCL were unloaded throughout stance. For the CrCL deficient stifle the peak CaCL force was 322% BW and occurred at 80% stance. The LCL and MCL were unloaded throughout stance.

4.3.1.2 Ligament Forces Summary for Tibial Plateau Angle Variation

Ligament forces for each phase of stance for varying TPA were determined in the CrCL intact and CrCL deficient stifle. Peak CrCL forces varied by 32% BW ranging from 17% BW to 49% BW for varying TPA in the CrCL intact stifle. Peak CaCL forces varied by 114% BW ranging from 208% BW to 322% BW in the CrCL deficient stifle. The peak CrCL forces for varying TPA for the CrCL intact stifle are shown in FIGURE 52, and the peak CaCL forces for varying TPA for the CrCL deficient stifle are shown in FIGURE 53.

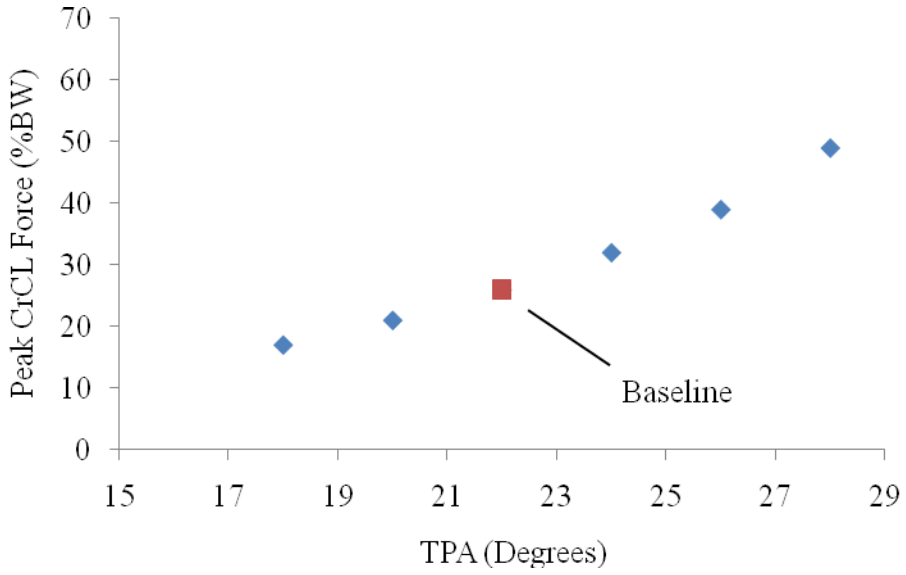

FIGURE 52 - Peak CrCL forces in the CrCL intact stifle for each TPA.

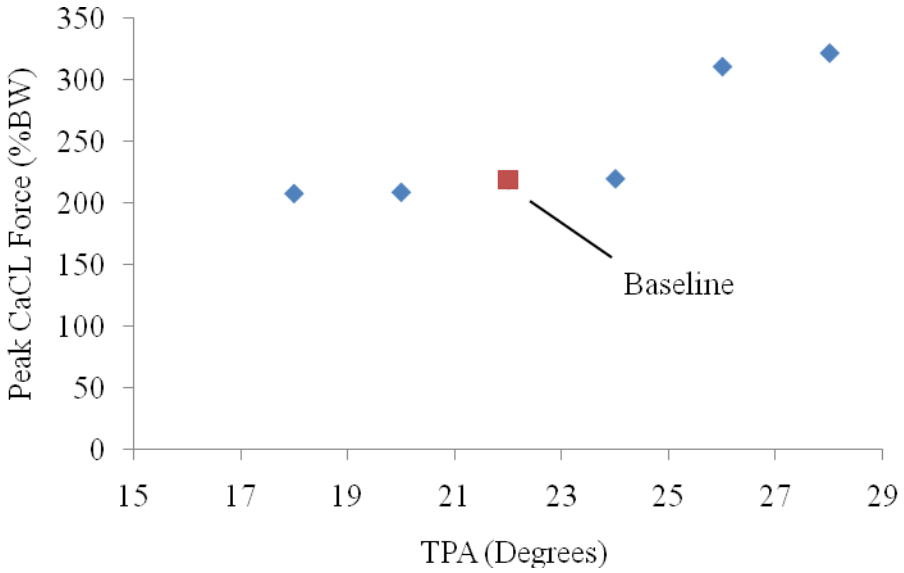

FIGURE 53 - Peak CaCL forces in the CrCL deficient stifle for each TPA.

4.3.1.3 Tibial Translation for Tibial Plateau Angle Variation

The relative tibial translation across the phases of stance is plotted in FIGURE 54.

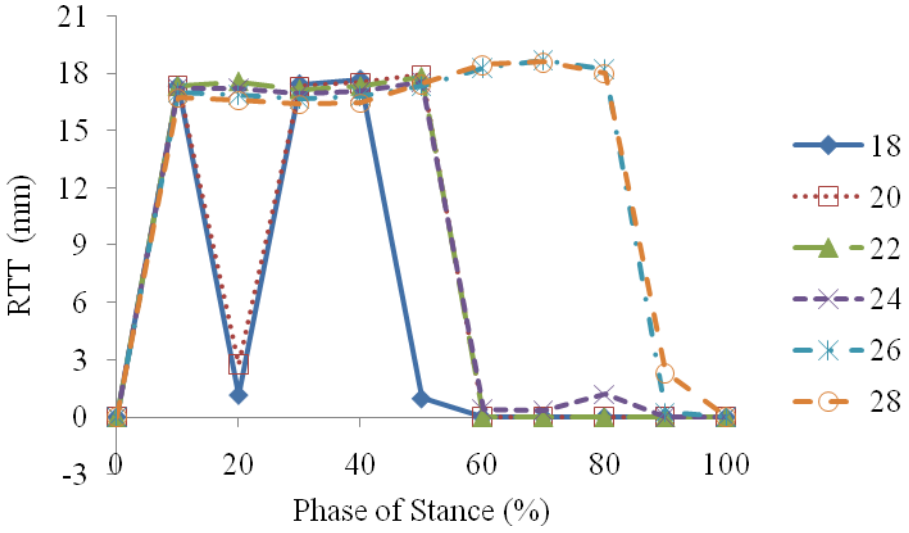

FIGURE 54 - Relative tibial translation between the CrCL intact and deficient stifle models for each TPA scenario during stance.

The higher TPAs showed more relative tibial translation activation in the later phases of stance while the lower TPAs showed reduced relative tibial translation activation in the earlier phases of stance.

4.3.1.4 Tibial Translation Summary for Tibial Plateau Angle Variation

The peak relative tibial translation, the phase of stance at which it occurred and the corresponding relative tibial translation per body mass and anatomical tibial translation for each TPA are listed in TABLE XI. The peak relative tibial translation values are plotted in FIGURE 55.

TABLE XI

PEAK TIBIAL TRANSLATION VALUES FOR EACH TPA EVALUATED

TPA (Degrees)	18.0	20.0	22.0	24.0	26.0	28.0
Stance Phase (%)	40	50	50	50	70	70
Peak RTT (mm)*	17.7	17.9	17.8	17.6	18.7	18.6
RTT/BM (mm/kg)**	0.55	0.56	0.56	0.55	0.58	0.58
ATT***	1.20	1.47	1.43	1.36	5.18	5.03

*RTT = Relative Tibial Translation = $(\mathrm{FT}_{\mathrm{deficient}})_{\mathrm{loaded}} - (\mathrm{FT}_{\mathrm{intact}})_{\mathrm{loaded}}$

**RTT/BM = Relative Tibial Translation per Body Mass

***ATT = Anatomical Tibial Translation = $\dfrac{(\mathrm{FT}_{\mathrm{deficient}})_{\mathrm{loaded}} - (\mathrm{FT}_{\mathrm{intact}})_{\mathrm{loaded}}}{(\mathrm{FT}_{\mathrm{intact}})_{\mathrm{loaded}}}$

where FT denotes the craniocaudal distance from a fixed point on the femur to a fixed point on the tibia, deficient denotes the CrCL was suppressed, intact denotes the CrCL was not suppressed and loaded denotes weight bearing

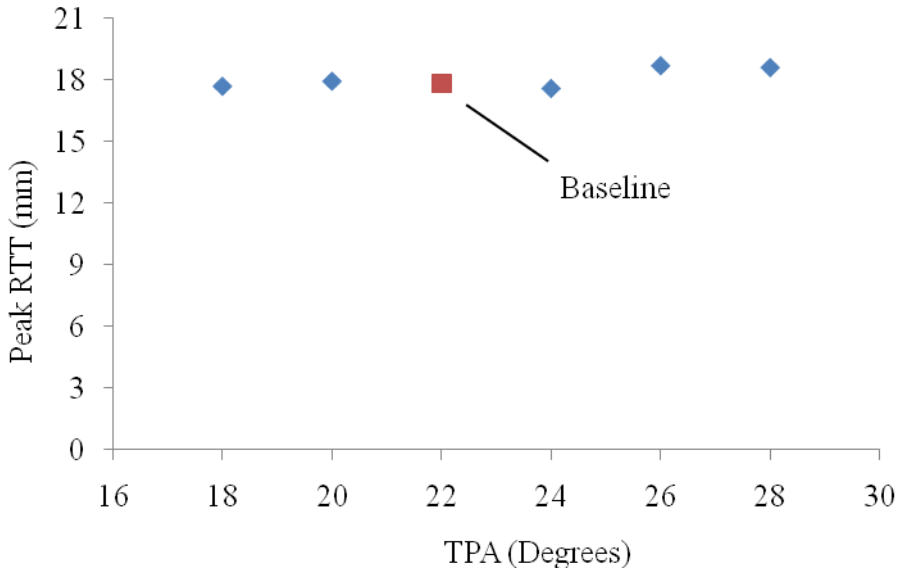

FIGURE 55 - Peak relative tibial translation for each TPA.

Peak relative tibial translation varied by +5.1/-1.1% from baseline for varying TPA.

4.3.2 Ligament Stiffness (All Stifle Ligaments)

4.3.2.1 Ligament Forces for Ligament Stiffness (All Stifle Ligaments) Variation

Ligament material property variation was simulated by altering the stifle ligament stiffness values. All model ligament stiffness values were altered from baseline by the same percentage. The five scenarios evaluated in the parametric sensitivity analysis consisted of percentage changes of -20%, -10%, 0% (baseline), 10% and 20%. Baseline stiffness values were 4230 N/ε, 7150 N/ε, 6350 N/ε and 3650 N/ε for the CrCL, CaCL, MCL and LCL, respectively. Therefore, ranges varied from 3380 N/ε to 5080 N/ε, from 5720 N/ε to 8580 N/ε, from 5080 N/ε to 7620 N/ε and from 2920 N/ε to 4380 N/ε for the CrCL, CaCL, MCL and LCL, respectively.

The ligament forces during stance for the CrCL intact and CrCL deficient stifle with a -20% ligament stiffness change are shown in FIGURE 56 and FIGURE 57, respectively.

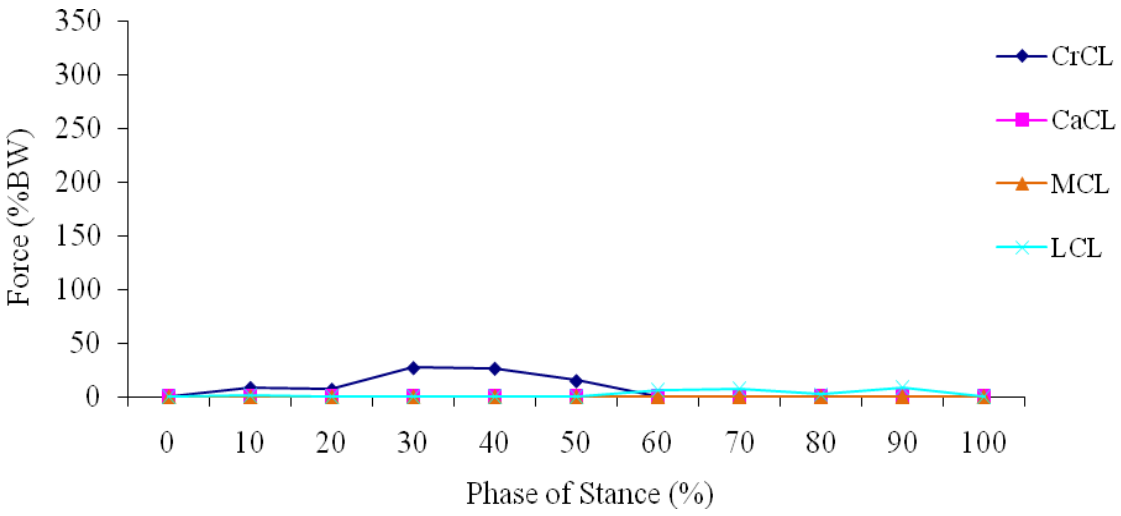

FIGURE 56 - Ligament forces for CrCL intact stifle (-20% stiffness change).

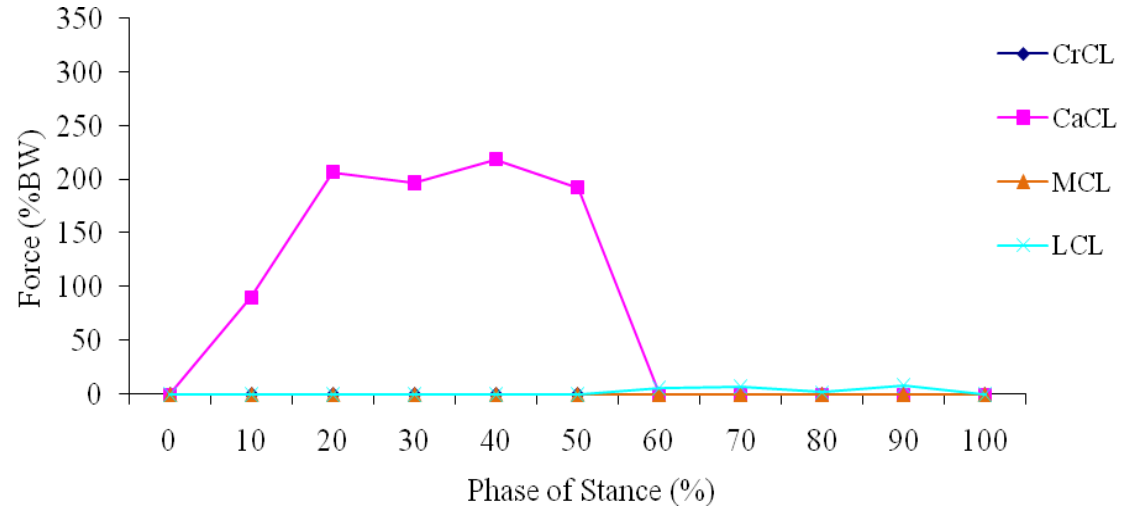

FIGURE 57 - Ligament forces for CrCL deficient stifle (-20% stiffness change).

For the CrCL intact stifle the peak CrCL force was 27% BW and occurred at 30% stance. The peak LCL force was 8% BW and occurred at 90% stance. The CaCL and MCL were unloaded throughout stance. For the CrCL deficient stifle the peak CaCL force was 219% BW and occurred at 40% stance. The peak LCL force was 8% BW and occurred at 90% stance. The MCL was unloaded throughout stance.

The ligament forces during stance for the CrCL intact and CrCL deficient stifle with a -10% ligament stiffness change are shown in FIGURE 58 and FIGURE 59, respectively.

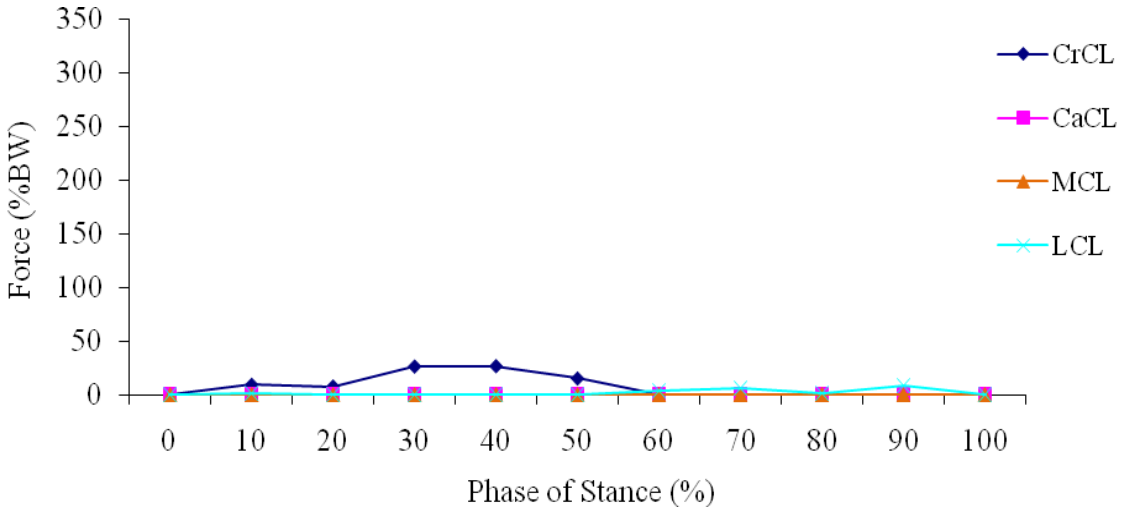

FIGURE 58 - Ligament forces for CrCL intact stifle (-10% stiffness change).

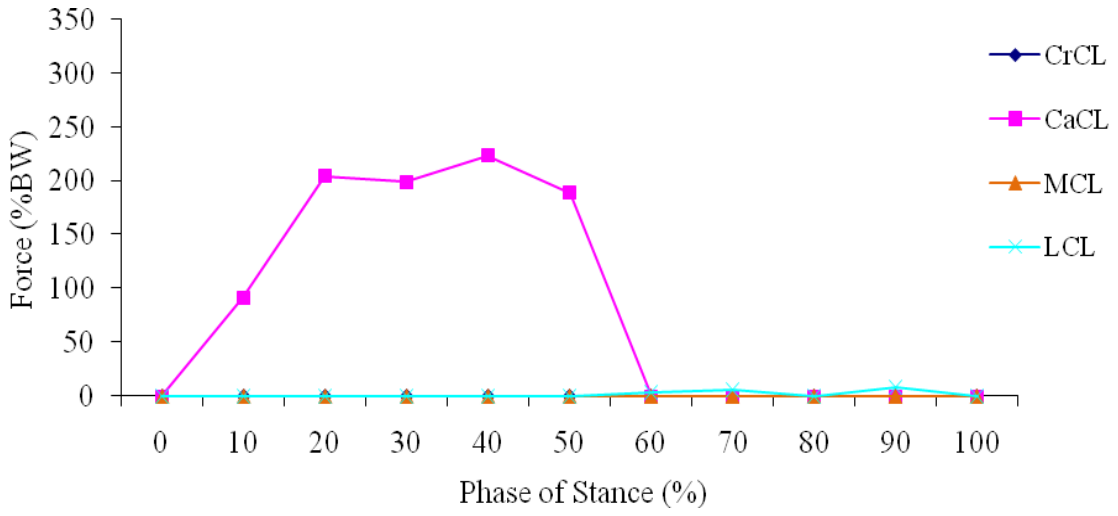

FIGURE 59 - Ligament forces for CrCL deficient stifle (-10% stiffness change).

For the CrCL intact stifle the peak CrCL force was 26% BW and occurred at 40% stance. The peak LCL force was 9% BW and occurred at 90% stance. The CaCL and MCL were unloaded throughout stance. For the CrCL deficient stifle the peak CaCL force was 223% BW and occurred at 40% stance. The peak LCL force was 8% BW and occurred at 90% stance. The MCL was unloaded throughout stance.

The ligament forces during stance for the CrCL intact and CrCL deficient stifle with a 0% (baseline) ligament stiffness change are shown in FIGURE 60 and FIGURE 61, respectively.

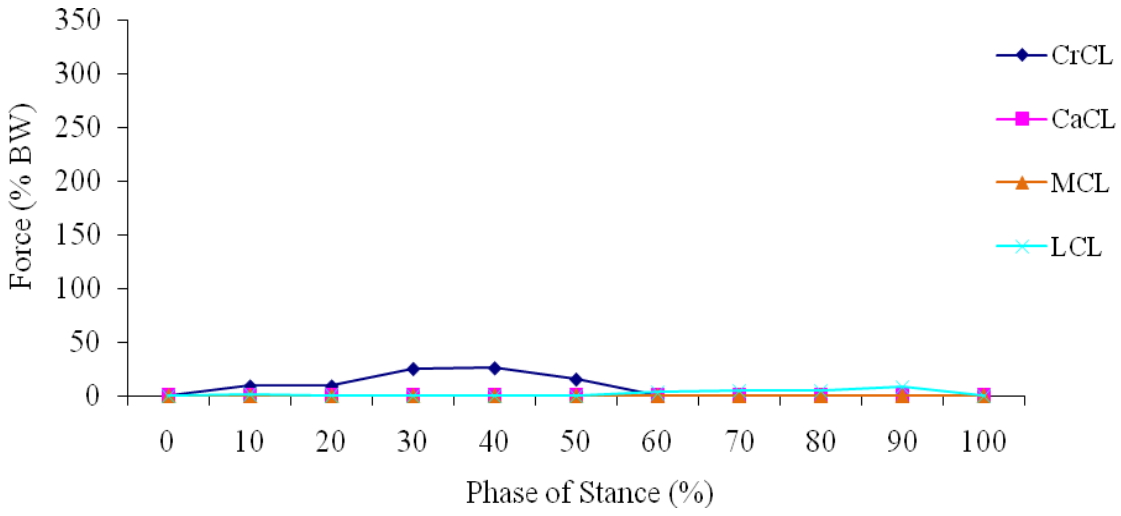

FIGURE 60 - Ligament forces for CrCL intact stifle (0% stiffness change).

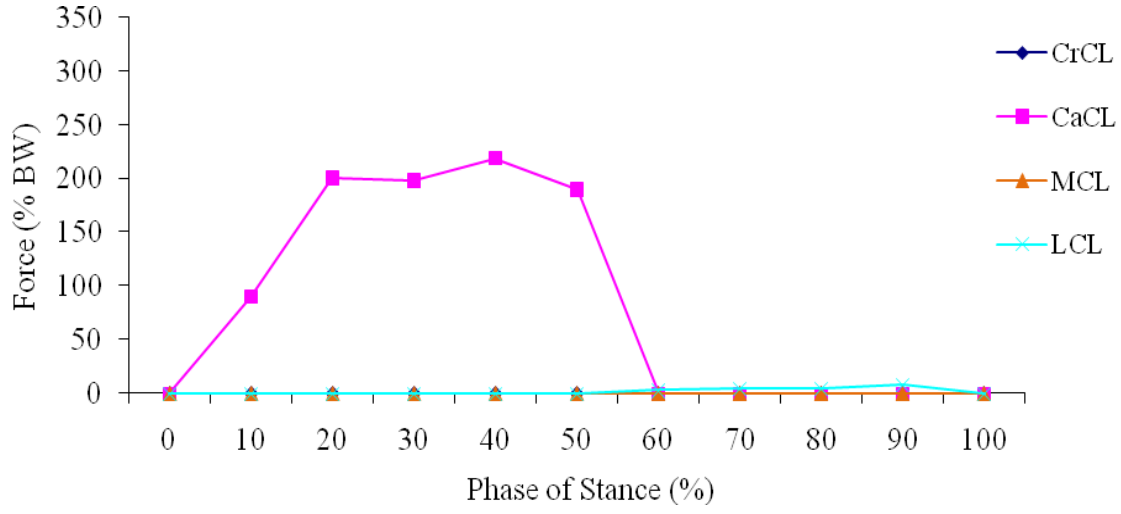

FIGURE 61 - Ligament forces for CrCL deficient stifle (0% stiffness change).

For the CrCL intact stifle the peak CrCL force was 26% body weight (BW) and occurred at 40% stance. The CaCL was unloaded thoughout stance. The peak LCL force was 8% BW and occurred at 90% stance. The MCL was unloaded throughout stance. For the

CrCL deficient stifle the peak CaCL force was 219% BW and occurred at 40% stance. The peak LCL force was 8% BW and occurred at 90% stance. The MCL was unloaded throughout stance.

The ligament forces during stance for the CrCL intact and CrCL deficient stifle with a 10% ligament stiffness change are shown in FIGURE 62 and FIGURE 63, respectively.

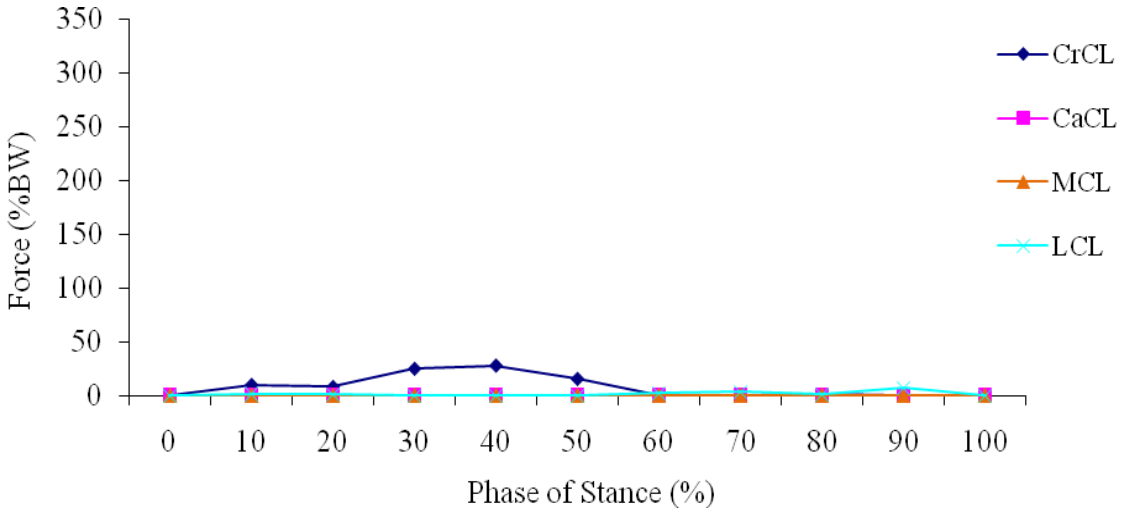

FIGURE 62 - Ligament forces for CrCL intact stifle (+10% stiffness change).

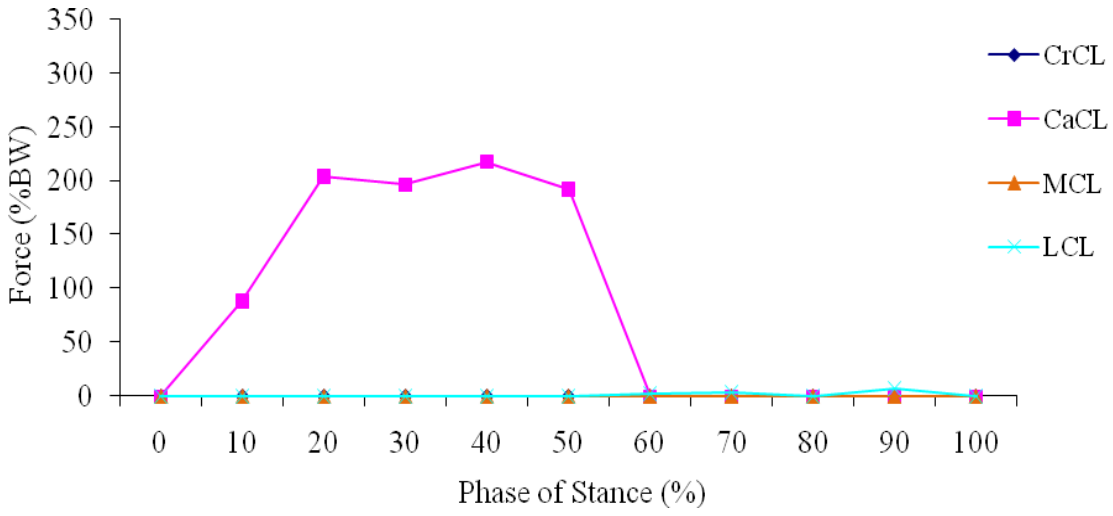

FIGURE 63 - Ligament forces for CrCL deficient stifle (+10% stiffness change).

For the CrCL intact stifle the peak CrCL force was 28% BW and occurred at 40% stance. The peak LCL force was 7% BW and occurred at 90% stance. The CaCL and MCL were unloaded throughout stance. For the CrCL deficient stifle the peak CaCL force was 218% BW and occurred at 40% stance. The peak LCL force was 7% BW and occurred at 90% stance. The MCL was unloaded throughout stance.

The ligament forces during stance for the CrCL intact and CrCL deficient stifle with a 20% ligament stiffness change are shown in FIGURE 64 and FIGURE 65, respectively.

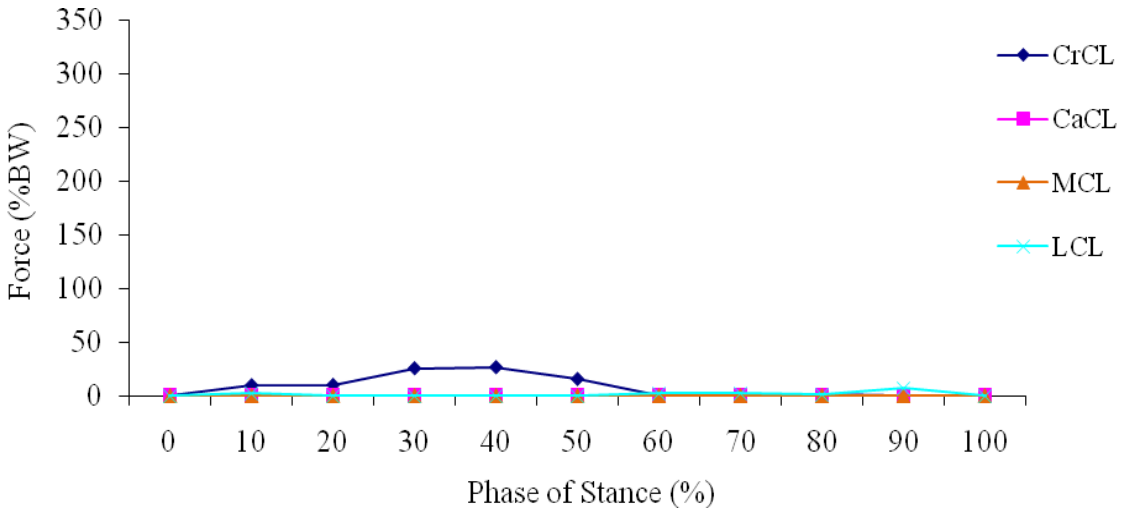

FIGURE 64 - Ligament forces for CrCL intact stifle (+20% stiffness change).

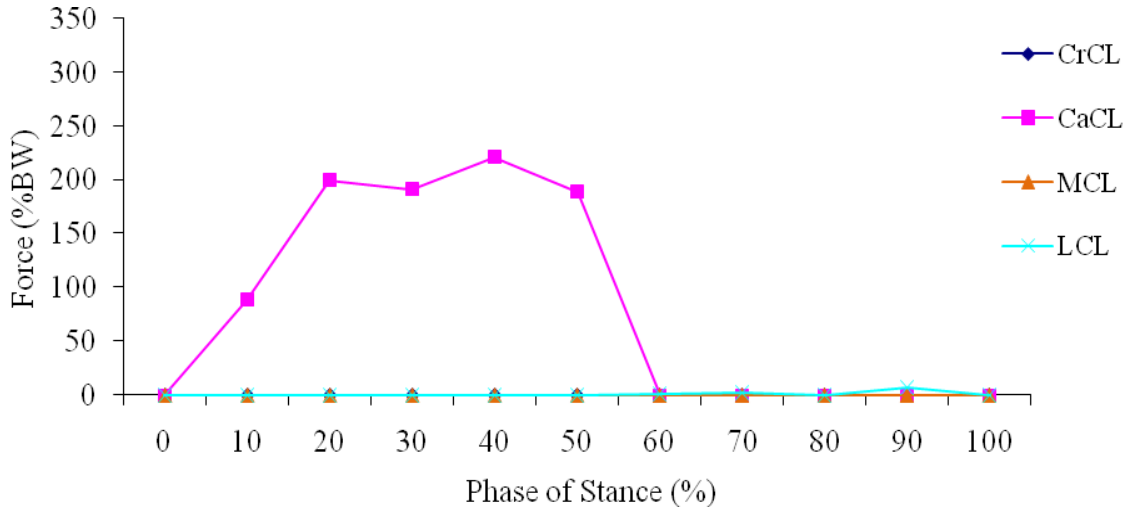

FIGURE 65 - Ligament forces for CrCL deficient stifle (+20% stiffness change).

For the CrCL intact stifle the peak CrCL force was 27% BW and occurred at 40% stance. The peak LCL force was 7% BW and occurred at 90% stance. The CaCL and MCL were unloaded throughout stance. For the CrCL deficient stifle the peak CaCL force was 221%

BW and occurred at 40% stance. The peak LCL force was 7% BW and occurred at 90% stance. The MCL was unloaded throughout stance.

4.3.2.2 Ligament Forces Summary for Ligament Stiffness (All Stifle Ligaments) Variation

Ligament forces for each phase of stance for varying ligament stiffness were determined in the CrCL intact and CrCL deficient stifle. Peak CrCL forces varied by 2% BW ranging from 26% BW to 28% BW for varying stifle ligament stiffness in the CrCL intact stifle. Peak CaCL forces varied by 5% BW ranging from 218% BW to 223% BW in the CrCL deficient stifle.The peak CrCL forces for varying ligament stiffness for the CrCL intact stifle are shown in FIGURE 66, and the peak CaCL forces for varying ligament stiffness for the CrCL deficient stifle are shown in FIGURE 67.

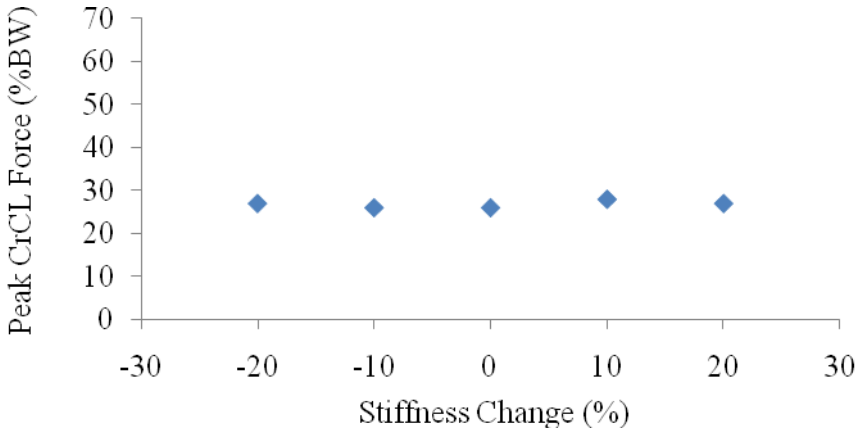

FIGURE 66 - Peak CrCL forces in the CrCL intact stifle for each percentage ligament stiffness change from the baseline stiffness.

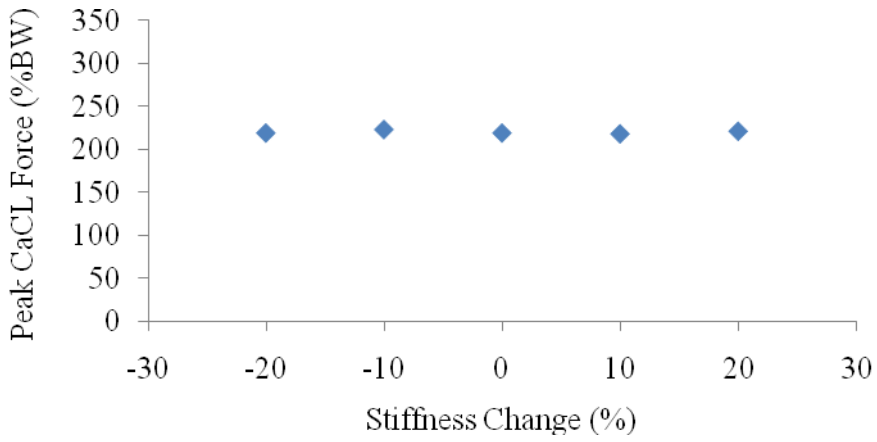

FIGURE 67 - Peak CaCL forces in the CrCL deficient stifle for each percentage ligament stiffness change from the baseline stiffness.

4.3.2.3 Tibial Translation for Ligament Stiffness (All Stifle Ligaments) Variation

The relative tibial translation across the phases of stance is plotted in FIGURE 68.

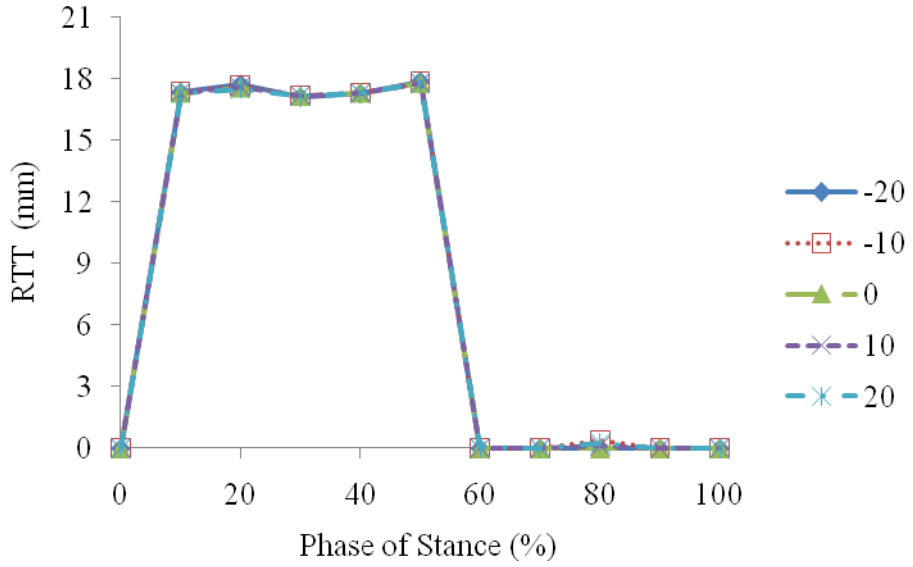

FIGURE 68 - Relative tibial translation between the CrCL intact and deficient stifle models for each percentage ligament stiffness change.

4.3.2.4 Tibial Translation Summary for Ligament Stiffness (All Stifle Ligaments) Variation

The peak relative tibial translation, the phase of stance at which it occurred and the corresponding relative tibial translation per body mass and anatomical tibial translation for each ligament stiffness change are listed in TABLE XII. The peak relative tibial translation values are plotted in FIGURE 69.

TABLE XII

PEAK TIBIAL TRANSLATION VALUES FOR EACH PERCENTAGE LIGAMENT STIFFNESS CHANGE EVALUATED

Change (%)	-20	-10	0	10	20
Stance Phase (%)	50	50	50	50	50
Peak RTT (mm)*	17.9	17.9	17.8	17.8	17.8
RTT/BM (mm/kg)**	0.56	0.56	0.56	0.56	0.56
ATT***	1.42	1.43	1.43	1.43	1.44

*RTT = Relative Tibial Translation = $(\mathrm{FT}_{\mathrm{deficient}})_{\mathrm{loaded}} - (\mathrm{FT}_{\mathrm{intact}})_{\mathrm{loaded}}$

**RTT/BM = Relative Tibial Translation per Body Mass

***ATT = Anatomical Tibial Translation = $\dfrac{(\mathrm{FT}_{\mathrm{deficient}})_{\mathrm{loaded}} - (\mathrm{FT}_{\mathrm{intact}})_{\mathrm{loaded}}}{(\mathrm{FT}_{\mathrm{intact}})_{\mathrm{loaded}}}$

where FT denotes the craniocaudal distance from a fixed point on the femur to a fixed point on the tibia, deficient denotes the CrCL was suppressed, intact denotes the CrCL was not suppressed and loaded denotes weight bearing

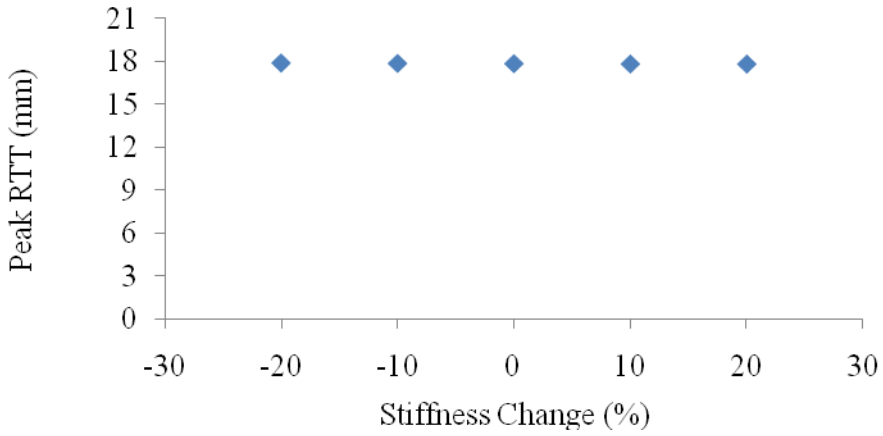

FIGURE 69 - Peak relative tibial translation for each TPA.

Peak relative tibial translation varied by +0.6/-0.0% from baseline for varying stiffness in all ligaments.

4.3.3 Ligament Stiffness (CrCL Only)

4.3.3.1 Ligament Forces for Ligament Stiffness (CrCL Only) Variation

To simulate variation of material properties in the CrCL only, the CrCL stiffness value was altered from baseline by discrete percentages. The five scenarios evaluated were CrCL stiffness percentage changes of -20%, -10%, 0% (baseline), 10% and 20%. The baseline CrCL stiffness was 4230 N/ε. Therefore, the CrCL stiffness range varied from 3380 N/ε to 5080 N/ε for the CrCL. The CrCL deficient stifle would produce the same results for all cases since only the CrCL stiffness was altered in this portion of the parametric analysis.

The ligament forces during stance for the CrCL intact stifle with a -20% CrCL stiffness change are shown in FIGURE 70.

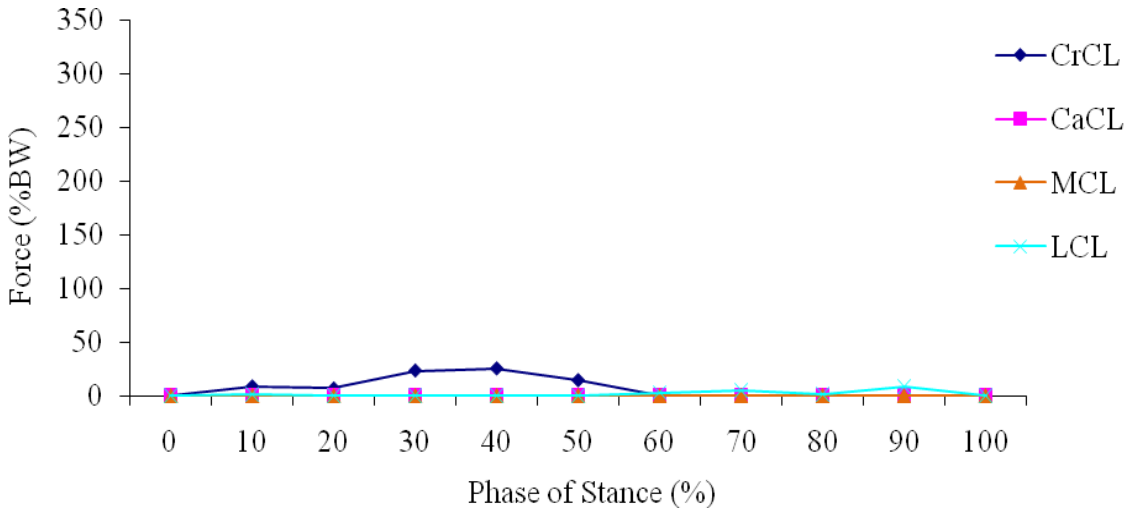

FIGURE 70 - Ligament forces for CrCL intact stifle (-20% CrCL stiffness change).

For the CrCL intact stifle the peak CrCL force was 26% BW and occurred at 40% stance. The peak LCL force was 8% BW and occurred at 90% stance. The CaCL and MCL were unloaded throughout stance.

The ligament forces during stance for the CrCL intact stifle with a -10% CrCL stiffness change are shown in FIGURE 71.

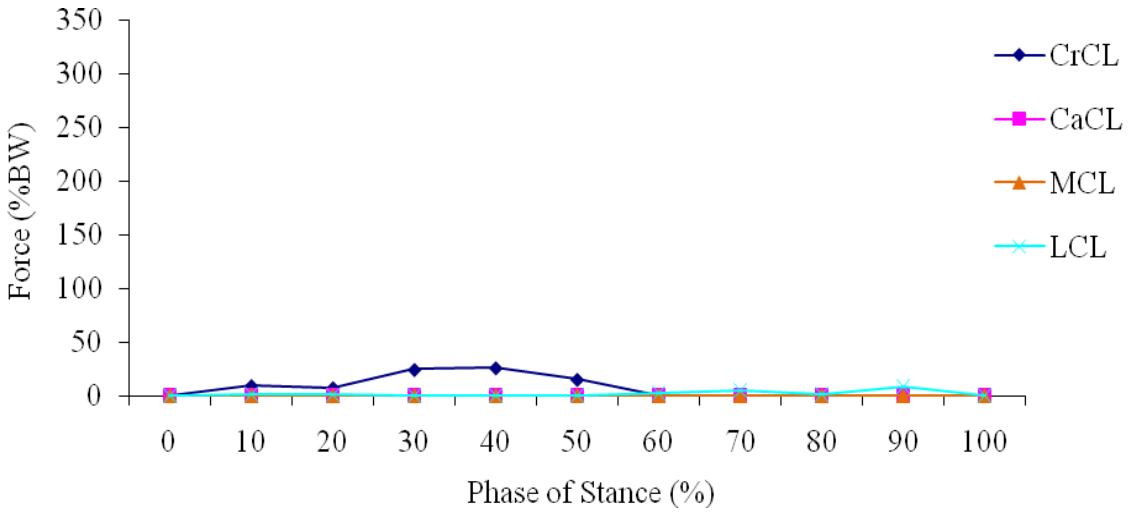

FIGURE 71 - Ligament forces for CrCL intact stifle (-10% CrCL stiffness change).

For the CrCL intact stifle the peak CrCL force was 26% BW and occurred at 40% stance. The peak LCL force was 8% BW and occurred at 90% stance. The CaCL and MCL were unloaded throughout stance.

The ligament forces during stance for the CrCL intact and CrCL deficient stifle with a 0% CrCL stiffness change are shown in FIGURE 72 and FIGURE 73, respectively. FIGURE 73 represents the CrCL deficient stifle for all CrCL stiffness variation because the CrCL stiffness acts only in the CrCL intact stifle.

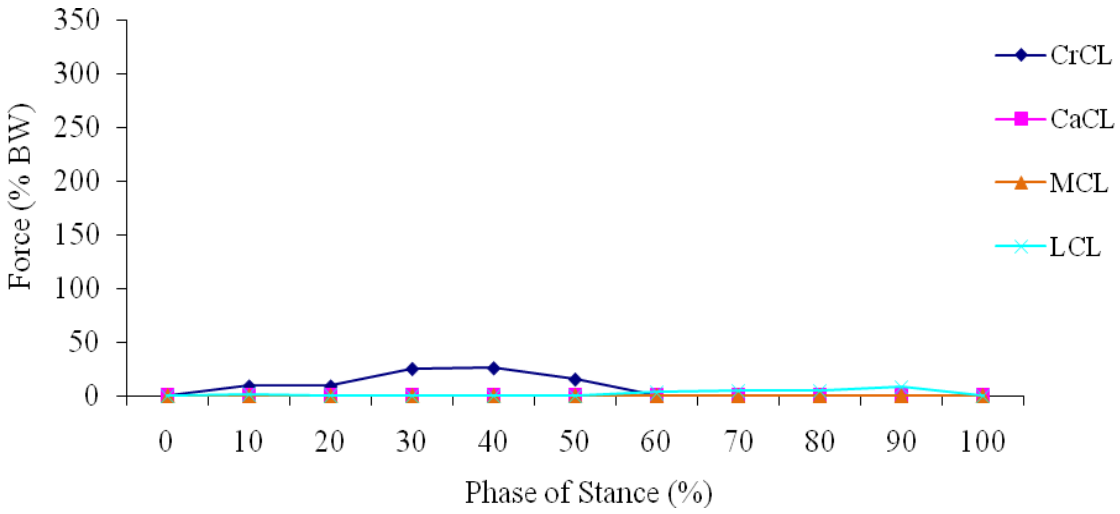

FIGURE 72 - Ligament forces for CrCL intact stifle (0% CrCL stiffness change).

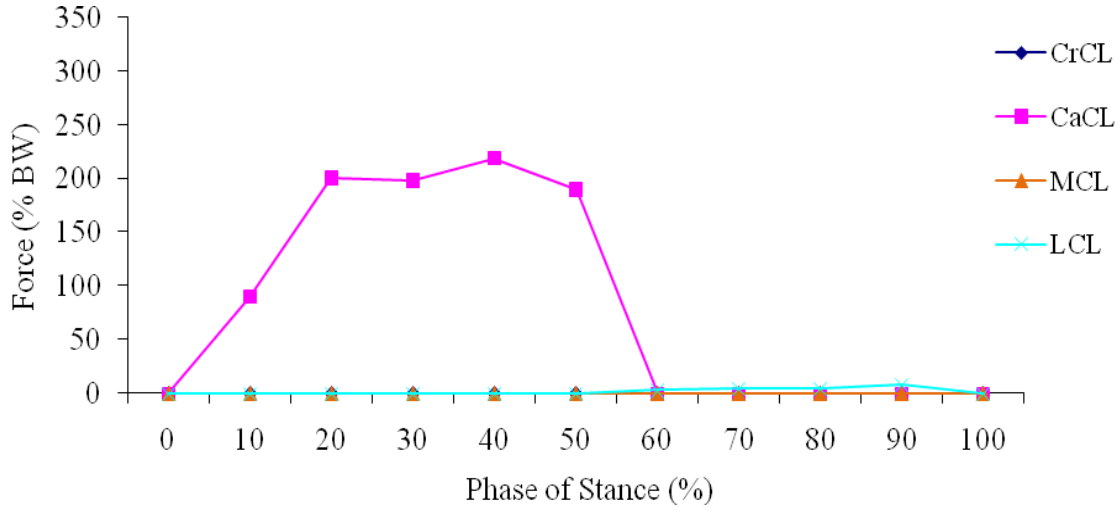

FIGURE 73 - Ligament forces for CrCL deficient stifle (0% CrCL stiffness change).

For the CrCL intact stifle the peak CrCL force was 26% body weight (BW) and occurred at 40% stance. The CaCL was unloaded thoughout stance. The peak LCL force was 8% BW and occurred at 90% stance. The MCL was unloaded throughout stance. For the

CrCL deficient stifle the peak CaCL force was 219% BW and occurred at 40% stance. The peak LCL force was 8% BW and occurred at 90% stance. The MCL was unloaded throughout stance.

The ligament forces during stance for the CrCL intact stifle with a 10% CrCL stiffness change are shown in FIGURE 74.

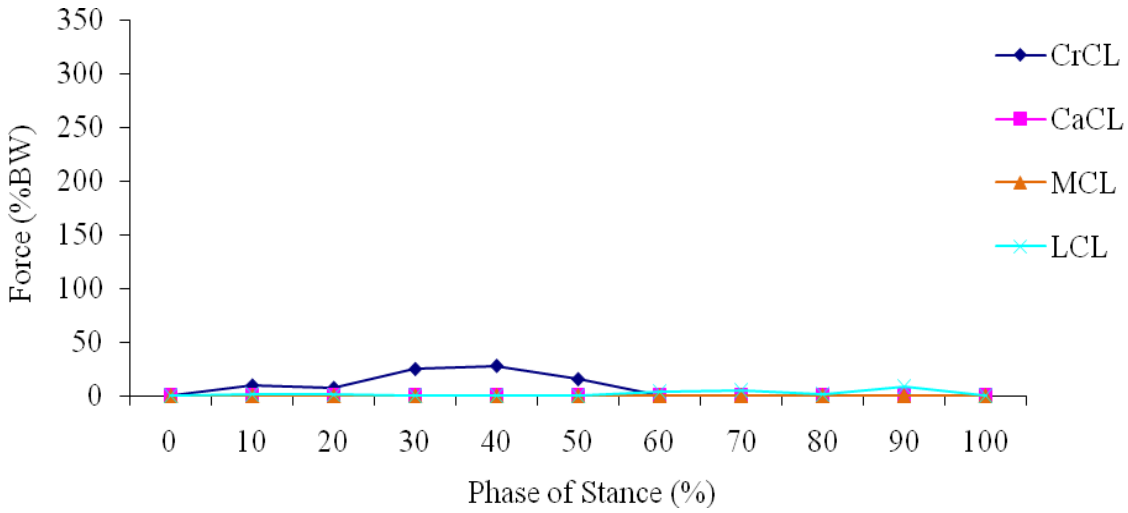

FIGURE 74 - Ligament forces for CrCL intact stifle (+10% CrCL stiffness change).

For the CrCL intact stifle the peak CrCL force was 28% BW and occurred at 40% stance. The peak LCL force was 8% BW and occurred at 90% stance. The CaCL and MCL were unloaded throughout stance.

The ligament forces during stance for the CrCL intact stifle with a 20% CrCL stiffness change are shown in FIGURE 75.

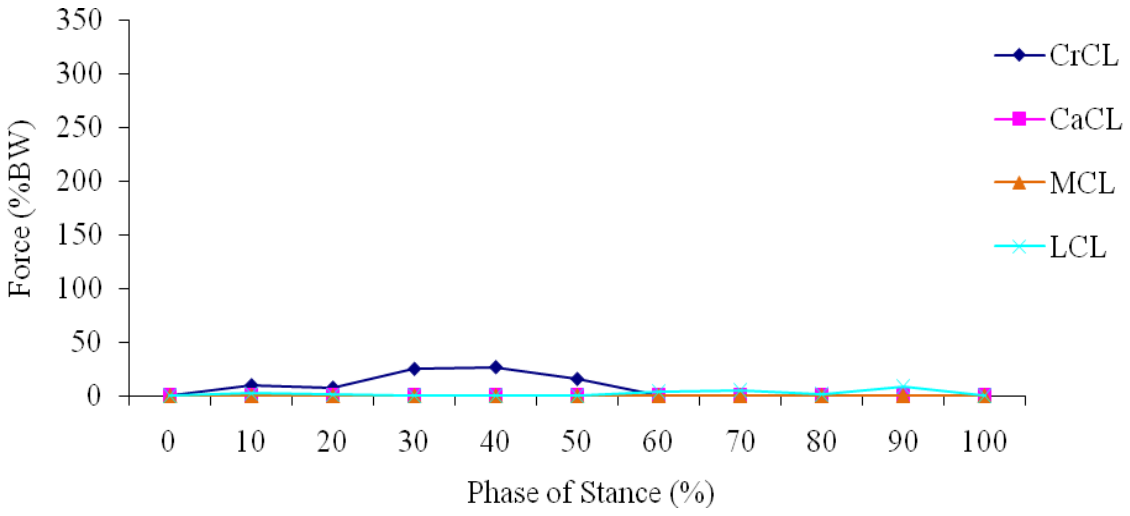

FIGURE 75 - Ligament forces for CrCL intact stifle (+20% CrCL stiffness change).

For the CrCL intact stifle the peak CrCL force was 27% BW and occurred at 40% stance. The peak LCL force was 8% BW and occurred at 90% stance. The CaCL and MCL were unloaded throughout stance.

4.3.3.2 Ligament Forces Summary for Ligament Stiffness (CrCL Only) Variation

Ligament forces for each phase of stance for varying CrCL stiffness were determined in the CrCL intact stifle. Peak CrCL forces varied by 2% BW ranging from 26% BW to 28% BW for varying CrCL stiffness in the CrCL intact stifle. The peak CrCL forces for varying CrCL stiffness for the intact stifle are shown in FIGURE 76.

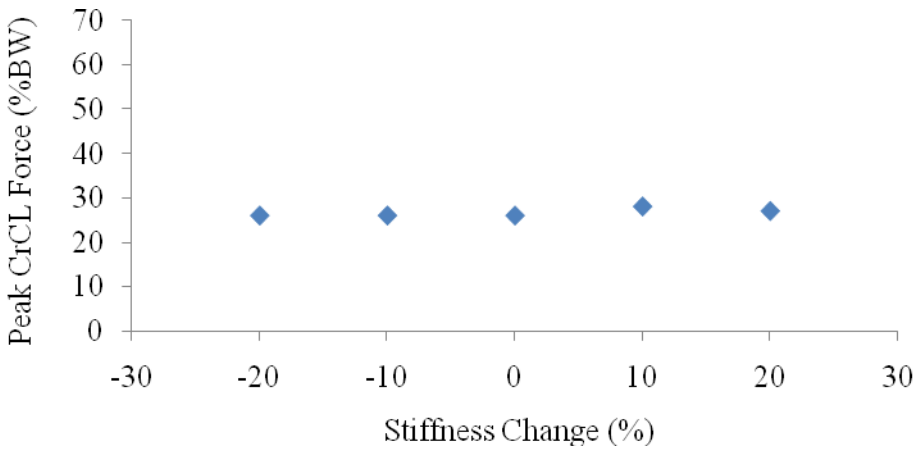

FIGURE 76 - Peak CrCL forces in the CrCL intact stifle for each percentage CrCL stiffness change.

4.3.3.3 Tibial Translation for Ligament Stiffness (CrCL Only) Variation

The relative tibial translation across the phases of stance is plotted in FIGURE 77.

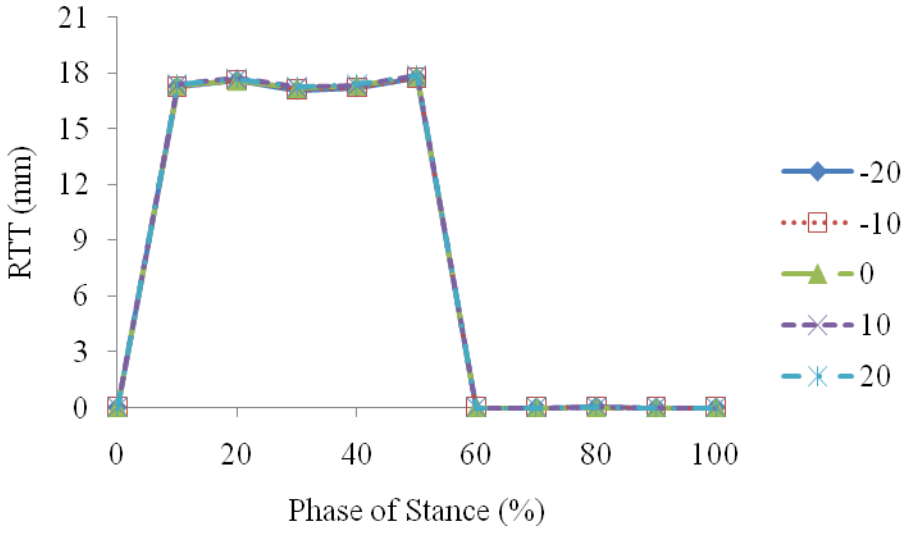

FIGURE 77 - Relative tibial translation between the CrCL intact and deficient stifle models for each percentage CrCL stiffness change.

4.3.3.4 Tibial Translation Summary for Ligament Stiffness (CrCL Only) Variation

The peak relative tibial translation, the phase of stance at which it occurred and the corresponding relative tibial translation per body mass and anatomical tibial translation for each CrCL stiffness change are listed in TABLE XIII. The peak relative tibial translation values are plotted in FIGURE 78.

TABLE XIII

PEAK TIBIAL TRANSLATION VALUES FOR EACH PERCENTAGE CRCL STIFFNESS CHANGE EVALUATED

Change (%)	-20	-10	0	10	20
Stance Phase (%)	50	50	50	50	50
Peak RTT (mm)*	17.7	17.8	17.8	17.9	17.9
RTT/BM (mm/kg)**	0.55	0.56	0.56	0.56	0.56
ATT***	1.41	1.42	1.43	1.44	1.44

*RTT = Relative Tibial Translation = $(\mathrm{FT}_{\mathrm{deficient}})_{\mathrm{loaded}} - (\mathrm{FT}_{\mathrm{intact}})_{\mathrm{loaded}}$

**RTT/BM = Relative Tibial Translation per Body Mass

***ATT = Anatomical Tibial Translation = $\dfrac{(\mathrm{FT}_{\mathrm{deficient}})_{\mathrm{loaded}} - (\mathrm{FT}_{\mathrm{intact}})_{\mathrm{loaded}}}{(\mathrm{FT}_{\mathrm{intact}})_{\mathrm{loaded}}}$

where FT denotes the craniocaudal distance from a fixed point on the femur to a fixed point on the tibia, deficient denotes the CrCL was suppressed, intact denotes the CrCL was not suppressed and loaded denotes weight bearing

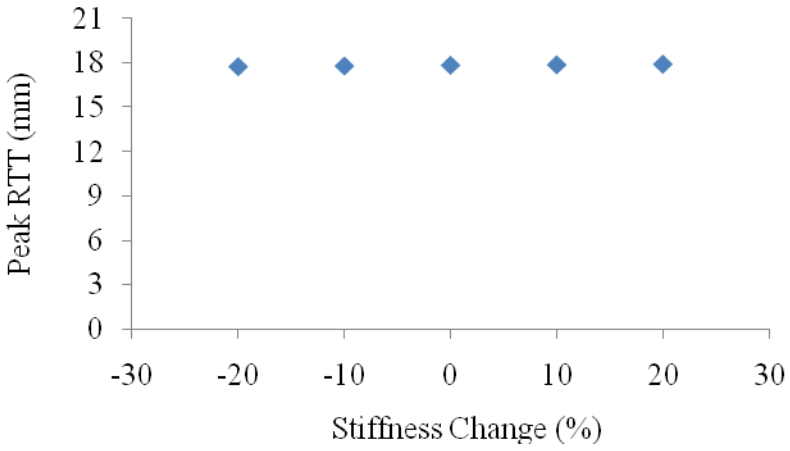

FIGURE 78 - Peak relative tibial translation for each percentage CrCL stiffness change.

Peak relative tibial translation varied by +0.6/-0.6% from baseline for varying CrCL stiffness.

4.3.4 Ligament Prestrain (All Stifle Ligaments)

4.3.4.1 Ligament Forces for Ligament Prestrain (All Stifle Ligaments) Variation

All model ligament prestrain values were altered from baseline by the same percentage to simulate variation in the amount of tautness in the stifle ligaments. The five scenarios evaluated were ligament prestrain percentage changes of -20%, -10%, 0% (baseline), 10% and 20%. The baseline reference prestrain values were 0.04, 0.04, -0.25 and 0.08 for the CrCL, CaCL, MCL and LCL, respectively. Therefore, ranges varied from 0.032 to 0.048, from 0.032 to 0.048, from -0.300 to -0.200 and from 0.064 to 0.096 for the CrCL, CaCL, MCL and LCL, respectively.

The ligament forces during stance for the CrCL intact and CrCL deficient stifle with a -20% ligament prestrain change are shown in FIGURE 79 and FIGURE 80, respectively.

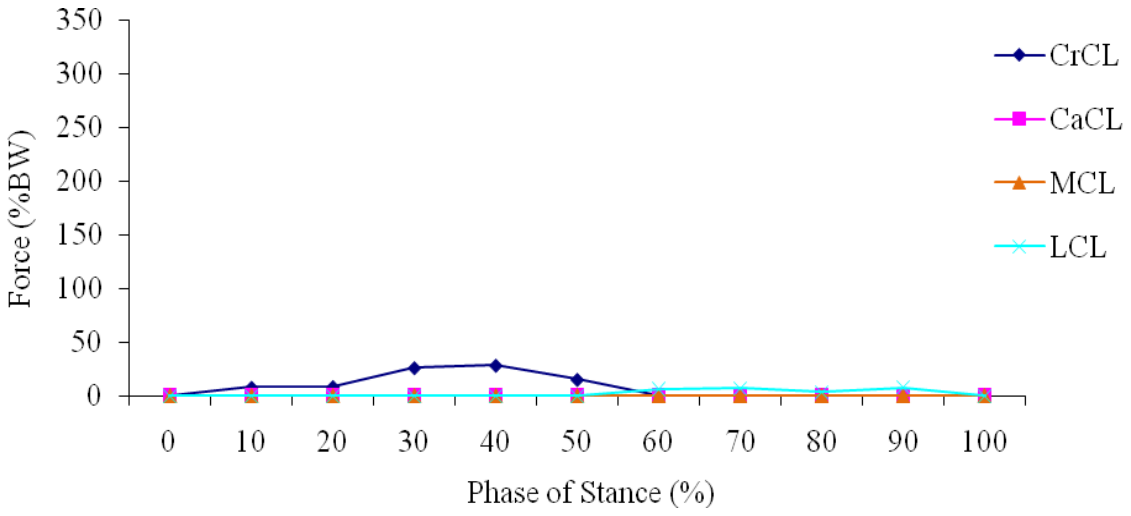

FIGURE 79 - Ligament forces for CrCL intact stifle (-20% prestrain change).

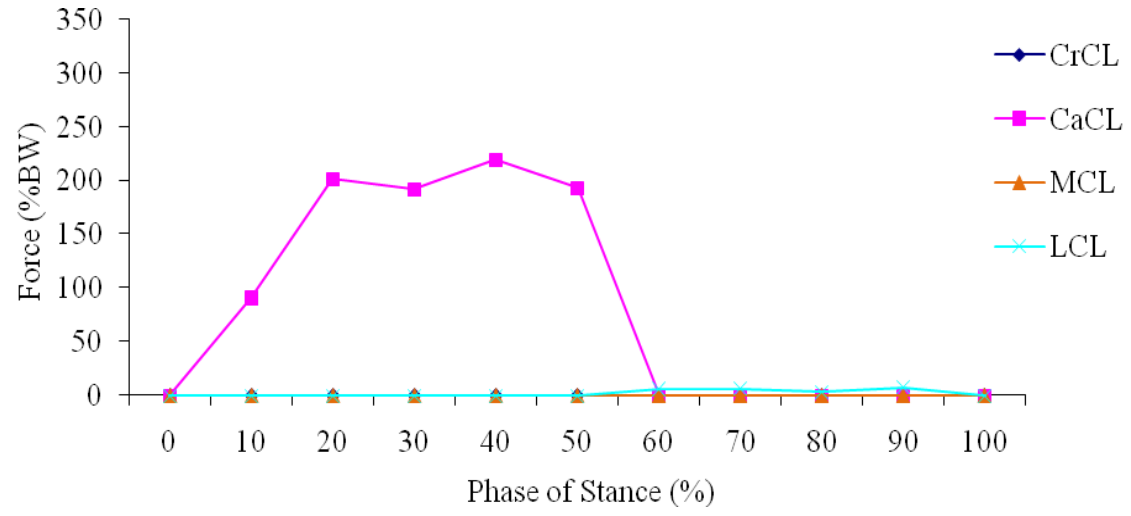

FIGURE 80 - Ligament forces for CrCL deficient stifle (-20% prestrain change).

For the CrCL intact stifle the peak CrCL force was 28% BW and occurred at 40% stance. The peak LCL force was 8% BW and occurred at 90% stance. The CaCL and MCL were unloaded throughout stance. For the CrCL deficient stifle the peak CaCL force was 219%

BW and occurred at 40% stance. The peak LCL force was 8% BW and occurred at 90% stance. The MCL was unloaded throughout stance.

The ligament forces during stance for the CrCL intact and CrCL deficient stifle with a -10% ligament prestrain change are shown in FIGURE 81 and FIGURE 82, respectively.

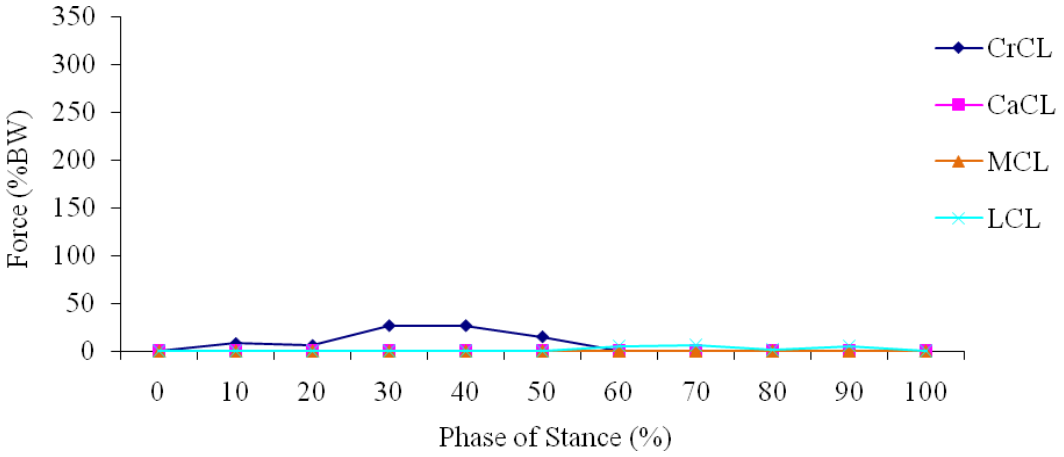

FIGURE 81 - Ligament forces for CrCL intact stifle (-10% prestrain change).

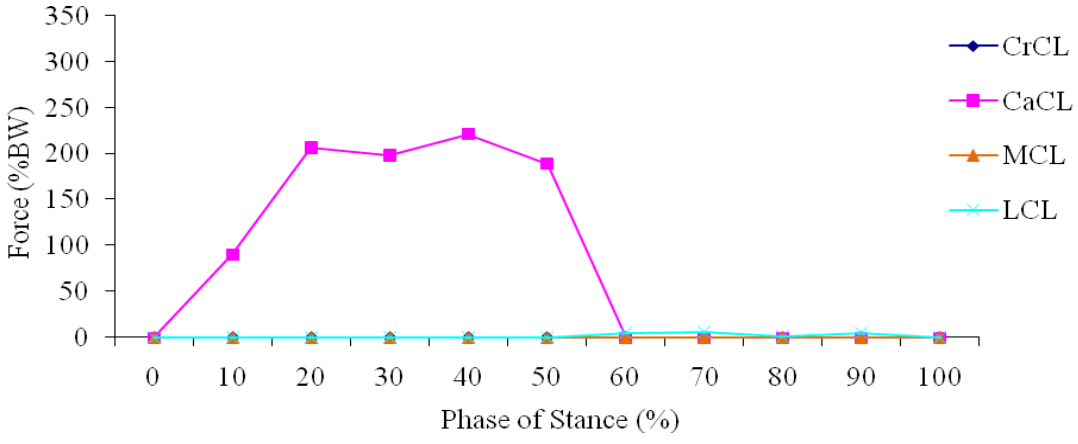

FIGURE 82 - Ligament forces for CrCL deficient stifle (-10% prestrain change).

For the CrCL intact stifle the peak CrCL force was 27% BW and occurred at 30% and 40% stance. The peak LCL force was 6% BW and occurred at 70% stance. The CaCL and MCL were unloaded throughout stance. For the CrCL deficient stifle the peak CaCL force was 221% BW and occurred at 40% stance. The peak LCL force was 6% BW and occurred at 70% stance. The MCL was unloaded throughout stance.

The ligament forces during stance for the CrCL intact and CrCL deficient stifle with a 0% ligament prestrain change are shown in FIGURE 83 and FIGURE 84, respectively.

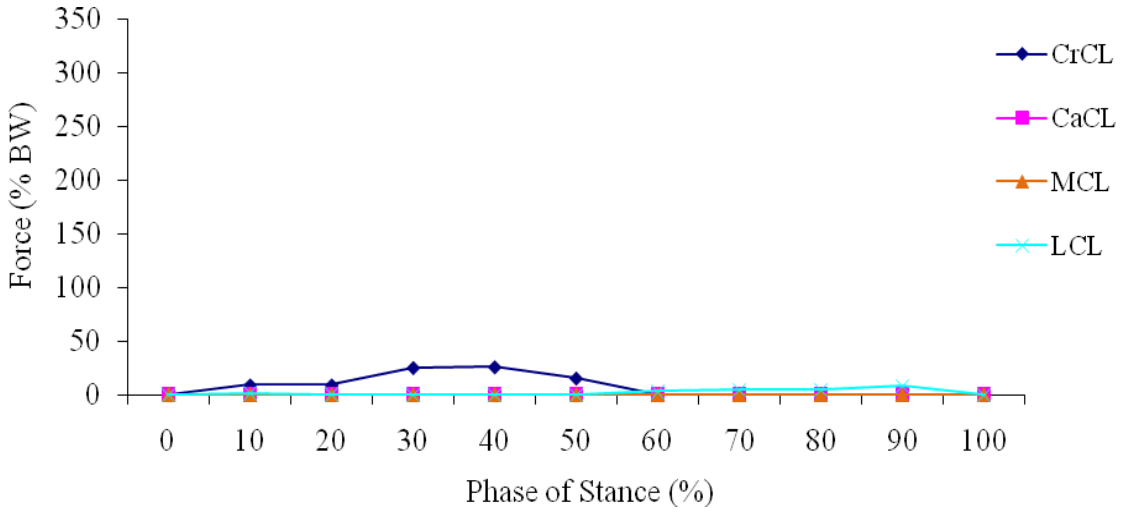

FIGURE 83 - Ligament forces for CrCL intact stifle (0% prestrain change).

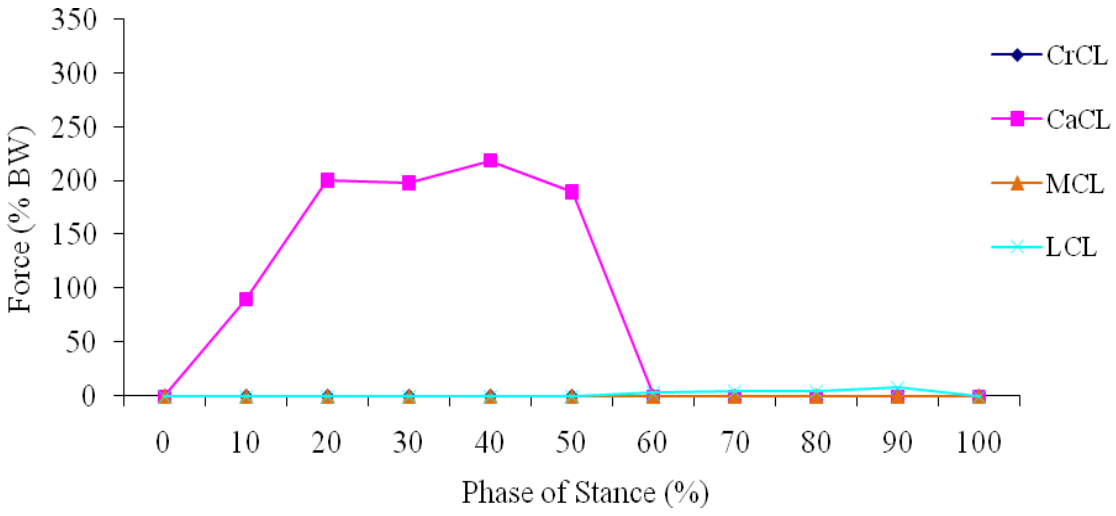

FIGURE 84 - Ligament forces for CrCL deficient stifle (0% prestrain change).

For the CrCL intact stifle the peak CrCL force was 26% body weight (BW) and occurred at 40% stance. The CaCL was unloaded thoughout stance. The peak LCL force was 8% BW and occurred at 90% stance. The MCL was unloaded throughout stance. For the CrCL deficient stifle the peak CaCL force was 219% BW and occurred at 40% stance. The peak LCL force was 8% BW and occurred at 90% stance. The MCL was unloaded throughout stance.

The ligament forces during stance for the CrCL intact and CrCL deficient stifle with a 10% ligament prestrain change are shown in FIGURE 85 and FIGURE 86, respectively.

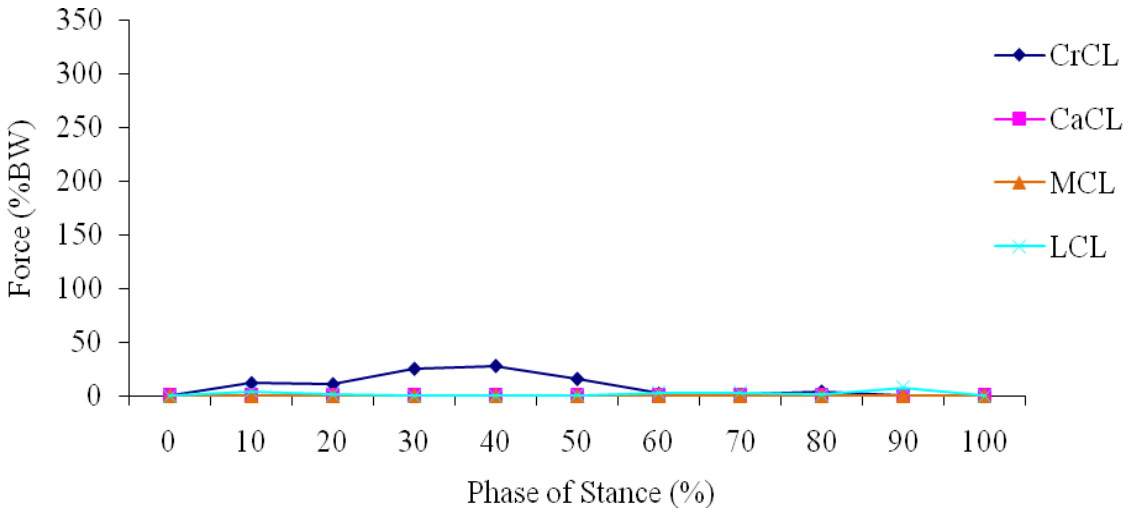

FIGURE 85 - Ligament forces for CrCL intact stifle (+10% prestrain change).

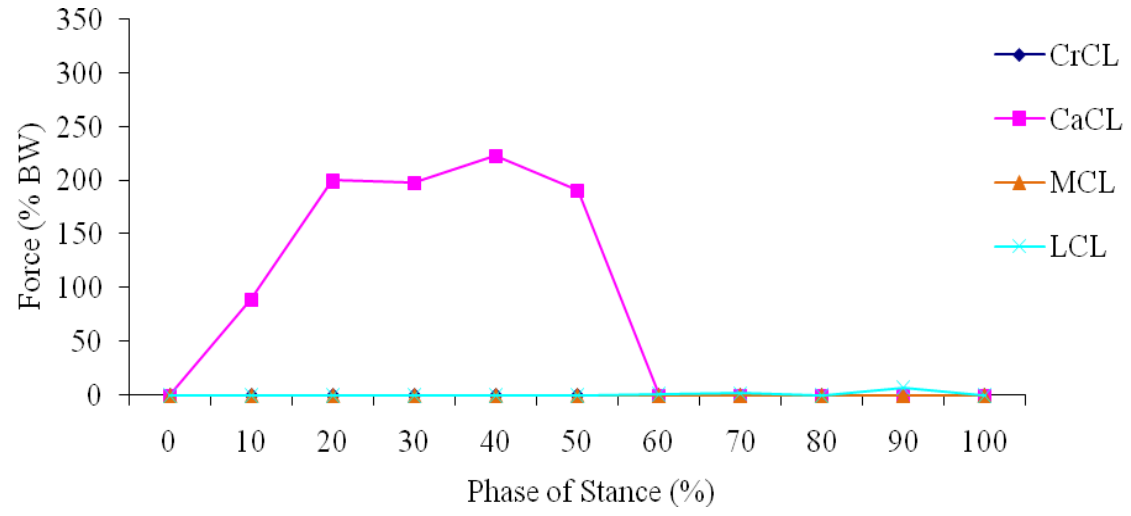

FIGURE 86 - Ligament forces for CrCL deficient stifle (+10% prestrain change).

For the CrCL intact stifle the peak CrCL force was 27% BW and occurred at 40% stance. The peak LCL force was 8% BW and occurred at 90% stance. The CaCL and MCL were unloaded throughout stance. For the CrCL deficient stifle the peak CaCL force was 223%

BW and occurred at 40% stance. The peak LCL force was 7% BW and occurred at 90% stance. The MCL was unloaded throughout stance.

The ligament forces during stance for the CrCL intact and CrCL deficient stifle with a 20% ligament prestrain change are shown in FIGURE 87 and FIGURE 88, respectively.

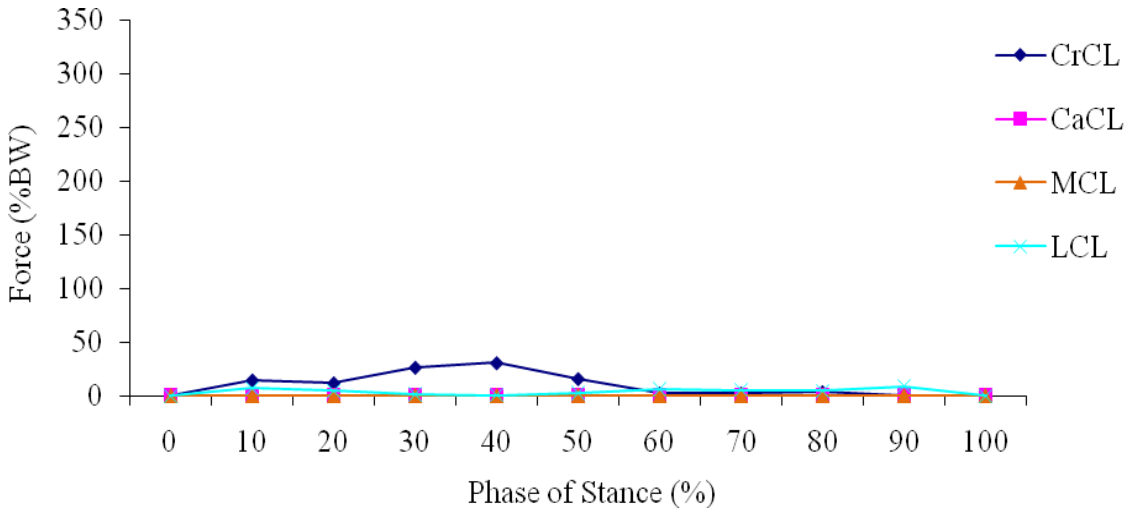

FIGURE 87 - Ligament forces for CrCL intact stifle (+20% prestrain change).

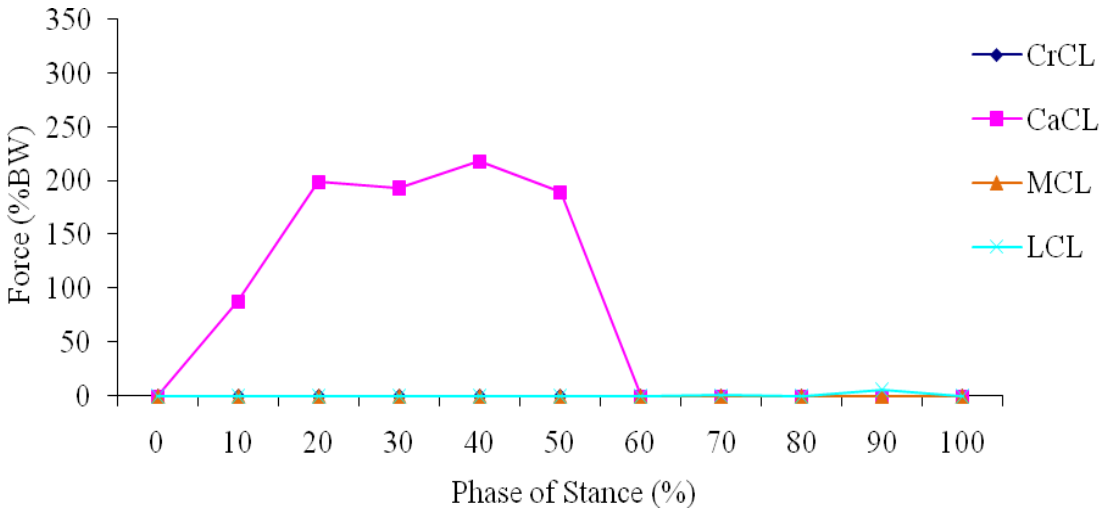

FIGURE 88 - Ligament forces for CrCL deficient stifle (+20% prestrain change).

For the CrCL intact stifle the peak CrCL force was 31% BW and occurred at 40% stance. The peak LCL force was 9% BW and occurred at 90% stance. The CaCL and MCL were unloaded throughout stance. For the CrCL deficient stifle the peak CaCL force was 218% BW and occurred at 40% stance. The peak LCL force was 6% BW and occurred at 90% stance. The MCL was unloaded throughout stance.

4.3.4.2 Ligament Forces Summary for Ligament Prestrain (All Stifle Ligaments) Variation

Ligament forces for each phase of stance for varying ligament prestrain were determined in the CrCL intact and CrCL deficient stifle. Peak CrCL forces varied by 5% BW ranging from 26% BW to 31% BW for varying prestrain in all ligaments for the CrCL intact stifle. Peak CaCL forces varied by 5% BW ranging from 218% BW to 223% BW for the CrCL deficient stifle. The peak CrCL forces for varying ligament prestrain

for the CrCL intact stifle are shown in FIGURE 89, and the peak CaCL forces for varying ligament prestrain for the CrCL deficient stifle are shown in FIGURE 90.

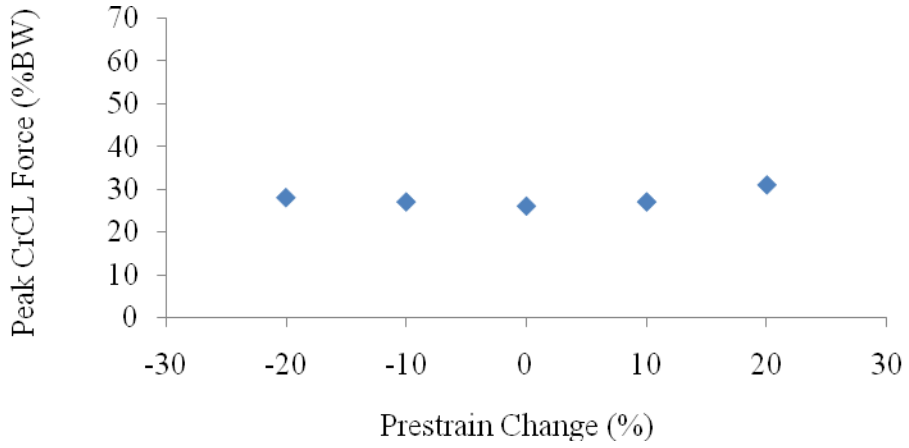

FIGURE 89 - Peak CrCL forces in the CrCL intact stifle for each percentage ligament prestrain change.

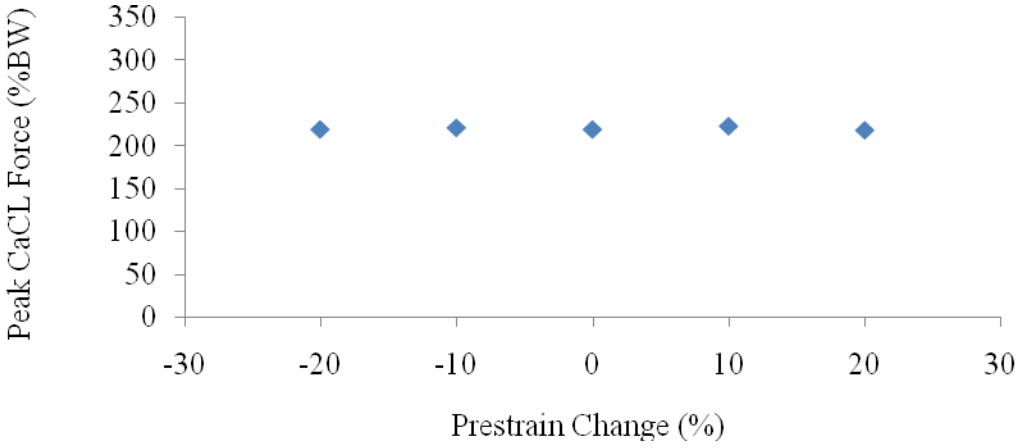

FIGURE 90 - Peak CaCL forces in the CrCL deficient stifle for each percentage ligament prestrain change.

4.3.4.3 Tibial Translation for Ligament Prestrain (All Stifle Ligaments) Variation

The relative tibial translation across the phases of stance is plotted in FIGURE 91.

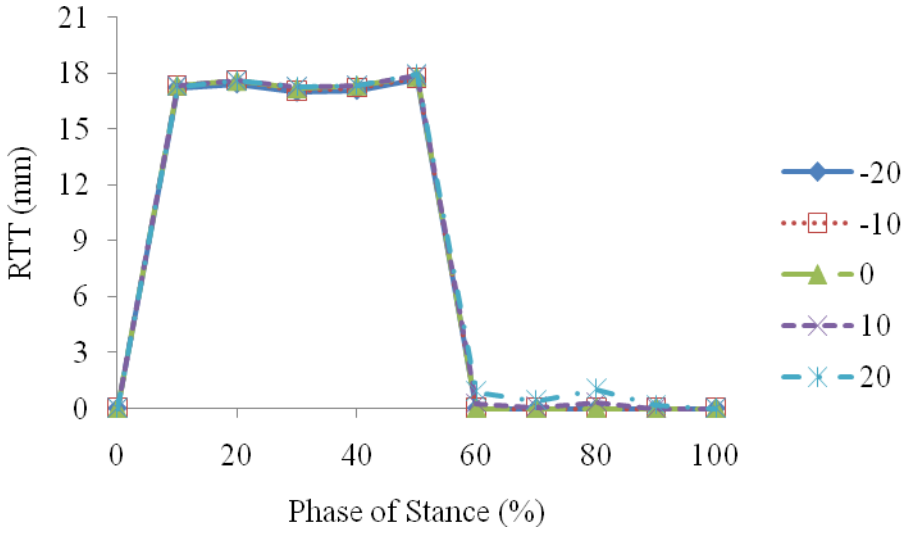

FIGURE 91 - Relative tibial translation between the CrCL intact and deficient stifle models for each percentage ligament prestrain change.

4.3.4.4 Tibial Translation Summary for Ligament Prestrain (All Stifle Ligaments) Variation

The peak relative tibial translation, the phase of stance at which it occurred and the corresponding relative tibial translation per body mass and anatomical tibial translation for each ligament prestrain percentage change are listed in TABLE XIV. The peak relative tibial translation values are plotted in FIGURE 92.

TABLE XIV

PEAK TIBIAL TRANSLATION VALUES FOR EACH PERCENTAGE LIGAMENT PRESTRAIN CHANGE EVALUATED

Change (%)	-20	-10	0	10	20
Stance Phase (%)	50	50	50	50	50
Peak RTT (mm)*	17.7	17.8	17.8	17.9	18.0
RTT/BM (mm/kg)**	0.55	0.56	0.56	0.56	0.56
ATT***	1.40	1.41	1.43	1.45	1.46

*RTT = Relative Tibial Translation = $(FT_{deficient})_{loaded} - (FT_{intact})_{loaded}$

**RTT/BM = Relative Tibial Translation per Body Mass

***ATT = Anatomical Tibial Translation = $\frac{(FT_{deficient})_{loaded} - (FT_{intact})_{loaded}}{(FT_{intact})_{loaded}}$

where FT denotes the craniocaudal distance from a fixed point on the femur to a fixed point on the tibia, deficient denotes the CrCL was suppressed, intact denotes the CrCL was not suppressed and loaded denotes weight bearing

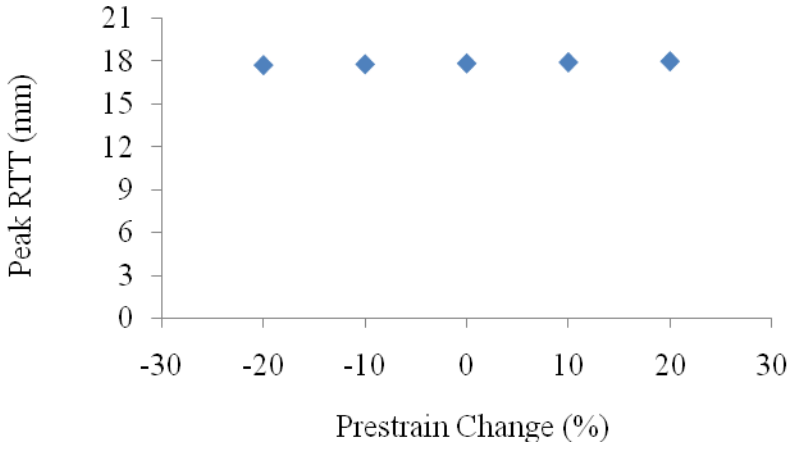

FIGURE 92 - Peak relative tibial translation for each percentage ligament prestrain change.

Peak relative tibial translation varied by +1.1/-0.6% from baseline for varying prestrain in all ligaments.

4.3.5 Ligament Prestrain (CrCL Only)

4.3.5.1 Ligament Forces for Ligament Prestrain (CrCL Only) Variation

The CrCL prestrain value was altered from baseline by discrete percentages to simulate variation in the amount of tautness in the CrCL only. The five scenarios evaluated were CrCL prestrain percentage changes of -20%, -10%, 0% (baseline), 10% and 20%. The baseline CrCL reference prestrain was 0.04. Therefore, the CrCL prestrain varied from 0.032 to 0.048. The CrCL deficient stifle would have the same results for all cases since only the CrCL prestrain was altered.

The ligament forces during stance for the CrCL intact stifle with a -20% CrCL prestrain change are shown in FIGURE 93.

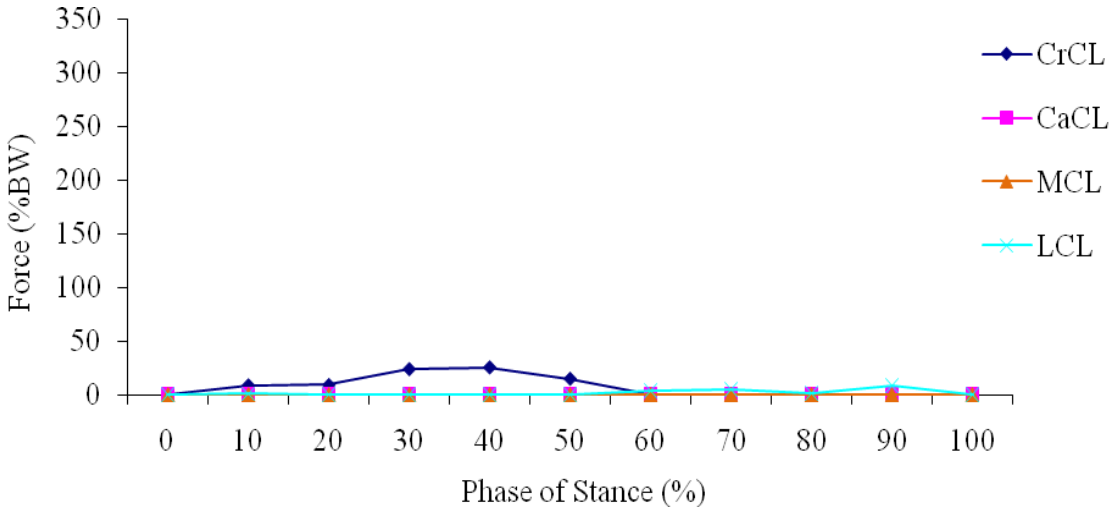

FIGURE 93 - Ligament forces for CrCL intact stifle (-20% CrCL prestrain change).

For the CrCL intact stifle the peak CrCL force was 26% BW and occurred at 40% stance. The peak LCL force was 8% BW and occurred at 90% stance. The CaCL and MCL were unloaded throughout stance.

The ligament forces during stance for the CrCL intact stifle with a -10% CrCL prestrain change are shown in FIGURE 94.

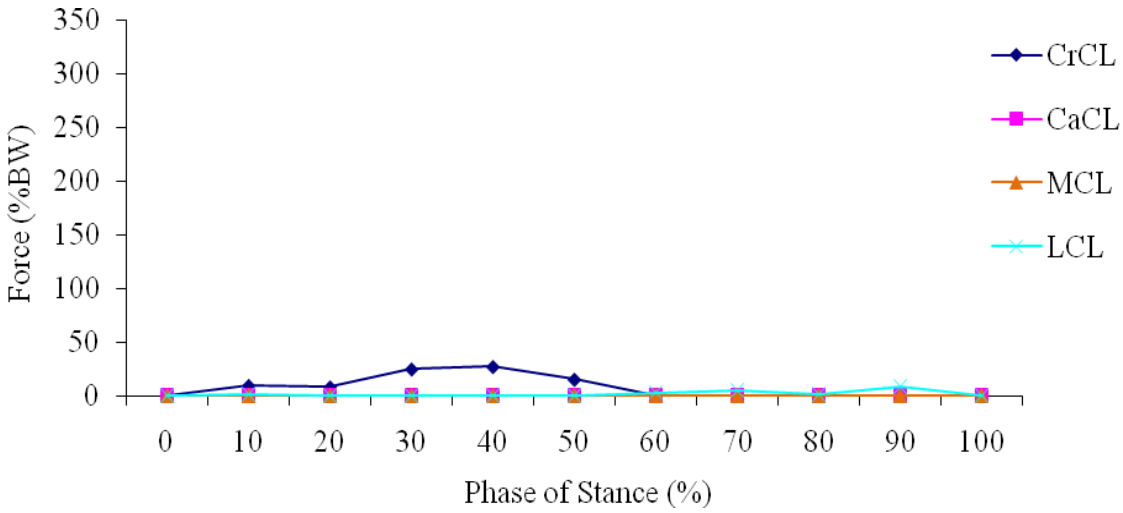

FIGURE 94 - Ligament forces for CrCL intact stifle (-10% CrCL prestrain change).

For the CrCL intact stifle the peak CrCL force was 27% BW and occurred at 40% stance. The peak LCL force was 8% BW and occurred at 90% stance. The CaCL and MCL were unloaded throughout stance.

The ligament forces during stance for the CrCL intact and CrCL deficient stifle with a 0% CrCL prestrain change are shown in FIGURE 95 and FIGURE 96, respectively. FIGURE 96 represents the CrCL deficient stifle for all CrCL stiffness variation because the CrCL stiffness acts only in the CrCL intact stifle.

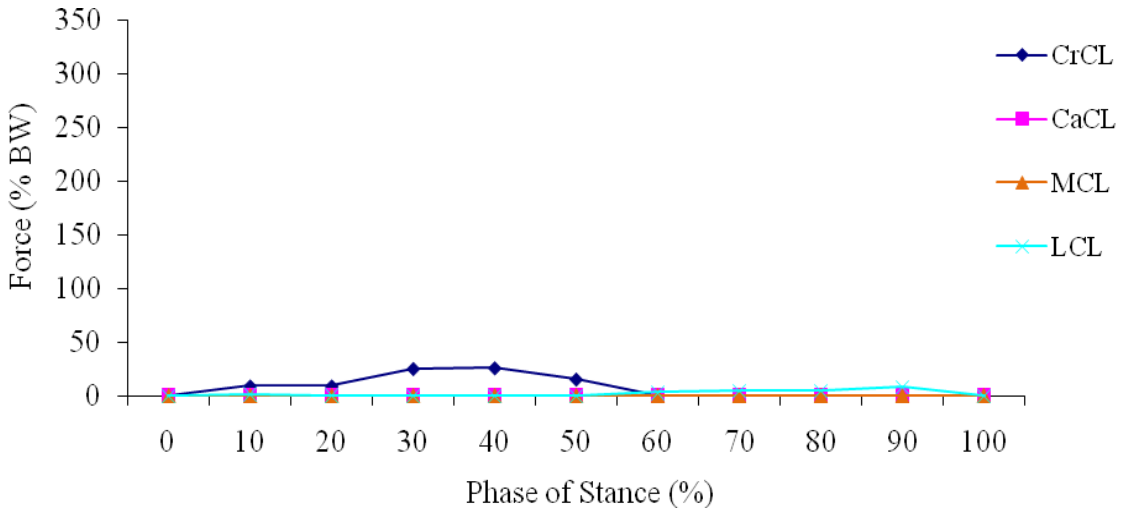

FIGURE 95 - Ligament forces for CrCL intact stifle (0% CrCL prestrain change).

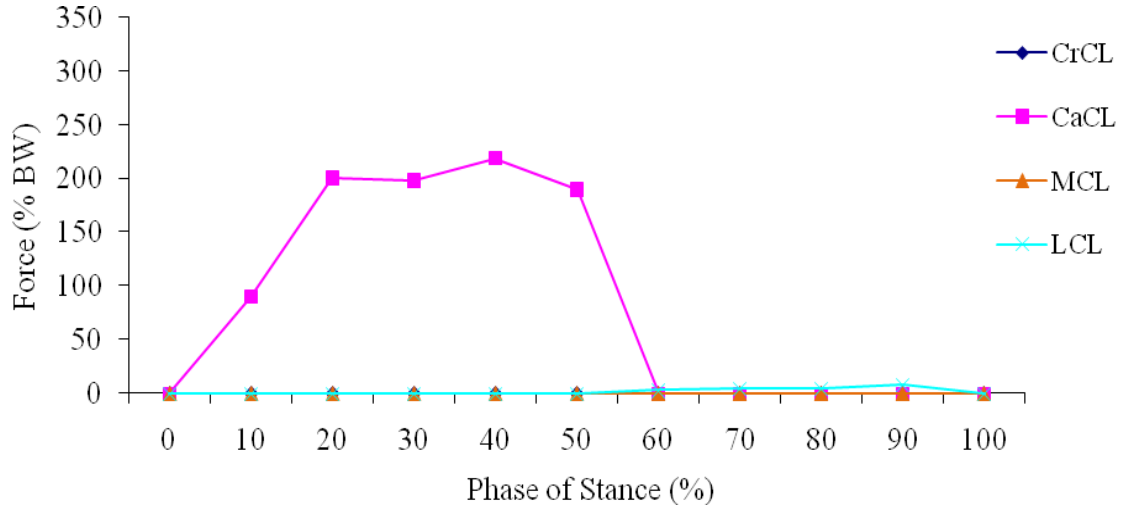

FIGURE 96 - Ligament forces for CrCL deficient stifle (0% CrCL prestrain change).

For the CrCL intact stifle the peak CrCL force was 26% body weight (BW) and occurred at 40% stance. The CaCL was unloaded thoughout stance. The peak LCL force was 8% BW and occurred at 90% stance. The MCL was unloaded throughout stance. For the

CrCL deficient stifle the peak CaCL force was 219% BW and occurred at 40% stance. The peak LCL force was 8% BW and occurred at 90% stance. The MCL was unloaded throughout stance.

The ligament forces during stance for the CrCL intact stifle with a 10% CrCL prestrain change are shown in FIGURE 97.

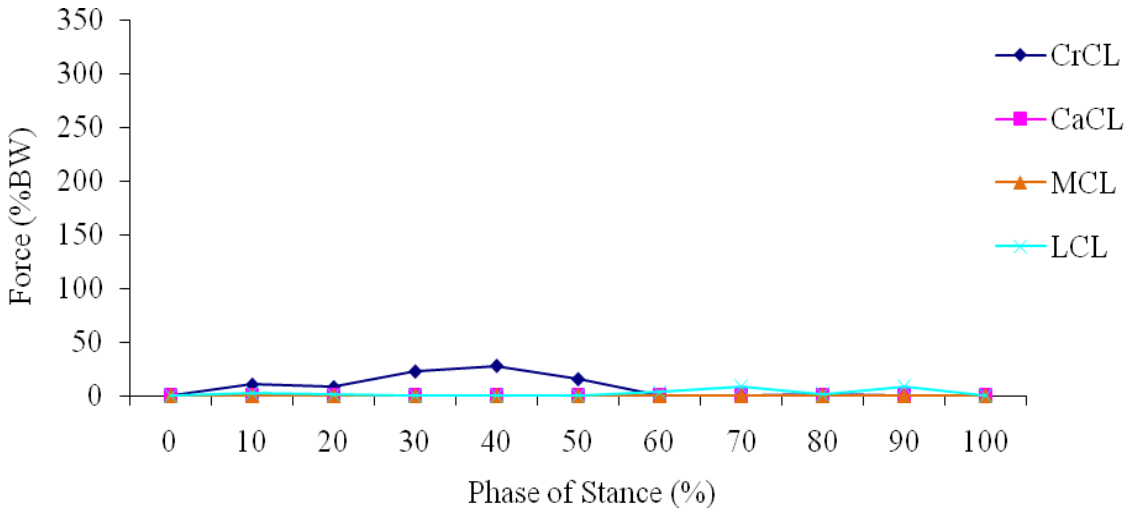

FIGURE 97 - Ligament forces for CrCL intact stifle (+10% CrCL prestrain change).

For the CrCL intact stifle the peak CrCL force was 28% BW and occurred at 40% stance. The peak LCL force was 9% BW and occurred at 70% stance. The CaCL and MCL were unloaded throughout stance.

The ligament forces during stance for the CrCL intact stifle with a 20% CrCL prestrain change are shown in FIGURE 98.

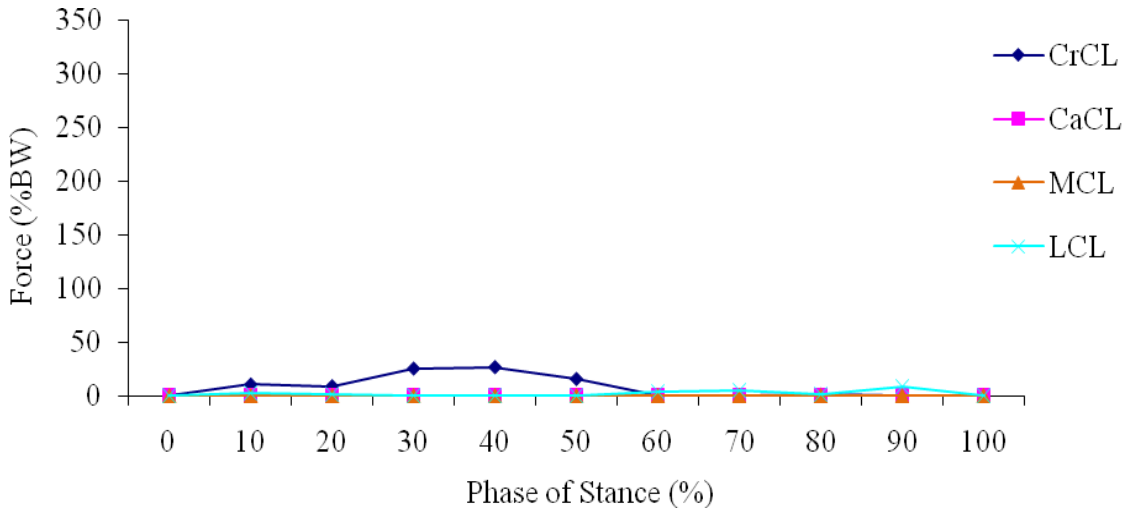

FIGURE 98 - Ligament forces for CrCL intact stifle (+20% CrCL prestrain change).

For the CrCL intact stifle the peak CrCL force was 27% BW and occurred at 40% stance. The peak LCL force was 8% BW and occurred at 90% stance. The CaCL and MCL were unloaded throughout stance.

4.3.5.2 Ligament Forces Summary for Ligament Prestrain (CrCL Only) Variation

Ligament forces for each phase of stance for varying CrCL prestrain were determined in the CrCL intact stifle. Peak CrCL forces varied by 2% BW from 26% BW to 28% BW for varying CrCL prestrain for the CrCL intact stifle. The peak CrCL forces for varying CrCL prestrain for the intact stifle are shown in FIGURE 99.

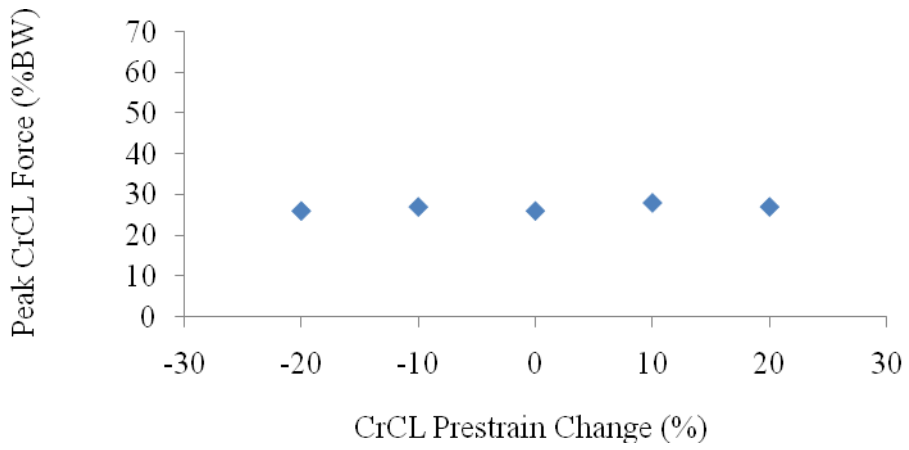

FIGURE 99 - Peak CrCL forces in the CrCL intact stifle for each percentage CrCL prestrain change.

4.3.5.3 Tibial Translation for Ligament Prestrain (CrCL Only) Variation

The relative tibial translation across the phases of stance is plotted in FIGURE 100.

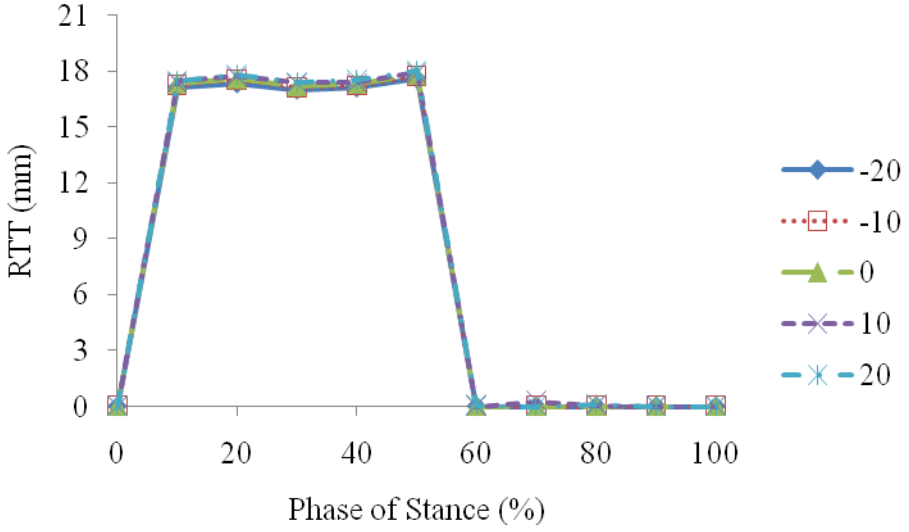

FIGURE 100 - Relative tibial translation between the CrCL intact and deficient stifle models for each percentage CrCL prestrain change.

4.3.5.4 Tibial Translation Summary for Ligament Prestrain (CrCL Only) Variation

The peak relative tibial translation, the phase of stance at which it occurred and the corresponding relative tibial translation per body mass and anatomical tibial translation for each percentage CrCL prestrain change are listed in TABLE XV. The peak relative tibial translation values are plotted in FIGURE 101.

TABLE XV

PEAK TIBIAL TRANSLATION VALUES FOR EACH PERCENTAGE CRCL PRESTRAIN CHANGE

Change (%)	-20	-10	0	10	20
Stance Phase (%)	50	50	50	50	50
Peak RTT (mm)*	17.6	17.7	17.8	17.9	18.0
RTT/BM (mm/kg)**	0.55	0.55	0.56	0.56	0.56
ATT***	1.39	1.41	1.43	1.45	1.47

*RTT = Relative Tibial Translation = $(\mathrm{FT}_{\mathrm{deficient}})_{\mathrm{loaded}} - (\mathrm{FT}_{\mathrm{intact}})_{\mathrm{loaded}}$

**RTT/BM = Relative Tibial Translation per Body Mass

***ATT = Anatomical Tibial Translation = $\dfrac{(\mathrm{FT}_{\mathrm{deficient}})_{\mathrm{loaded}} - (\mathrm{FT}_{\mathrm{intact}})_{\mathrm{loaded}}}{(\mathrm{FT}_{\mathrm{intact}})_{\mathrm{loaded}}}$

where FT denotes the craniocaudal distance from a fixed point on the femur to a fixed point on the tibia, deficient denotes the CrCL was suppressed, intact denotes the CrCL was not suppressed and loaded denotes weight bearing

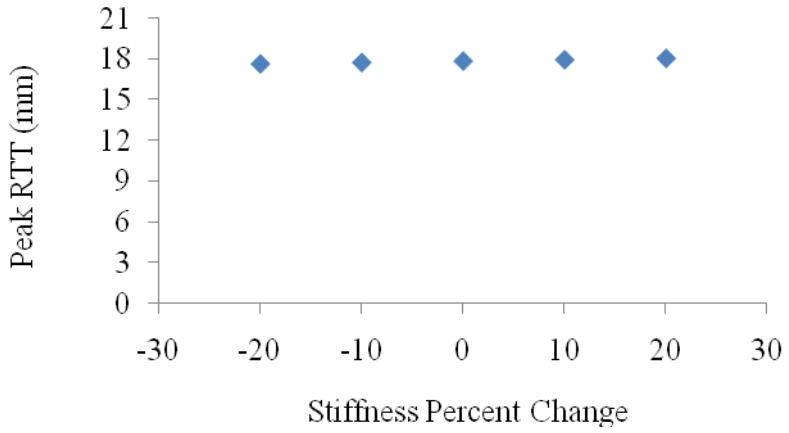

FIGURE 101 - Peak relative tibial translation for each percentage CrCL prestrain change.

Peak relative tibial translation varied by +1.1/-1.1% from baseline for varying CrCL prestrain.

4.3.6 Muscle Force Magnitude

4.3.6.1 Ligament Forces for Muscle Force Magnitude Variation

All model muscle force magnitude values were altered from baseline by the same percentages to simulate variation in the extent of hind limb muscle activation. The five scenarios evaluated were muscle force magnitude percentage changes of -20%, -10%, 0% (baseline), 10% and 20%. The baseline muscle force magnitudes are described in TABLE VIII.

The ligament forces during stance for the CrCL intact and CrCL deficient stifle with a -20% muscle force magnitude change are shown in FIGURE 102 and FIGURE 103, respectively.

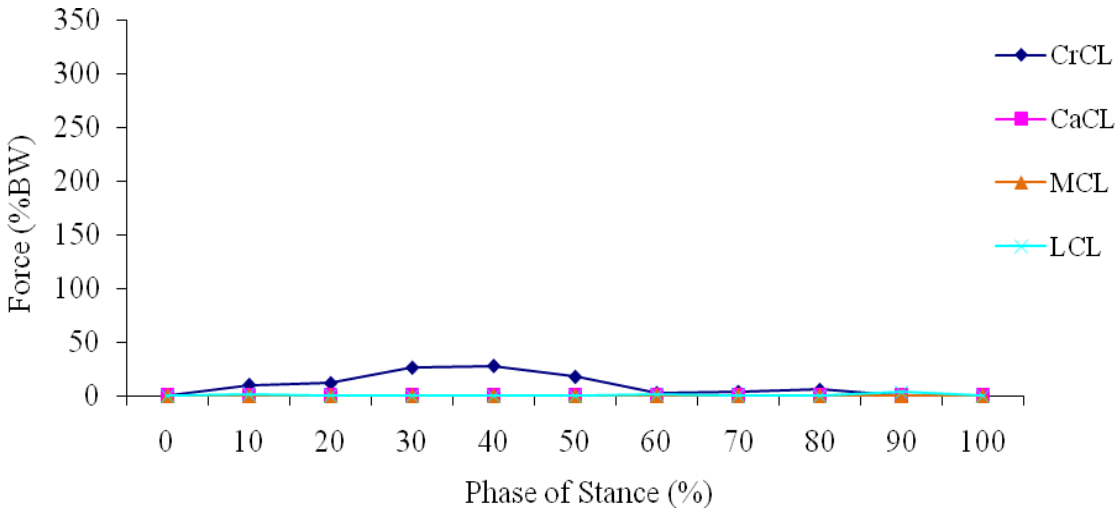

FIGURE 102 - Ligament forces for CrCL intact stifle (-20% muscle force magnitude change).

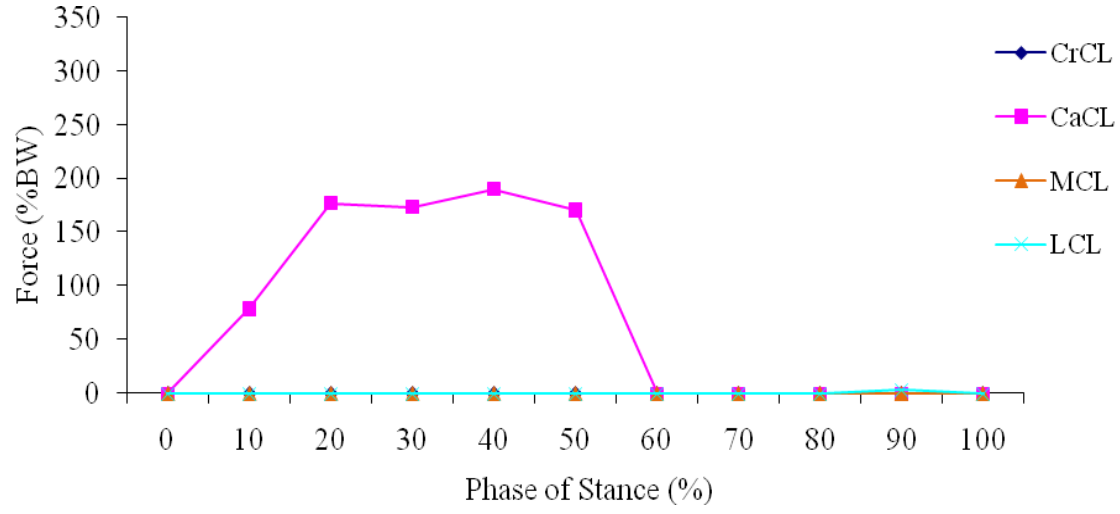

FIGURE 103 - Ligament forces for CrCL deficient stifle (-20% muscle force magnitude change).

For the CrCL intact stifle the peak CrCL force was 27% BW and occurred at 40% stance. The peak LCL force was 3% BW and occurred at 90% stance. The CaCL and MCL were unloaded throughout stance. For the CrCL deficient stifle the peak CaCL force was 190% BW and occurred at 40% stance. The peak LCL force was 3% BW and occurred at 90% stance. The MCL was unloaded throughout stance.

The ligament forces during stance for the CrCL intact and CrCL deficient stifle with a -10% muscle force magnitude change are shown in FIGURE 104 and FIGURE 105, respectively.

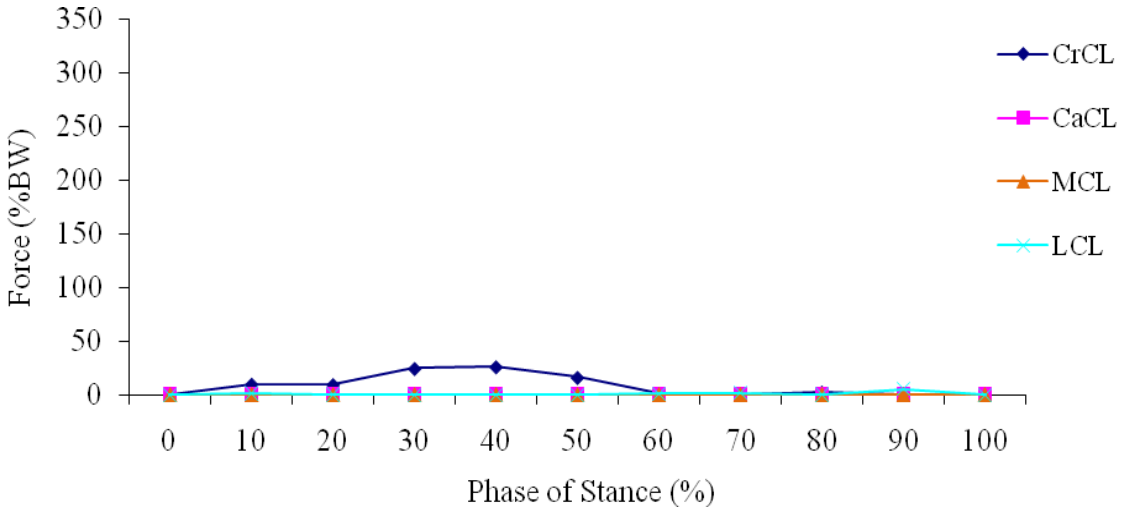

FIGURE 104 - Ligament forces for CrCL intact stifle (-10% muscle force magnitude change).

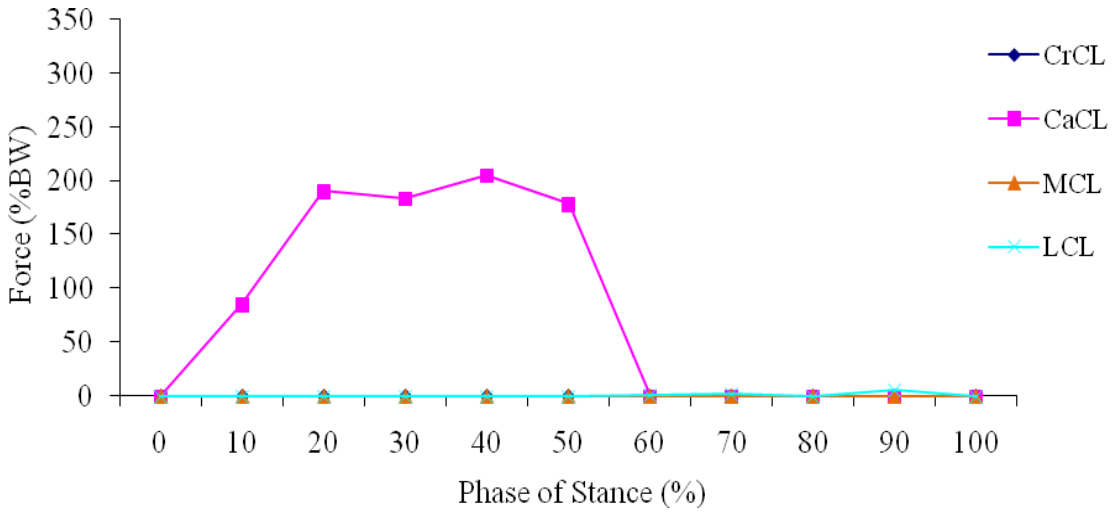

FIGURE 105 - Ligament forces for CrCL deficient stifle (-10% muscle force magnitude change).

For the CrCL intact stifle the peak CrCL force was 26% BW and occurred at 40% stance. The peak LCL force was 5% BW and occurred at 90% stance. The CaCL and MCL were unloaded throughout stance. For the CrCL deficient stifle the peak CaCL force was 205% BW and occurred at 40% stance. The peak LCL force was 5% BW and occurred at 90% stance. The MCL was unloaded throughout stance.

The ligament forces during stance for the CrCL intact and CrCL deficient stifle with a 0% muscle force magnitude change are shown in FIGURE 106 and FIGURE 107, respectively.

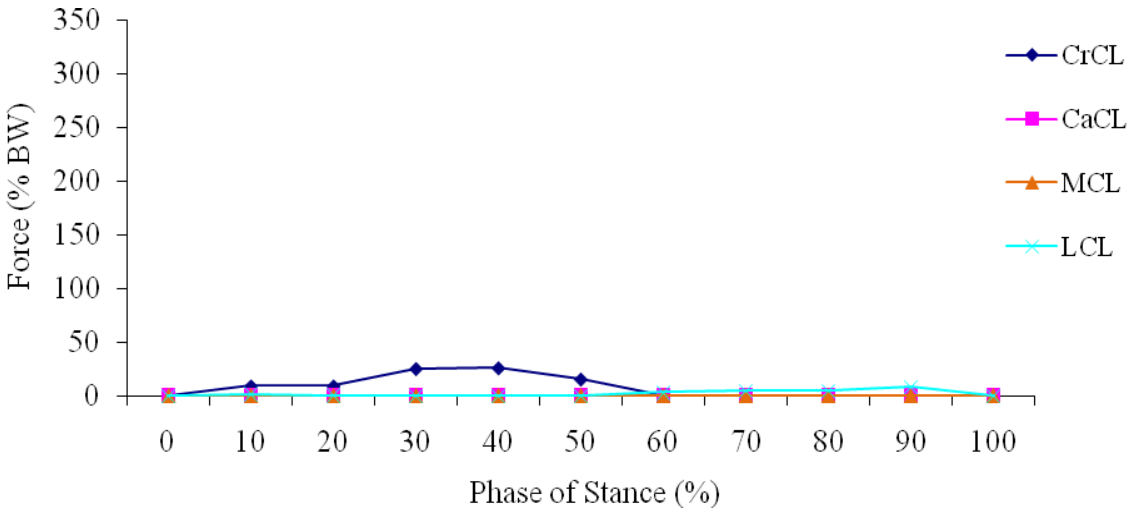

FIGURE 106 - Ligament forces for CrCL intact stifle (0% muscle force magnitude change).

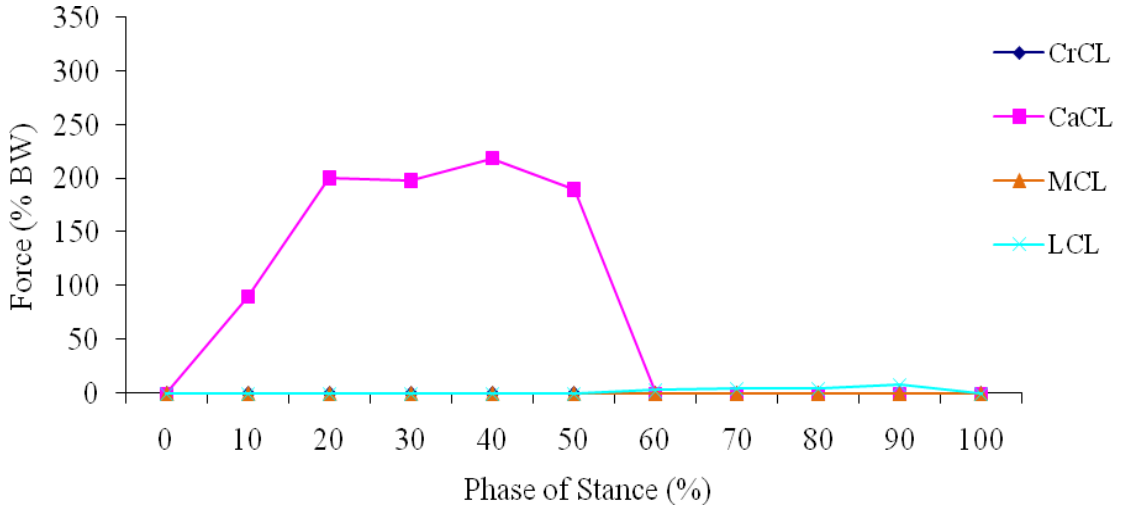

FIGURE 107 - Ligament forces for CrCL deficient stifle (0% muscle force magnitude change).

For the CrCL intact stifle the peak CrCL force was 26% body weight (BW) and occurred at 40% stance. The CaCL was unloaded thoughout stance. The peak LCL force was 8% BW and occurred at 90% stance. The MCL was unloaded throughout stance. For the CrCL deficient stifle the peak CaCL force was 219% BW and occurred at 40% stance. The peak LCL force was 8% BW and occurred at 90% stance. The MCL was unloaded throughout stance.

The ligament forces during stance for the CrCL intact and CrCL deficient stifle with a 10% muscle force magnitude change are shown in FIGURE 108 and FIGURE 109, respectively.

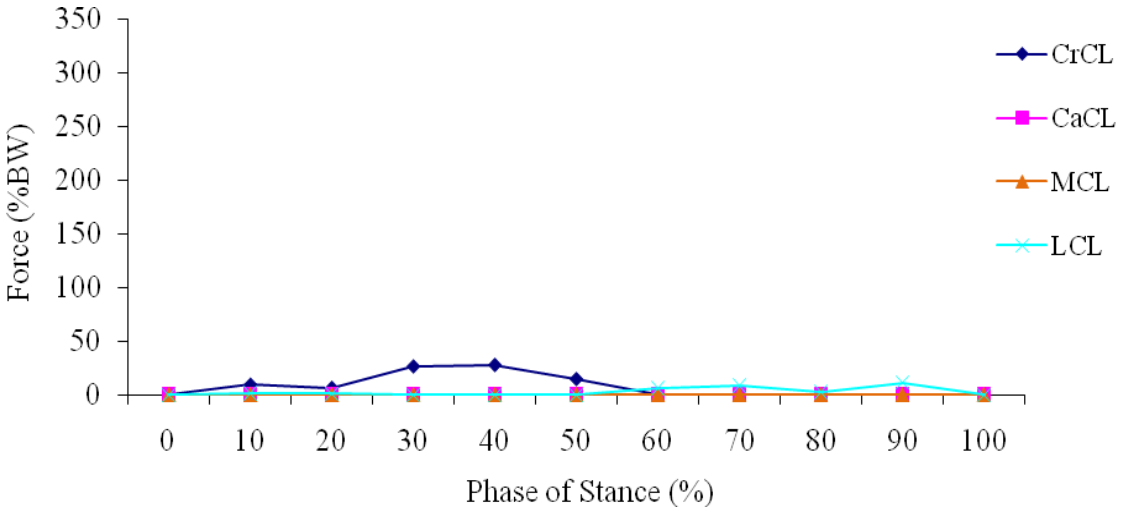

FIGURE 108 - Ligament forces for CrCL intact stifle (+10% muscle force magnitude change).

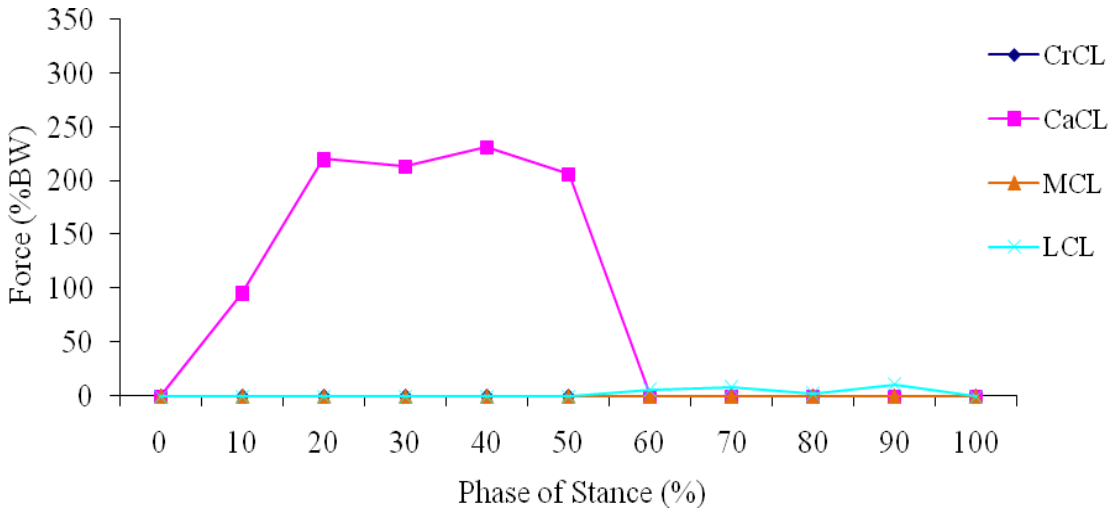

FIGURE 109 - Ligament forces for CrCL deficient stifle (+10% muscle force magnitude change).

For the CrCL intact stifle the peak CrCL force was 27% BW and occurred at 40% stance. The peak LCL force was 11% BW and occurred at 90% stance. The CaCL and MCL were unloaded throughout stance. For the CrCL deficient stifle the peak CaCL force was 231% BW and occurred at 40% stance. The peak LCL force was 11% BW and occurred at 90% stance. The MCL was unloaded throughout stance.

The ligament forces during stance for the CrCL intact and CrCL deficient stifle with a 20% muscle force magnitude change are shown in FIGURE 110 and FIGURE 111, respectively.

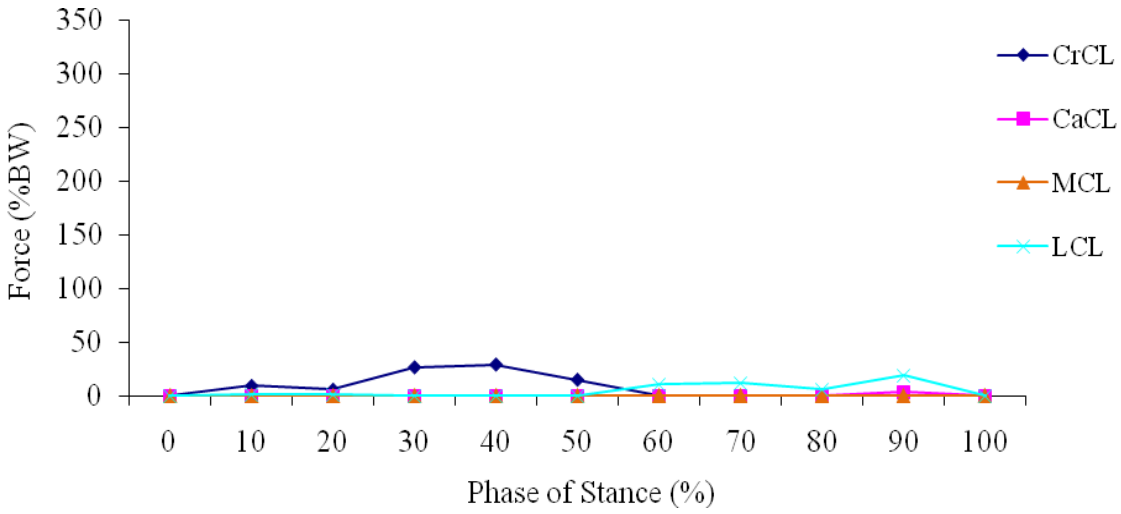

FIGURE 110 - Ligament forces for CrCL intact stifle (+20% muscle force magnitude change).

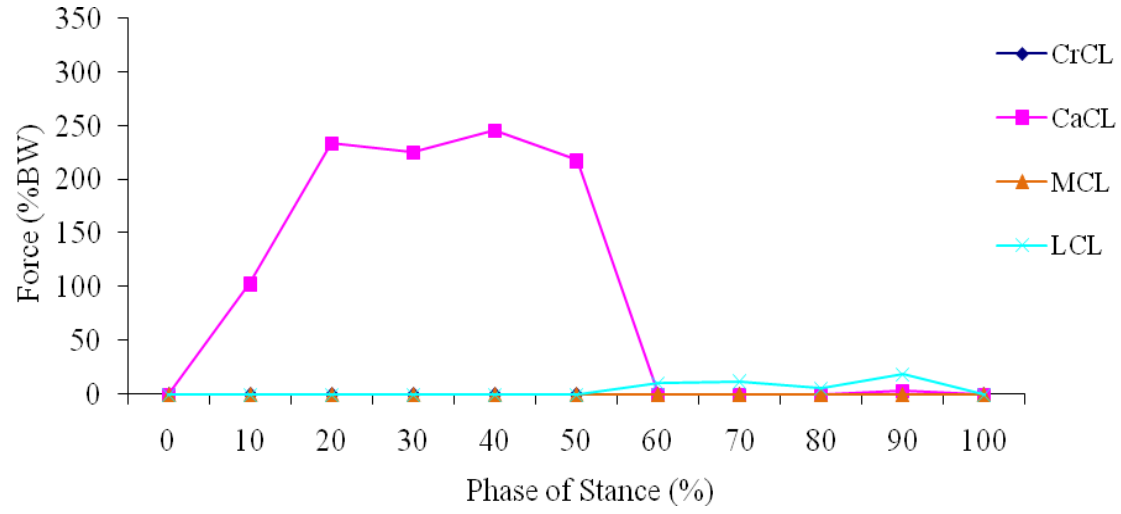

FIGURE 111 - Ligament forces for CrCL deficient stifle (+20% muscle force magnitude change).

For the CrCL intact stifle the peak CrCL force was 29% BW and occurred at 40% stance. The peak LCL force was 19% BW and occurred at 90% stance. The peak CaCL force was 3% BW and occurred at 90% stance. The MCL was unloaded throughout stance. For the CrCL deficient stifle the peak CaCL force was 245% BW and occurred at 40% stance. The peak LCL force was 19% BW and occurred at 90% stance. The MCL was unloaded throughout stance.

4.3.6.2 Ligament Forces Summary for Muscle Force Magnitude Ligament Variation

Ligament forces for each phase of stance for varying muscle force magnitude were determined in the CrCL intact and CrCL deficient stifle. Peak CrCL forces varied by 3% BW ranging from 26% BW to 29% BW for varying muscle force magnitude for the CrCL intact stifle. Peak CaCL forces varied by 44% BW ranging from 190% Bw to 234% BW for the CrCL deficient stifle. The peak CrCL forces for varying muscle force magnitude for the CrCL intact stifle are shown in FIGURE 112, and the peak CaCL forces for varying muscle force magnitude for the CrCL deficient stifle are shown in FIGURE 113.

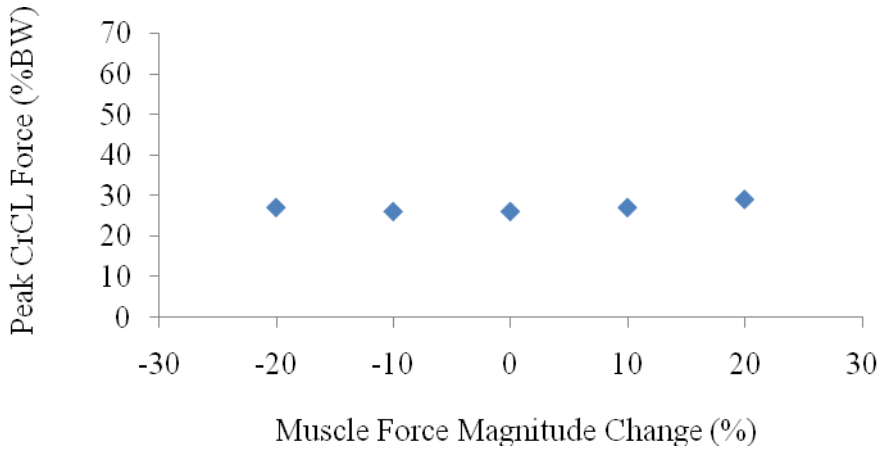

FIGURE 112 - Peak CrCL forces in the CrCL intact stifle for each percentage muscle magnitude change.

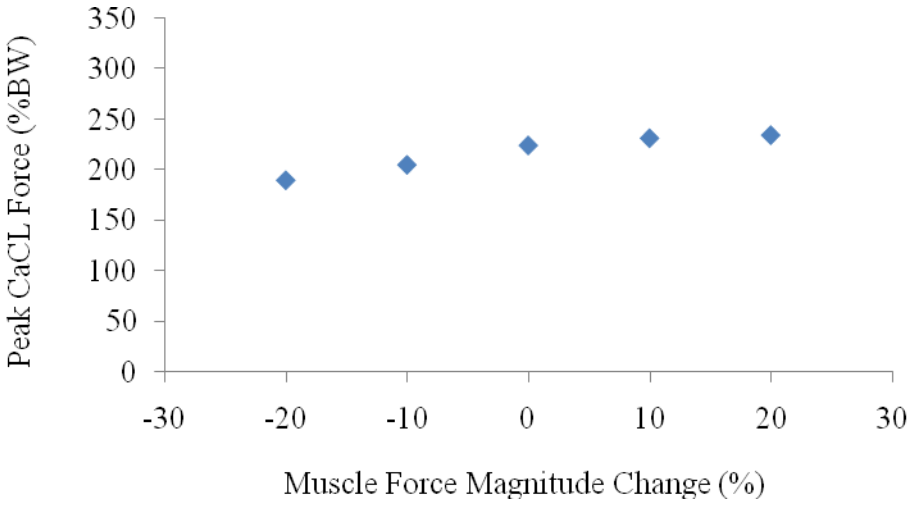

FIGURE 113 - Peak CaCL forces in the CrCL deficient stifle for each percentage muscle magnitude change.

4.3.6.3 Tibial Translation for Muscle Force Magnitude Variation

The relative tibial translation across the phases of stance is plotted in FIGURE 114.

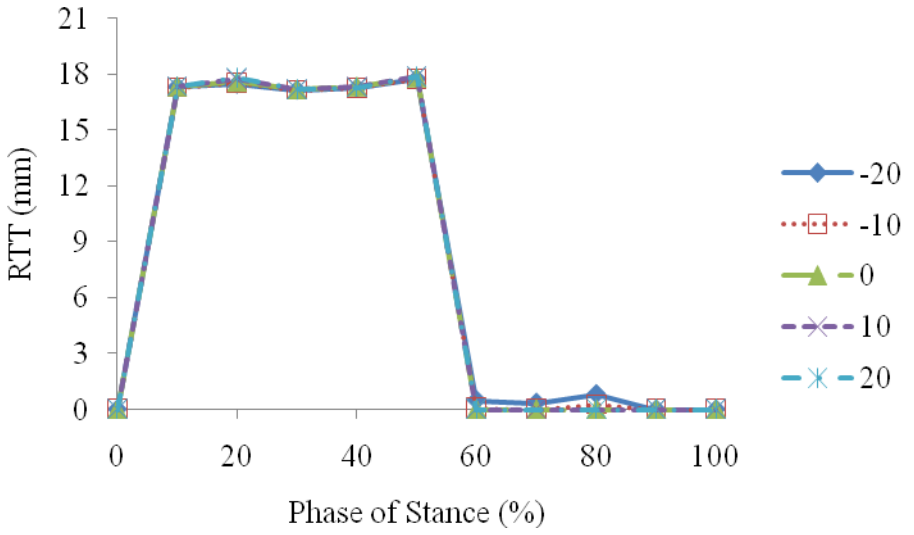

FIGURE 114 - Relative tibial translation between the CrCL intact and deficient stifle models for each percentage muscle magnitude change.

4.3.6.4 Tibial Translation Summary for Muscle Force Magnitude Variation

The peak relative tibial translation, the phase of stance at which it occurred and the corresponding relative tibial translation per body mass and anatomical tibial translation for each percentage muscle magnitude change are listed in TABLE XVI. The peak relative tibial translation values are plotted in FIGURE 115.

TABLE XVI

PEAK TIBIAL TRANSLATION VALUES FOR EACH PERCENTAGE MUSCLE MAGNITUDE CHANGE EVALUATED

Change (%)	-20	-10	0	10	20
Stance Phase (%)	50	50	50	50	50
Peak RTT (mm)*	17.7	17.8	17.8	17.9	17.9
RTT/BM** (mm/kg)	0.55	0.56	0.56	0.56	0.56
ATT***	1.42	1.42	1.43	1.44	1.43

*RTT = Relative Tibial Translation = $(FT_{deficient})_{loaded} - (FT_{intact})_{loaded}$

**RTT/BM = Relative Tibial Translation per Body Mass

***ATT = Anatomical Tibial Translation = $\frac{(FT_{deficient})_{loaded} - (FT_{intact})_{loaded}}{(FT_{intact})_{loaded}}$

where FT denotes the craniocaudal distance from a fixed point on the femur to a fixed point on the tibia, deficient denotes the CrCL was suppressed, intact denotes the CrCL was not suppressed and loaded denotes weight bearing

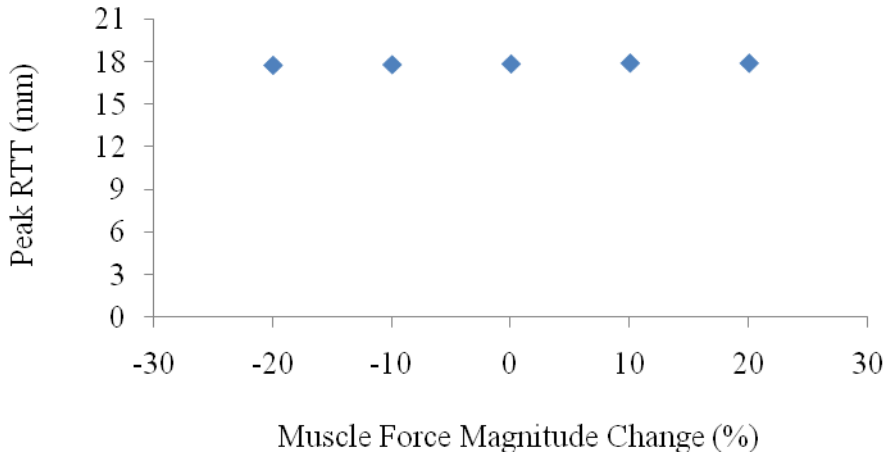

FIGURE 115 - Peak relative tibial translation values for each percentage muscle magnitude change.

Peak relative tibial translation varied by +0.6/-0.6% from baseline for varying muscle force magnitude.

4.3.7 Patellar Ligament Line of Action Angle

4.3.7.1 Ligament Forces for Patellar Ligament Line of Action Angle Variation

The patellar ligament line of action angle (PLLAA) was altered from baseline by an angular rotation to simulate variation in the direction of the quadriceps force. The nine scenarios evaluated were a PLLAAs of -20°, -15°, -10°, -5°, 0° (baseline), 5°, 10°, 15°, and 20° relative to baseline. FIGURE 116 illustrates the altered PLLAA with a positive change in direction from baseline.

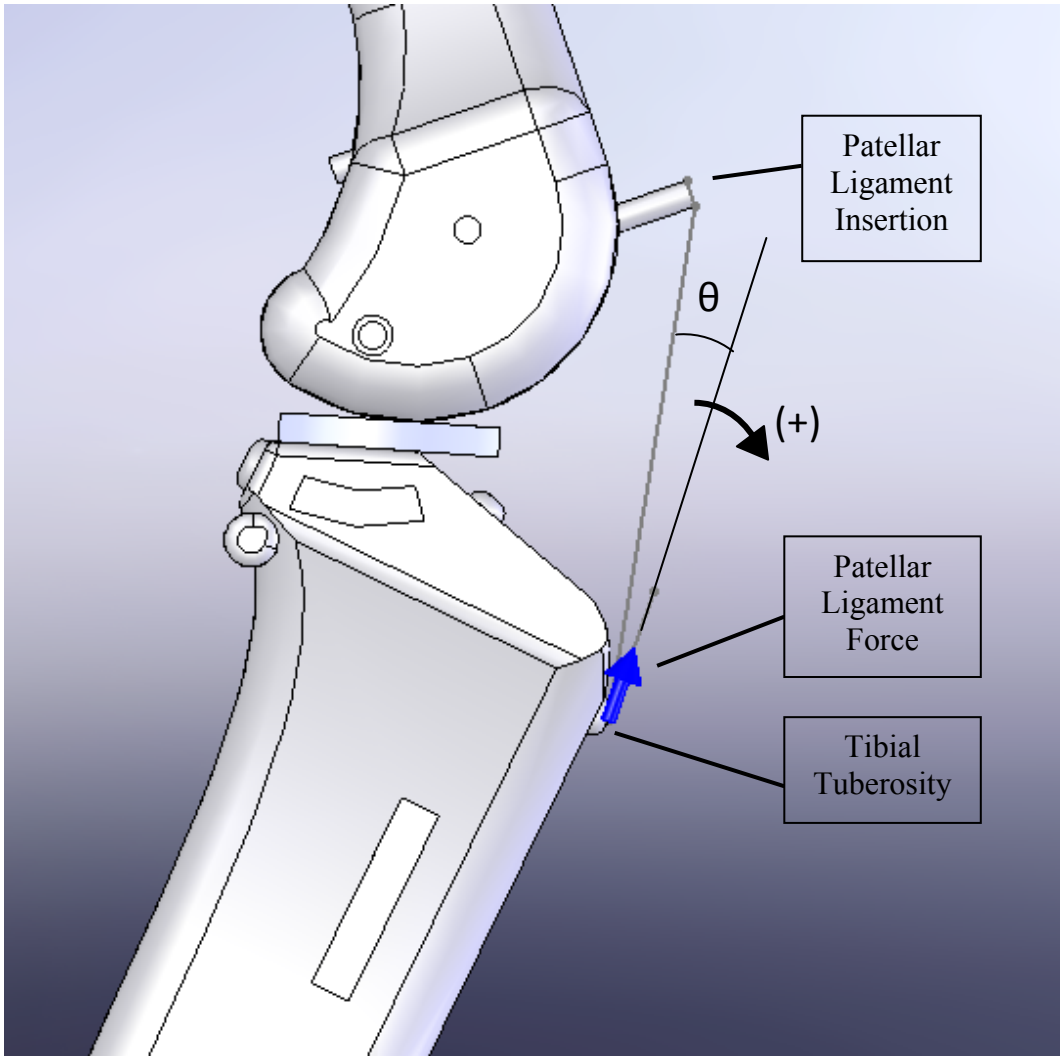

FIGURE 116 – Patellar ligament line of action angle.

The ligament forces during stance for the CrCL intact and CrCL deficient stifle with a -20° PLLAA are shown in FIGURE 117 and FIGURE 118, respectively.

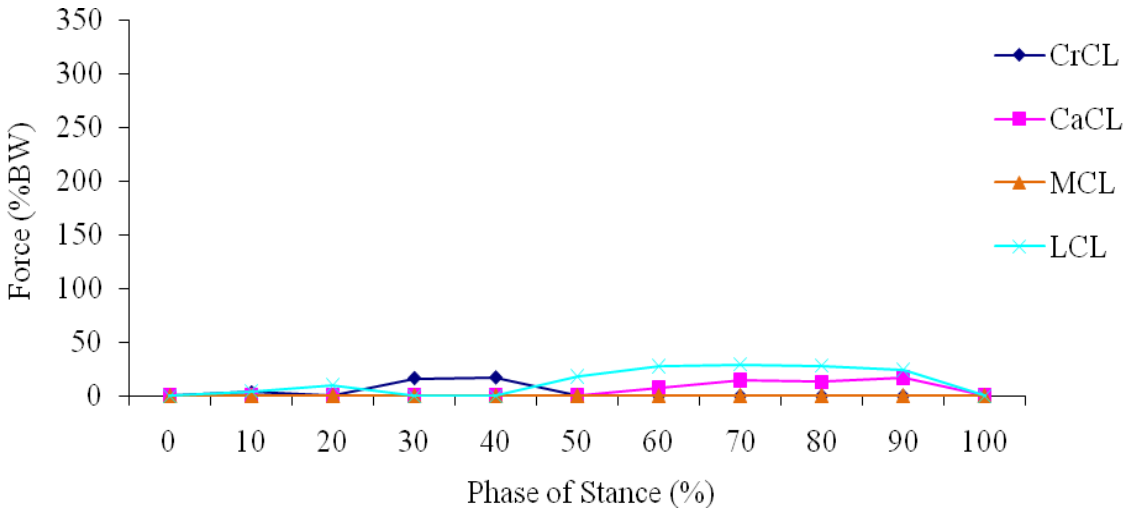

FIGURE 117 - Ligament forces for CrCL intact stifle (-20° PLLAA).

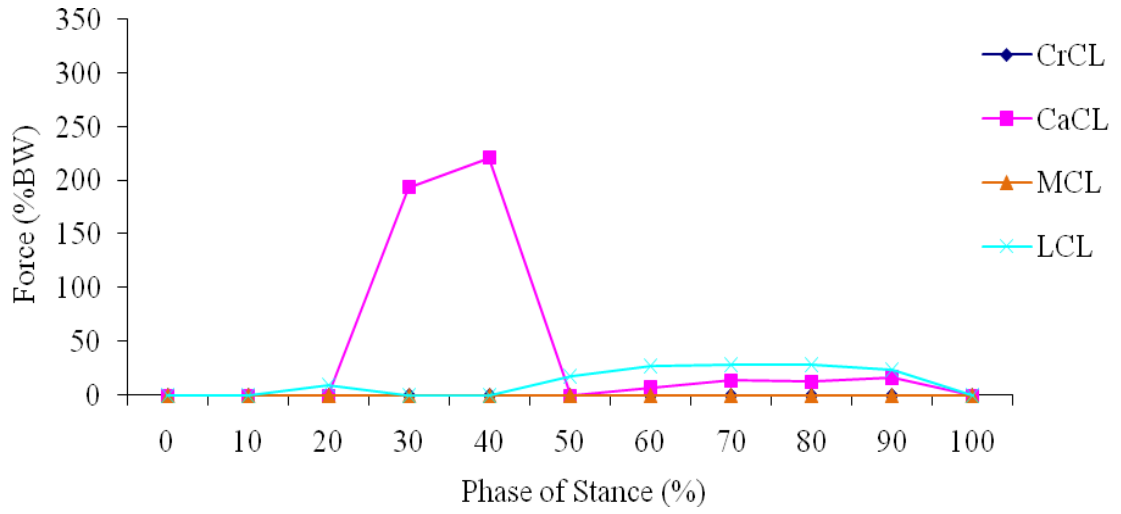

FIGURE 118 - Ligament forces for CrCL deficient stifle (-20° PLLAA).

For the CrCL intact stifle the peak CrCL force was 17% BW and occurred at 40% stance. The peak CaCL force was 17% BW and occurred at 90% stance. The peak LCL force was 29% BW and occurred at 70% stance. The MCL was unloaded throughout stance.

For the CrCL deficient stifle the peak CaCL force was 221% BW and occurred at 40% stance. The peak LCL force was 29% BW and occurred at 70% stance. The MCL was unloaded throughout stance.

The ligament forces during stance for the CrCL intact and CrCL deficient stifle with a -15° PLLAA are shown in FIGURE 119 and FIGURE 120, respectively.

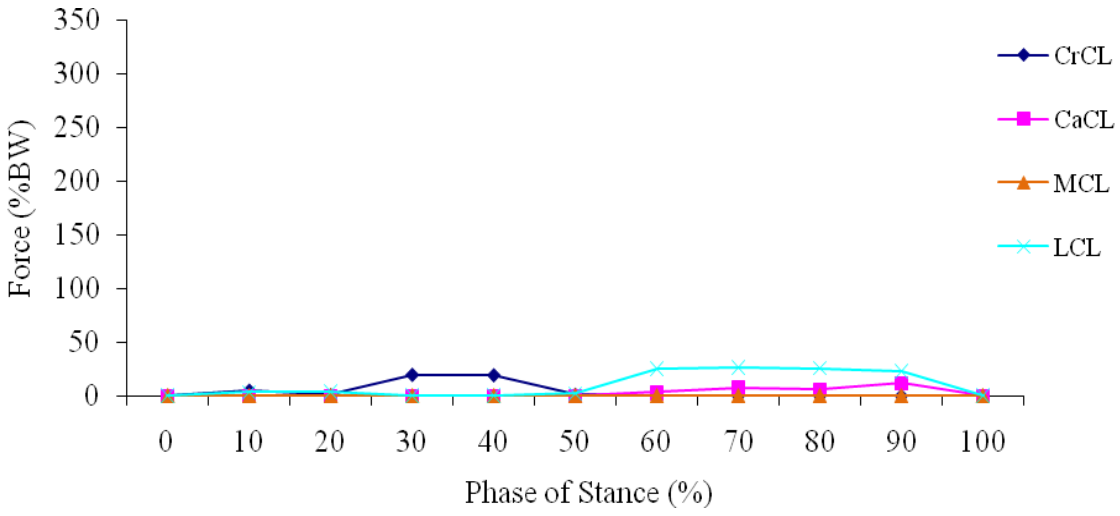

FIGURE 119 - Ligament forces for CrCL intact stifle (-15° PLLAA).

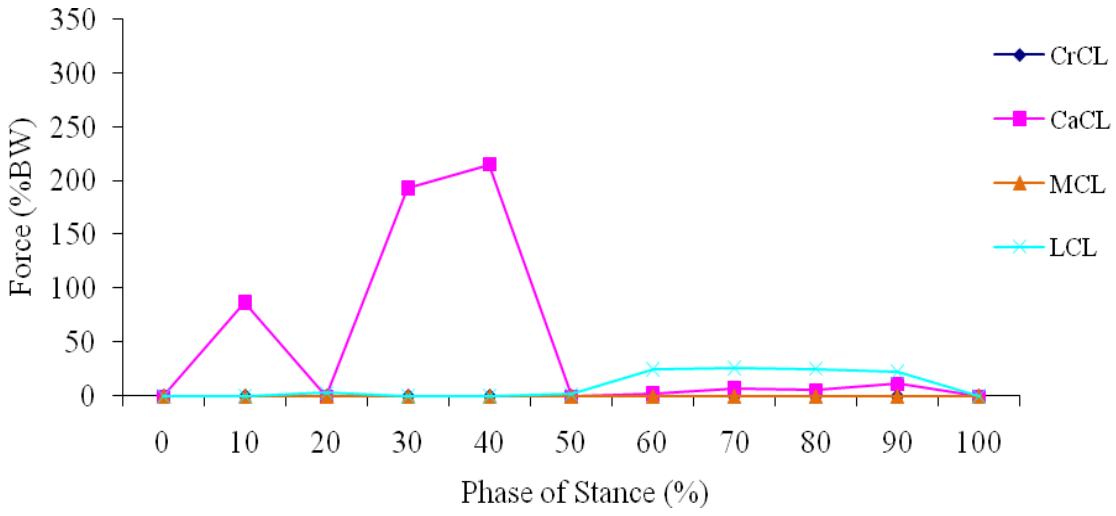

FIGURE 120 - Ligament forces for CrCL deficient stifle (-15° PLLAA).

For the CrCL intact stifle the peak CrCL force was 19% BW and occurred at 30% stance. The peak CaCL force was 12% BW and occurred at 90% stance. The peak LCL force was 26% BW and occurred at 70% stance. The MCL was unloaded throughout stance. For the CrCL deficient stifle the peak CaCL force was 215% BW and occurred at 40% stance. The peak LCL force was 26% BW and occurred at 70% stance. The MCL was unloaded throughout stance.

The ligament forces during stance for the CrCL intact and CrCL deficient stifle with a -10° PLLAA are shown in FIGURE 121 and FIGURE 122, respectively.

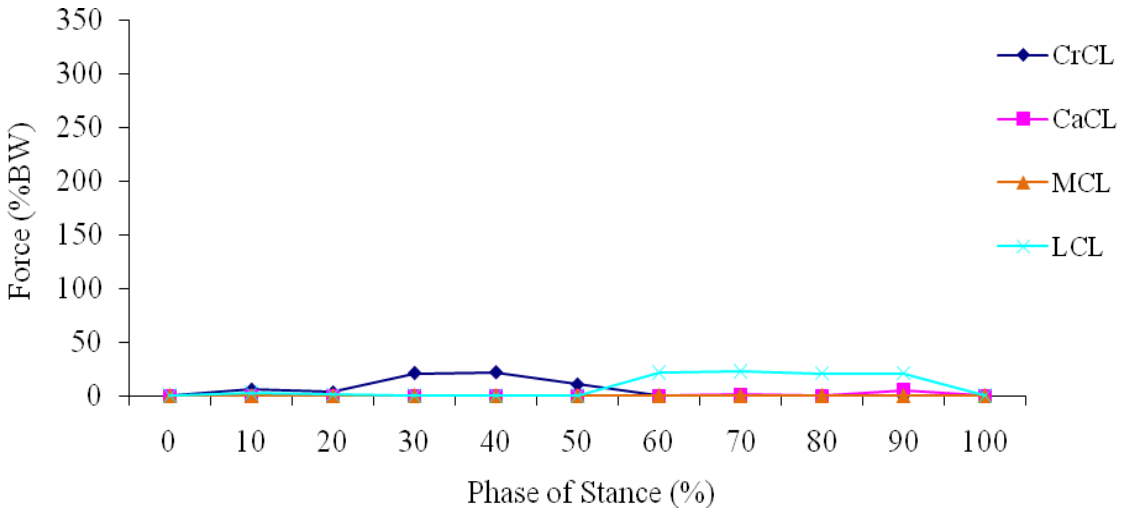

FIGURE 121 - Ligament forces for CrCL intact stifle (-10° PLLAA).

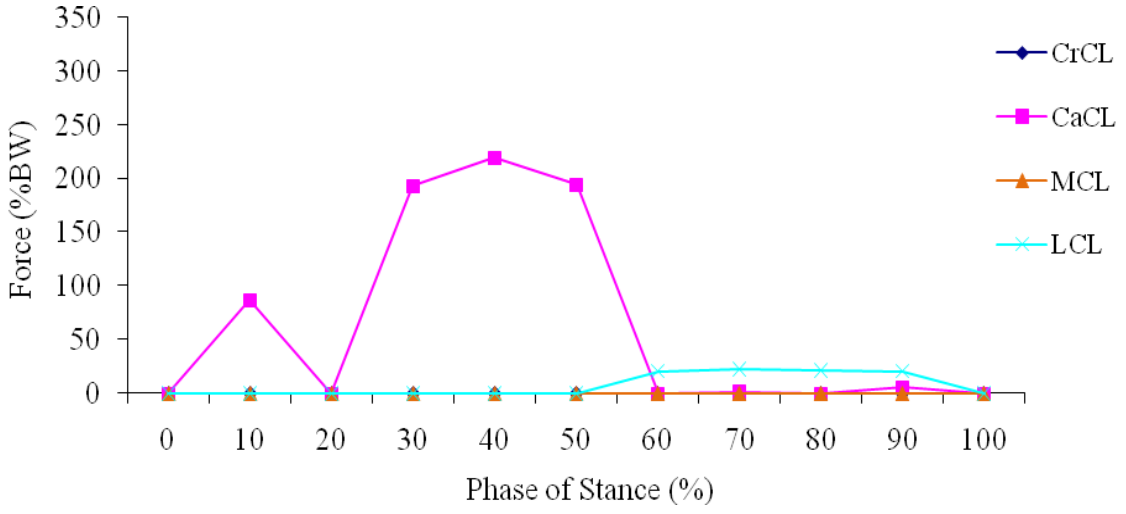

FIGURE 122 - Ligament forces for CrCL deficient stifle (-10° PLLAA).

For the CrCL intact stifle the peak CrCL force was 22% BW and occurred at 40% stance. The peak CaCL force was 5% BW and occurred at 90% stance. The peak LCL force was 23% BW and occurred at 70% stance. The MCL was unloaded throughout stance. For the

CrCL deficient stifle the peak CaCL force was 219% BW and occurred at 40% stance. The peak LCL force was 23% BW and occurred at 70% stance. The MCL was unloaded throughout stance.

The ligament forces during stance for the CrCL intact and CrCL deficient stifle with a -5° PLLAA are shown in FIGURE 123 and FIGURE 124, respectively.

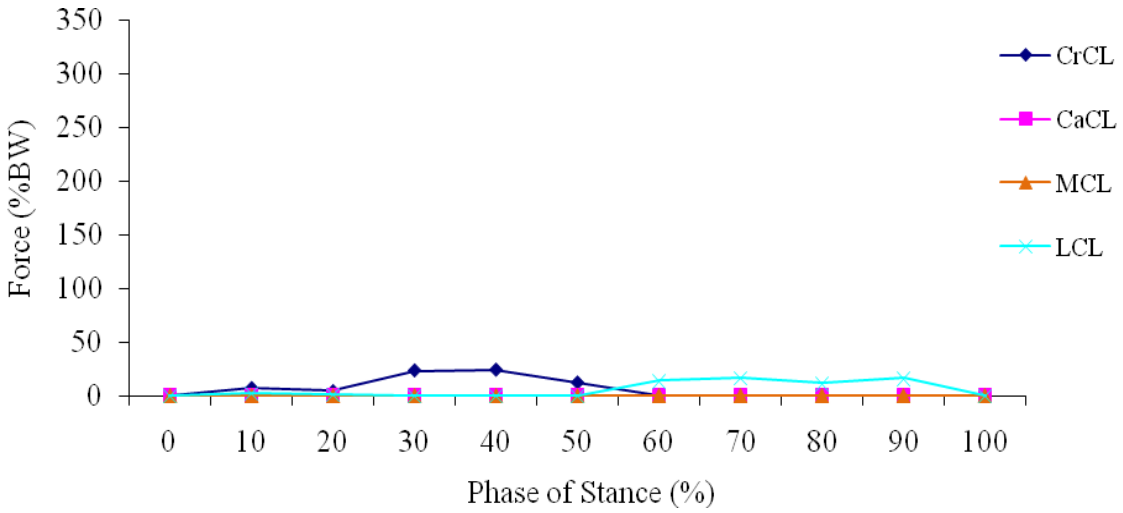

FIGURE 123 - Ligament forces for CrCL intact stifle (-5° PLLAA).

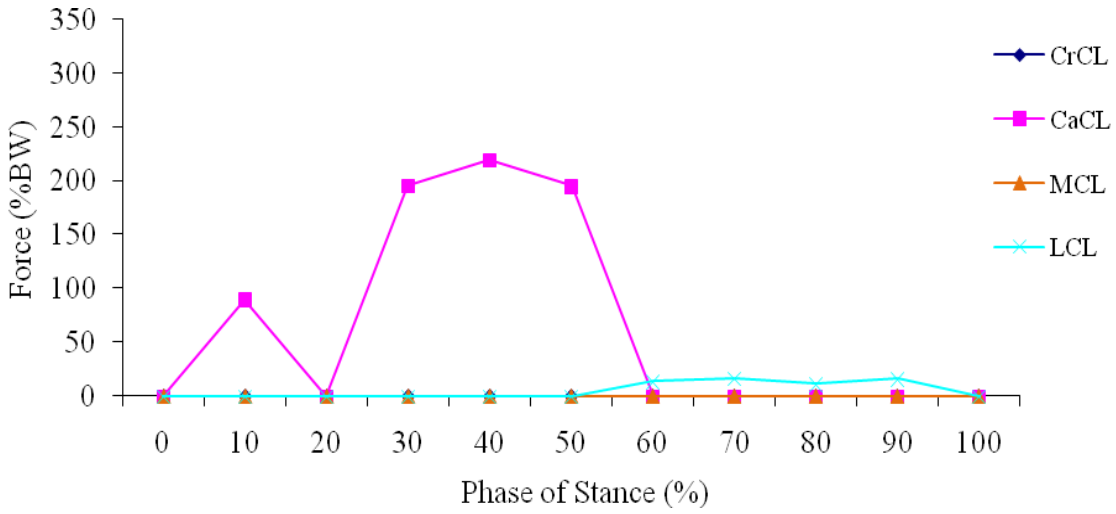

FIGURE 124 - Ligament forces for CrCL deficient stifle (-5° PLLAA).

For the CrCL intact stifle the peak CrCL force was 24% BW and occurred at 40% stance. The peak LCL force was 16% BW and occurred at 70% stance. The CaCL and MCL were unloaded throughout stance. For the CrCL deficient stifle the peak CaCL force was 219% BW and occurred at 40% stance. The peak LCL force was 16% BW and occurred at 70% stance. The MCL was unloaded throughout stance.

The ligament forces during stance for the CrCL intact and CrCL deficient stifle with a 0° PLLAA are shown in FIGURE 125 and FIGURE 126, respectively.

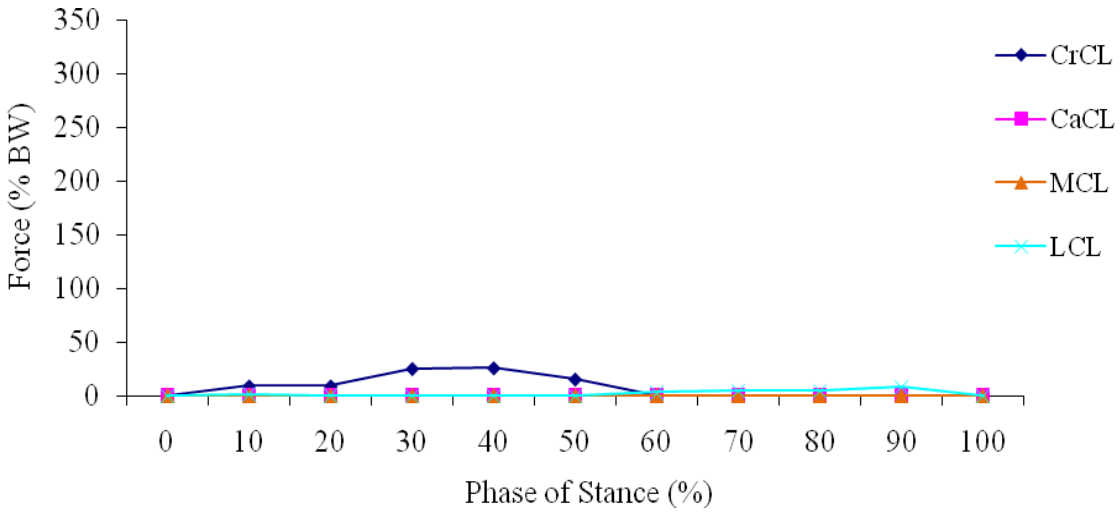

FIGURE 125 - Ligament forces for CrCL intact stifle (0° PLLAA).

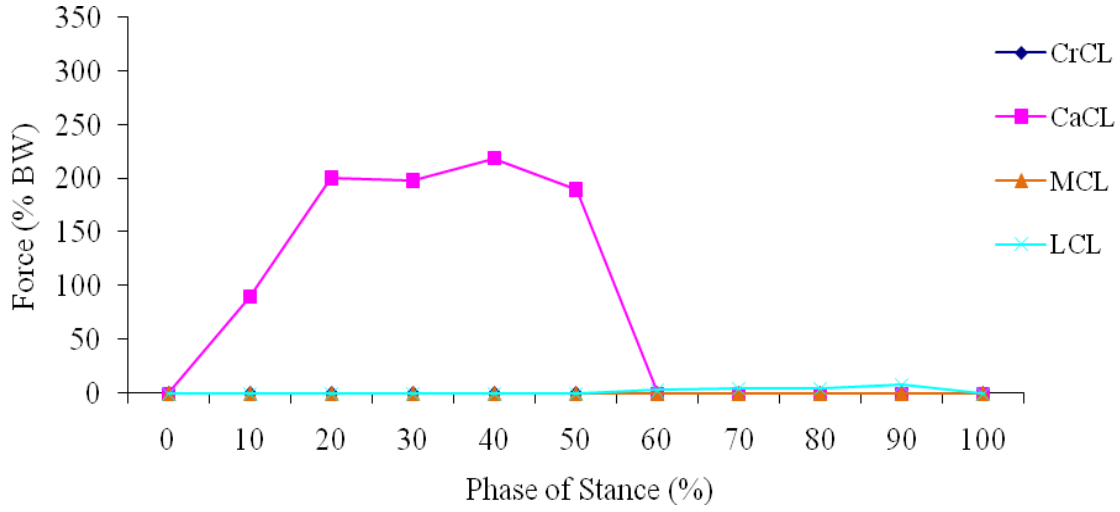

FIGURE 126 - Ligament forces for CrCL deficient stifle (0° PLLAA).

For the CrCL intact stifle the peak CrCL force was 26% body weight (BW) and occurred at 40% stance. The CaCL was unloaded thoughout stance. The peak LCL force was 8% BW and occurred at 90% stance. The MCL was unloaded throughout stance. For the

CrCL deficient stifle the peak CaCL force was 219% BW and occurred at 40% stance. The peak LCL force was 8% BW and occurred at 90% stance. The MCL was unloaded throughout stance.

The ligament forces during stance for the CrCL intact and CrCL deficient stifle with a 5° PLLAA are shown in FIGURE 127 and FIGURE 128, respectively.

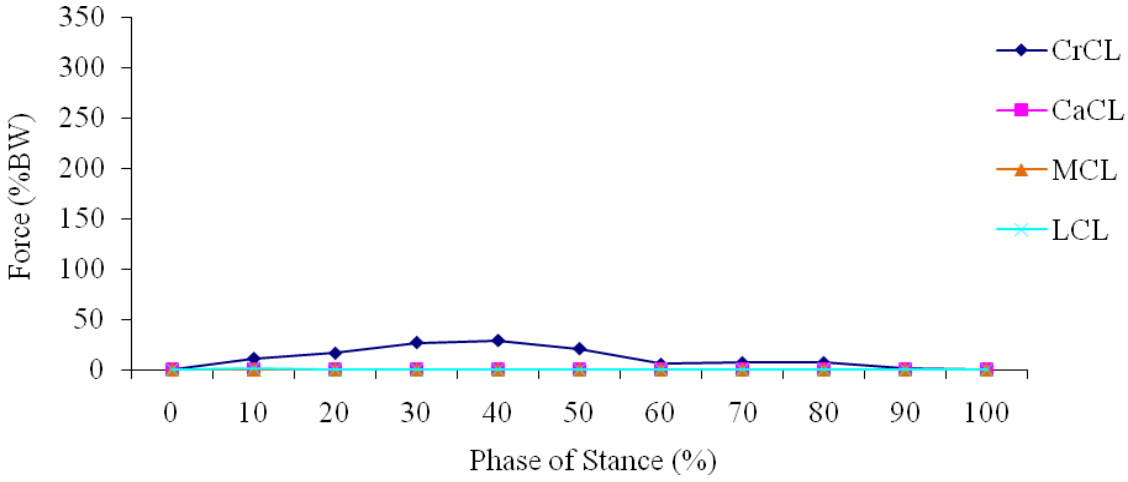

FIGURE 127 - Ligament forces for CrCL intact stifle (+5° PLLAA).

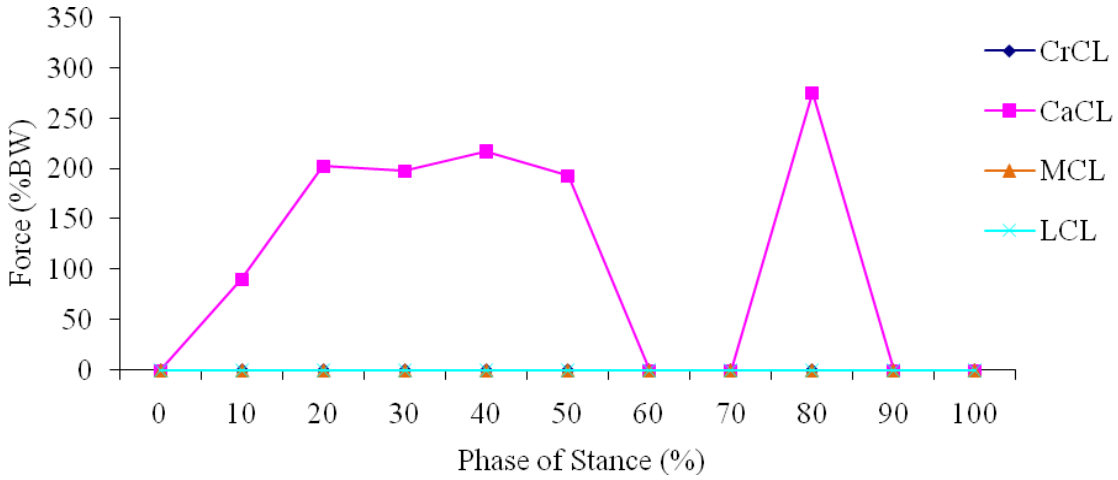

FIGURE 128 - Ligament forces for CrCL deficient stifle (+5° PLLAA).

For the CrCL intact stifle the peak CrCL force was 29% BW and occurred at 40% stance. The peak LCL force was 1% BW and occurred at 90% stance. The CaCL and MCL were unloaded throughout stance. For the CrCL deficient stifle the peak CaCL force was 275% BW and occurred at 80% stance. The LCL and MCL were unloaded throughout stance.

The ligament forces during stance for the CrCL intact and CrCL deficient stifle with a 10° PLLAA are shown in FIGURE 129 and FIGURE 130, respectively.

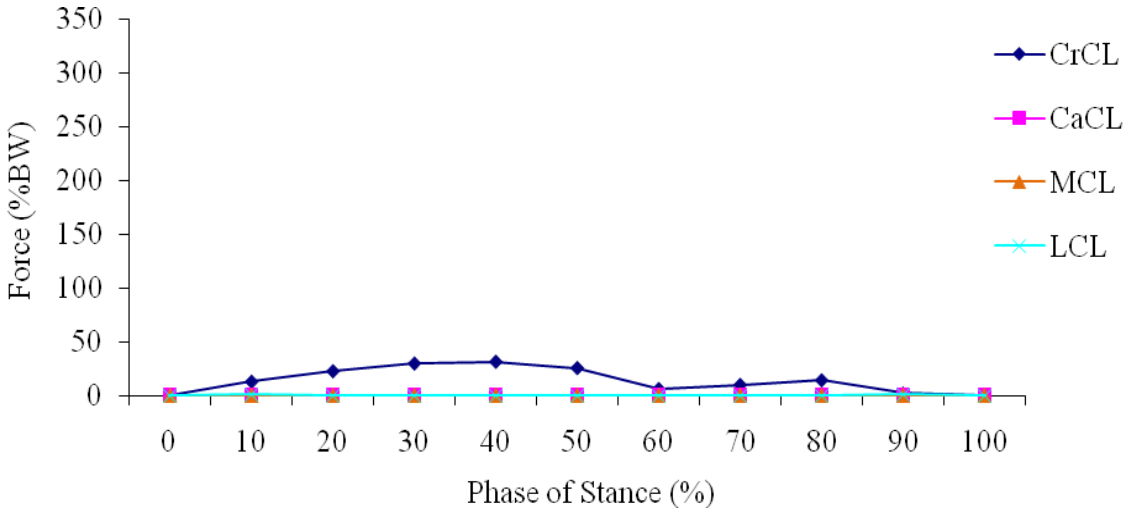

FIGURE 129 - Ligament forces for CrCL intact stifle (+10° PLLAA).

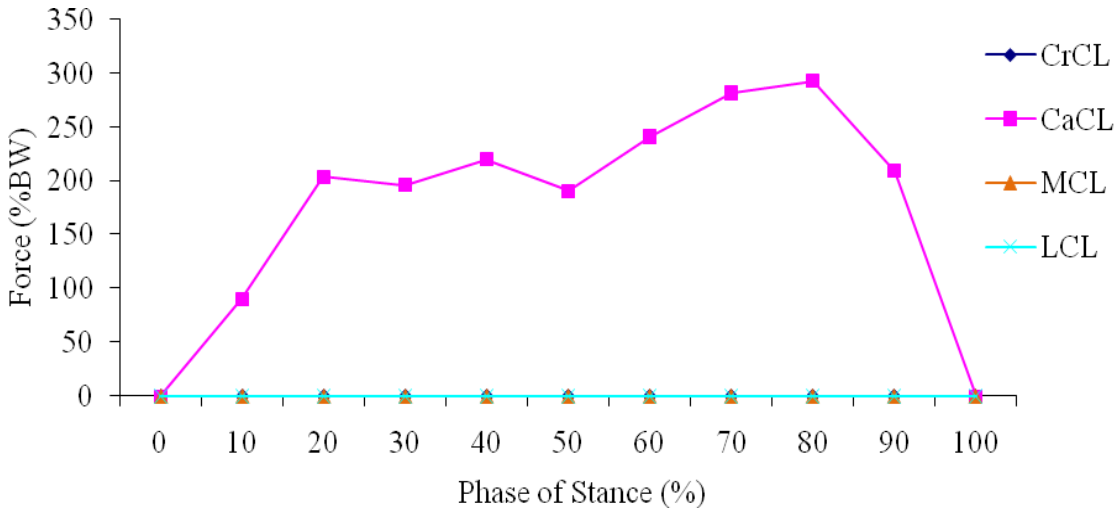

FIGURE 130 - Ligament forces for CrCL deficient stifle (+10° PLLAA).

For the CrCL intact stifle the peak CrCL force was 31% BW and occurred at 40% stance. The peak LCL force was 1% BW and occurred at 90% stance. The CaCL and MCL were unloaded throughout stance. For the CrCL deficient stifle the peak CaCL force was 292% BW and occurred at 80% stance. The LCL and MCL were unloaded throughout stance.

The ligament forces during stance for the CrCL intact and CrCL deficient stifle with a 15° PLLAA are shown in FIGURE 131 and FIGURE 132, respectively.

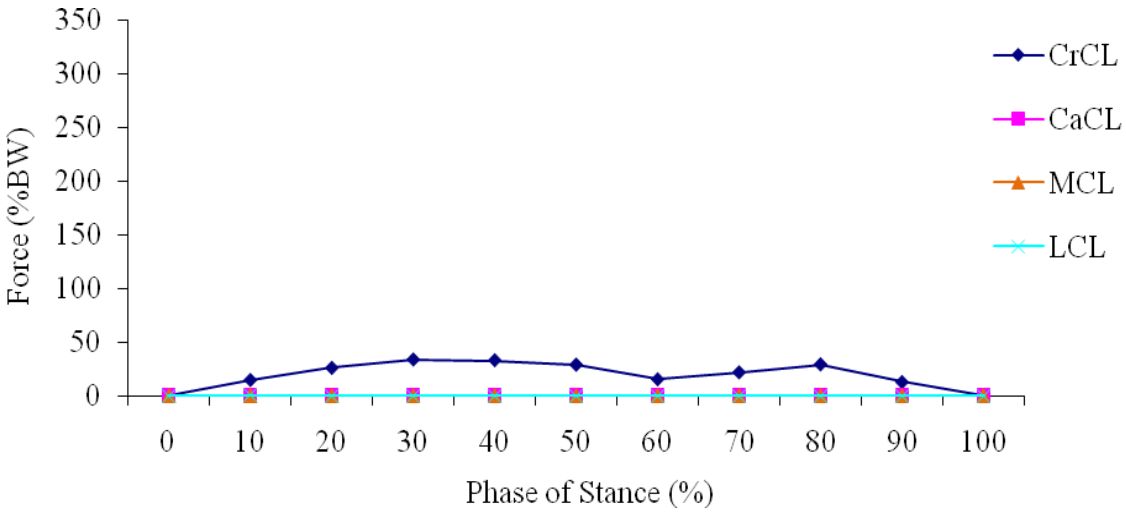

FIGURE 131 - Ligament forces for CrCL intact stifle (+15° PLLAA).

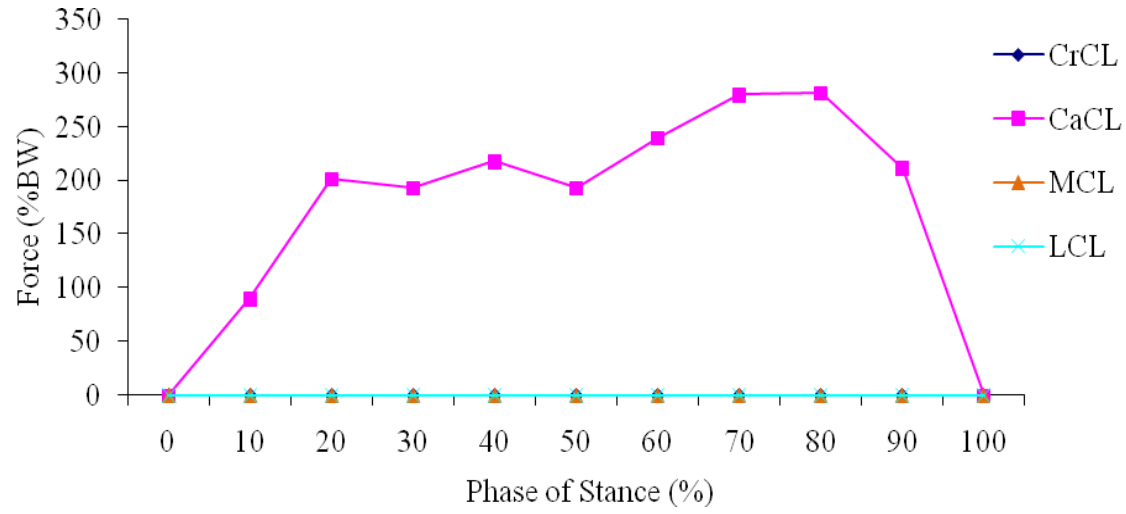

FIGURE 132 - Ligament forces for CrCL deficient stifle (+15° PLLAA).

For the CrCL intact stifle the peak CrCL force was 34% BW and occurred at 30% stance. The peak LCL force was 1% BW and occurred at 10% stance. The CaCL and MCL were

unloaded throughout stance. For the CrCL deficient stifle the peak CaCL force was 282% BW and occurred at 80% stance. The LCL and MCL were unloaded throughout stance.

The ligament forces during stance for the CrCL intact and CrCL deficient stifle with a 20° PLLAA are shown in FIGURE 133 and FIGURE 134, respectively.

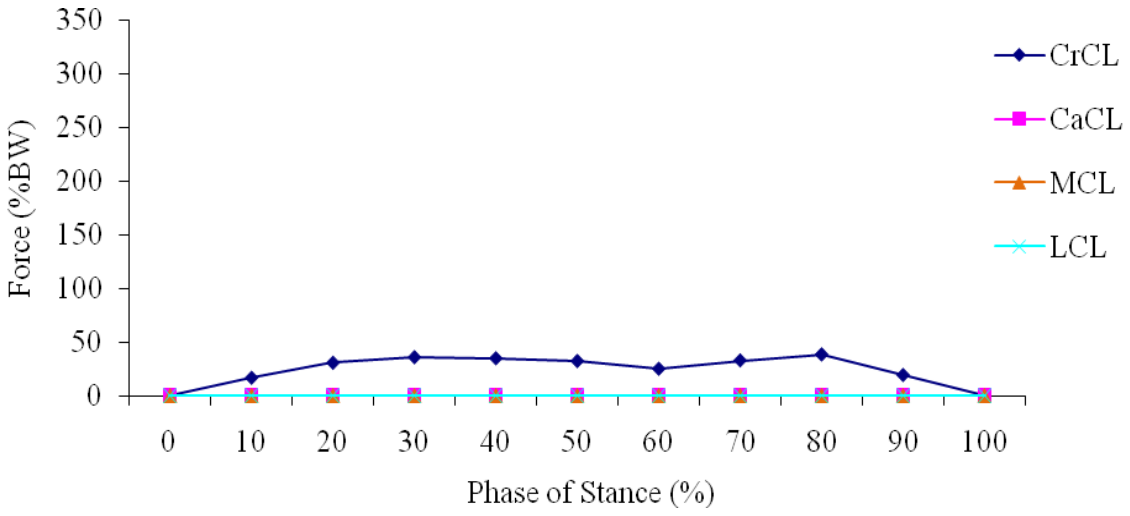

FIGURE 133 - Ligament forces for CrCL intact stifle (+20° PLLAA).

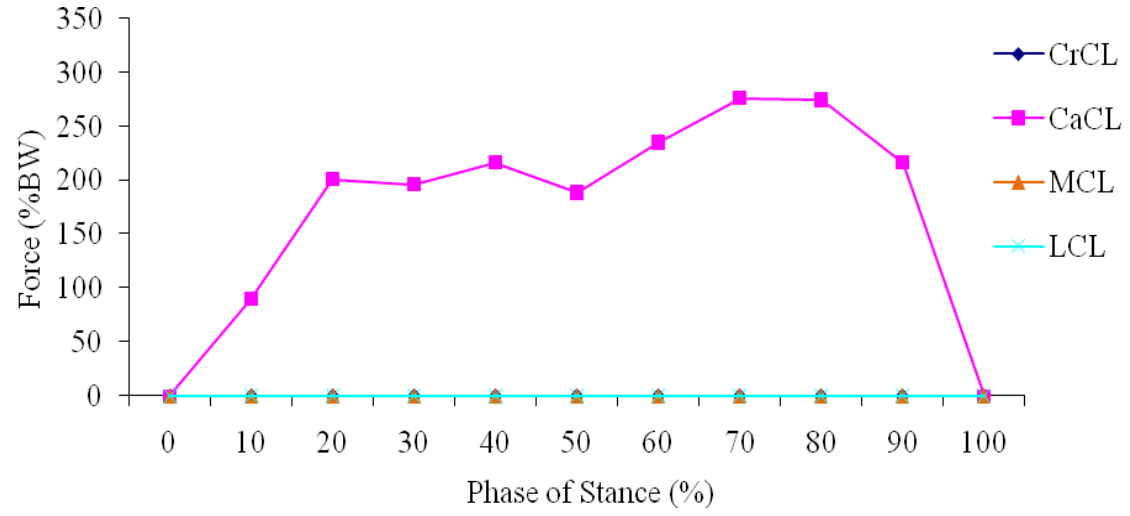

FIGURE 134 - Ligament forces for CrCL deficient stifle (+20° PLLAA).

For the CrCL intact stifle the peak CrCL force was 38% BW and occurred at 80% stance. The CaCL, LCL and MCL were unloaded throughout stance. For the CrCL deficient stifle the peak CaCL force was 276% BW and occurred at 70% stance. The LCL and MCL were unloaded throughout stance.

4.3.7.2 Ligament Forces Summary for Patellar Ligament Line of Action Angle Variation

Ligament forces for each phase of stance for varying PLLAA were determined in the CrCL intact and CrCL deficient stifle. Peak CrCL forces varied by 21% BW ranging from 17% BW to 38% BW for varying PLLAA for the CrCL intact stifle. Peak CaCL forces varied by 77% BW ranging from 215% BW to 292% BW for the CrCL deficient stifle. The peak CrCL forces for varying PLLAA for the CrCL intact stifle are shown in FIGURE 135, and the peak CaCL forces for varying PLLAA for the CrCL deficient stifle are shown in FIGURE 136.

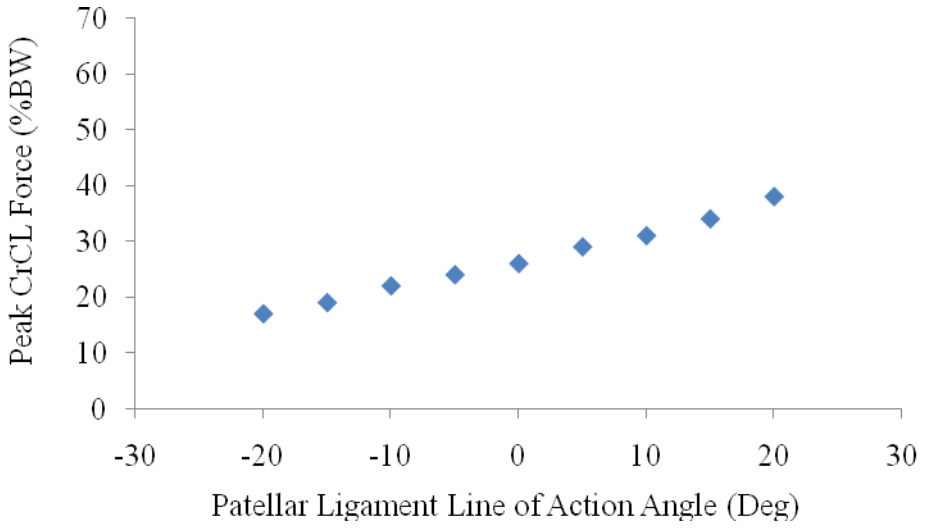

FIGURE 135 - Peak CrCL forces in the CrCL intact stifle for each PLLAA.

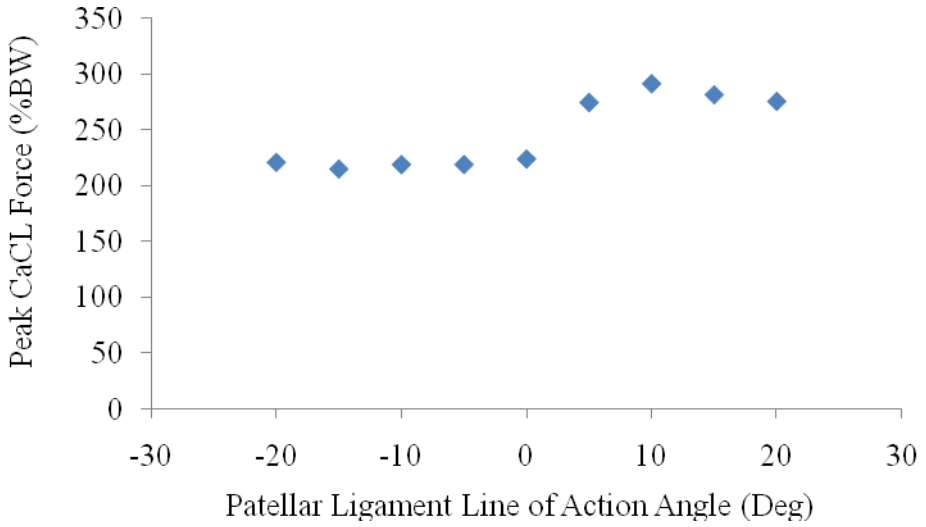

FIGURE 136 - Peak CaCL forces in the CrCL deficient stifle for each PLLAA.

4.3.7.3 Tibial Translation for Patellar Ligament Line of Action Angle Variation

The relative tibial translation across the phases of stance is plotted in FIGURE 137.

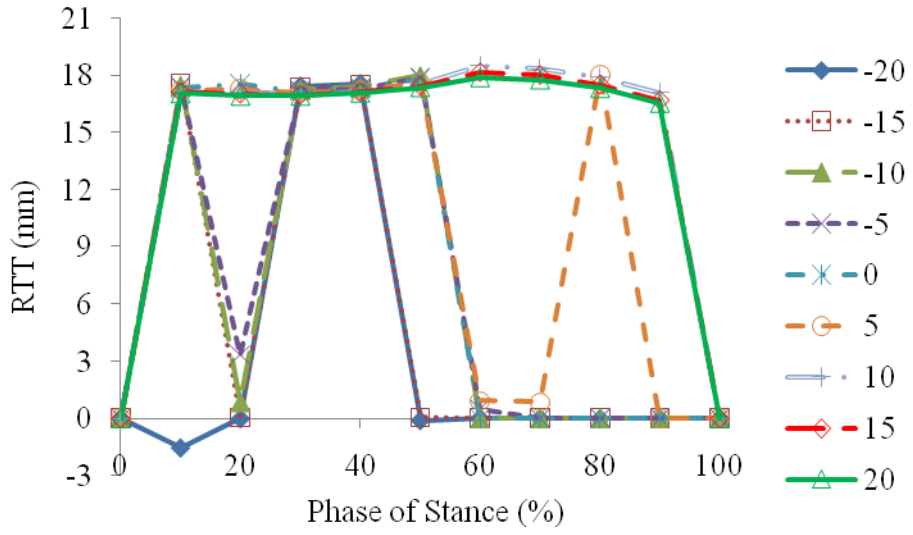

FIGURE 137 - Relative tibial translation between the CrCL intact and deficient stifle models for each PLLAA.

4.3.7.4 Tibial Translation Summary for Patellar Ligament Line of Action Angle Variation

The peak relative tibial translation, the phase of stance at which it occurred and the corresponding relative tibial translation per body mass and anatomical tibial translation for each PLLAA are listed in TABLE XVII. The peak relative tibial translation values are plotted in FIGURE 138.

TABLE XVII

PEAK TIBIAL TRANSLATION VALUES FOR EACH PATELLAR LIGAMENT LINE OF ACTION ANGLE EVALUATED

Change (%)	-20	-15	-10	-5	0	5	10	15	20
Stance Phase (%)	40	10	50	50	50	80	60	60	60
RTT (mm)*	17.5	17.6	18.0	17.9	17.8	18.1	18.5	18.2	17.9
RTT/BM (mm/kg)**	0.55	0.55	0.56	0.56	0.56	0.56	0.58	0.57	0.56
ATT***	1.12	1.02	1.46	1.45	1.43	903	2.36	2.22	2.12

*RTT = Relative Tibial Translation = $\left(FT_{deficient}\right)_{loaded} - \left(FT_{intact}\right)_{loaded}$

**RTT/BM = Relative Tibial Translation per Body Mass

***ATT = Anatomical Tibial Translation = $\frac{\left(FT_{deficient}\right)_{loaded} - \left(FT_{intact}\right)_{loaded}}{\left(FT_{intact}\right)_{loaded}}$

where FT denotes the craniocaudal distance from a fixed point on the femur to a fixed point on the tibia, deficient denotes the CrCL was suppressed, intact denotes the CrCL was not suppressed and loaded denotes weight bearing

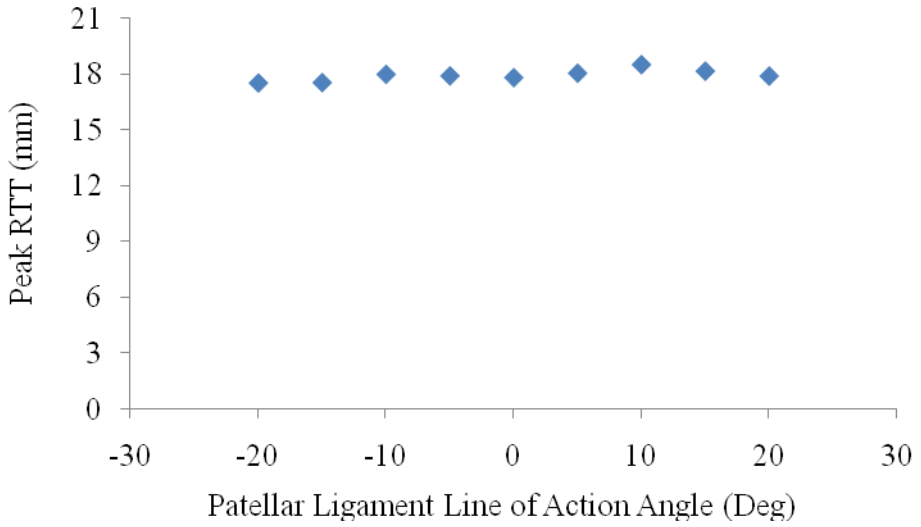

FIGURE 138 - Peak relative tibial translation values for each PLLAA.

Peak relative tibial translation varied by +3.9/-1.7% from baseline for varying patellar ligament line of action direction.

4.3.8 Ground Reaction Force

4.3.8.1 Ligament Forces for Ground Reaction Force Variation

The GRF magnitude values were altered from baseline by discrete percentages to simulate variation in weight for the same dog height. The five scenarios evaluated were GRF magnitude percentage changes of -20%, -10%, 0% (baseline), 10% and 20% from baseline. Baseline GRF values are described in TABLE VII.

The ligament forces during stance for the CrCL intact and CrCL deficient stifle with a -20% GRF change are shown in FIGURE 139 and FIGURE 140, respectively.

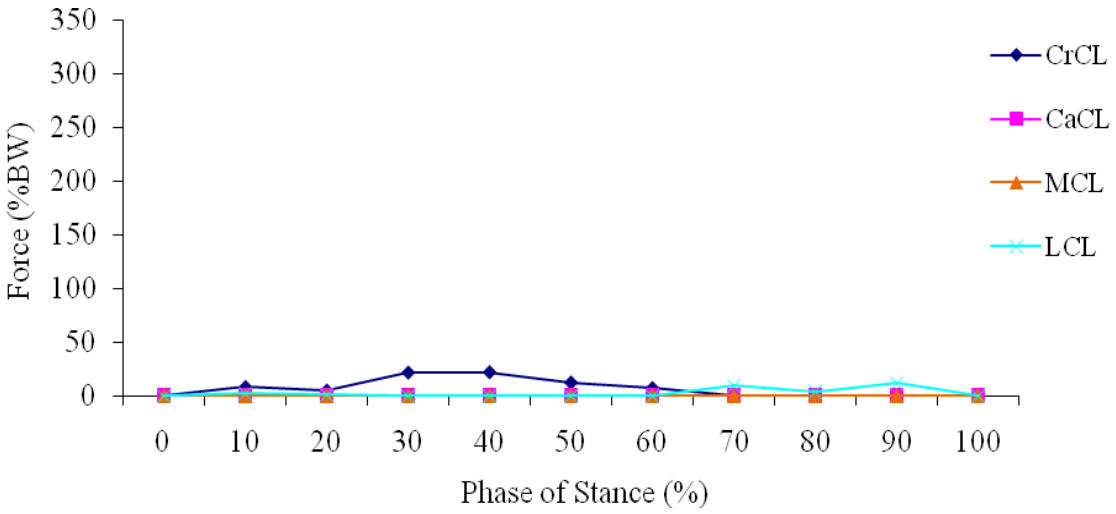

FIGURE 139 - Ligament forces for CrCL intact stifle (-20% GRF magnitude change).

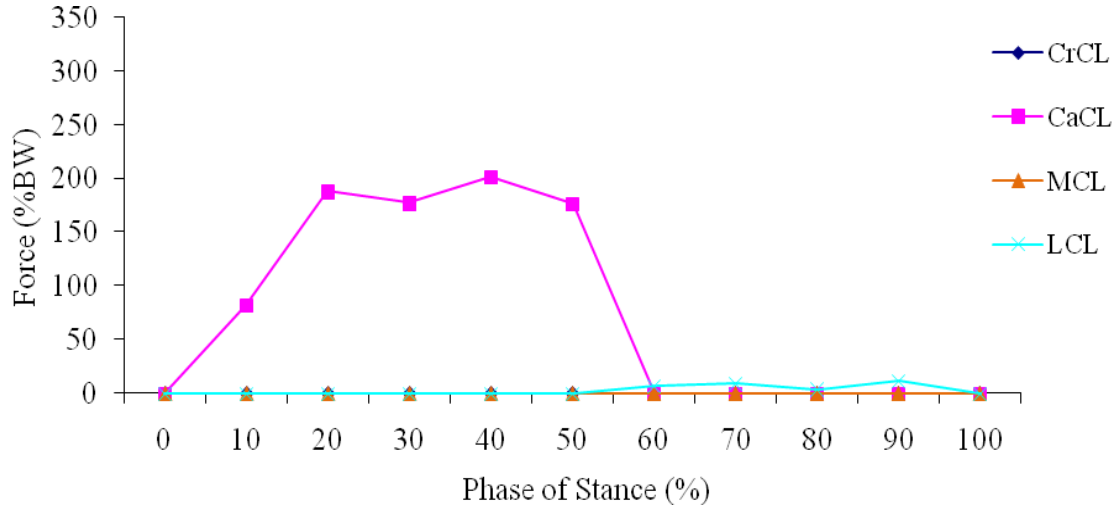

FIGURE 140 - Ligament forces for CrCL deficient stifle (-20% GRF magnitude change).

For the CrCL intact stifle the peak CrCL force was 22% BW and occurred at 40% stance. The peak LCL force was 12% BW and occurred at 90% stance. The CaCL and MCL were unloaded throughout stance. For the CrCL deficient stifle the peak CaCL force was

201% BW and occurred at 40% stance. The peak LCL force was 12% BW and occurred at 90% stance. The MCL was unloaded throughout stance.

The ligament forces during stance for the CrCL intact and CrCL deficient stifle with a -10% GRF change are shown in FIGURE 141 and FIGURE 142, respectively.

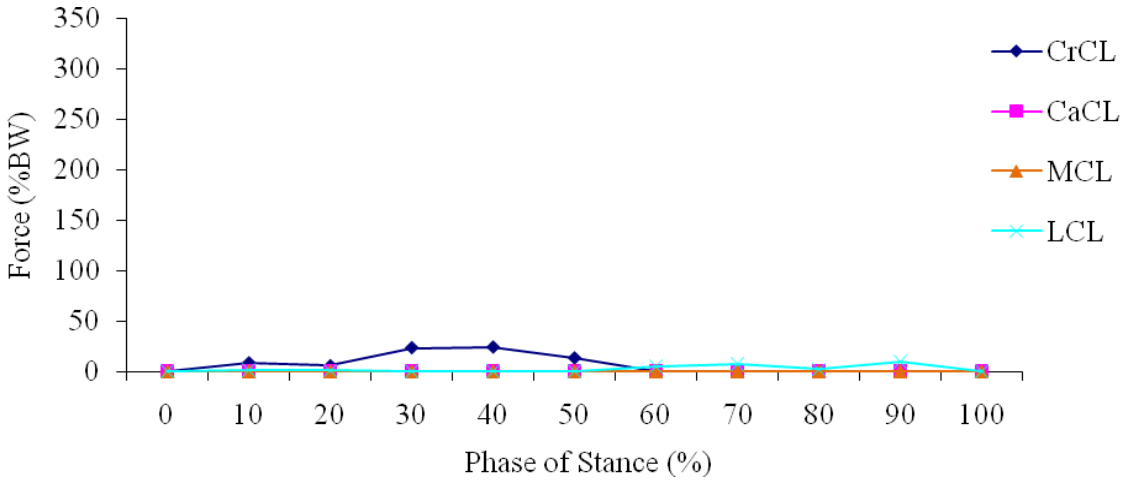

FIGURE 141 - Ligament forces for CrCL intact stifle (-10% GRF magnitude change).

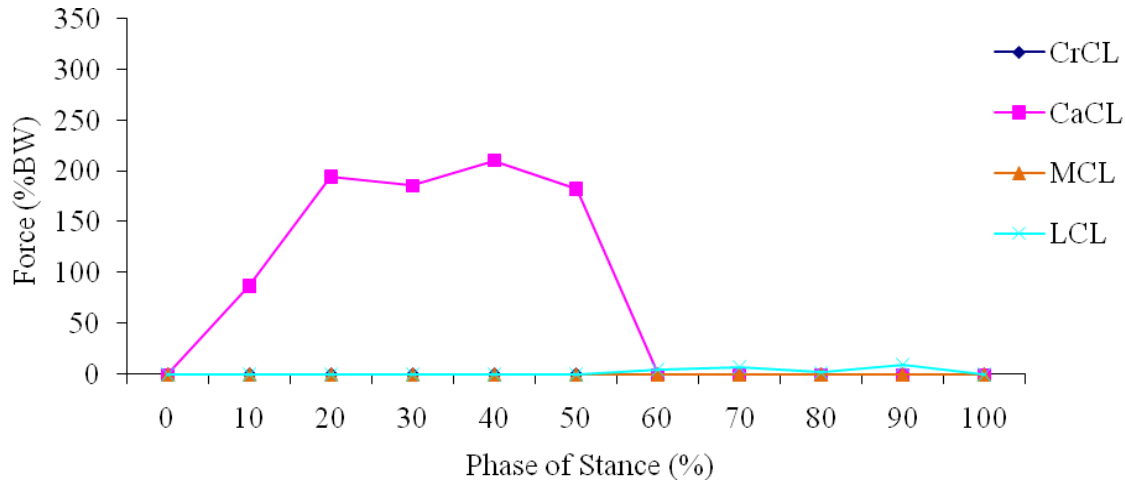

FIGURE 142 - Ligament forces for CrCL deficient stifle (-10% GRF magnitude change).

For the CrCL intact stifle the peak CrCL force was 24% BW and occurred at 40% stance. The peak LCL force was 10% BW and occurred at 90% stance. The CaCL and MCL were unloaded throughout stance. For the CrCL deficient stifle the peak CaCL force was 210% BW and occurred at 40% stance. The peak LCL force was 10% BW and occurred at 90% stance. The MCL was unloaded throughout stance.

The ligament forces during stance for the CrCL intact and CrCL deficient stifle with a 0% GRF change are shown in FIGURE 143 and FIGURE 144, respectively.

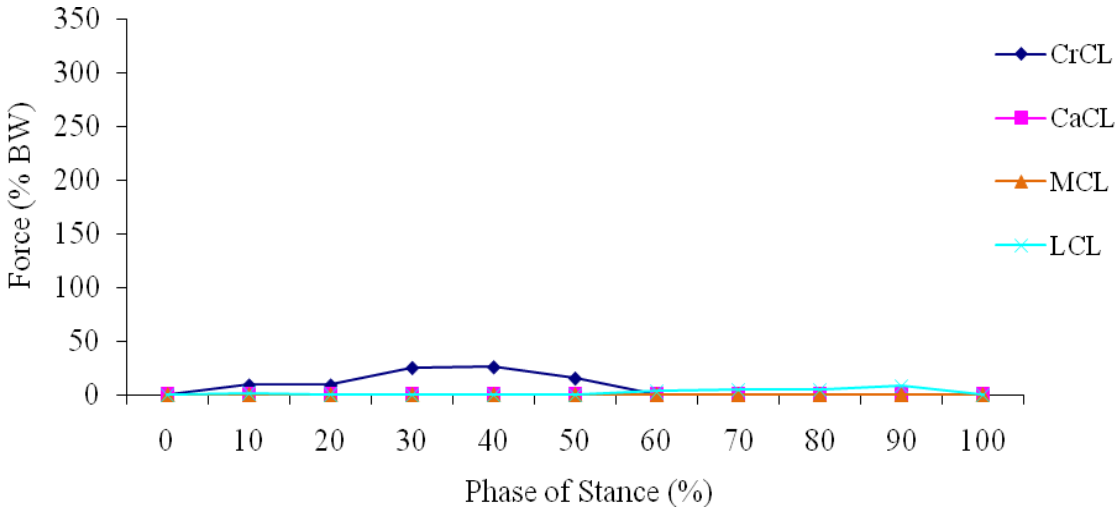

FIGURE 143 - Ligament forces for CrCL intact stifle (0% GRF magnitude change).

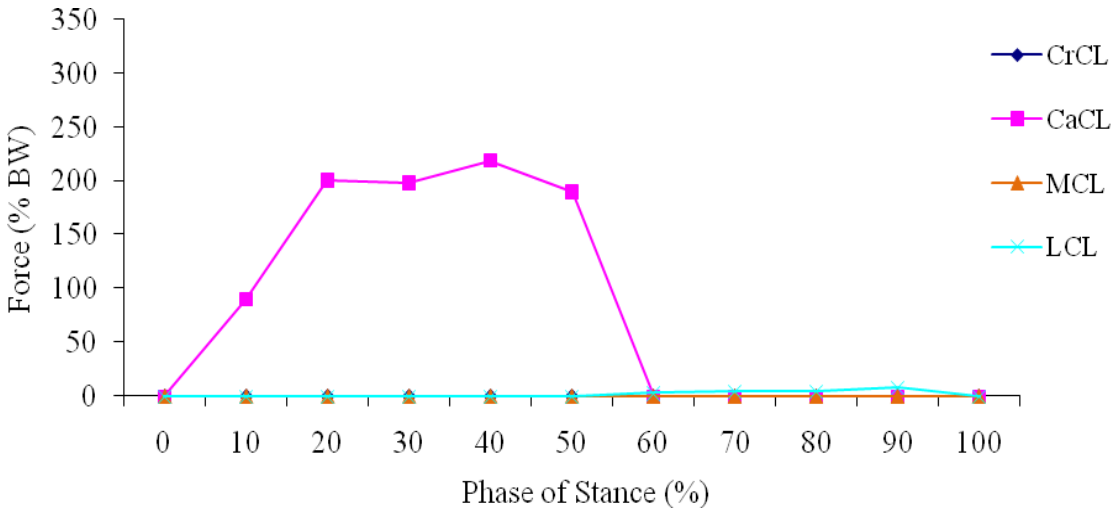

FIGURE 144 - Ligament forces for CrCL deficient stifle (0% GRF magnitude change).

For the CrCL intact stifle the peak CrCL force was 26% body weight (BW) and occurred at 40% stance. The CaCL was unloaded thoughout stance. The peak LCL force was 8% BW and occurred at 90% stance. The MCL was unloaded throughout stance. For the CrCL deficient stifle the peak CaCL force was 219% BW and occurred at 40% stance. The peak LCL force was 8% BW and occurred at 90% stance. The MCL was unloaded throughout stance.

The ligament forces during stance for the CrCL intact and CrCL deficient stifle with a 10% GRF change are shown in FIGURE 145 and FIGURE 146, respectively.

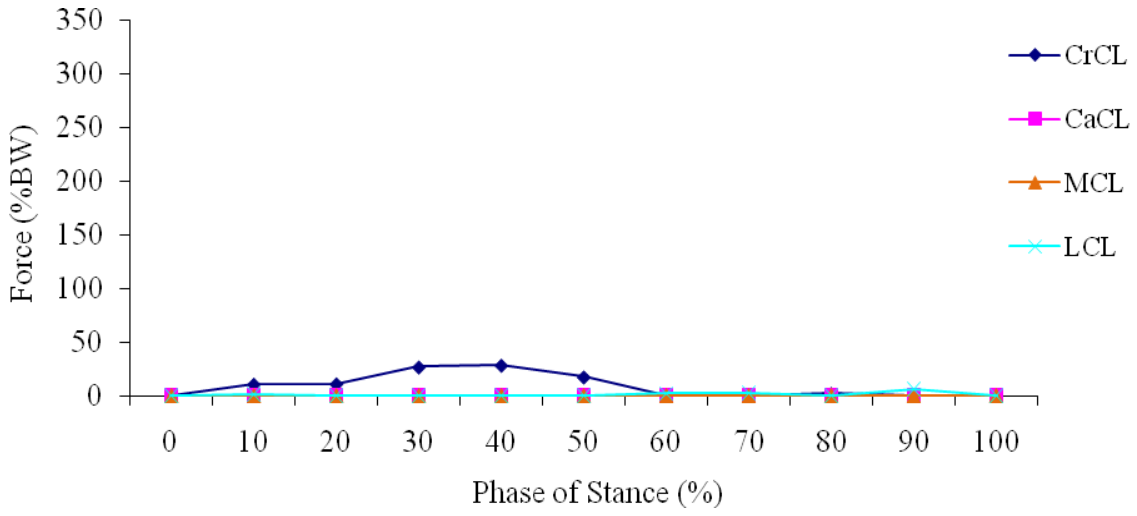

FIGURE 145 - Ligament forces for CrCL intact stifle (+10% GRF magnitude change).

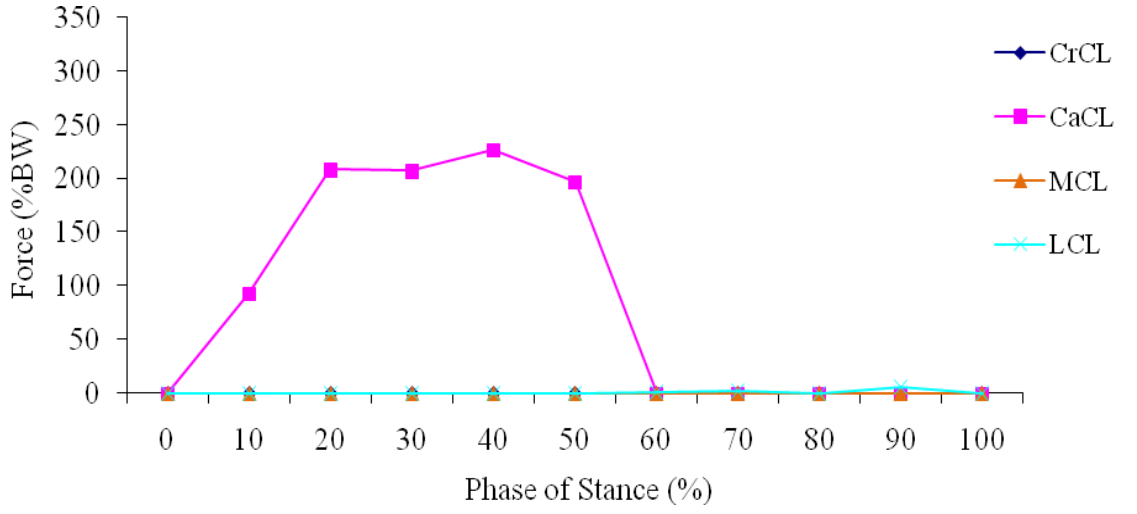

FIGURE 146 - Ligament forces for CrCL deficient stifle (+10% GRF magnitude change).

For the CrCL intact stifle the peak CrCL force was 28% BW and occurred at 40% stance. The peak LCL force was 6% BW and occurred at 90% stance. The CaCL and MCL were unloaded throughout stance. For the CrCL deficient stifle the peak CaCL force was 227%

BW and occurred at 40% stance. The peak LCL force was 6% BW and occurred at 90% stance. The MCL was unloaded throughout stance.

The ligament forces during stance for the CrCL intact and CrCL deficient stifle with a 20% GRF change are shown in FIGURE 147 and FIGURE 148, respectively.

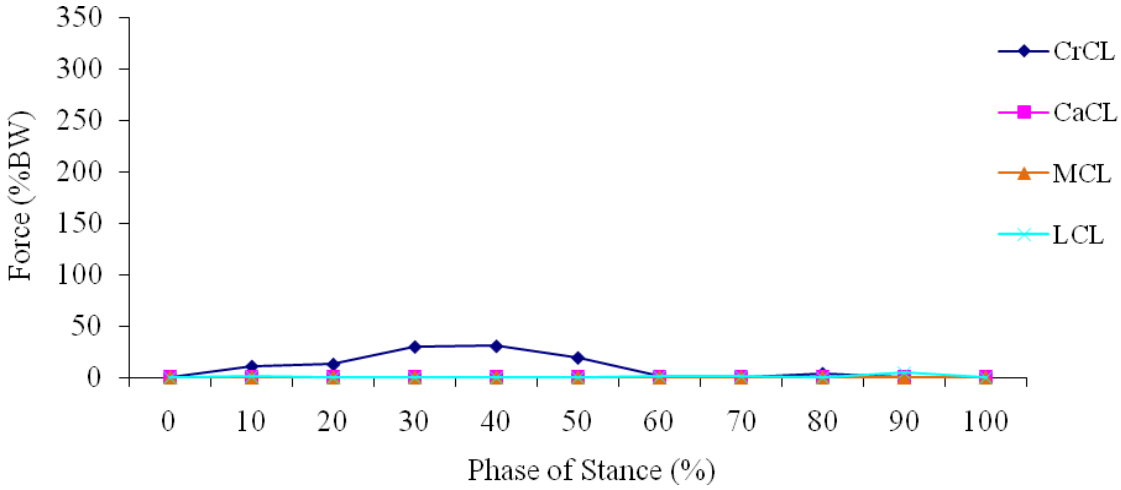

FIGURE 147 - Ligament forces for CrCL intact stifle (+20% GRF magnitude change).

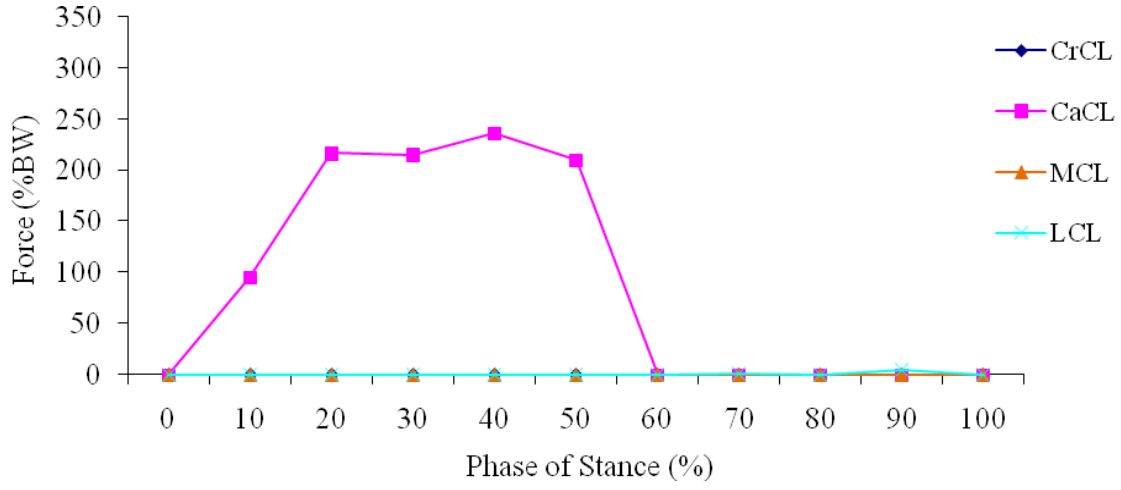

FIGURE 148 - Ligament forces for CrCL deficient stifle (+20% GRF magnitude change).

For the CrCL intact stifle the peak CrCL force was 31% BW and occurred at 40% stance. The peak LCL force was 5% BW and occurred at 90% stance. The CaCL and MCL were unloaded throughout stance. For the CrCL deficient stifle the peak CaCL force was 236% BW and occurred at 40% stance. The peak LCL force was 5% BW and occurred at 90% stance. The MCL was unloaded throughout stance.

4.3.8.2 Ligament Forces Summary for Ground Reaction Force Variation

Ligament forces for each phase of stance for varying ground reaction force were determined in the CrCL intact and CrCL deficient stifle. Peak CrCL forces varied by 9% BW ranging from 22% BW to 31% BW for varying GRF magnitude for the CrCL intact stifle. Peak CaCL forces varied by 35% BW ranging from 201% BW to 236% BW for the CrCL deficient stifle. The peak CrCL forces for varying GRF magnitude for the CrCL intact stifle are shown in FIGURE 149, and the peak CaCL forces for varying GRF magnitude for the CrCL deficient stifle are shown in FIGURE 150.

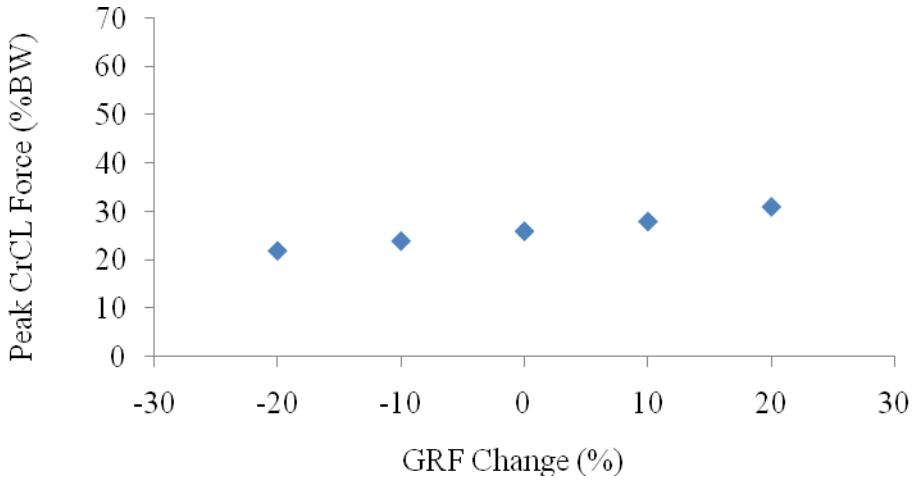

FIGURE 149 - Peak CrCL forces in the CrCL intact stifle for each percentage GRF magnitude change.

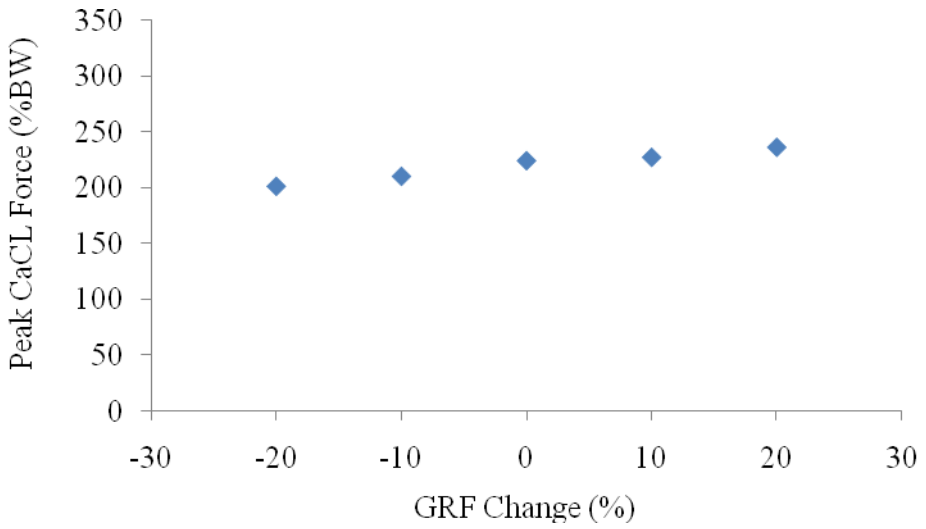

FIGURE 150 - Peak CaCL forces in the CrCL deficient stifle for each percentage GRF magnitude change.

4.3.8.3 Tibial Translation for Ground Reaction Force Variation

The relative tibial translation across the phases of stance is plotted in FIGURE 151.

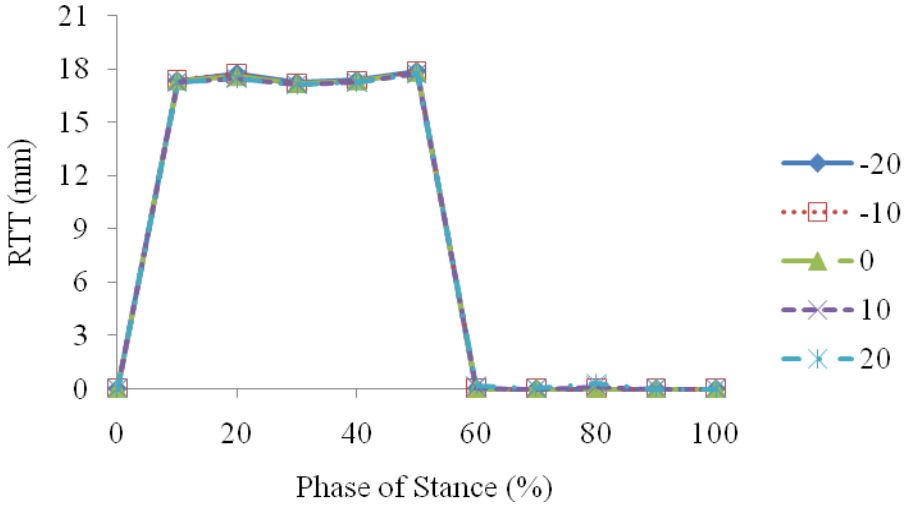

FIGURE 151 - Relative tibial translation between the CrCL intact and deficient stifle models for each percentage GRF magnitude change.

4.3.8.4 Tibial Translation Summary for Ground Reaction Force Variation

The peak relative tibial translation, the phase of stance at which it occurred and the corresponding relative tibial translation per body mass and anatomical tibial translation for each percentage GRF magnitude change are listed in TABLE XVIII. The peak relative tibial translation values are plotted in FIGURE 152.

TABLE XVIII

PEAK TIBIAL TRANSLATION VALUES FOR EACH PERCENTAGE GRF MAGNITUDE CHANGE EVALUATED

Change (%)	-20	-10	0	10	20
Stance Phase (%)	50	50	50	50	50
RTT (mm)*	17.9	17.9	17.8	17.8	17.7
RTT/BM (mm/kg)**	0.56	0.56	0.56	0.56	0.55
ATT***	1.45	1.44	1.43	1.42	1.41

*RTT = Relative Tibial Translation = $(\mathrm{FT}_{\mathrm{deficient}})_{\mathrm{loaded}} - (\mathrm{FT}_{\mathrm{intact}})_{\mathrm{loaded}}$

**RTT/BM = Relative Tibial Translation per Body Mass

***ATT = Anatomical Tibial Translation = $\dfrac{(\mathrm{FT}_{\mathrm{deficient}})_{\mathrm{loaded}} - (\mathrm{FT}_{\mathrm{intact}})_{\mathrm{loaded}}}{(\mathrm{FT}_{\mathrm{intact}})_{\mathrm{loaded}}}$

where FT denotes the craniocaudal distance from a fixed point on the femur to a fixed point on the tibia, deficient denotes the CrCL was suppressed, intact denotes the CrCL was not suppressed and loaded denotes weight bearing

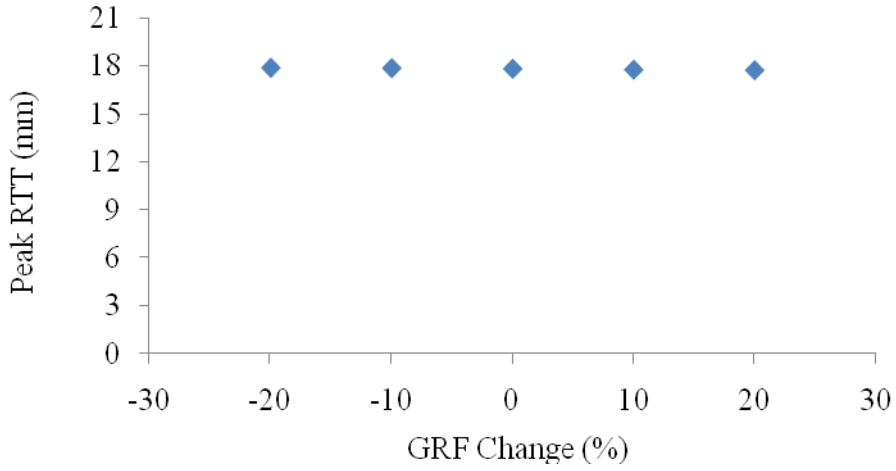

FIGURE 152 - Peak relative tibial translation values for each percentage GRF magnitude change.

Peak relative tibial translation varied by +0.6/-0.6% from baseline for varying ground reaction force.

4.3.9 Body Mass

4.3.9.1 Ligament Forces for Body Mass Variation

Body mass values were altered from baseline by discrete percentages to simulate variation in dog stature. The five scenarios evaluated were body mass percentage changes of -20%, -10%, 0% (baseline), 10% and 20% from baseline. The baseline body mass was 32 kg so variation ranged from 26 kg to 38 kg.

The ligament forces during stance for the CrCL intact and CrCL deficient stifle with a -20% body mass change are shown in FIGURE 153 and FIGURE 154, respectively.

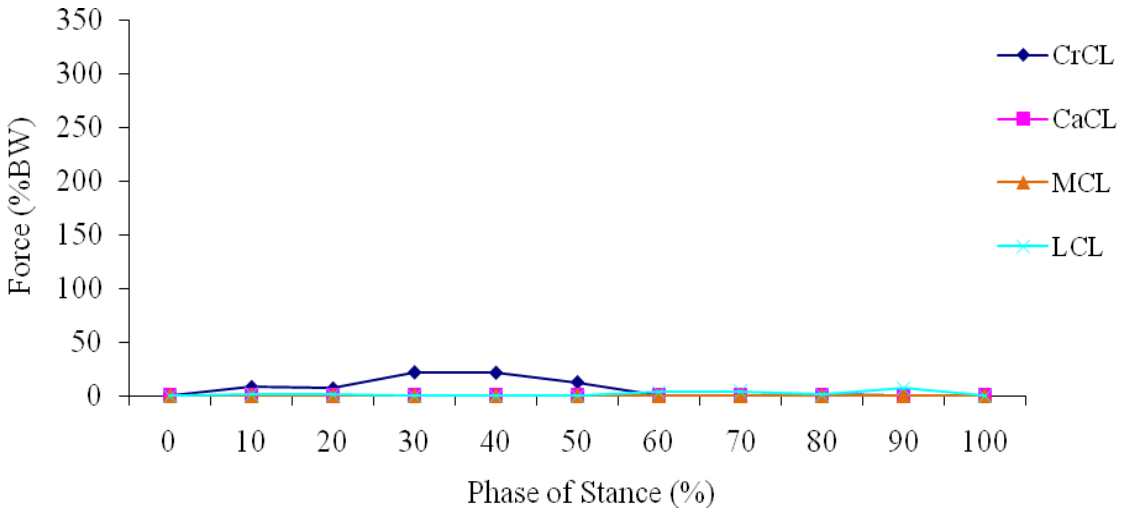

FIGURE 153 - Ligament forces for CrCL intact stifle (-20% body mass change).

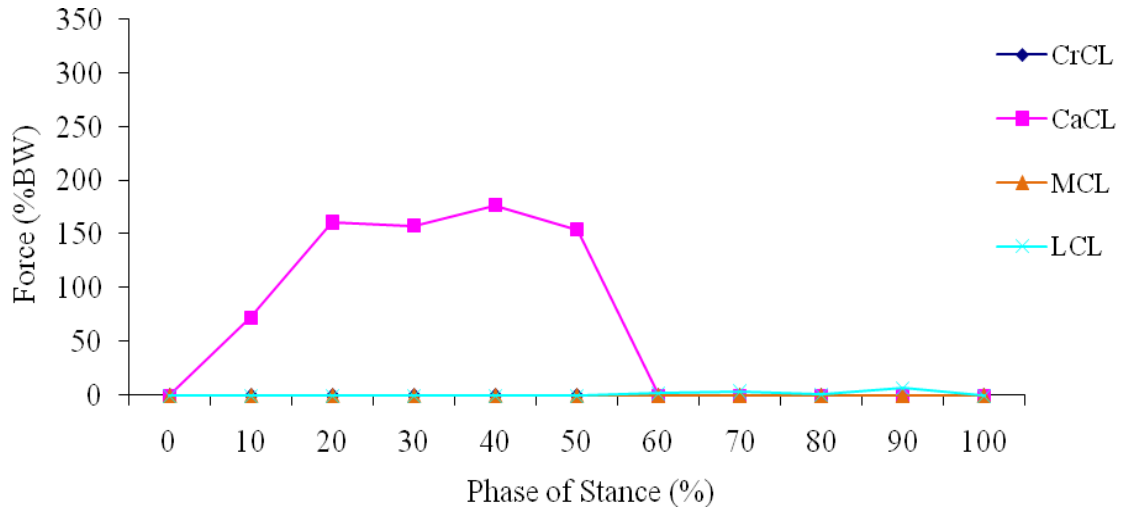

FIGURE 154 - Ligament forces for CrCL deficient stifle (-20% body mass change).

For the CrCL intact stifle the peak CrCL force was 22% BW and occurred at 30% stance. The peak LCL force was 7% BW and occurred at 90% stance. The CaCL and MCL were unloaded throughout stance. For the CrCL deficient stifle the peak CaCL force was 177%

BW and occurred at 40% stance. The peak LCL force was 7% BW and occurred at 90% stance. The MCL was unloaded throughout stance.

The ligament forces during stance for the CrCL intact and CrCL deficient stifle with a -10% body mass change are shown in FIGURE 155 and FIGURE 156, respectively.

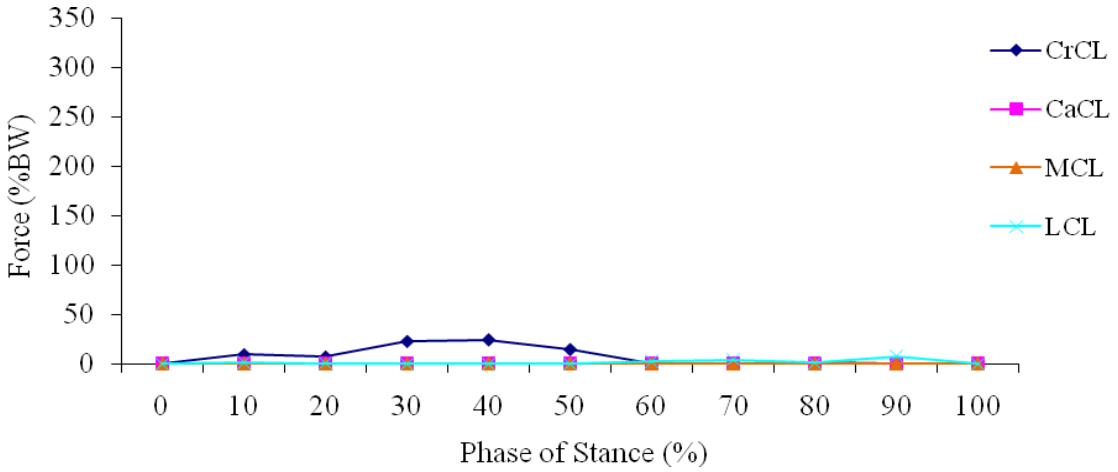

FIGURE 155 - Ligament forces for CrCL intact stifle (-10% body mass change).

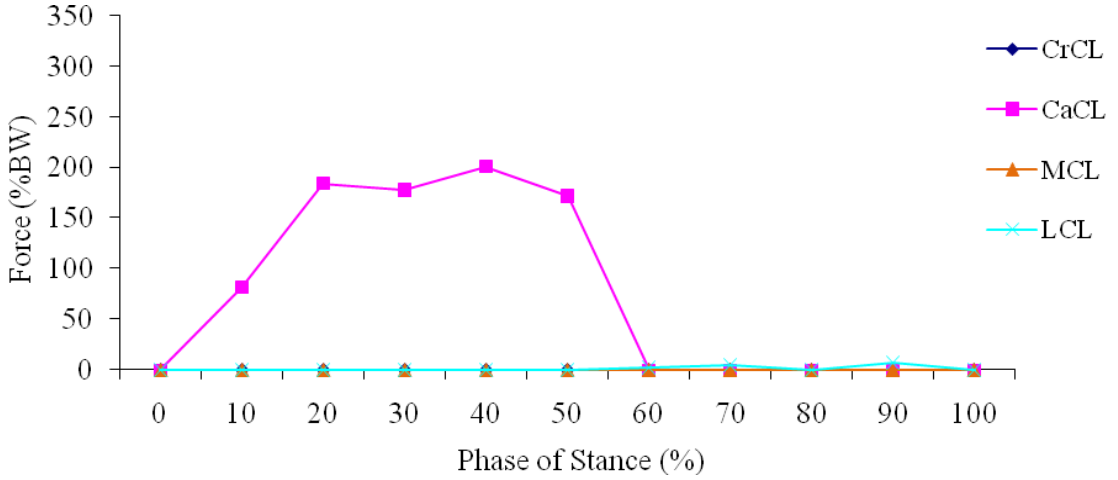

FIGURE 156 - Ligament forces for CrCL deficient stifle (-10% body mass change).

For the CrCL intact stifle the peak CrCL force was 24% BW and occurred at 40% stance. The peak LCL force was 8% BW and occurred at 90% stance. The CaCL and MCL were unloaded throughout stance. For the CrCL deficient stifle the peak CaCL force was 200% BW and occurred at 40% stance. The peak LCL force was 7% BW and occurred at 90% stance. The MCL was unloaded throughout stance.

The ligament forces during stance for the CrCL intact and CrCL deficient stifle with a 0% body mass change are shown in FIGURE 157 and FIGURE 158, respectively.

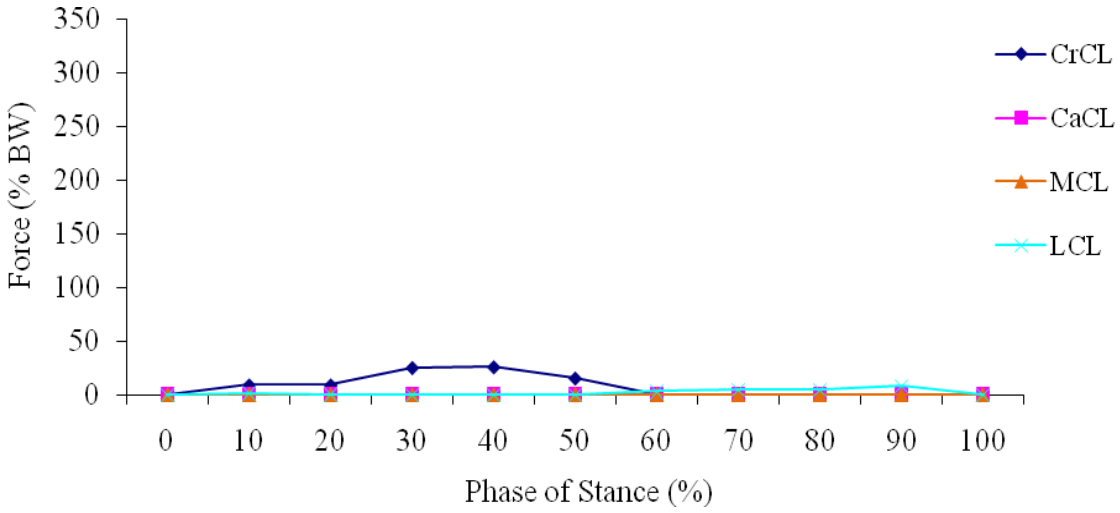

FIGURE 157 - Ligament forces for CrCL intact stifle (0% body mass change).

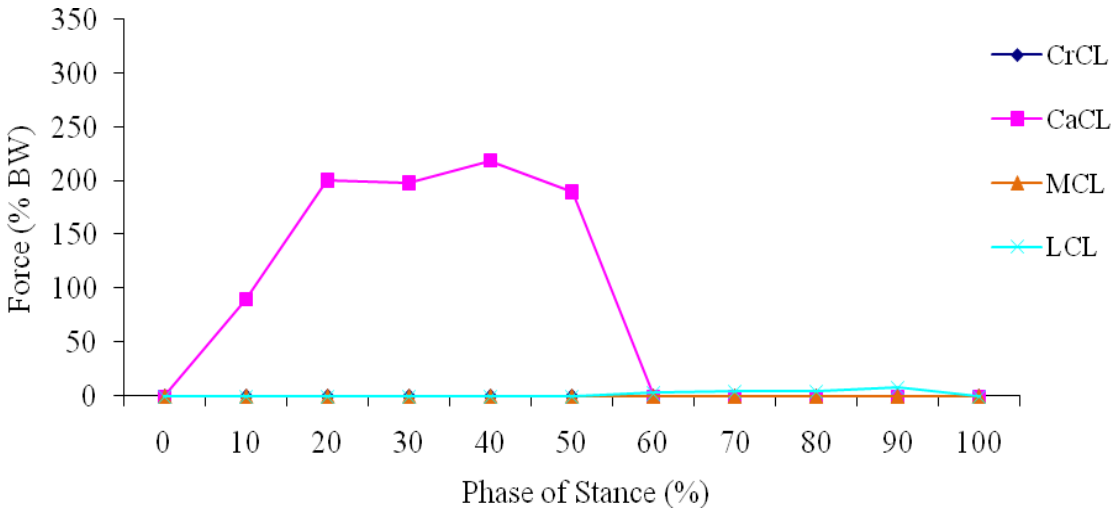

FIGURE 158 - Ligament forces for CrCL deficient stifle (0% body mass change).

For the CrCL intact stifle the peak CrCL force was 26% body weight (BW) and occurred at 40% stance. The CaCL was unloaded thoughout stance. The peak LCL force was 8% BW and occurred at 90% stance. The MCL was unloaded throughout stance. For the CrCL deficient stifle the peak CaCL force was 219% BW and occurred at 40% stance. The peak LCL force was 8% BW and occurred at 90% stance. The MCL was unloaded throughout stance.

The ligament forces during stance for the CrCL intact and CrCL deficient stifle with a 10% body mass change are shown in FIGURE 159 and FIGURE 160, respectively.

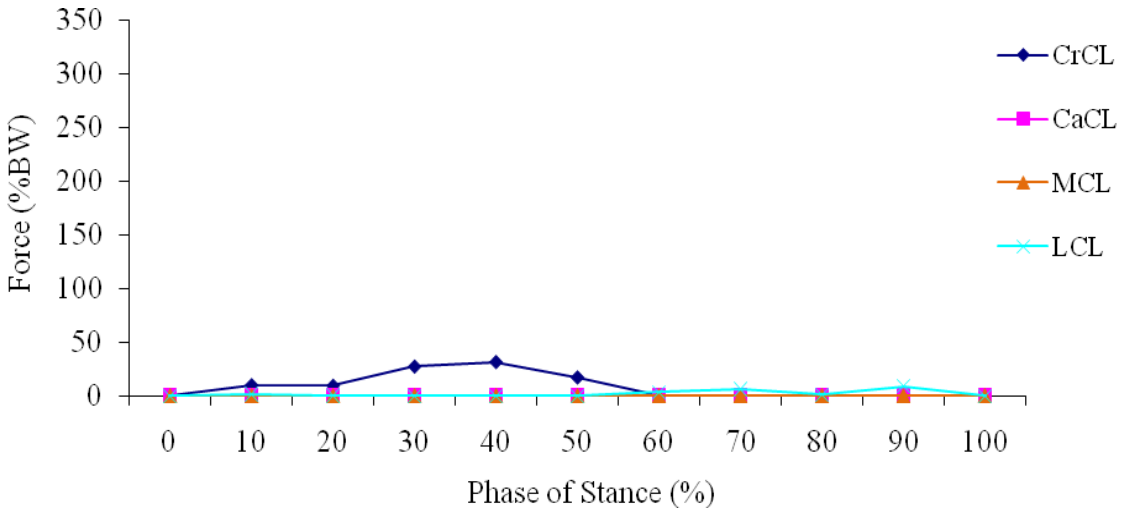

FIGURE 159 - Ligament forces for CrCL intact stifle (+10% body mass change).

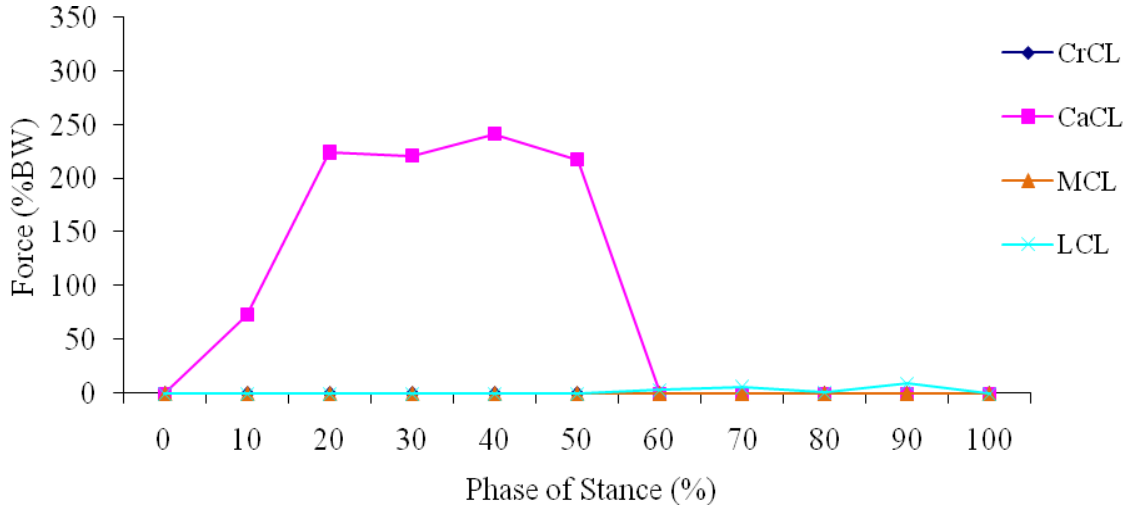

FIGURE 160 - Ligament forces for CrCL deficient stifle (+10% body mass change).

For the CrCL intact stifle the peak CrCL force was 31% BW and occurred at 40% stance. The peak LCL force was 9% BW and occurred at 90% stance. The CaCL and MCL were unloaded throughout stance. For the CrCL deficient stifle the peak CaCL force was 241%

BW and occurred at 40% stance. The peak LCL force was 9% BW and occurred at 90% stance. The MCL was unloaded throughout stance.

The ligament forces during stance for the CrCL intact and CrCL deficient stifle with a 20% body mass change are shown in FIGURE 161 and FIGURE 162, respectively.

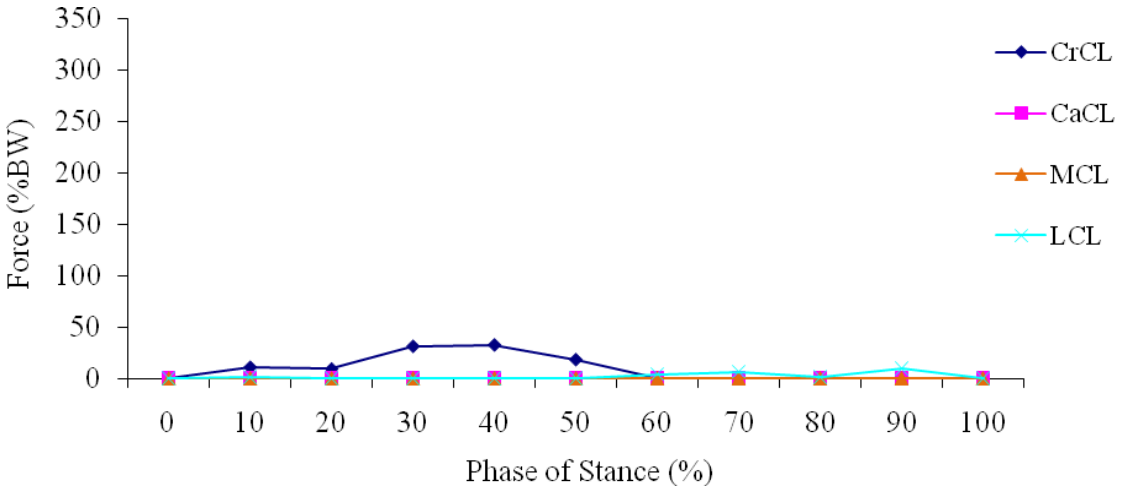

FIGURE 161 - Ligament forces for CrCL intact stifle (+20% body mass change).

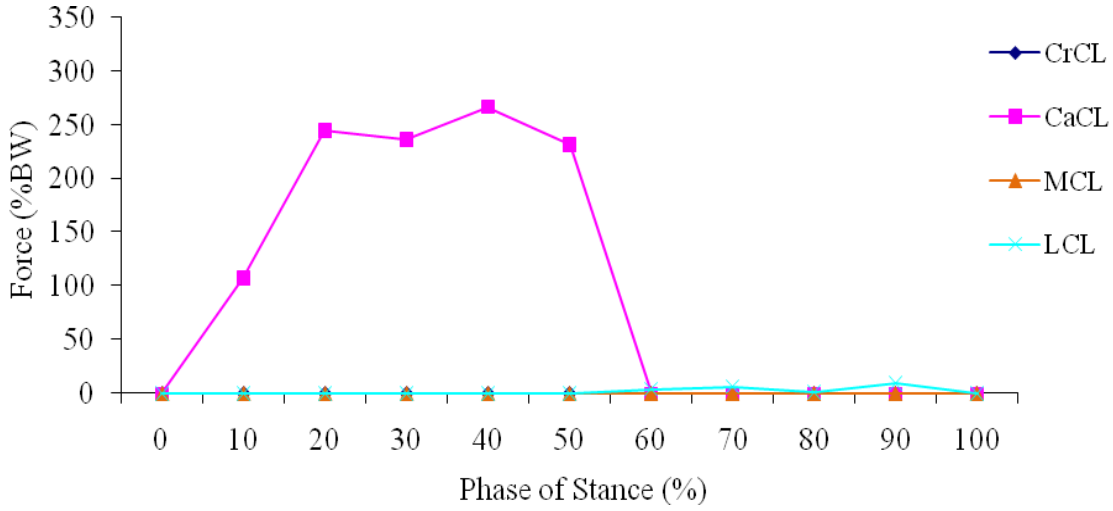

FIGURE 162 - Ligament forces for CrCL deficient stifle (+20% body mass change).

For the CrCL intact stifle the peak CrCL force was 32% BW and occurred at 40% stance. The peak LCL force was 10% BW and occurred at 90% stance. The CaCL and MCL were unloaded throughout stance. For the CrCL deficient stifle the peak CaCL force was 266% BW and occurred at 40% stance. The peak LCL force was 10% BW and occurred at 90% stance. The MCL was unloaded throughout stance.

4.3.9.2 Ligament Forces Summary for Body Mass Variation

Ligament forces for each phase of stance for varying body mass were determined in the CrCL intact and CrCL deficient stifle. Peak CrCL forces varied by 10% BW ranging from 22% BW to 32% BW for varying body mass in the CrCL intact stifle. Peak CaCL forces varied by 89% BW ranging from 177% BW to 266% BW for the CrCL deficient stifle. The peak CrCL forces for varying body mass for the CrCL intact stifle are shown in FIGURE 163, and the peak CaCL forces for varying body mass for the CrCL deficient stifle are shown in FIGURE 164.

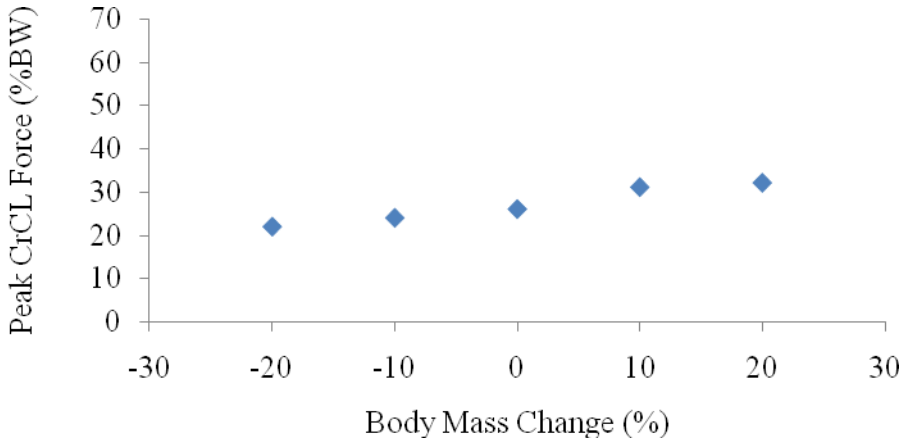

FIGURE 163 - Peak CrCL forces in the CrCL intact stifle for each percentage change in body mass.

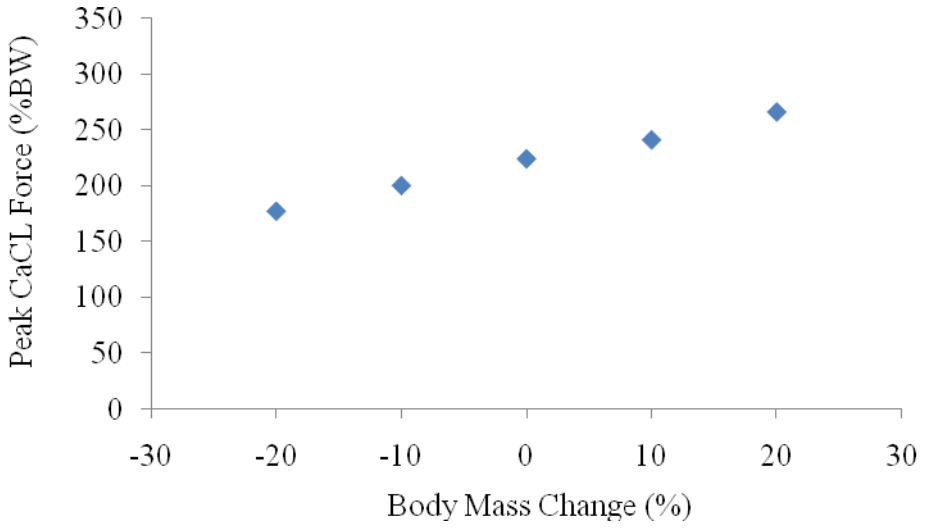

FIGURE 164 - Peak CaCL forces in the CrCL deficient stifle for each percentage change in body mass.

4.3.9.3 Tibial Translation for Body Mass Variation

The relative tibial translation across the phases of stance is plotted in FIGURE 165.

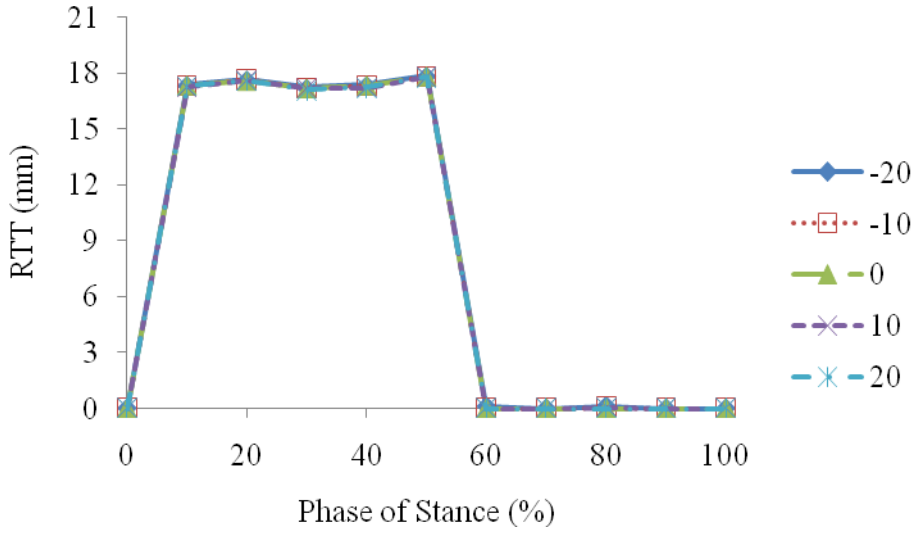

FIGURE 165 - Relative tibial translation between the CrCL intact and deficient stifle models for each change in body mass percentage.

4.3.9.4 Tibial Translation for Body Mass Variation

The peak relative tibial translation, the phase of stance at which it occurred and the corresponding relative tibial translation per body mass and anatomical tibial translation for each percentage change in body mass are listed in TABLE XIX. The peak relative tibial translation values are plotted in FIGURE 166.

TABLE XIX

PEAK TIBIAL TRANSLATION VALUES FOR EACH PERCENTAGE BODY MASS CHANGE EVALUATED

Change (%)	-20	-10	0	10	20
Stance Phase (%)	50	50	50	50	50
Peak RTT (mm)*	17.9	17.8	17.8	17.8	17.8
RTT/BM (mm/kg)**	0.56	0.56	0.56	0.56	0.56
ATT***	1.44	1.43	1.43	1.42	1.42

*RTT = Relative Tibial Translation = $(\mathrm{FT}_{\mathrm{deficient}})_{\mathrm{loaded}} - (\mathrm{FT}_{\mathrm{intact}})_{\mathrm{loaded}}$

**RTT/BM = Relative Tibial Translation per Body Mass

***ATT = Anatomical Tibial Translation = $\dfrac{(\mathrm{FT}_{\mathrm{deficient}})_{\mathrm{loaded}} - (\mathrm{FT}_{\mathrm{intact}})_{\mathrm{loaded}}}{(\mathrm{FT}_{\mathrm{intact}})_{\mathrm{loaded}}}$

where FT denotes the craniocaudal distance from a fixed point on the femur to a fixed point on the tibia, deficient denotes the CrCL was suppressed, intact denotes the CrCL was not suppressed and loaded denotes weight bearing

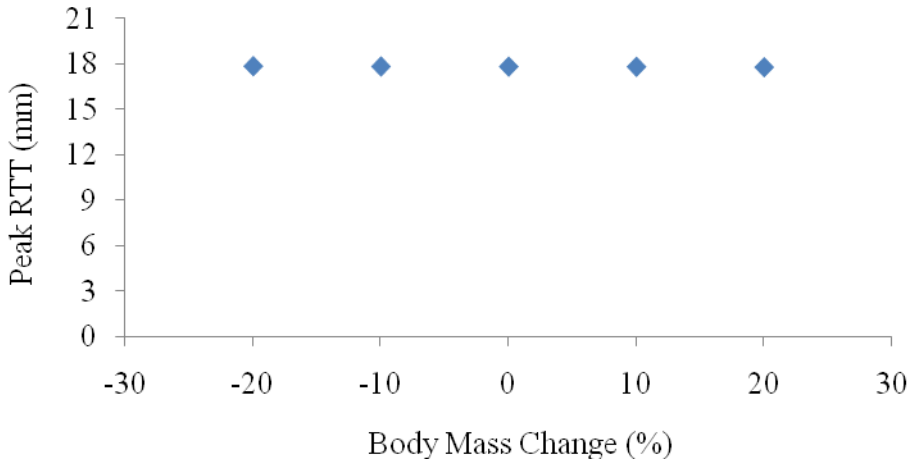

FIGURE 166 - Peak relative tibial translation values for each change in body mass percentage.

Peak relative tibial translation varied by +0.6/-0.0% from baseline for varying body mass.

4.3.10 Femoromeniscal Friction Coefficients

4.3.10.1 Ligament Forces for Femoromeniscal Friction Coefficients Variation

Femoromeniscal friction coefficients were altered from baseline in 0.02 increments to simulate synovial joint variation that may result from osteoarthritis. The four scenarios evaluated were static and dynamic femoromeniscal contact friction coefficients that included 0.03, 0.05 (baseline), 0.07 and 0.09.

The ligament forces during stance for the CrCL intact and CrCL deficient stifle with a friction coefficient of 0.03 are shown in FIGURE 167 and FIGURE 168, respectively.

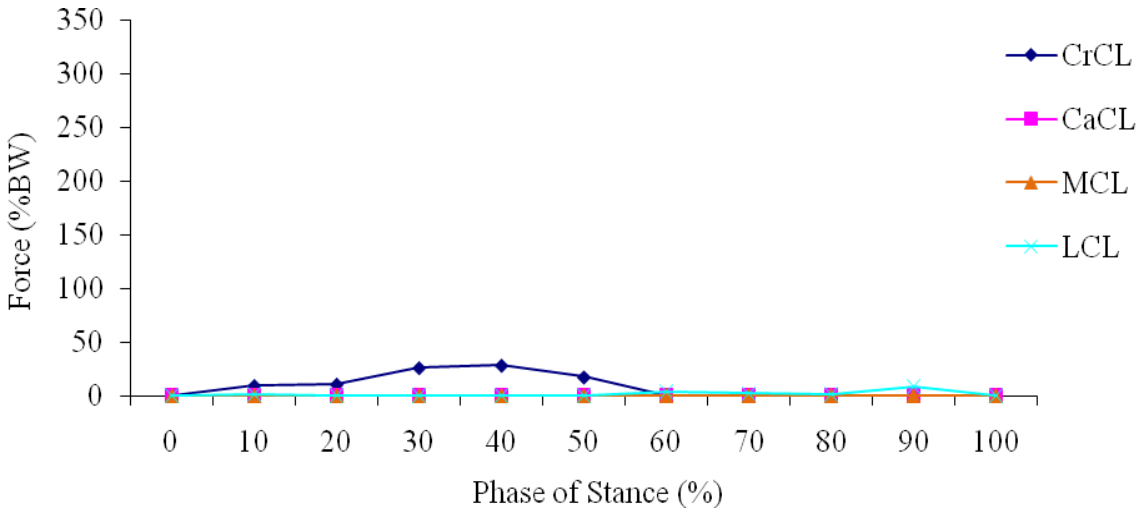

FIGURE 167 - Ligament forces for CrCL intact stifle (0.03 friction coefficient).

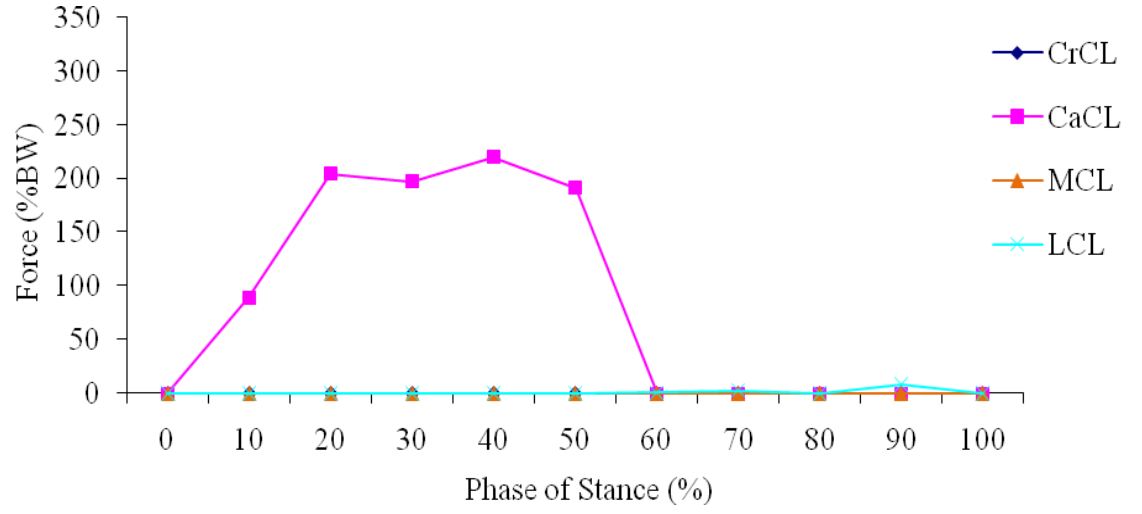

FIGURE 168 - Ligament forces for CrCL deficient stifle (0.03 friction coefficient).

For the CrCL intact stifle the peak CrCL force was 28% BW and occurred at 40% stance. The peak LCL force was 8% BW and occurred at 90% stance. The CaCL and MCL were unloaded throughout stance. For the CrCL deficient stifle the peak CaCL force was 220%

BW and occurred at 40% stance. The peak LCL force was 8% BW and occurred at 90% stance. The MCL was unloaded throughout stance.

The ligament forces during stance for the CrCL intact and CrCL deficient stifle with a friction coefficient of 0.05 (baseline) are shown in FIGURE 169 and FIGURE 170, respectively.

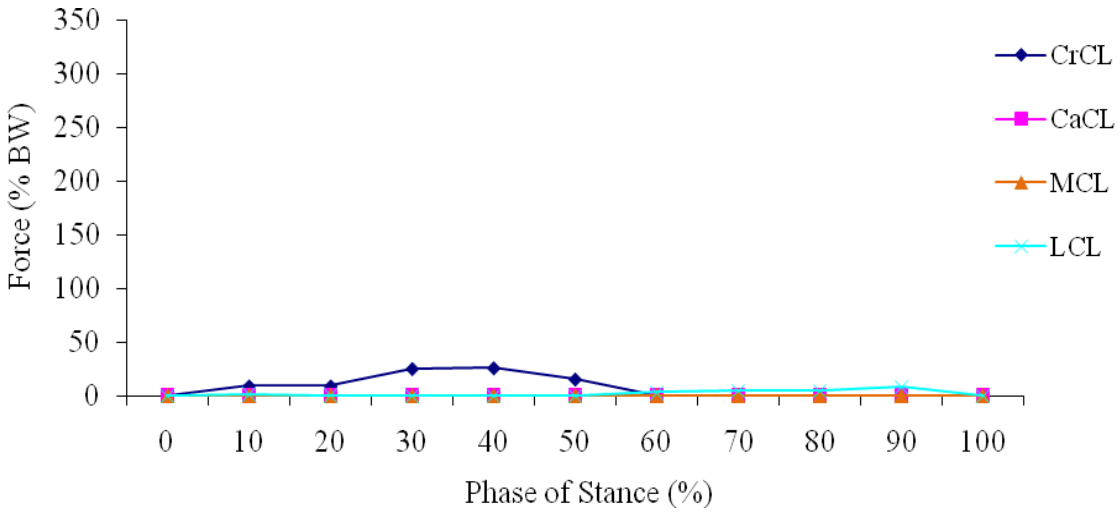

FIGURE 169 - Ligament forces for CrCL intact stifle (0.05 friction coefficient).

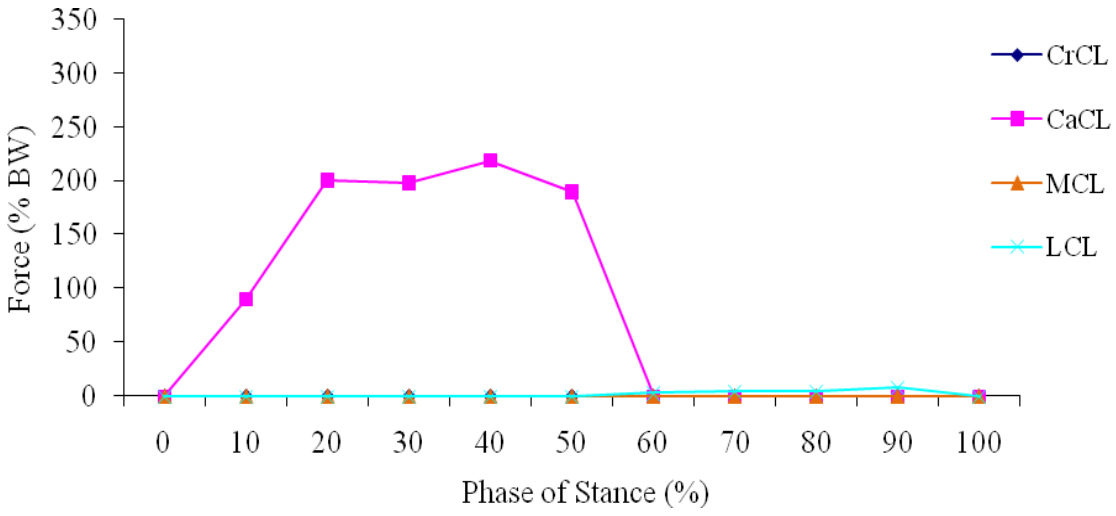

FIGURE 170 - Ligament forces for CrCL deficient stifle (0.05 friction coefficient).

For the CrCL intact stifle the peak CrCL force was 26% body weight (BW) and occurred at 40% stance. The CaCL was unloaded thoughout stance. The peak LCL force was 8% BW and occurred at 90% stance. The MCL was unloaded throughout stance. For the CrCL deficient stifle the peak CaCL force was 219% BW and occurred at 40% stance. The peak LCL force was 8% BW and occurred at 90% stance. The MCL was unloaded throughout stance.

The ligament forces during stance for the CrCL intact and CrCL deficient stifle with a friction coefficient of 0.07 are shown in FIGURE 171 and FIGURE 172, respectively.

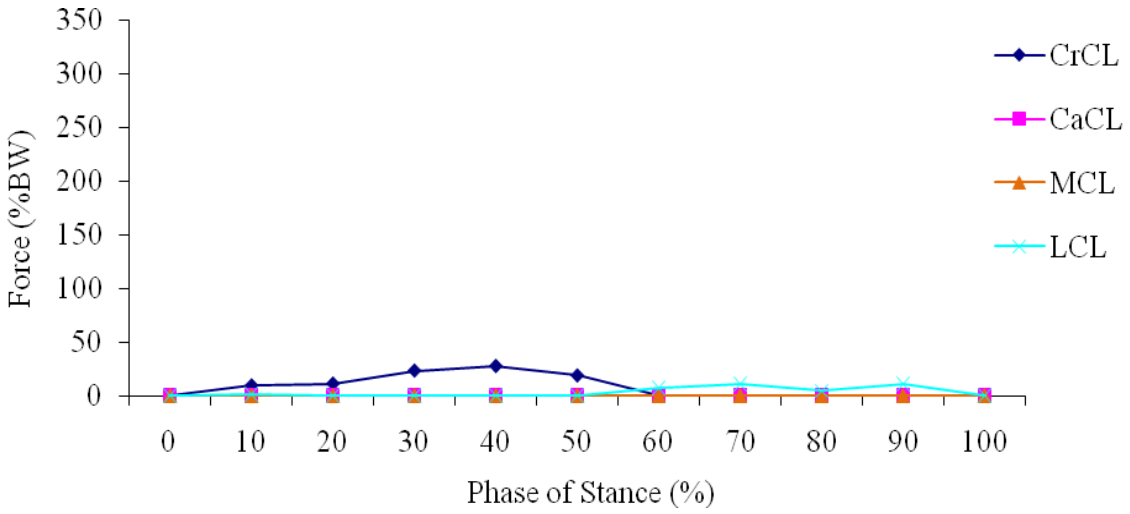

FIGURE 171 - Ligament forces for CrCL intact stifle (0.07 friction coefficient).

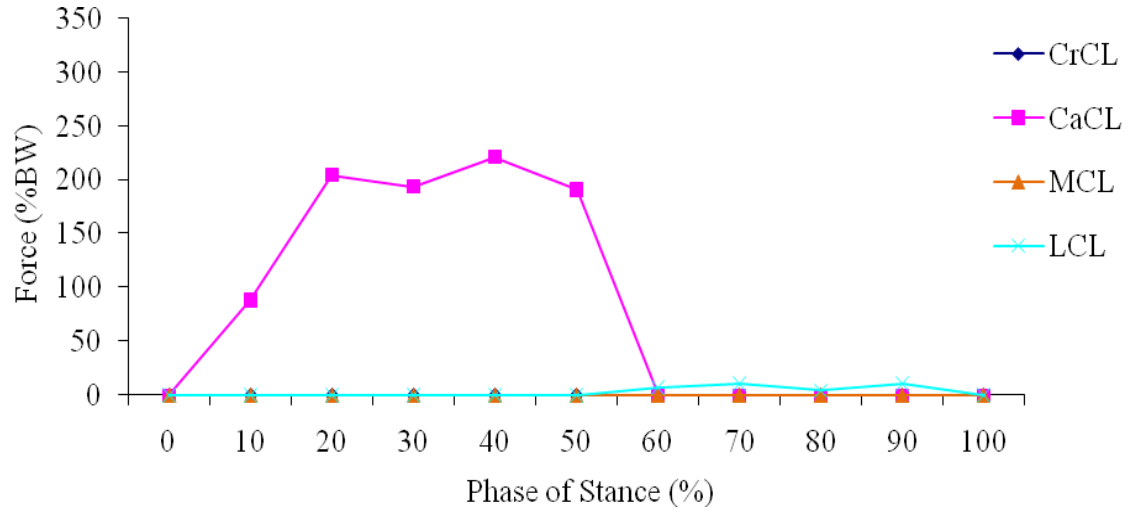

FIGURE 172 - Ligament forces for CrCL deficient stifle (0.07 friction coefficient).

For the CrCL intact stifle the peak CrCL force was 27% BW and occurred at 40% stance. The peak LCL force was 11% BW and occurred at 90% stance. The CaCL and MCL were unloaded throughout stance. For the CrCL deficient stifle the peak CaCL force was

221% BW and occurred at 40% stance. The peak LCL force was 11% BW and occurred at 90% stance. The MCL was unloaded throughout stance.

The ligament forces during stance for the CrCL intact and CrCL deficient stifle with a friction coefficient of 0.09 are shown in FIGURE 173 and FIGURE 174, respectively.

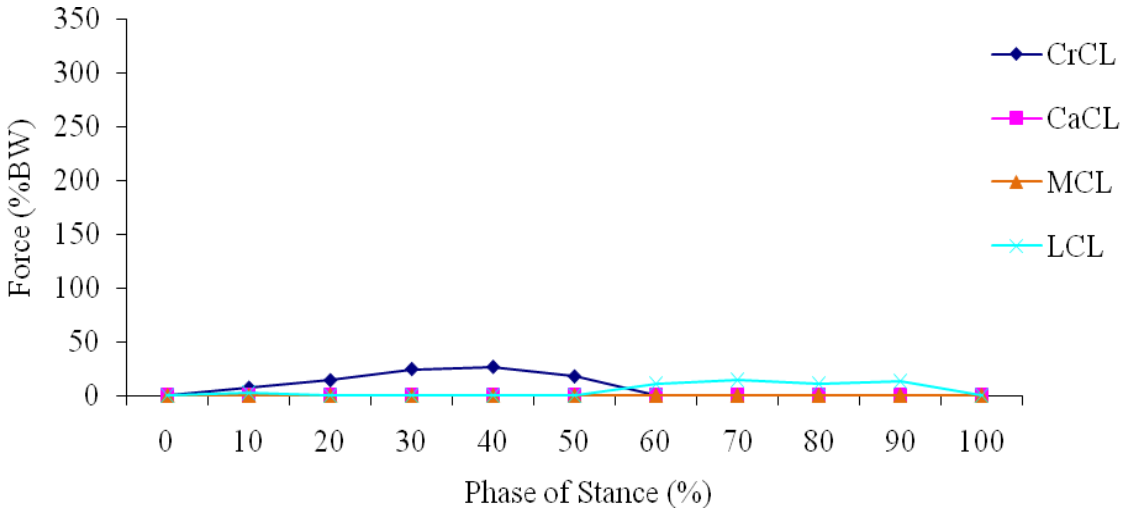

FIGURE 173 - Ligament forces for CrCL intact stifle (0.09 friction coefficient).

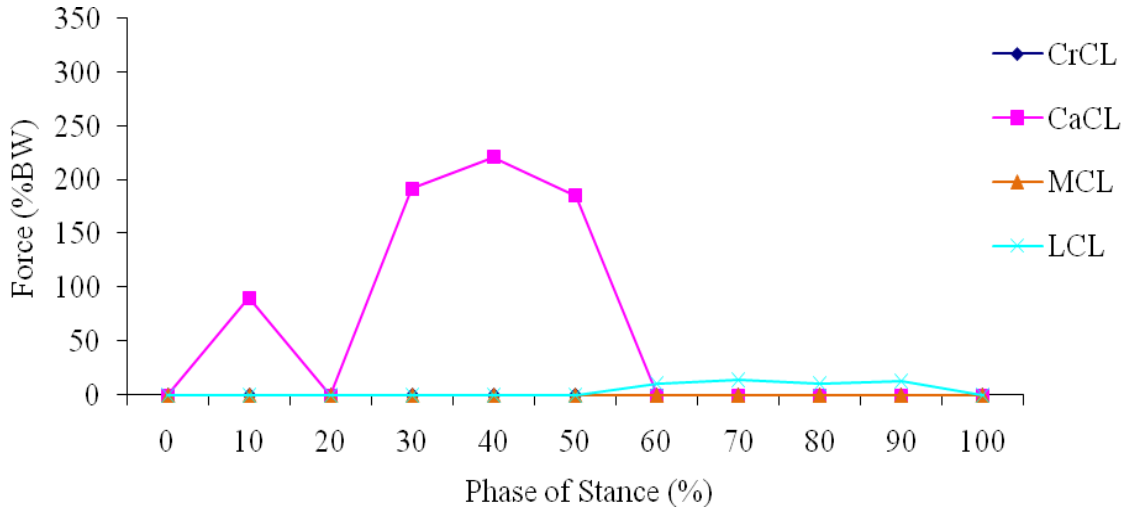

FIGURE 174 - Ligament forces for CrCL deficient stifle (0.09 friction coefficient).

For the CrCL intact stifle the peak CrCL force was 26% BW and occurred at 40% stance. The peak LCL force was 14% BW and occurred at 70% stance. The CaCL and MCL were unloaded throughout stance. For the CrCL deficient stifle the peak CaCL force was 221% BW and occurred at 40% stance. The peak LCL force was 14% BW and occurred at 70% stance. The MCL was unloaded throughout stance.

4.3.10.2 Ligament Forces Summary for Femoromeniscal Friction Coefficients Variation

Ligament forces for each phase of stance for varying femoromeniscal friction coefficients were determined in the CrCL intact and CrCL deficient stifle. Peak CrCL forces varied by 2% BW ranging from 26% BW to 28% BW for varying femoromeniscal friction coefficient for the CrCL intact stifle. Peak CaCL forces varied by 4% BW ranging from 220% BW to 224% BW for the CrCL deficient stifle. The peak CrCL forces for varying femoromeniscal friction coefficient for the CrCL intact stifle are shown in FIGURE 175, and the peak CaCL forces for varying femoromeniscal friction coefficient for the CrCL deficient stifle are shown in FIGURE 176.

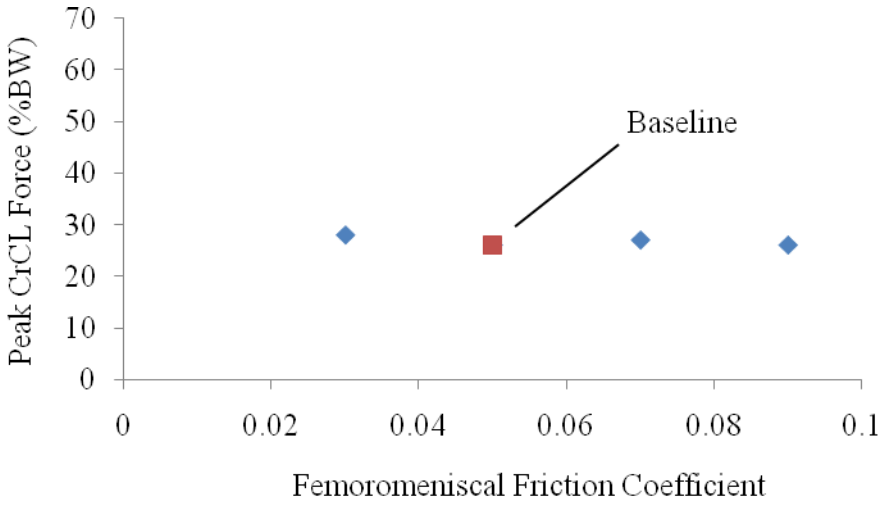

FIGURE 175 - Peak CrCL forces in the CrCL intact stifle for each femoromeniscal friction coefficient.

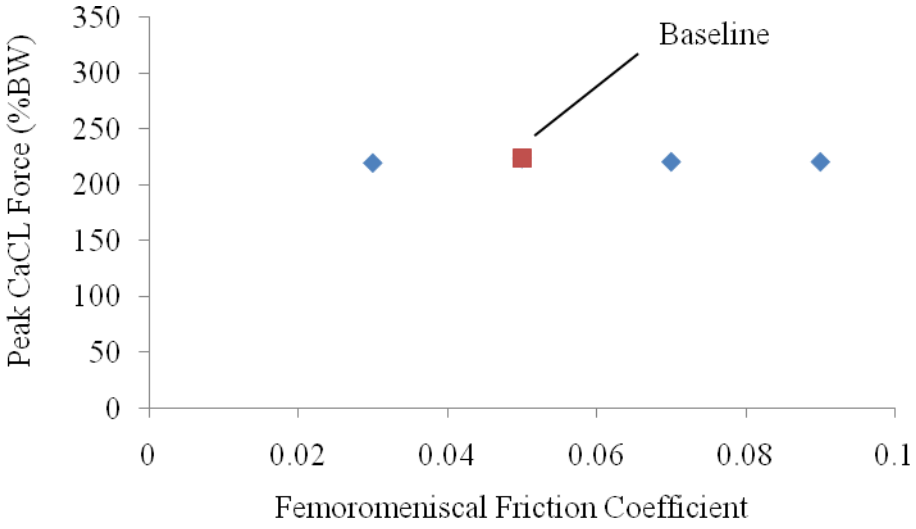

FIGURE 176 - Peak CaCL forces in the CrCL deficient stifle for each femoromeniscal friction coefficient.

4.3.10.3 Tibial Translation for Femoromeniscal Friction Coefficients Variation

The relative tibial translation across the phases of stance is plotted in FIGURE 177.

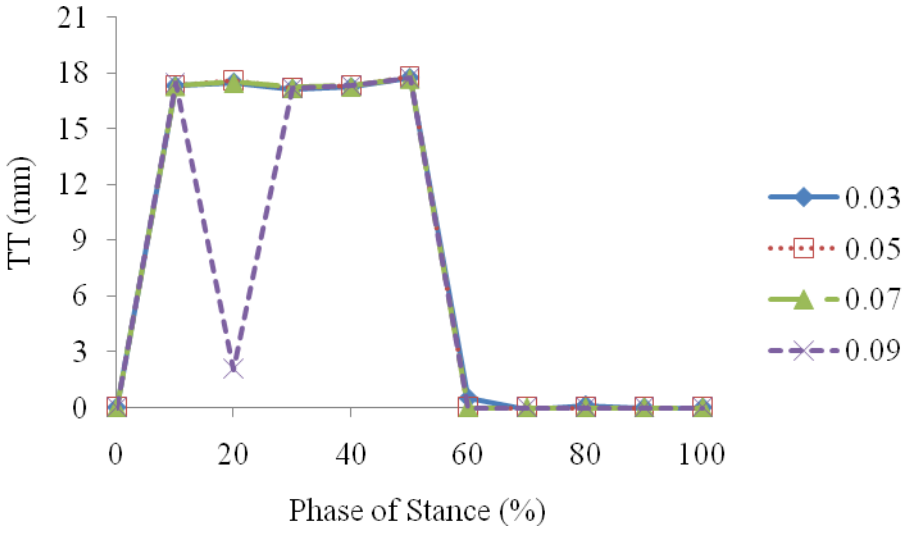

FIGURE 177 - Relative tibial translation between the CrCL intact and deficient stifle models for each femoromeniscal friction coefficient.

4.3.10.4 Tibial Translation Summary for Femoromeniscal Friction Coefficients Variation

The peak relative tibial translation, the phase of stance at which it occurred and the corresponding relative tibial translation per body mass and anatomical tibial translation for each femoromeniscal friction coefficient are listed in TABLE XX. The peak relative tibial translation values are plotted in FIGURE 178.

TABLE XX

PEAK TIBIAL TRANSLATION VALUES FOR EACH FEMOROMENISCAL FRICTION COEFFICIENT EVALUATED

Friction Coefficient	0.03	0.05	0.07	0.09
Stance Phase (%)	50	50	50	50
Peak RTT (mm)*	17.8	17.8	17.7	17.7
RTT/BM (mm/kg)**	0.56	0.56	0.55	0.56
ATT***	1.42	1.43	1.41	1.41

*RTT = Relative Tibial Translation = $(\mathrm{FT}_{\mathrm{deficient}})_{\mathrm{loaded}} - (\mathrm{FT}_{\mathrm{intact}})_{\mathrm{loaded}}$

**RTT/BM = Relative Tibial Translation per Body Mass

***ATT = Anatomical Tibial Translation = $\dfrac{(\mathrm{FT}_{\mathrm{deficient}})_{\mathrm{loaded}} - (\mathrm{FT}_{\mathrm{intact}})_{\mathrm{loaded}}}{(\mathrm{FT}_{\mathrm{intact}})_{\mathrm{loaded}}}$

where FT denotes the craniocaudal distance from a fixed point on the femur to a fixed point on the tibia, deficient denotes the CrCL was suppressed, intact denotes the CrCL was not suppressed and loaded denotes weight bearing

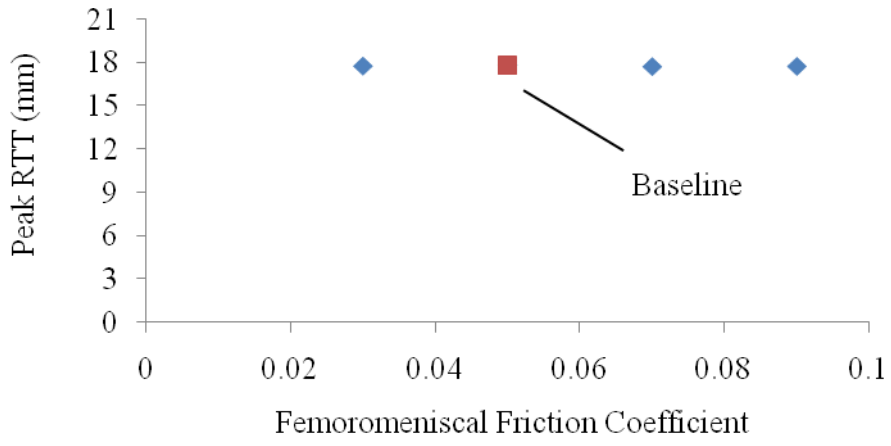

FIGURE 178 - Peak relative tibial translation for each femoromeniscal friction coefficient.

Peak relative tibial translation varied by +0.0/-0.6% from baseline for varying femoromeniscal friction coefficients.

4.3.11 Femoral Condyle Radius

4.3.11.1 Ligament Forces for Femoral Condyle Radius Variation

Femoral condyle radius was altered to simulate variation in femoral condyle shape between breeds. The six scenarios evaluated were femoral condyle radii of 6 mm, 10 mm, 14 mm, 16 mm (baseline), 18 mm and 22 mm. The femoral condyle radius in the model is described in FIGURE 179.

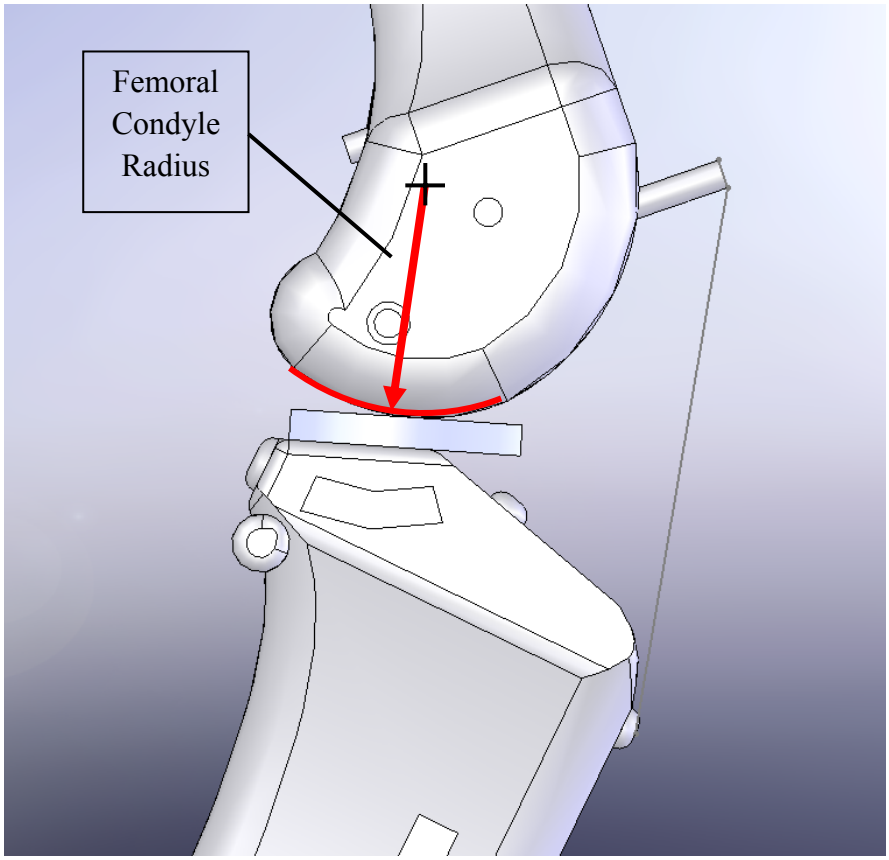

FIGURE 179 – Model femoral condyle radius.

The ligament forces during stance for the CrCL intact and CrCL deficient stifle with a 6 mm femoral condyle radius are shown in FIGURE 180 and FIGURE 181, respectively.

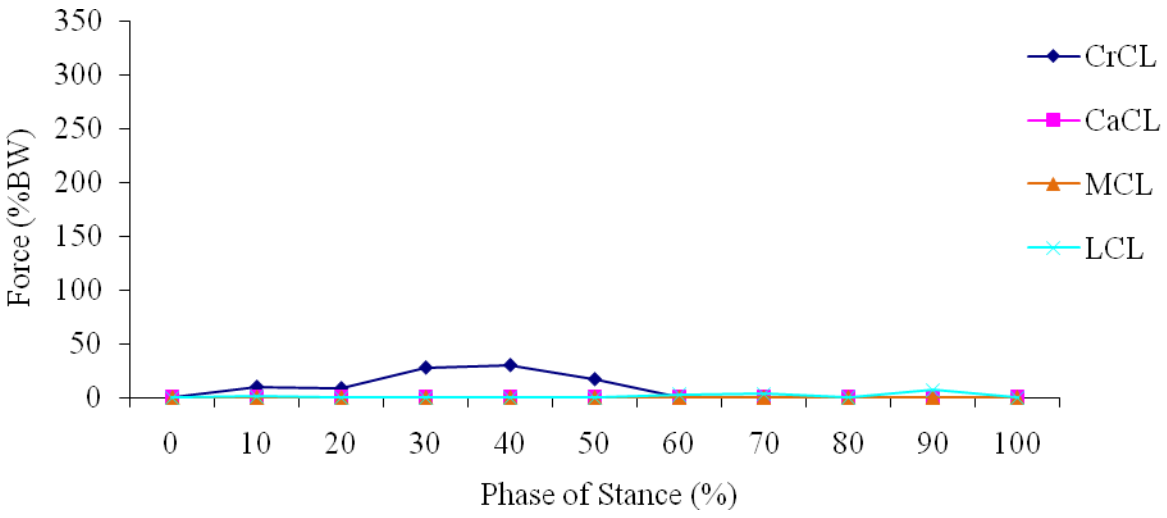

FIGURE 180 - Ligament forces for CrCL intact stifle (6 mm femoral condyle radius).

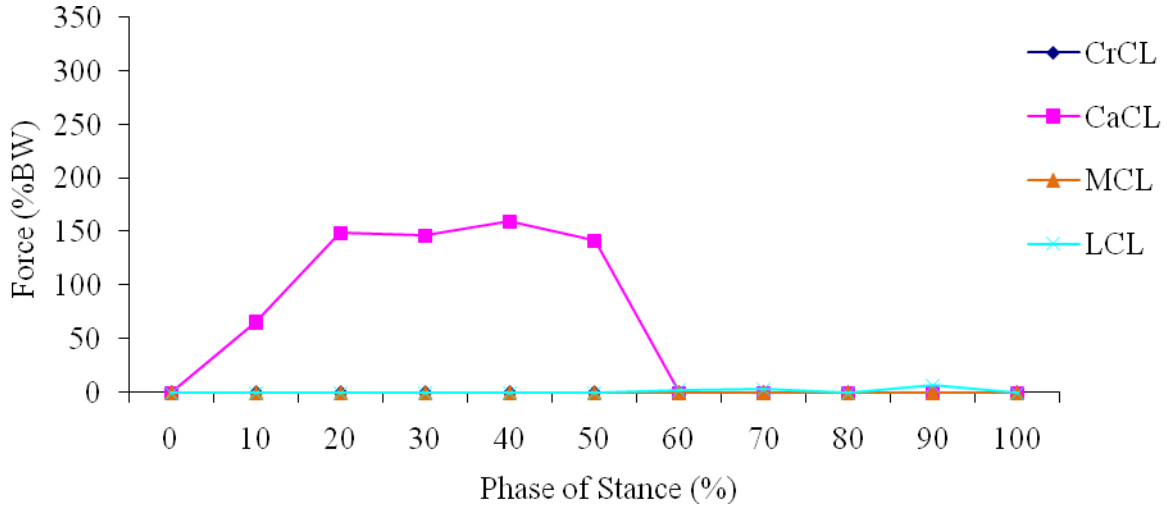

FIGURE 181 - Ligament forces for CrCL deficient stifle (6 mm femoral condyle radius).

For the CrCL intact stifle the peak CrCL force was 30% BW and occurred at 40% stance. The peak LCL force was 7% BW and occurred at 90% stance. The CaCL and MCL were unloaded throughout stance. For the CrCL deficient stifle the peak CaCL force was 160% BW and occurred at 40% stance. The peak LCL force was 7% BW and occurred at 90% stance. The MCL was unloaded throughout stance.

The ligament forces during stance for the CrCL intact and CrCL deficient stifle with a 10 mm femoral condyle radius are shown in FIGURE 182 and FIGURE 183, respectively.

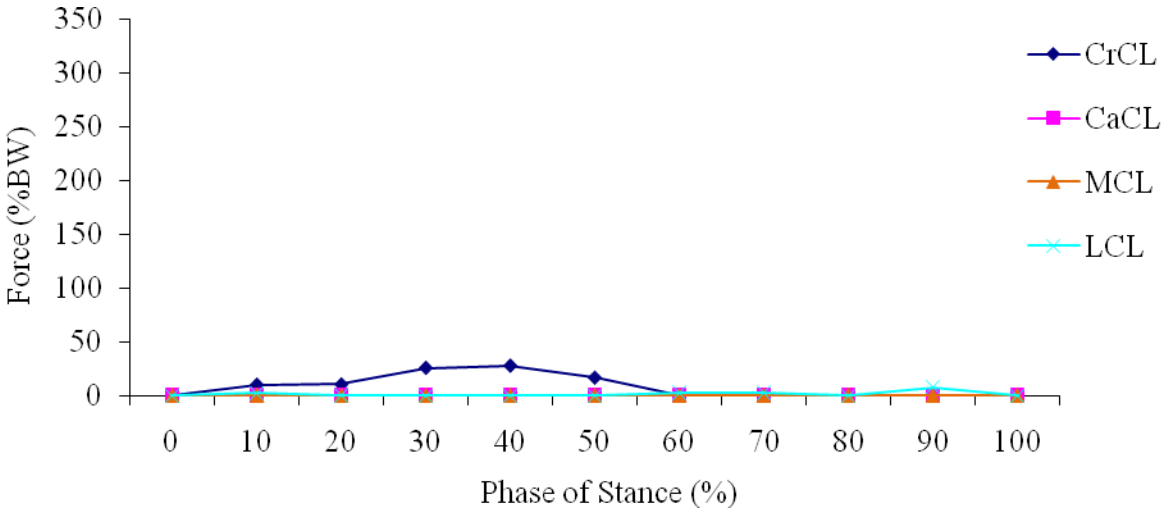

FIGURE 182 - Ligament forces for CrCL intact stifle (10 mm femoral condyle radius).

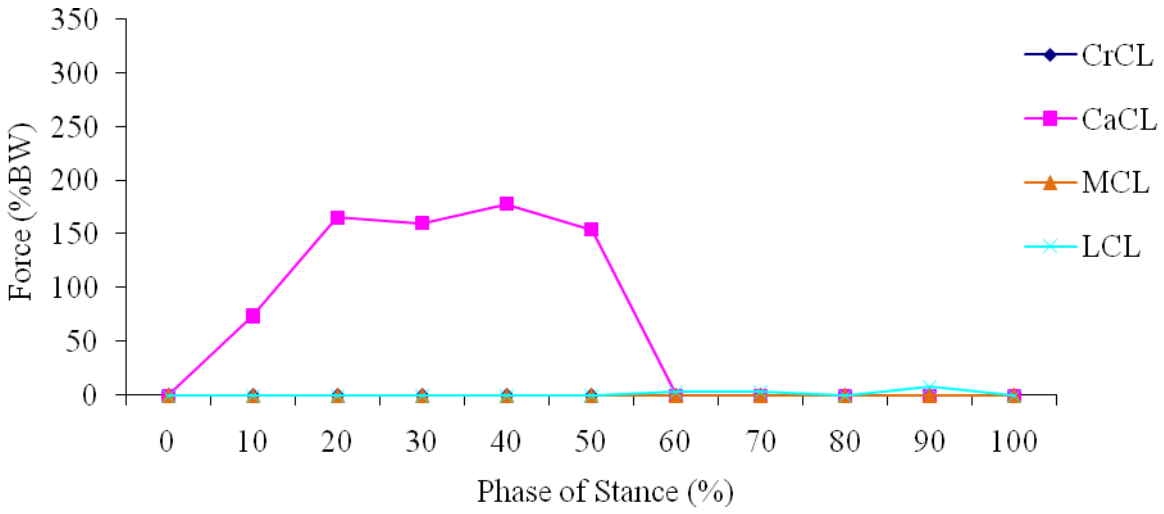

FIGURE 183 - Ligament forces for CrCL deficient stifle (10 mm femoral condyle radius).

For the CrCL intact stifle the peak CrCL force was 27% BW and occurred at 40% stance. The peak LCL force was 8% BW and occurred at 90% stance. The CaCL and MCL were unloaded throughout stance. For the CrCL deficient stifle the peak CaCL force was 178% BW and occurred at 40% stance. The peak LCL force was 8% BW and occurred at 90% stance. The MCL was unloaded throughout stance.

The ligament forces during stance for the CrCL intact and CrCL deficient stifle with a 14 mm femoral condyle radius are shown in FIGURE 184 and FIGURE 185, respectively.

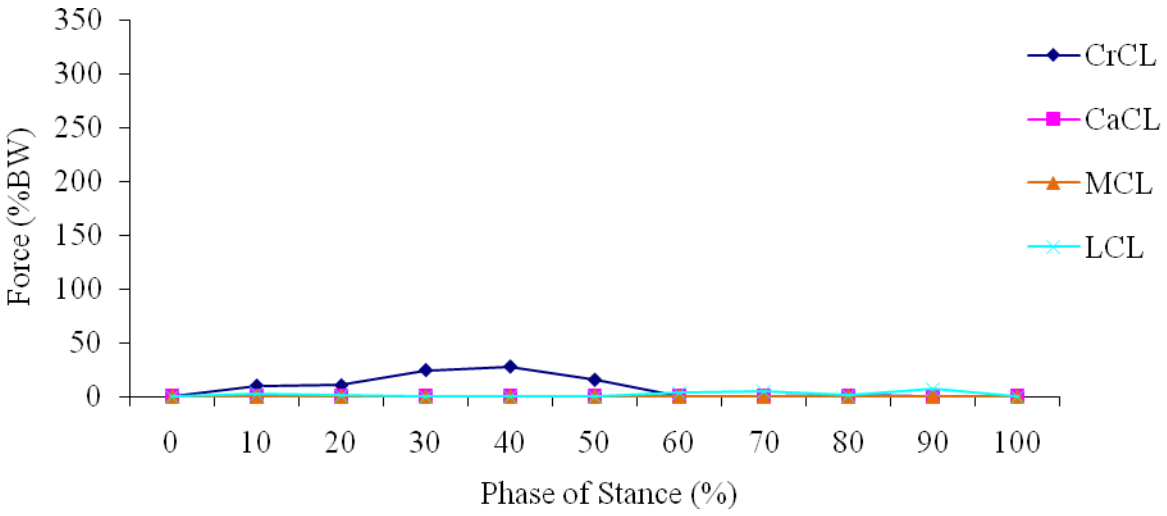

FIGURE 184 - Ligament forces for CrCL intact stifle (14 mm femoral condyle radius).

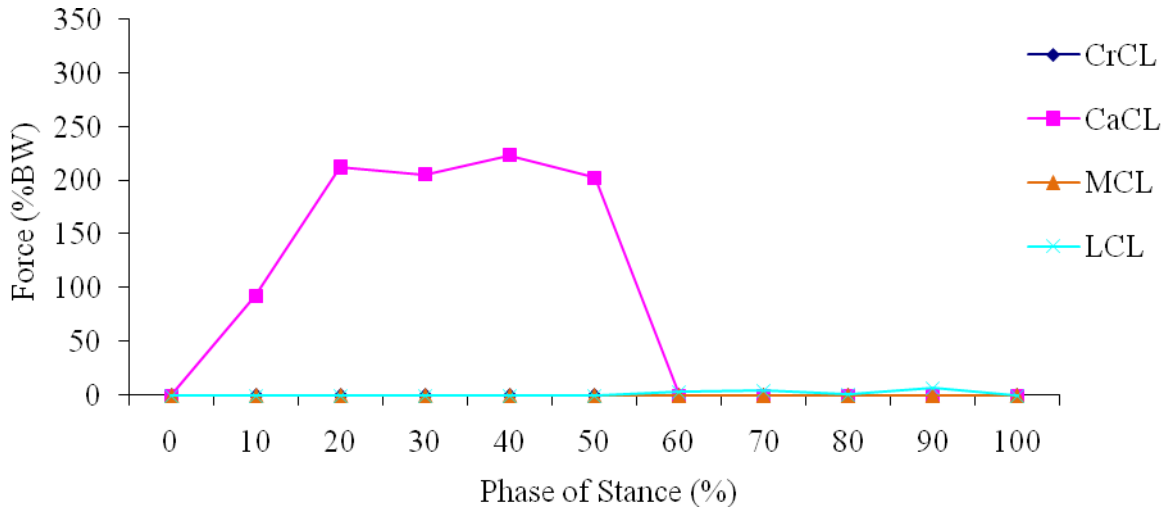

FIGURE 185 - Ligament forces for CrCL deficient stifle (14 mm femoral condyle radius).

For the CrCL intact stifle the peak CrCL force was 28% BW and occurred at 40% stance. The peak LCL force was 7% BW and occurred at 90% stance. The CaCL and MCL were

unloaded throughout stance. For the CrCL deficient stifle the peak CaCL force was 224% BW and occurred at 40% stance. The peak LCL force was 7% BW and occurred at 90% stance. The MCL was unloaded throughout stance.

The ligament forces during stance for the CrCL intact and CrCL deficient stifle with a 16 mm (baseline) femoral condyle radius are shown in FIGURE 186 and FIGURE 187, respectively.

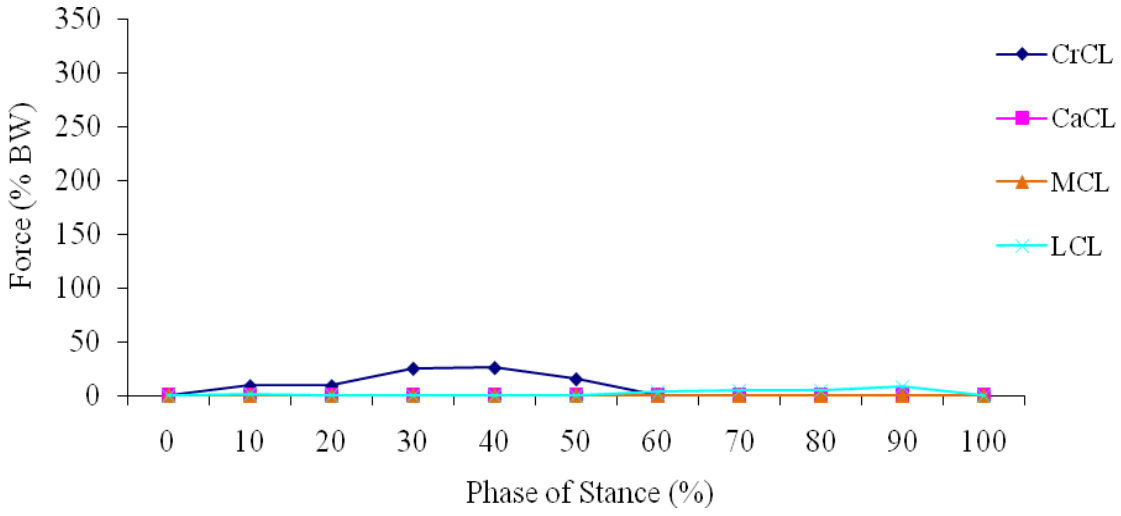

FIGURE 186 - Ligament forces for CrCL intact stifle (16 mm femoral condyle radius).

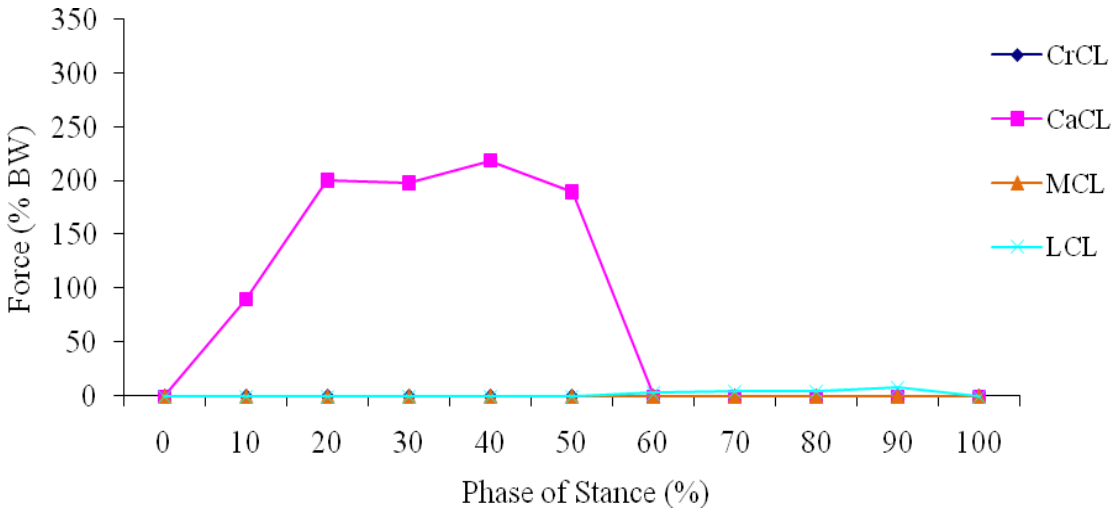

FIGURE 187 - Ligament forces forh CrCL deficient stifle (16 mm femoral condyle radius).

For the CrCL intact stifle the peak CrCL force was 26% body weight (BW) and occurred at 40% stance. The CaCL was unloaded thoughout stance. The peak LCL force was 8% BW and occurred at 90% stance. The MCL was unloaded throughout stance. For the CrCL deficient stifle the peak CaCL force was 219% BW and occurred at 40% stance. The peak LCL force was 8% BW and occurred at 90% stance. The MCL was unloaded throughout stance.

The ligament forces during stance for the CrCL intact and CrCL deficient stifle with an 18 mm femoral condyle radius are shown in FIGURE 188 and FIGURE 189, respectively.

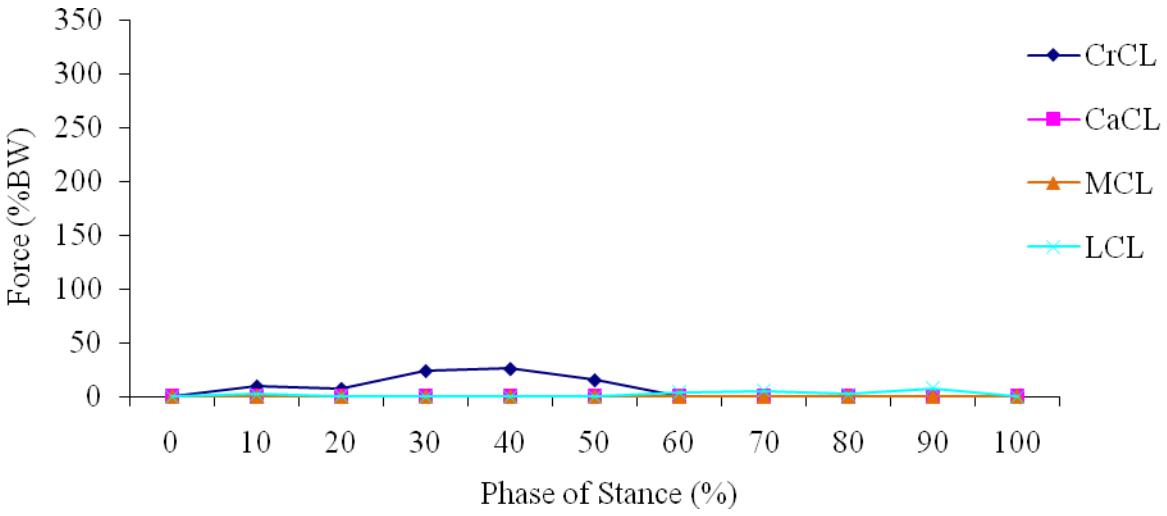

FIGURE 188 - Ligament forces for CrCL intact stifle (18 mm femoral condyle radius).

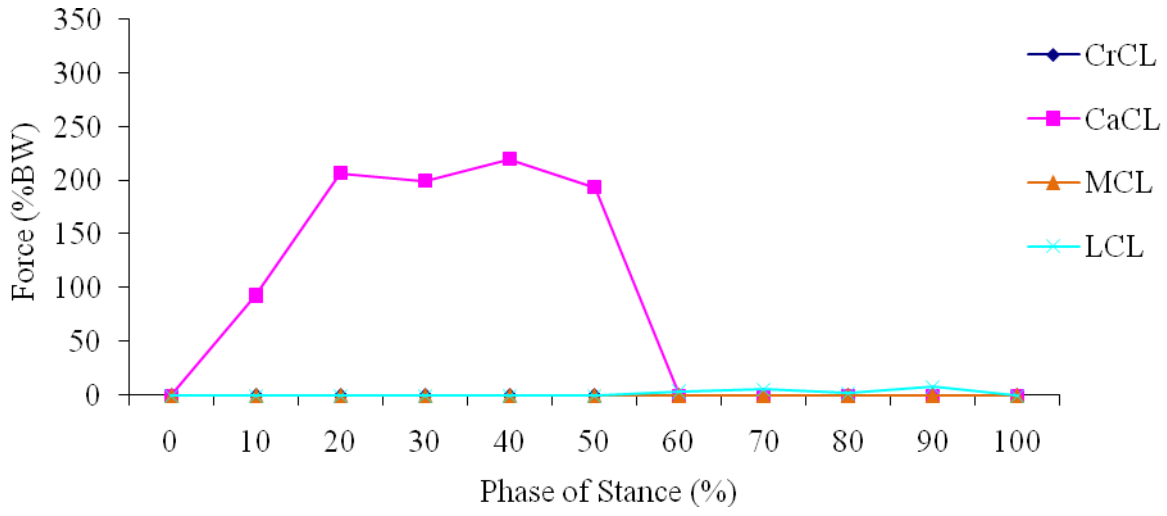

FIGURE 189 - Ligament forces for CrCL deficient stifle (18 mm femoral condyle radius).

For the CrCL intact stifle the peak CrCL force was 26% BW and occurred at 40% stance. The peak LCL force was 8% BW and occurred at 90% stance. The CaCL and MCL were

unloaded throughout stance. For the CrCL deficient stifle the peak CaCL force was 220% BW and occurred at 40% stance. The peak LCL force was 8% BW and occurred at 90% stance. The MCL was unloaded throughout stance.

The ligament forces during stance for the CrCL intact and CrCL deficient stifle with a 22 mm femoral condyle radius are shown in FIGURE 190 and FIGURE 191, respectively.

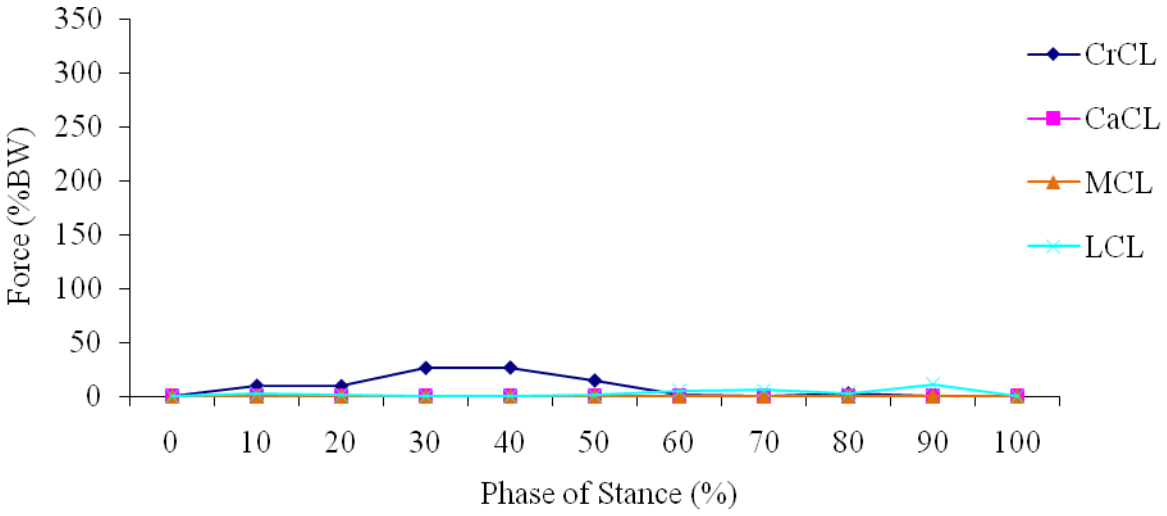

FIGURE 190 - Ligament forces for CrCL intact stifle (22 mm femoral condyle radius).

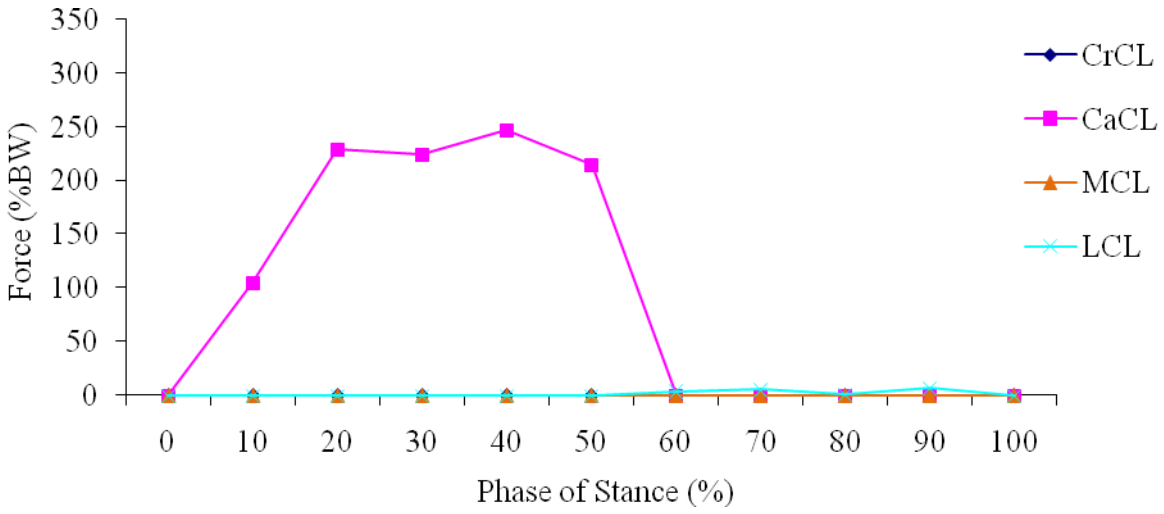

FIGURE 191 - Ligament forces for CrCL deficient stifle (22 mm femoral condyle radius).

For the CrCL intact stifle the peak CrCL force was 27% BW and occurred at 40% stance. The peak LCL force was 11% BW and occurred at 90% stance. The CaCL and MCL were unloaded throughout stance. For the CrCL deficient stifle the peak CaCL force was 247% BW and occurred at 40% stance. The peak LCL force was 7% BW and occurred at 90% stance. The MCL was unloaded throughout stance.

4.3.11.2 Ligament Forces Summary for Femoral Condyle Radius Variation

Ligament forces for each phase of stance for varying femoral condyle radius were determined in the CrCL intact and CrCL deficient stifle. Peak CrCL forces varied by 4% BW ranging from 26% BW to 30% BW across the femoral condyle radii evaluated for the CrCL intact stifle. Peak CaCL forces varied by 87% BW ranging from 160% BW to 247% BW across the femoral condyle radii evaluated for the CrCL deficient stifle. The

peak CrCL forces across the femoral condyle radii evaluated for the CrCL intact stifle are shown in FIGURE 192, and the peak CaCL forces across the femoral condyle radii evaluated for the CrCL deficient stifle are shown in FIGURE 193.

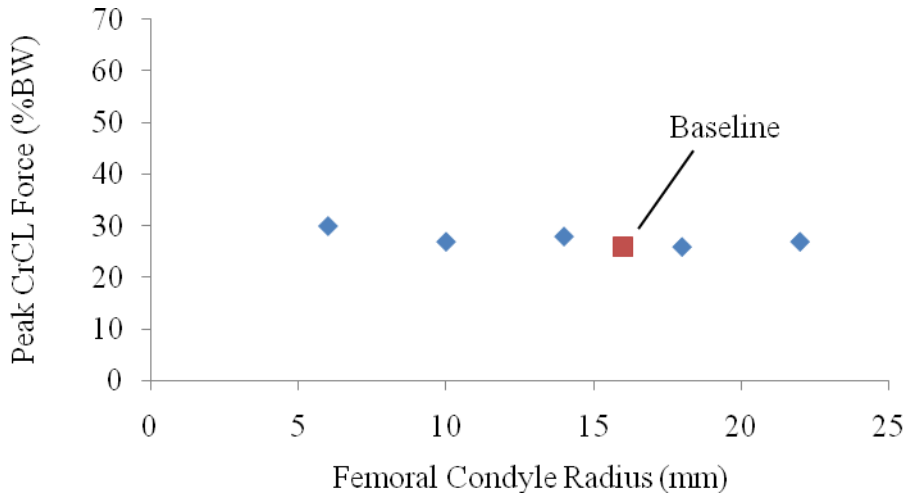

FIGURE 192 - Peak CrCL forces in the CrCL intact stifle for each femoral condyle radius.

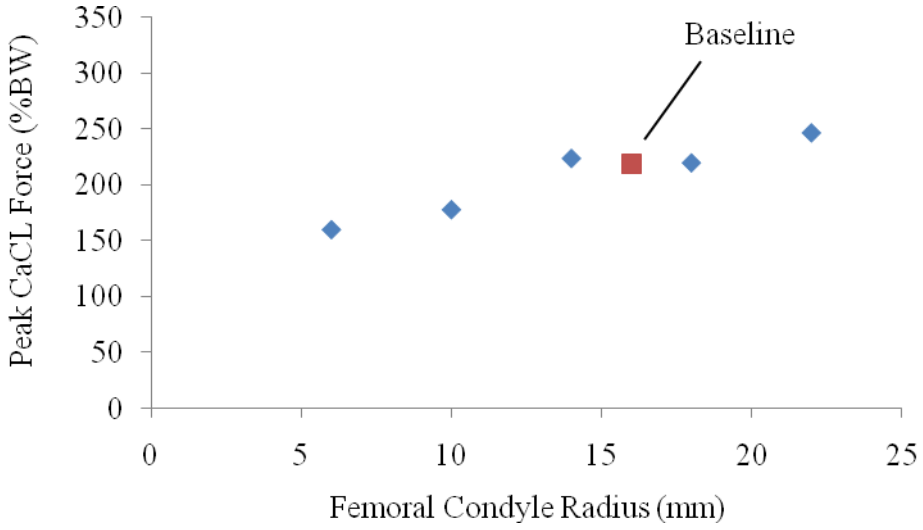

FIGURE 193 - Peak CaCL forces in the CrCL deficient stifle for each femoral condyle radius.

4.3.11.3 Tibial Translation for Femoral Condyle Radius Variation

The relative tibial translation across the phases of stance is plotted in FIGURE 194.

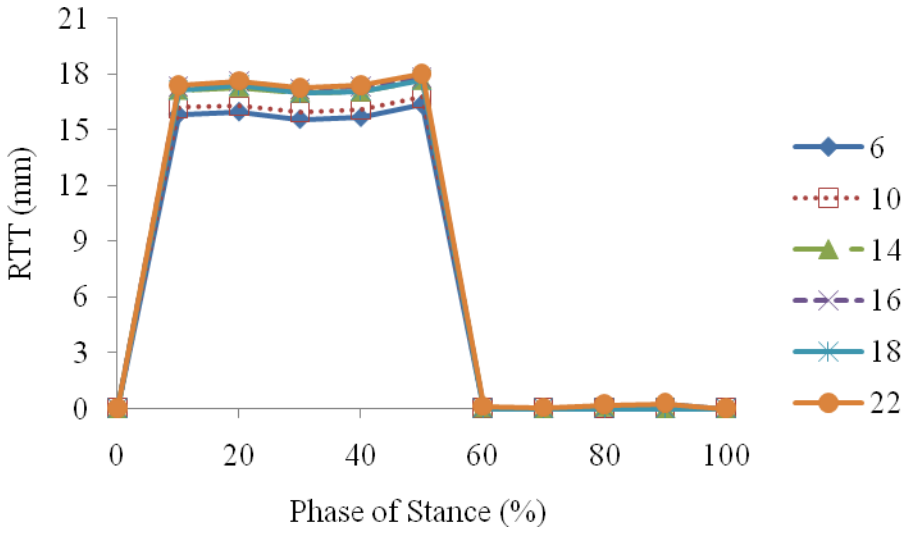

FIGURE 194 - Relative tibial translation between the CrCL intact and deficient stifle models for each femoral condyle radius.

4.3.11.4 Tibial Translation Summary for Femoral Condyle Radius Variation

The peak relative tibial translation, the phase of stance at which it occurred and the corresponding relative tibial translation per body mass and anatomical tibial translation for each femoral condyle radius are listed in TABLE XXI. The peak relative tibial translation values are plotted in FIGURE 195.

TABLE XXI

PEAK TIBIAL TRANSLATION VALUES FOR EACH FEMORAL CONDYLE RADIUS EVALUATED

Radius (mm)	6	10	14	16	18	22
Stance Phase (%)	50	50	50	50	50	50
Peak RTT (mm)*	16.4	16.8	17.7	17.8	17.7	18.0
RTT/BM (mm/kg)**	0.51	0.52	0.55	0.56	0.55	0.56
ATT***	1.29	1.34	1.42	1.43	1.42	1.47

*RTT = Relative Tibial Translation = $(FT_{deficient})_{loaded} - (FT_{intact})_{loaded}$

**RTT/BM = Relative Tibial Translation per Body Mass

***ATT = Anatomical Tibial Translation = $\frac{(FT_{deficient})_{loaded} - (FT_{intact})_{loaded}}{(FT_{intact})_{loaded}}$

where FT denotes the craniocaudal distance from a fixed point on the femur to a fixed point on the tibia, deficient denotes the CrCL was suppressed, intact denotes the CrCL was not suppressed and loaded denotes weight bearing

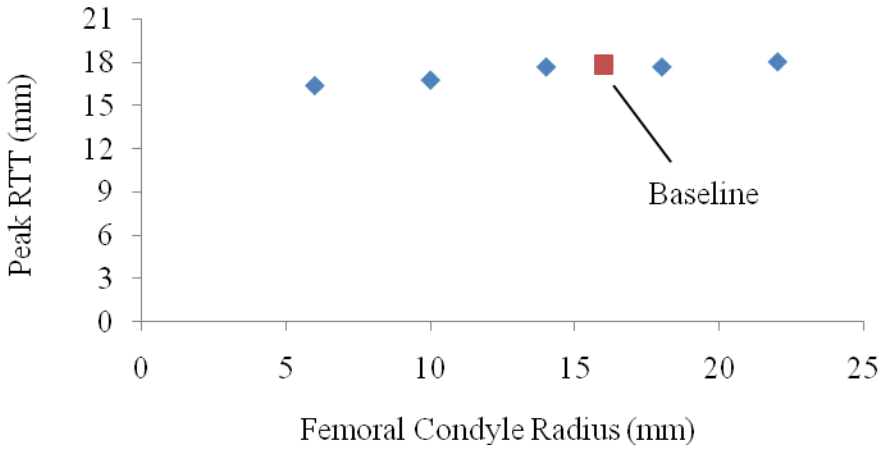

FIGURE 195 - Peak relative tibial translation values for each femoral condyle radius.

Peak relative tibial translation varied by +1.2/-8.2% from baseline for varying femoral condyle radius.

4.4 Parametric Analysis Results Summary

The parametric sensitivity analysis has shown the CrCL force response for the CrCL intact stifle was most sensitive to tibial plateau angle and patellar ligament line of action angle. Variation of ligament stiffness in all ligaments, CrCL stiffness only, ligament prestrain in all ligaments, CrCL prestrain only, muscle force magnitude, ground reaction force magnitude, body mass, femoromeniscal friction coefficients and femoral condyle radius had the least effect on CrCL force response for the CrCL intact stifle compared to baseline. The CrCL force sensitivity of the model for each parameter varied is shown in FIGURE 196.

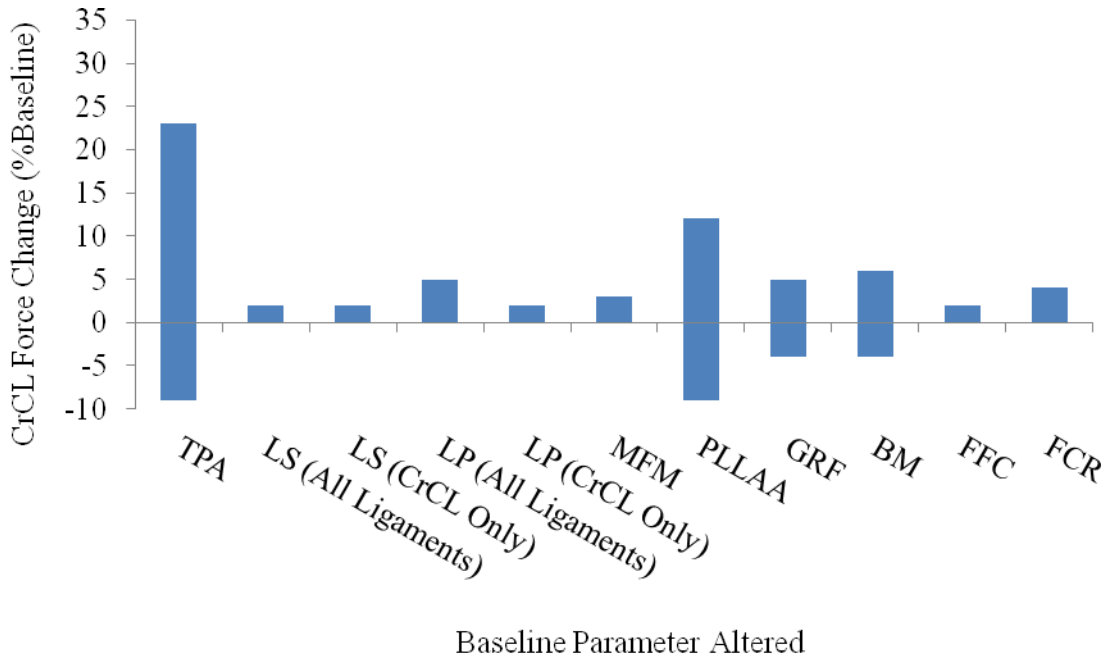

FIGURE 196 - Sensitivity of the CrCL force response for each parameter varied in the CrCL intact stifle.

The CaCL force response for the CrCL deficient stifle was most sensitive to tibial plateau angle, patellar ligament line of action angle, muscle force magnitude, ground reaction force magnitude, body mass, and femoral condyle radius. Variation of ligament stiffness in all ligaments, ligament prestrain in all ligaments and femoromeniscal friction coefficients had the least effect on CaCL force response for the CrCL deficient stifle compared to baseline. Variation of CrCL stiffness only and CrCL prestrain only would have no effect on the CrCL deficient stifle. The CaCL force sensitivity of the model for each parameter varied is shown in FIGURE 197.

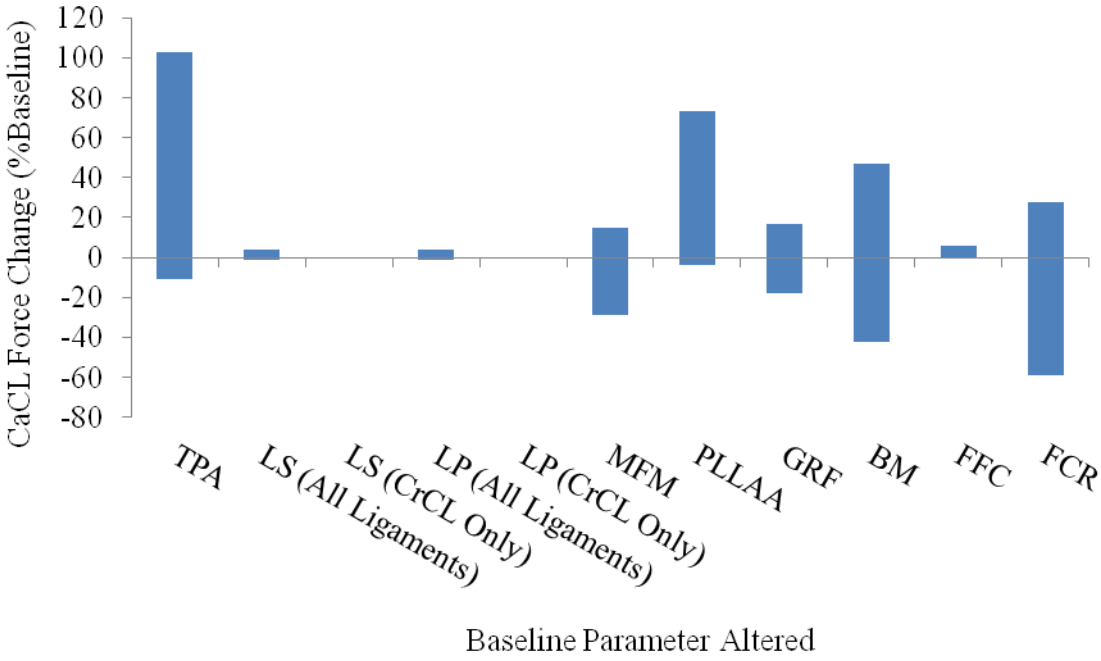

FIGURE 197 - Sensitivity of the CaCL force response for each parameter varied in the CrCL deficient stifle.

The peak relative tibial translation was most sensitive to tibial plateau angle, patellar ligament line of action angle and femoral condyle radius. Variation of ligament stiffness in all ligaments, ligament stiffness in the CrCL only, ligament prestrain in all ligaments, ligament prestrain in the CrCL only, muscle force magnitude, ground reaction

force magnitude, body mass, and femoromeniscal friction coefficients had the least effect on relative tibial translation compared to baseline. The peak relative tibial translation sensitivity of the model for each parameter varied is shown in FIGURE 198.

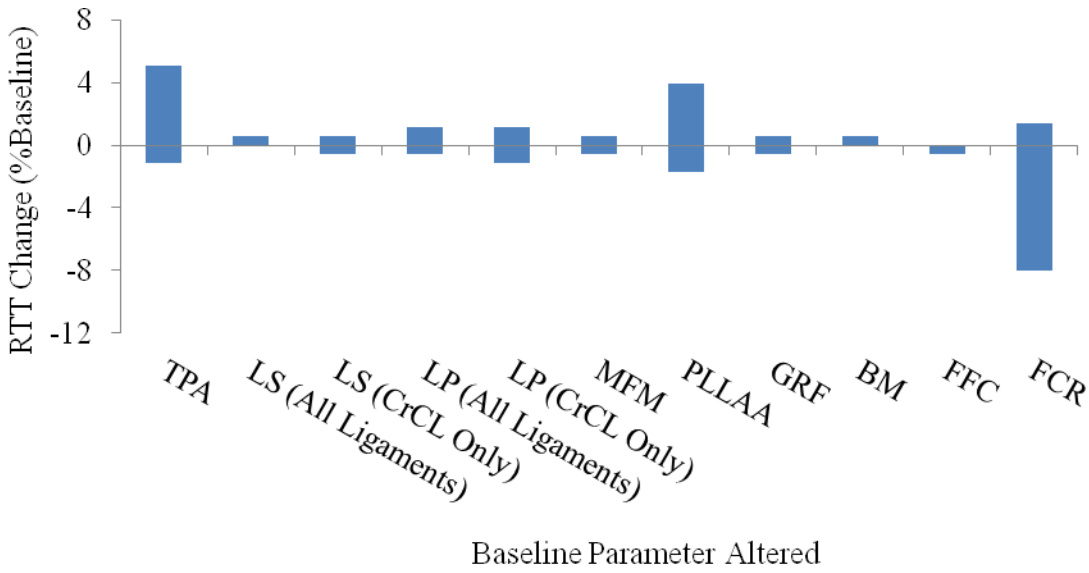

FIGURE 198 - Sensitivity of the peak relative tibial translation between the CrCL intact and CrCL deficient stifle for each parameter varied.

Collectively, the stifle outcome measures of CrCL force in the CrCl intact stifle, CaCL force in the CrCL deficient stifle and relative tibial translation were most sensitive to changes to tibial plateau angle and patellar ligament line of action angle. The outcome measures of CaCL force in the CrCL deficient stifle and relative tibial translation were sensitive to femoral condyle radius. The CaCL force response in the CrCL deficient stifle was moderately sensitive to changes to muscle force magnitude, ground reaction force magnitude and body mass. The stifle outcome measures were least sensitive to ligament stiffness in all ligaments, CrCL stiffness, ligament prestrain in all ligaments, CrCL prestrain and femoromeniscal friction coefficients.

V. DISCUSSION

5.1 Model Description

Despite the challenges of biomechanical simulation, a validated computer model has the capability to incorporate parametric analyses to explore the effects of various parameters on key outcomes without the need to conduct animal studies. The model developed in this study was an approximation of the canine hind limb capable of simulating both a CrCL intact and CrCL deficient stifle. This is the first three dimensional canine hind limb computer model able to determine ligament forces, tibial translation, and visually describe both the CrCL intact and CrCL deficient stifle for discrete phases of stance.

Using the verified model, a parametric sensitivity analysis was conducted to evaluate the influence of several parameters, thought to be associated with CrCL deficiency, on ligament forces and tibial translation. The parameters varied were based on clinically relevant or approximated input values and were easily incorporated and assessed in this computer model. It is important to note that though the predetermined parameters such as stifle ligament prestrain and hind limb muscle forces were based on values reported in the scientific literature, some values reported were approximations and in need of further justification. Therefore the computer model is a representation of these

reported parameters, and its validity is additionally subject to the validity of these reported approximations.

5.1.1 Ligament Forces

In general it was found that the CrCL was the primary load-bearing ligament in the CrCL intact stifle, and the CaCL was the primary load-bearing ligament in the CrCL deficient stifle. The LCL and MCL generally carried less load than the CrCL and CaCL.

As previously described the CrCL is generally taut in extension and loose in flexion (Arnoczky and Marshall 1977). This would indicate that the CrCL would be in greater tension in the early phases of stance when the hind limb is in increased extension. The peak loads in the anterior cruciate ligament of goats were measured in vivo in the first 40% of stance during a slow walk (Holden, Grood et al. 1994). Furthermore, a mathematical model also indicated peak CrCL loads in the canine stifle at 40% stance (Shahar and Banks-Sills 2004). In this study the computer model developed also demonstrated peak CrCL loads at 40% stance with CrCL loads reducing to zero in the latter portions of stance.

Similarly, it was reported that the CaCL is generally loose in extension and taut in flexion (Arnoczky and Marshall 1977). This would correspond with the CaCL being in greater tension in the later phases of stance when the hind limb is in increased flexion. The CaCL remained unloaded throughout stance in the modeled CrCL intact stifle. Similar results were reported by Shahar using a mathematical model (Shahar and Banks-Sills 2004).

Unlike the cruciate ligaments, the collateral ligaments remain approximately constant in length in both the flexion and extension portions of the stance phase (Vasseur

and Arnoczky 1981). This would suggest less variation in the collateral ligament forces during stance due to changes in the stifle angle. In this study the MCL and LCL, both carrying negligible load, maintained more constant loading patterns than the CrCL throughout stance in the CrCL intact stifle.

In the CrCL deficient stifle, the CaCL force increased compared to the CaCL force in the CrCL intact stifle. In this study the peak CaCL load occurred at 40% stance in the CrCL deficient stifle model while it occurred at 50% stance in a mathematical model study conducted by Shahar (Shahar and Banks-Sills 2004). In our study force trends within the MCL and LCL remained the same in the CrCL intact and CrCL deficient stifle. This would indicate the CaCL is therefore the sole load bearing ligament following CrCL suppression. An in vitro study has also noted increased loads in the CaCL following CrCL suppression (Warzee, Dejardin et al. 2001) at mid stride as was present in this model. All ligament forces were below the proposed failure threshold of four times body weight indicated by a previous canine CrCL material testing study (Wingfield, Amis et al. 2000) so the assumption that no ligament failed during simulation was considered valid.

Though the loading patterns during stance were similar to those reported in a previous study using a mathematical model (Shahar and Banks-Sills 2004), the ligament force magnitudes reported in that study were less than the results predicted based on our computer model. Shahar reported CrCL loads peaking at 12% body weight (BW) in the CrCL intact stifle while the CaCL load peaked at 11% BW following CrCL suppression. In this study the computer model predicted peak CrCL loads of 26% BW. Following CrCL suppression, the CaCL load peaked at 219% BW. This disparity could be due to the

much lower ligament stiffness values used in Shahar's mathematical model. In our study ligament stiffness values developed from reported tensile testing (Wingfield, Amis et al. 2000) were more than twice those used by Shahar for the mathematical model. Ligament stiffnesses of 1600 N/ε, 3000 N/ε, 900 N/ε and 700 N/ε for the CrCL, CaCL, MCL and LCL, respectively, were used in the mathematical model by Shahar.

Since the CrCL serves to prevent tibial translation (Arnoczky and Marshall 1977; Slocum and Devine 1983), the correlation between the increased CrCL loading in the CrCL intact stifle in the first half of stance and the presence of tibial translation following CrCL suppression in the first half of stance supports the functional role of the CrCL in the model.

A few scenarios in this study showed the presence of CaCL force anomalies in the CrCL deficient stifle. These scenarios had instances where the CaCL force suddenly changed from a nonzero value to a zero value and then returned to a nonzero value. Scenarios such as these are present in the CrCL deficient stifle for a TPA of 18° and 20° at 20% stance. This anomaly was no longer present for the CrCL deficient stifle with a TPA of 22°. This change indicates a transition occurring in the model near 20% stance. A similar trend was present in a previously reported mathematical model (Shahar and Banks-Sills 2004), but its presence was not discussed. FIGURE 199 shows the CaCL forces for TPAs of 18°, 20° and 22°.

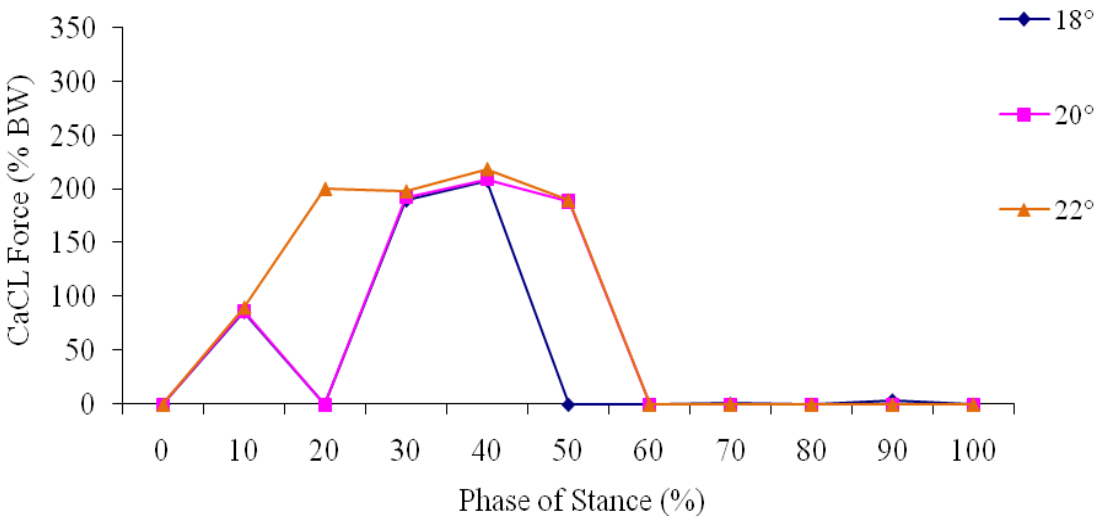

FIGURE 199 – CaCL forces for three TPA scenarios in the CrCL deficient stifle.

To better understand the discontinuity occurring near 20% stance for the 18° and 20° TPA, free body diagrams that include the model input forces for these three tibial plateau angles at 10%, 20% and 30% stance were developed for the hind limb. A representative instance of the sagittal forces present in each scenario is depicted in FIGURE 200.

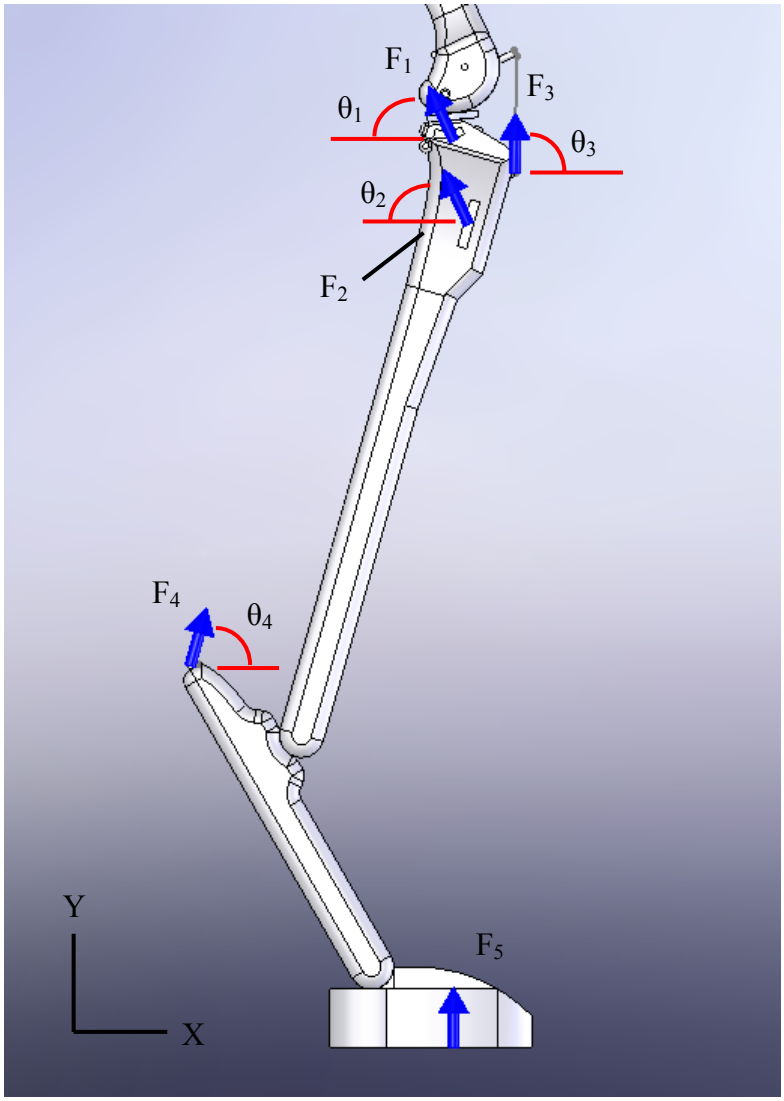

FIGURE 200 –Model muscle and ground reaction input forces and their associated angles. F_1 is the medial femoral stifle flexors, F_2 is the lateral femoral stifle flexors, F_3 is the femoral stifle extensors, F_4 is the tibial stifle flexors and F_5 is the GRF.

TABLE XXII lists the variables noted in FIGURE 200 for the 10%, 20% and 30% phases of stance while

TABLE XXIII lists the resulting force components in the X and Y directions.

TABLE XXII

MUSCLE AND GROUND REACTION INPUT FORCES AND ANGLES FOR THREE PHASES OF STANCE

	F_1 (N)	F_2 (N)	F_3 (N)	F_4 (N)	F_5 (N)	θ_1 (°)	θ_2 (°)	θ_3 (°)	θ_4 (°)
10%	5	26	55	26	44	65	65	89	74
20%	12	71	151	22	112	66	66	87	72
30%	22	38	69	77	137	67	67	87	71

TABLE XXIII

SUMMATION OF FORCES IN THE X AND Y DIRECTIONS FOR THREE PHASES OF STANCE

	ΣF_X (N)	ΣF_Y (N)
10%	-5	152
20%	-19	360
30%	5	333

The summed forces in TABLE XXIII are not dependent on the TPA parameter varied. Therefore, these summed forces were converted to directional forces corresponding to each TPA relative to horizontal as depicted in FIGURE 201.

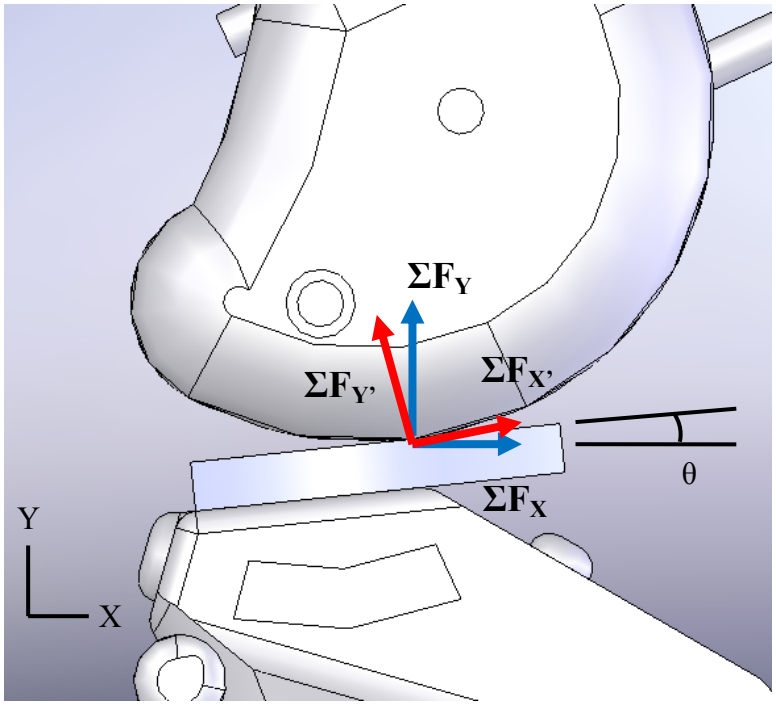

FIGURE 201 –Force components at distal femur. X' is parallel to the meniscal surface and Y' is perpendicular to the meniscal surface.

The resulting converted force components in FIGURE 201 in the X' and Y' directions for each TPA are listed in TABLE XXIV.

TABLE XXIV

CONVERTED FORCE COMPONENTS IN THE X' AND Y' DIRECTIONS FOR THREE TIBIAL PLATEAU ANGLES AT THREE PHASES OF STANCE

TPA	Stance Phase	θ (°)	$\Sigma F_{X'}$ (N)	$\Sigma F_{Y'}$ (N)
18°	10%	2	0.31	151.73
	20%	0	-19.00	360.00
	30%	-1	-0.81	332.86
20°	10%	4	5.62	151.28
	20%	2	-6.42	359.12
	30%	1	10.81	333.04
22°	10%	6	10.92	150.64
	20%	4	6.16	357.80
	30%	3	22.42	332.81

For the two scenarios, TPAs of 18° and 20° at 20% stance, resulting in a zero CaCL load, there is a negative X' component. This negative component would act to counter cranial tibial translation thus greatly reducing loading on the CaCL. Since this negative X' component helped to prevent excessive cranial tibial translation while still allowing small cranial tibial translation (FIGURE 54) for these two scenarios, the CaCL was unloaded.

Other varied parameters also occasionally showed these anomaly points of zero CaCL load in the CrCL deficient stifle. Similar relationships may have resulted for patellar ligament line of action angles of -15°, -10° and -5° at 20% stance. These angles introduced a more caudally directed quadriceps force, which increased the negative magnitude of the X' force component thereby reucing cranial tibial translation as indicated in FIGURE 137 at 20% stance. Additionally, this behavior was present for the 0.09 femoromeniscal friction coefficient scenario. The higher friction coefficient would tend to reduce cranial tibial translation as indicated in FIGURE 177 at 20% stance.

5.1.2 Tibial Translation

The amount of tibial translation found using our computer model with a CrCL deficient stifle is similar to that reported in an in vitro study by Warzee simulating mid-stride stance (Warzee, Dejardin et al. 2001). An average relative tibial translation of 18.9 +/- 3.4 mm following CrCL transection from dogs ranging from 27 to 36 kg was reported by Warzee (Warzee, Dejardin et al. 2001). Peak relative tibial translation using our model was 17.8 mm and also occurred at mid-stance. A comparison of relative measures indicates a relative tibial translation per body mass of 0.56 mm/kg and an anatomical tibial translation (relative tibial translation divided by the CrCL intact tibial translation, FT_{Intact}) of 1.43 using our model. The in vitro study by Warzee yielded a relative tibial

translation per body mass of 0.59 mm/kg and an anatomical tibial translation of 1.19. These measures of tibial translation for similarly sized dogs at mid-stride showed good agreement between our model's predictions and the in vitro study. A visual representation of the cranial tibial translation prior to and following CrCL transection in our computer model and Warzee's in vitro study is shown in FIGURE 202 and FIGURE 203, respectively.

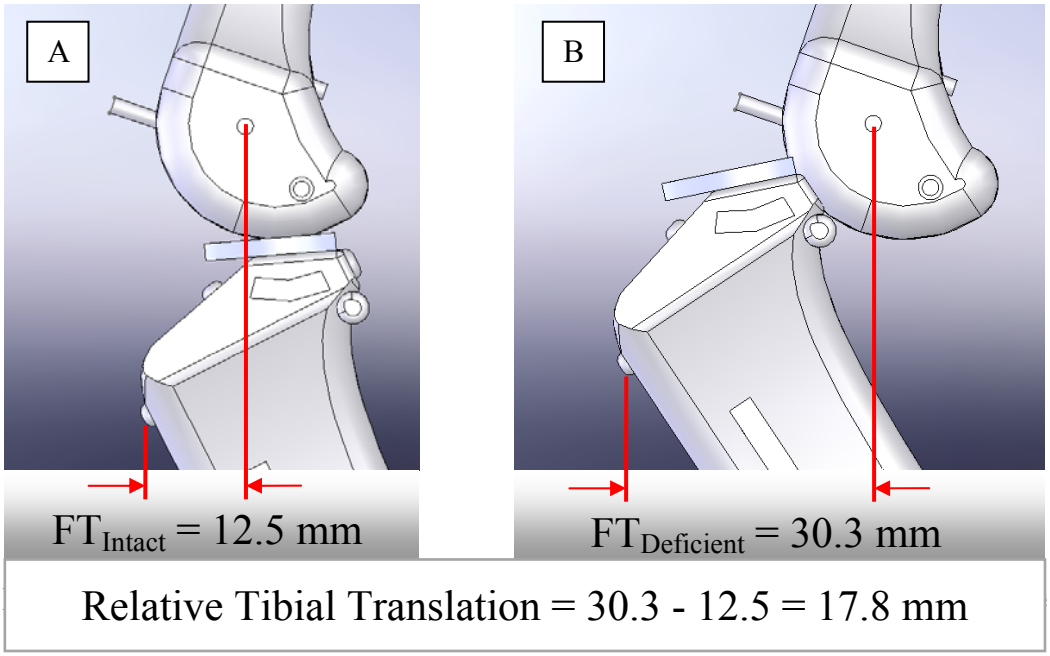

FIGURE 202 – Lateral view of relative cranial tibial translation. Relative tibial translation is the difference between the CrCL intact tibial translation (FT_{Intact}) (A) and CrCL deficient tibial translation ($FT_{Deficient}$).

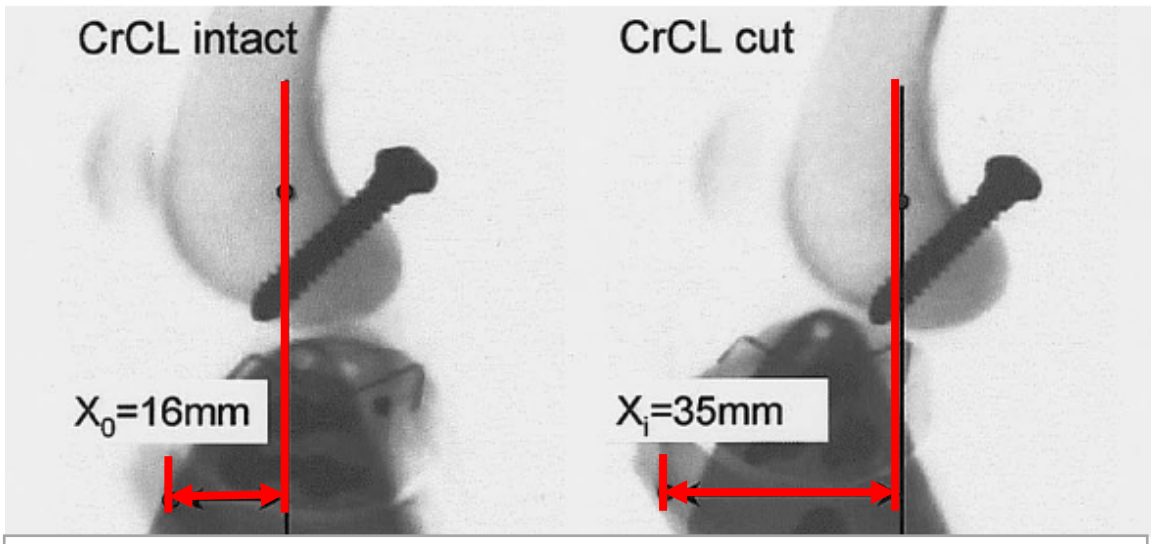

FIGURE 203 – Lateral radiograph of relative cranial tibial translation. Relative tibial translation is the difference between the CrCL intact tibial translation (X_0) and CrCL deficient tibial translation (X_i) (Warzee, Dejardin et al. 2001).

5.2 Parametric Sensitivity Analysis

The sensitivity of model outcome measures was assessed by systematically altering model characteristics. Since our computer model is a simplified version of the canine hind limb which is reliant upon several predetermined parameters such as stifle ligament stiffness, TPA and ground reaction force, the sensitivity of model outcomes to these parameters indicated which parameters have the greatest effect. Sensitivity of model outcome measures to these varied parameters may also indicate which parameters are more likely to influence CrCL deficiency.

5.2.1 Tibial Plateau Angle

Tibial plateau angle was one of three parameters for which the model outcomes were most sensitive. Tibial plateau angles ranging from 18° to 28° were evaluated. The model predicted trends of increased ligament forces and increased tibial translation for increased TPA compared to the baseline 22° TPA. Tibial plateau angles ranging from 18° to 25° have been reported for various breeds, both with and without CrCL deficiency (Morris and Lipowitz 2001). Using the CrCL intact model, for TPAs of 24°, 26° and 28° the model demonstrated not only increased CrCL loads of up to 49% BW in the early phases of stance, but the CrCL was also loaded in later phases of stance. This may be indicative of predisposition to CrCL failure in dogs with higher TPAs as has been previously suggested (Morris and Lipowitz 2001).

Subsequently, as was demonstrated in the baseline 22° TPA version of the computer model, the CaCL tended to become the primary load bearing ligament following CrCL suppression. During phases of stance where the CrCL was loaded in the CrCL intact stifle, the CaCL, which was not loaded in the CrCL intact stifle, became loaded in the CrCL deficient stifle. The increased CrCL loads in the CrCL intact stifle for higher TPAs was reflected as increased CaCL loads in the CrCL deficient stifle.

Relative tibial translation between the CrCL intact and CrCL deficient stifle for TPAs of 26° and 28° were nonzero following mid-stride with peak relative tibial translation occuring at 70% stance. Only the CrCL was loaded after mid-stride in the CrCL intact stifle for these two TPA scenarios. This suggests the CrCL was a primary factor inhibiting tibial translation in later phases of stance for 26° and 28° TPAs.

Overall, these results of increasing relative tibial translation and increasing ligament forces with increasing TPA support the previously proposed reasoning that the TPA affects the stability of the canine stifle (Slocum and Devine 1983; Slocum and Devine 1984; Slocum and Slocum 1993; Morris and Lipowitz 2001; Warzee, Dejardin et al. 2001; Reif, Hulse et al. 2002; Talaat, Kowaleski et al. 2006; Boudrieau 2009).

5.2.2 Ligament Stiffness (All Ligaments)

Ligament stiffness was investigated as a parameter due to the biomechanical role of the stifle ligaments as passive stifle joint restraints. The ligament stiffness of the CrCL has been previously reported for two breeds (Wingfield, Amis et al. 2000), but biomechanical information for the remaining stifle ligaments was unavailable. Approximations were adapted from CT data to develop input stiffness values for the remaining ligaments based on the proportional cross sectional area relationships between the CrCL and the remaining stifle ligaments. The baseline ligament stiffness values were 4230 N/ε, 7150 N/ε, 3650 N/ε and 6350 N/ε for the CrCL, CaCL, LCL and MCL, respectively. Uncertainty in these approximations, as well as uncertainty due to scaling the assigned stiffness for the CrCL from two breeds, was accounted for through variation of all ligament stiffness values through the range of +/-20% in the parametric sensitivity analysis. Variation through the range of +/-20% of the assigned ligament stiffness values was demonstrated to have little effect on model outcome measures. Therefore, the ligament stiffness assumptions had negligible effect on model outcomes for the range of values evaluated. Clinically, this lack of sensitivity to variation in all ligament stiffness values suggests the passive restraint imposed by the ligaments across the range of

stiffness values evaluated did not affect stifle biomechanics during the stance portion of walking gait.

5.2.3 Ligament Stiffness (CrCL Only)

Since the CrCL has previously been reported to show the most degeneration of any of the four stifle ligaments (Vasseur, Pool et al. 1985), variation of CrCL stiffness was thought to be representative of changes to the CrCL as a result of this degeneration. Variation through the range of +/-20% of the assigned 4230 N/ε CrCL stiffness was demonstrated to have little effect on the intact stifle model outcome measures. Clinically, as with variation of all ligament stiffness values, this lack of sensitivity to variation in CrCL-only stiffness suggests the passive restraint imposed by the CrCL across the range of stiffness values evaluated did not affect stifle biomechanics during the stance portion of walking gait. This lack of outcome sensitivty to CrCL stiffness also suggests small changes in CrCL stiffness due to degeneration or a partial tear may not have an appreciable effect on stifle biomechanics. However, we evaluated a small range of ligament stiffness values which may not account for the presence of degeneration or a partial tear.

5.2.4 Ligament Prestrain (All Ligaments)

Stress within each respective stifle ligament is related to the amount of strain inherently present within each respective ligament. The amount of prestrain within each stifle ligament was assigned in the model based on previously reported values at full stifle extension developed from human studies (Blankevoort, Kuiper et al. 1991; Shahar and Banks-Sills 2004). The baseline ligament prestrain values were 0.04, 0.04, 0.08 and -0.25

for the CrCL, CaCL, LCL and MCL, respectively. Uncertainty due to these approximations was assessed by varying the ligament prestrain values through the range of +/-20% in the parametric sensitivity analysis. Variation through the range of +/-20% of the assigned ligament prestrain values was demonstrated to have little effect on the model outcome measures. Clinically, this lack of sensitivity of the model to variation in ligament prestrain across the range of values evaluated suggests stifle biomechanics were not affected during the stance portion of walking gait for small variation in the amount of stretch in each respective ligament.

5.2.5 Ligament Prestrain (CrCL Only)

Since the CrCL has previously been reported to show the most degeneration of any of the four stifle ligaments (Vasseur, Pool et al. 1985), variation of CrCL prestrain alone was thought to be representative of changes to the CrCL as a result of this increased likelihood of degeneration. The baseline CrCL prestrain was 0.04. Variation through the range of +/-20% of the assigned CrCL prestrain value was demonstrated to have little effect on the model outcome measures. Clinically, this lack of sensitivity of the model to variation in CrCL prestrain across the range of values evaluated suggests stifle biomechanics were not affected during the stance portion of walking gait for small variation in the amount of stretch in the CrCL.

5.2.6 Muscle Force Magnitude

Muscle forces applied within the model were approximated based on previously reported values developed for the stance phase of gait using an optimization technique that sought to minimize the maximal muscle stress of the hind limb muscles (Shahar and

Banks-Sills 2004). These reported muscle forces were adapted in this study by grouping key hind limb muscles into the following four groups: femoral stifle extensors, medial femoral stifle flexors, lateral femoral stifle flexors and tibial stifle flexors. Each of the four muscle force groups lines of action were maintained throughout the analysis. Uncertainty in these reported muscle forces, as well as the grouping of these muscle forces, was assessed by varying all input muscle forces through the range of +/-20%. Variation through the range of +/-20% of the assigned muscle force magnitudes was demonstrated to have little effect on the CrCL force and tibial translation model outcome measures. The CaCL force, however, varied by 44% BW ranging from a minimum of 190% BW to a maximum of 234% BW following suppression of the CrCL with variation in muscle force. The magnitude of the CaCL force in the CrCL deficient stifle model increased with increasing muscle force magnitude. Relative tibial translation was not affected by muscle force magnitude variation across the range evaluated. Clinically, though hindlimb muscles may help stabilize the stifle during stance, an imbalance in these stabilizing muscles may lead to instability in the CrCL deficient stifle and increased loads in the remaining passive restraints, such as the CaCL. This imbalance may become more pronounced as the magnitude of the muscle forces increases.

5.2.7 Patellar Ligament Line of Action Angle

It has been reported through an in vitro study that a patellar ligament line of action angle (PLLAA) greater than perpendicular to the tibial plateau at mid stance will cause cranial tibial translation (Apelt, Kowaleski et al. 2007). To investigate this finding, PLLAA was systematically varied across the range of +/-20°. FIGURE 204 shows the

PLLAA as defined in our model where positive rotation about the tibial tuberosity is in the cranial direction.

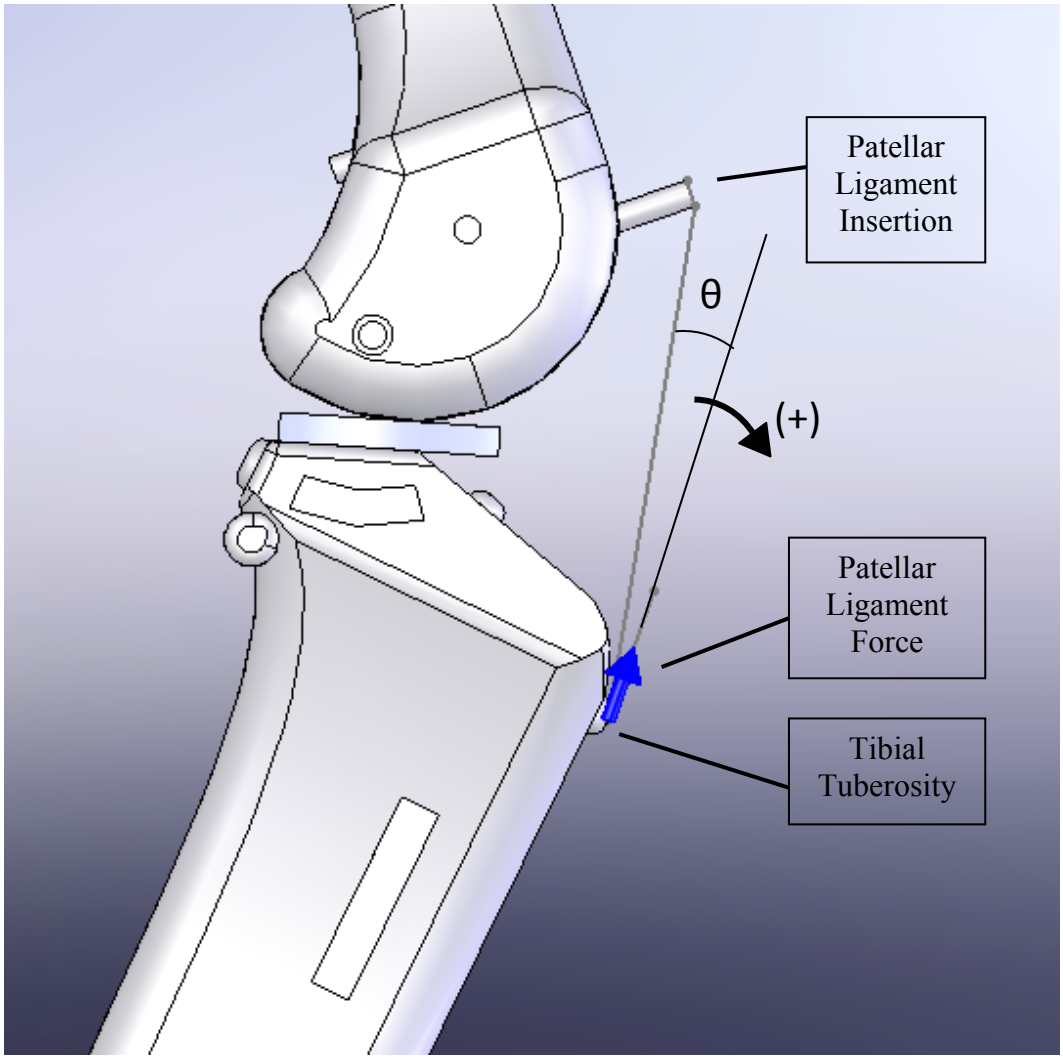

FIGURE 204 – PLLAA as previously described.

Patellar ligament line of action angle was also one of three parameters for which the model outcomes were most sensitive. The model predicted trends of increasing CrCL forces in the CrCL intact stifle, increasing CaCL force in the CrCL deficient stifle and increasing relative tibial translation for increased PLLAA.

As the PLLAA increased, the cranial component of the quadriceps force transferred through the patellar ligament increased. Likewise, as the PLLAA decreased, the cranial component of the quadriceps force transferred through the patellar ligament decreased as the quadriceps force became more caudally oriented. Therefore, peak CrCL loads steadily increased with increasing PLLAA.

Beginning with a 5° PLLAA increase in the CrCL intact stifle, the CrCL was loaded in later phases of stance. As the PLLAA increased, the load carried by the CrCL in the later phases of stance also increased. As with the increase in TPA, in the CrCL deficient stifle the CaCL carried the load in the later phases of stance that had been carried by the CrCL in the intact stifle. This relationship is similarly demonstrated in the model by the nonzero relative tibial translation in later phases of stance for increased PLLAA.

Additionally, decreasing the PLLAA so as to incorporate a more caudally oriented quadriceps force reduced CrCL loads in the intact stifle, CaCL loads in the CrCL deficient stifle and relative tibial translation. Relative tibial translation was not present in the later phases of stance for decreased PLLAA, which corresponded with the baseline model. Relative tibial translation was even reduced in some cases during the early phases of stance. These results therefore support the previously proposed reasoning that the direction of the patellar ligament affects the stability of the canine stifle (Hoffmann, Miller et al. 2006; Apelt, Kowaleski et al. 2007; Boudrieau 2009).

5.2.8 Ground Reaction Force

Ground reaction forces were based on previously reported values for large breed dogs for the stance phase of a slow-walking gait (Budsberg, Verstraete et al. 1987;

Shahar and Banks-Sills 2004). Uncertainty in these values due to their application to our model, which was developed from one dog, was assessed by varying GRF through the range of +/-20% in the parametric sensitivity analysis. Additionally, variation in GRF profiles could result for varied walking speeds. Variation through the range of +/-20% of the assigned ground reaction force magnitudes was demonstrated to have little effect on the CrCL force and tibial translation outcome measures in the model. The CaCL force, however, varied by 35% BW ranging from a minimum of 201% BW to an maximum of 236% BW following suppression of the CrCL with GRF changes. The magnitude of the CaCL force in the CrCL deficient stifle increased with increasing GRF magnitude. Peak CaCL loads in the CrCL deficient stifle occurred prior to mid-stance and corresponded with peak input GRF magnitudes. Clinically, the CaCL would be expected to carry additional load resulting from the increased GRF. Therefore, overweight dogs would be predisposed to further injury following CrCL deficiency as previously suggested (Morris and Lipowitz 2001).

5.2.9 Body Mass

A dog of equal height but different body mass was simulated by varying the body mass as well as the parameters associated with body mass including ground reaction forces, muscle forces and ligament cross sectional areas through the range of +/-20% in the parametric sensitivity analysis. Variation through the range of +/-20% of the assigned parameters derived from body mass was demonstrated to have little effect on the CrCL force and tibial translation outcome measures in the intact stifle model. The CaCL force, however, varied by 89% BW ranging from a minimum of 177% BW to a maximum of 266% BW following suppression of the CrCL. The magnitude of the CaCL force in the

CrCL deficient stifle increased with increasing body mass. Since both increases in muscle force magnitude and GRF magnitude were previously found to increase CaCL forces in the CrCL deficient stifle, the combination of these increases would be expected to also increase CaCL forces. Clinically, the passive restraints in the CrCL deficient stifle, especially the CaCL, would be expected to carry additional load. Dogs of greater body mass would be predisposed to possible injury following CrCL deficiency. Previous studies have reported larger dogs are less likely to recover function following CrCL deficiency without surgical correction (Vasseur, Pool et al. 1985; Lazar, Berry et al. 2005).

5.2.10 Femoromeniscal Friction Coefficients

Friction between the articulating surfaces of the stifle was varied in the model to encompass previously reported bovine stifle joint femoromeniscal friction coefficients (McCann, Ingham et al. 2009). These values ranging from 0.03 to 0.09 represented a healthy and osteoarthritic bovine stifle since increased femoromeniscal friction coefficients were shown to result in osteoarthritic bovine stifles (McCann, Ingham et al. 2009). Variation of the static and dynamic femoromeniscal friction coefficients to values within this published bovine stifle range was demonstrated to have little effect on the outcome measures in the model. Clinically, osteoarthritis has previously been reported to continue to progress following stabilization of the CrCL deficient stifle (Thieman, Tomlinson et al. 2006). The lack of sensitivity of the model to osteoarthritic femoromeniscal friction suggests this model may not be able to describe the biomechanics associated with the presence or absence of osteoarthritis.

5.2.11 Femoral Condyle Radius

Alteration of the geometry of the femur has not to our knowledge been the basis of any CrCL deficiency corrective surgical procedures. Femoral condyle radius (FCR) was introduced as a parameter capable of describing one aspect of the distal femur that varies among breeds. A FCR range of 6 mm to 22 mm corresponding to a Dachshund and a Great Dane, respectively, were evaluated in this model. The baseline FCR was 16 mm.

The model outcomes of CaCL force and relative tibial translation in the CrCL deficient stifle were sensitive to variation in FCR. Peak CrCL loads in the intact stifle were not sensitive to variation in FCR, while peak CaCL loads in the CrCL deficient stifle and relative tibial translation generally increased with increasing FCR. Relative tibial translation was present in only the first half of the stance phase for all FCRs evaluated. However, peak CrCL loads in the intact stifle were not sensitive to variation in FCR.

It was expected that the smaller FCR corresponding to a breed such as the Greyhound or Dachshund, that is less likely to experience CrCL deficiency (Witsberger, Villamil et al. 2008) would have decreased ligament loads and tibial translation. The model, however, predicted little variation in the CrCL loads in the CrCL intact stifle. But unlike TPA and PLLAA, the FCR is a result of the femur geometry, which, due to skeletal scaling variation among breeds, would be determined by the breed of dog. Even though the values used for changes in the FCR were based on measurements from various breeds, alteration of the FCR in the model may not be fully representative of femur scale variation that differs among breeds. Additionally, body mass variance associated with breed was not accounted for in conjunction with breed variation of FCR. Therefore, the

model may not be representative of breed variation based solely on FCR variation, and other parameters describing the distal femur, the mass of the dog and associated corresponding characteristics affecting gait may need to also be assessed for their role in CrCL loading and stifle biomechanics.

CaCL forces in the CrCL deficient stifle and relative tibial translation increased with increasing FCR. These results support clinical findings which suggest larger dogs are less likely to fully recover following CrCL deficiency without surgical intervention (Vasseur, Pool et al. 1985; Lazar, Berry et al. 2005).

5.3 Results Summary and Clinical Implications

Of the parameters varied, the three parameters for which model outcomes were most sensitive were the tibial plateau angle, patellar ligament line of action angle and the femoral condyle radius. Two of these parameters, TPA and PLLAA, have been the biomechanical basis for several CrCL deficiency corrective surgical procedures.

Alteration of the TPA plays a prominent role in the cranial tibial wedge osteotomy (CTWO), tibial plateau leveling osteotomy (TPLO) and triple tibial osteotomy (TTO). The TPLO (as seen in FIGURE 16) involves a radial cut in the proximal tibia and then rotates the tibial fragment to alter the TPA to be more perpendicular to the tibial functional axis (Slocum and Slocum 1993). The CTWO (as seen in FIGURE 15) and TTO (as seen in FIGURE 19) both involve a wedge cut in the proximal tibia shaft (Slocum and Devine 1984; Bruce, Rose et al. 2007). Closing this wedge cut by rotating the proximal tibia cranially alters the TPA to be more perpendicular to the tibial functional axis. It was found in this study that a TPA closer to perpendicular to the tibial functional axis reduced CrCL forces in the CrCL intact stifle, reduced CaCL forces in the

CrCL deficient stifle and reduced relative tibial translation. Therefore, the findings of our study would tend to support the biomechanical approach of these corrective procedures.

Alteration of the patellar ligament line of action angle is the basis of the tibial tuberosity advancement (TTA) and is also a component of the triple tibial osteotomy (Hoffmann, Miller et al. 2006; Bruce, Rose et al. 2007). The TTA (as seen in FIGURE 18) involves a cut in the proximal tibia and a spacer advances the tibial tuberosity cranially. This advancement alters the PLLAA to be more perpendicular to the TPA. The TTO (as seen in FIGURE 19) also involves a cut in the proximal tibia, but this procedure uses the closing of the previously described wedge cut to advance the tibial tuberosity cranially. As with the TTA, the TTO alters the PLLAA to be more perpendicular to the TPA. It was found in this study that a PLLAA that was closer to perpendicular to the TPA reduced CrCL forces in the CrCL intact stifle, reduced CaCL forces in the CrCL deficient stifle and reduced relative tibial translation. Therefore, the findings of our study would tend to support the biomechanical approach of these corrective procedures as well.

The role of the FCR in stifle joint stability has not to our knowledge been extensively studied and has not been the basis for any corrective surgical procedures. It was found in this study that increasing FCR resulted in increased CaCL forces and increased relative tibial translation in the CrCL deficient stifle.

Though this model was not used to determine the validity of these corrective surgical procedures or assess stifle biomechanics following these corrective procedures, it does provide preliminary support of the primary biomechanical rationale for these procedures. A lower TPA corresponded with reduced ligament forces in the CrCL intact and deficient stifle, and relative tibial translation was reduced. Also, a PLLAA closer to

perpendicular to the tibial plateau corresponded with reduced ligament forces in the CrCL intact and deficient stifle, and relative tibial translation was reduced.

This model did not, however, assess these parameters to the extent that they are altered in corrective surgical procedures. Average postoperative TPAs from the CTWO, TPLO and TTO range from perpendicular to the tibia functional axis, which was assumed to be a TPA of 0°, to 16° (Slocum and Devine 1984; Slocum and Slocum 1993; Bruce, Rose et al. 2007). In our study, the TPA was altered to a minimum of 18° and a maximum of 28°. Similarly following TTA and TTO, patellar ligament line of action angles relative to the TPA ranged from 89° to 100° (Hoffmann, Miller et al. 2006; Bruce, Rose et al. 2007) while our model was used to evaluate PLLAA at mid-stance ranging from 64° to 104°. Also, the PLLAA in this study was altered without modifiying the tibial tuberosity location. Therefore, the results presented here may not be reflective of stifle biomechanics resulting from these surgical corrective procedures.

Although our model outcomes were found to be sensitive to FCR, currently there are no surgical procedures which attempt to address this factor. The majority of osteotomy corrective surgical procedures have focused on alteration of the tibia. The results presented here suggest the distal femoral shape may also contribute to stifle stability. Femoral condyle radius was investigated as a possible parameter associated with stifle stability, but this parameter and others associated with the distal femur shape have not been clearly defined in previous studies. Further research examining the role of the distal femur shape in stifle stability is warranted.

This computer model attempted to assess individual parameters and their roles in stifle biomechanics. It was demonstrated through the model outcome measures that

multiple individual parameters can affect the stability of the stifle, but combinations of these altered parameters remains unknown. Additionally, this model made no attempt to investigate the effects of ligament degredation over time on stifle biomechanics. It has previously been reported that the morphology of the CaCL changes following CrCL deficiency, possibly as a result of repetitive microtrauma resulting from stifle instability (Zachos, Arnoczky et al. 2002). Since this computer model determined consistently increased CaCL loads following CrCL suppression with variation in tibial plateau angle, muscle force magnitude, patellar ligament line of action angle, ground reaction force, body mass and femoral condyle radius, the investigation of both the immediate and longterm effects of CrCL deficiency and stifle stabilization through surgical means is warranted.

VI. LIMITATIONS

Several limitations exist within this study and the development of this canine hind limb computer simulation model.

- This computer model is a simplification of a complex biomechanical system.
- Dynamic effects were not considered in this quasi-static model.
- As a first approximation, geometry and individual bones of the hind limb were developed using geometric modeling functions available in the SolidWorks modeling software and were based on anatomical images.
- The three dimensional hind limb bone elements were confined to translation and rotation in the sagittal plane, which reduced the number of available degrees of freedom from six to three.
- Ligaments were approximated as single elements connecting the origin and insertion and were not treated as three dimensional structures capable of articulating around other structures.
- Viscoelastic ligament material properties were not accounted for in the model.
- All ligament material properties were based on CrCL material properties reported in the literature for Rottweilers and Greyhounds (Wingfield, Amis et al. 2000).
- Muscle actuation was simplified by grouping muscles, and the magnitudes of muscle forces were approximated through the use of previously reported optimization techniques (Shahar and Banks-Sills 2004).

- The stifle joint capsule, menisci curvature and material properties were neglected in the model.
- The location of contact between the femur and meniscus was approximated.
- The location of the patella relative to the femur remained constant.
- The model was developed based upon a single Labrador Retriever.
- Hind limb skeletal dimensions were based upon locations of boney landmarks rather than radiological data.
- The ground reaction forces used were based upon the scientific literature and not on a specific dog.
- Attempts to verify the computer model in this study were primarily based on a previously reported mathematical model and an in vitro study which both have inherent limitations.

VII. RECOMMENDATIONS

In order to address the limitations described, several recommendations can be made.

- A model developed from radiological scans would improve the skeletal anatomical accuracy.
- Ligament size, shape and exact insertion location could also be incorporated into the model using radiological scans.
- Subject-specific ground reaction force data could be obtained and incorporated into the model.
- Utilization of all degrees of freedom and the inclusion of dynamic behavior would increase the complexity of the model but would give a more representative depiction of the canine hind limb.
- The use of more directly applicable musculoskeletal simulation software could improve the approximations for soft tissue response and dynamic biomechanical behavior.
- A parameter-based model development batch process could reduce the time needed to develop breed-specific models.

VIII. FUTURE WORK

This model was used as a tool to develop hypotheses for studies to be conducted in the future. Future dissertation work will be based on the development of a model utilizing radiological scan images, subject-specific kinetic and kinematic gait data, and we will consider the use of Software for Interactive Musculoskeletal Modeling, SIMM (MusculoGraphics, Inc., Santa Rosa, CA) for model development. Future models will be used to biomechanically evaluate procedures used to stabilize the CrCL deficient canine stifle.

IX. CONCLUSIONS

The three dimensional solid body computer model developed in this study was a first approximation of the canine hind limb during the stance phase of walking gait and is the first such model developed for the canine hind limb. This model was developed from a 32 kg Labrador Retriever and was used to simulate both a CrCL intact and CrCL deficient stifle. Stifle ligament forces and tibial translation were measured in both the CrCL intact and CrCL deficient stifle. A systematic variation of several parameters was conducted to assess the model sensitivity to parameters thought to be associated with CrCL deficiency. Verification of the model was confirmed through reasonable agreement with a previously reported mathematical model and an in vitro study. The goals of this study were to describe CrCL intact and CrCL deficient stifle biomechanics and their relation to parameters which may be associated with CrCL deficiency.

Suppression of the CrCL in the computer model consistently increased CaCL load profiles during stance. When the CrCL was suppressed, tibial translation was found to occur to an extent similar to that found in a previous in vitro study. Tibial plateau angle, patellar ligament line of action angle and femoral condyle radius were parameters for which model outcomes were most sensitive.

In the CrCL intact stifle the CrCL peak load during stance increased with increasing TPA and increasing PLLAA. In the CrCL deficient stifle the CaCL peak load during stance increased with increasing TPA, PLLAA, muscle force magnitude, ground

reaction force magnitude, body mass and FCR. Additionally, the peak relative tibial translation between the CrCL intact and CrCL deficient stifle during stance increased with increasing TPA, increasing PLLAA and increasing FCR in the CrCL deficient model.

This model serves as a basis from which more anatomically accurate canine hind limb models could be developed to simulate and assess corrective CrCL deficiency surgical procedures.

REFERENCES

Adams, D. R. (1986). Canine Anatomy: A Systemic Study. Ames, Iowa State University Press.

Apelt, D., M. P. Kowaleski, et al. (2007). "Effect of tibial tuberosity advancement on cranial tibial subluxation in canine cranial cruciate-deficient stifle joints: an in vitro experimental study." Vet Surg **36**(2): 170-7.

Aragon, C. L. and S. C. Budsberg (2005). "Applications of evidence-based medicine: cranial cruciate ligament injury repair in the dog." Vet Surg **34**(2): 93-8.

Arnoczky, S. P. and J. L. Marshall (1977). "The cruciate ligaments of the canine stifle: an anatomical and functional analysis." Am J Vet Res **38**(11): 1807-14.

Arnoczky, S. P., P. A. Torzilli, et al. (1977). "Biomechanical evaluation of anterior cruciate ligament repair in the dog. An analysis of the instant center of motion." J Am Anim Hosp Assoc **13**: 553-558.

Baroni, E., R. R. Matthias, et al. (2003). "Comparison of radiographic assessments of the tibial plateau slope in dogs." Am J Vet Res **64**(5): 586-9.

Blankevoort, L. and R. Huiskes (1991). "Ligament-bone interaction in a three-dimensional model of the knee." J Biomech Eng **113**(3): 263-9.

Blankevoort, L., J. H. Kuiper, et al. (1991). "Articular contact in a three-dimensional model of the knee." J Biomech **24**(11): 1019-31.

Boudrieau, R. J. (2009). "Tibial plateau leveling osteotomy or tibial tuberosity advancement?" Vet Surg **38**(1): 1-22.

Brianza, S. Z., P. D'Amelio, et al. (2007). "Allometric scaling and biomechanical behavior of the bone tissue: an experimental intraspecific investigation." Bone **40**(6): 1635-42.

Bruce, W. J., A. Rose, et al. (2007). "Evaluation of the triple tibial osteotomy. A new technique for the management of the canine cruciate-deficient stifle." Vet Comp Orthop Traumatol **20**(3): 159-68.

Budsberg, S. C., M. C. Verstraete, et al. (1987). "Force plate analysis of the walking gait in healthy dogs." Am J Vet Res **48**(6): 915-918.

Conzemius, M. G., R. B. Evans, et al. (2005). "Effect of surgical technique on limb function after surgery for rupture of the cranial cruciate ligament in dogs." J Am Vet Med Assoc **226**(2): 232-6.

DeCamp, C. E. (1997). "Kinetic and kinematic gait analysis and the assessment of lameness in the dog." Vet Clin North Am Small Anim Pract **27**(4): 825-40.

DeCamp, C. E., C. M. Riggs, et al. (1996). "Kinematic evaluation of gait in dogs with cranial cruciate ligament rupture." Am J Vet Res **57**(1): 120-6.

Fung, Y. C. (1993). Biomechanics: mechanical Properties of Living Tissues. New York, Springer.

Havig, M. E., J. Dyce, et al. (2007). "Relationship of tibial plateau slope to limb function in dogs treated with a lateral suture technique for stabilization of cranial cruciate ligament deficient stifles." Vet Surg **36**(3): 245-51.
Hoffmann, D. E., J. M. Miller, et al. (2006). "Tibial tuberosity advancement in 65 canine stifles." Vet Comp Orthop Traumatol **19**(4): 219-27.
Holden, J. P., E. S. Grood, et al. (1994). "In vivo forces in the anterior cruciate ligament: direct measurements during walking and trotting in a quadruped." J Biomech **27**(5): 517-26.
Hottinger, H. A., C. E. DeCamp, et al. (1996). "Noninvasive kinematic analysis of the walk in healthy large-breed dogs." Am J Vet Res **57**(3): 381-388.
Jaegger, G., D. J. Marcellin-Little, et al. (2002). "Reliability of goniometry in Labrador Retrievers." Am J Vet Res **63**(7): 979-86.
Jandi, A. S. and A. J. Schulman (2007). "Incidence of motion loss of the stifle joint in dogs with naturally occurring cranial cruciate ligament rupture surgically treated with tibial plateau leveling osteotomy: longitudinal clinical study of 412 cases." Vet Surg **36**(2): 114-21.
Kim, S. E., A. Pozzi, et al. (2009). "Effect of tibial plateau leveling osteotomy on femorotibial contact mechanics and stifle kinematics." Vet Surg **38**(1): 23-32.
Kim, S. E., A. Pozzi, et al. (2009). "Effect of tibial tuberosity advancement on femorotibial contact mechanics and stifle kinematics." Vet Surg **38**(1): 33-9.
Kim, S. E., A. Pozzi, et al. (2008). "Tibial osteotomies for cranial cruciate ligament insufficiency in dogs." Vet Surg **37**(2): 111-25.
Kowaleski, M. P., D. Apelt, et al. (2005). "The effect of tibial plateau leveling osteotomy position on cranial tibial subluxation: an in vitro study." Vet Surg **34**(4): 332-6.
Lazar, T. P., C. R. Berry, et al. (2005). "Long-term radiographic comparison of tibial plateau leveling osteotomy versus extracapsular stabilization for cranial cruciate ligament rupture in the dog." Vet Surg **34**(2): 133-41.
Liacouras, P. C. and J. S. Wayne (2007). "Computational modeling to predict mechanical function of joints: application to the lower leg with simulation of two cadaver studies." J Biomech Eng **129**(6): 811-17.
Liska, W. D., D. J. Marcellin-Little, et al. (2007). "Custom total knee replacement in a dog with femoral condylar bone loss." Vet Surg **36**(4): 293-301.
McCann, L., E. Ingham, et al. (2009). "Influence of the meniscus on friction and degradation of cartilage in the natural knee joint." Osteoarthritis Cartilage.
Morris, E. and A. J. Lipowitz (2001). "Comparison of tibial plateau angles in dogs with and without cranial cruciate ligament injuries." J Am Vet Med Assoc **218**(3): 363-6.
Osmond, C. S., D. J. Marcellin-Little, et al. (2006). "Morphometric assessment of the proximal portion of the tibia in dogs with and without cranial cruciate ligament rupture." Vet Radiol Ultrasound **47**(2): 136-41.
Pacchiana, P. D., E. Morris, et al. (2003). "Surgical and postoperative complications associated with tibial plateau leveling osteotomy in dogs with cranial cruciate ligament rupture: 397 cases (1998-2001)." J Am Vet Med Assoc **222**(2): 184-93.
Pozzi, A., M. P. Kowaleski, et al. (2006). "Effect of medial meniscal release on tibial translation after tibial plateau leveling osteotomy." Vet Surg **35**(5): 486-94.

Priddy, N. H., 2nd, J. L. Tomlinson, et al. (2003). "Complications with and owner assessment of the outcome of tibial plateau leveling osteotomy for treatment of cranial cruciate ligament rupture in dogs: 193 cases (1997-2001)." J Am Vet Med Assoc **222**(12): 1726-32.

Rayward, R. M., D. G. Thomson, et al. (2004). "Progression of osteoarthritis following TPLO surgery: a prospective radiographic study of 40 dogs." J Small Anim Pract **45**(2): 92-7.

Reif, U., D. A. Hulse, et al. (2002). "Effect of tibial plateau leveling on stability of the canine cranial cruciate-deficient stifle joint: an in vitro study." Vet Surg **31**(2): 147-54.

Reif, U. and C. W. Probst (2003). "Comparison of tibial plateau angles in normal and cranial cruciate deficient stifles of Labrador retrievers." Vet Surg **32**(4): 385-9.

Robertson, D. G. E., G. E. Caldwell, et al. (2004). Research Methods in Biomechanics. Champaign, Human Kinetics.

Robinson, D. A., D. R. Mason, et al. (2006). "The effect of tibial plateau angle on ground reaction forces 4-17 months after tibial plateau leveling osteotomy in Labrador Retrievers." Vet Surg **35**(3): 294-9.

Schaefer, S. L., C. E. DeCamp, et al. (1998). "Kinematic gait analysis of hind limb symmetry in dogs at the trot." Am J Vet Res **59**(6): 680-5.

Shahar, R. and L. Banks-Sills (2002). "Biomechanical analysis of the canine hind limb: calculation of forces during three-legged stance." Vet J **163**(3): 240-50.

Shahar, R. and L. Banks-Sills (2004). "A quasi-static three-dimensional, mathematical, three-body segment model of the canine knee." J Biomech **37**(12): 1849-59.

Shahar, R. and J. Milgram (2001). "Morphometric and anatomic study of the hind limb of a dog." Am J Vet Res **62**(6): 928-33.

Shahar, R. and J. Milgram (2006). "Biomechanics of tibial plateau leveling of the canine cruciate-deficient stifle joint: a theoretical model." Vet Surg **35**(2): 144-9.

Slatter, D. H. (2003). Textbook of small animal surgery. Philadelphia, Saunders.

Slocum, B. and T. Devine (1983). "Cranial tibial thrust: a primary force in the canine stifle." J Am Vet Med Assoc **183**(4): 456-9.

Slocum, B. and T. Devine (1984). "Cranial tibial wedge osteotomy: a technique for eliminating cranial tibial thrust in cranial cruciate ligament repair." J Am Vet Med Assoc **184**(5): 564-9.

Slocum, B. and T. D. Slocum (1993). "Tibial plateau leveling osteotomy for repair of cranial cruciate ligament rupture in the canine." Vet Clin North Am Small Anim Pract **23**(4): 777-95.

Talaat, M. B., M. P. Kowaleski, et al. (2006). "Combination tibial plateau leveling osteotomy and cranial closing wedge osteotomy of the tibia for the treatment of cranial cruciate ligament-deficient stifles with excessive tibial plateau angle." Vet Surg **35**(8): 729-39.

Thieman, K. M., J. L. Tomlinson, et al. (2006). "Effect of meniscal release on rate of subsequent meniscal tears and owner-assessed outcome in dogs with cruciate disease treated with tibial plateau leveling osteotomy." Vet Surg **35**(8): 705-10.

Vasseur, P. B. and S. P. Arnoczky (1981). "Collateral ligaments of the canine stifle joint: anatomic and functional analysis." Am J Vet Res **42**(7): 1133-7.

Vasseur, P. B., R. R. Pool, et al. (1985). "Correlative biomechanical and histologic study of the cranial cruciate ligament in dogs." Am J Vet Res **46**(9): 1842-54.
Warzee, C. C., L. M. Dejardin, et al. (2001). "Effect of tibial plateau leveling on cranial and caudal tibial thrusts in canine cranial cruciate-deficient stifles: an in vitro experimental study." Vet Surg **30**(3): 278-86.
Wentink, G. H. (1976). "The action of the hind limb musculature of the dog in walking." Acta Anat (Basel) **96**(1): 70-80.
Wilke, V. L., D. A. Robinson, et al. (2005). "Estimate of the annual economic impact of treatment of cranial cruciate ligament injury in dogs in the United States." J Am Vet Med Assoc **227**(10): 1604-7.
Wingfield, C., A. A. Amis, et al. (2000). "Comparison of the biomechanical properties of rottweiler and racing greyhound cranial cruciate ligaments." J Small Anim Pract **41**(7): 303-7.
Witsberger, T. H., J. A. Villamil, et al. (2008). "Prevalence of and risk factors for hip dysplasia and cranial cruciate ligament deficiency in dogs." J Am Vet Med Assoc **232**(12): 1818-24.
Zachos, T. A., S. P. Arnoczky, et al. (2002). "The effect of cranial cruciate ligament insufficiency on caudal cruciate ligament morphology: An experimental study in dogs." Vet Surg **31**(6): 596-603.

VITA

Nathan Brown was born on March 16, 1984 in Louisville, Kentucky. He graduated from Jeffersonville High School in Jeffersonville, Indiana in 2002. Nathan attended the University of Louisville and earned a Bachelor of Science degree in mechanical engineering with a minor in creative art in 2007. While pursuing a Master of Engineering degree in mechanical engineering, he was a teaching assistant for mechanical engineering experimental measurements. He also worked as a graduate assistant processing motion capture data. In March 2008 he was awarded the Grosscurth Fellowship to continue his research at the University of Louisville in pursuit of a PhD.